ACCURATE MEASUREMENTS OF THE THERMAL CONDUCTIVITY OF GASES

Markos Assael

M.Sc.,D I C,B.Sc.(Eng),A C G I

Department of Chemical Engineering and Chemical Technology
Imperial College
London

July 1980

A thesis submitted for the degree of Doctor of Philosophy
of the University of London

ABSTRACT

The thesis describes measurements of the thermal conductivity of the monatomic gases Helium, Neon, Argon, Krypton and Xenon and binary mixtures of Helium/Neon and Argon/Krypton. Measurements are also reported for the polyatomic gases Hydrogen, Nitrogen, Carbon Monoxide and Methane as well as binary mixtures of Hydrogen with Neon, Argon, Krypton and Nitrogen. The measurements have been carried out in a transient hot wire apparatus designed and constructed especially for this work, at 35 °C in the pressure range 0.5 to 10 MPa. The uncertainty in the reported data is estimated to be no more then $\pm 0.2\%$; an estimate which is confirmed by a comparison with low density viscosities for the monatomic gases using an exact result of the kinetic theory.

The new results for binary monatomic gas mixtures are so accurate that higher order kinetic theory formulae had to be developed to provide a satisfactory description of them at low density. The high accuracy achieved at elevated densities is used to demonstrate the inadequacies of the present theories of the density dependence of the transport coefficients for gases and gas mixtures. A semi-empirical procedure for the density dependence of the thermal conductivity of gas mixtures is, however remarkably succesful.

For polyatomic gases and their mixtures the new results indicate that existing kinetic theory formulae are again inadequate. It is shown how improved theoretical expressions would enable useful molecular information to be obtained from the experimental data at low density. In the particular cases of Nitrogen and Carbon Monoxide, despite the limitations of the theory, the present data strongly suggest that diffusion of internal energy in the gases is significantly slower then the transport of mass, in contrast to the prediction of the only available theoretical analysis. The density dependence of the thermal conductivity of the polyatomic mixtures is however well described by the same semi-empirical scheme which is succesful for the monatomic mixtures.

to my parents

CONTENTS

ACKNOWLEDGEMENTS

The author wishes to extend his deepest appreciation to his supervisor, Dr W.A.Wakeham, for his excellent counsel and guidance during the course of this work. The author is also indebted to Mr J.Menashe for his assistance and suggestions.

Special thanks are due to Mr A.Lucas for his help in designing and manufacturing the mechanical parts, to Mr M.J.Dix for the design of the electronic components and to Mr R.Wood for his continuous help. Thanks are also due to Dr H.J.Michels for his help with the calibration of the sample cylinders and the platinum resistance thermometers, and to Mr V.Vesovic for his assistance with some collision integrals calculations.

Finally, the author wishes to thank his parents for ther constant encouragement and financial support.

INTRODUCTION

The difficulty of performing accurate measurements of the thermal conductivity of fluids has been recognised for a considerable time. As recently as 1977 a review of the available experimental data for the most frequently studied systems, the monatomic gases, revealed that few of the results were consistent with accurate viscosities for the same gases. Furthermore, the discrepancies between various sets of experimental data were almost one order of magnitude larger than their claimed uncertainty. Because an accurate knowledge of the viscosity and thermal conductivity of a polyatomic gas provides information about inelastic processes it was evident that measurements of the thermal conductivity of a comparable accuracy to that achieved for viscosity ($\pm$0.2%) should be performed.

In a paper presented in Chempor 1978 in Braga,Portugal, we have also shown that uncertainties in the transport coefficients have a significant effect upon the technical design of any heat process equipment and may result in unnecessary capital expenditure. It was shown that uncertainties in the thermal conductivity of the fluids used, which can easily amount up to 20%, can have an almost proportional effect to the size of the particular equipment.

This thesis begins with a survey of the various techniques for fluid thermal conductivity measurements which establishes the need for more accurate measurements. In the second Chapter, the existing theories for the thermal conductivity of gases and gas mixtures at low and elevated densities are discussed and extended, so as to be of comparable accuracy with the experimental results obtained. This Chapter also illustrates how molecular information can be derived from transport property measurements. In the subsequent Chapter the theory of a refined technique based on the transient hot wire is given. In Chapter four the apparatus itself and the experimental procedure are described. The entire body of experimental data obtained in this work for a number of monatomic and polyatomic gases and gas mixtures is given in

Chapter five, for a temperature of 35 'C. Chapter six then details the interpretation of the experimental data in terms of the kinetic theory of gases, and demonstrates that in order for the maximum molecular information to be derived from the accurate experimental data obtained, more accurate kinetic theory expressions must be developed.Finally, in Chapter seven suggestions for future work involving the extenssion of the range of the present equipment to temperatures as low as -200 'C and as high as +200 'C will be discussed.

• ONE

METHODS OF MEASURING THE THERMAL CONDUCTIVITY

1. INTRODUCTION

The thermal conductivity coefficient 'λ', is defined by the Fourier law as :-

$$\frac{\partial Q}{\partial t} = - \lambda \cdot A \cdot \nabla^2 T \qquad (1.1)$$

where, Q represents the conductive heat flow, A the area at right angle to the heat flow, and T the temperature in the medium. Heat transport by conduction in a medium is caused by the molecular exchange of energy associated with the thermal random motion of the molecules. This must be clearly distinguished from convective heat transfer, in which heat is transferred by the translation of elements of fluids (large on a molecular scale) and from radiative transfer which occurs by the emission and absorption of electromagnetic radiation by molecules in translucent substances. In order to perform accurate measurements of the thermal conductivity of fluids, the foregoing discussion shows that experimental conditions must be arranged so that all energy is transported by conduction. At this point it should be noted that, as convection will always be present in fluids subject to a temperature gradient, conditions should be arranged such that its effect is insignificant. A suitable working equation for the equipment to measure the thermal conductivity of fluids can then be obtained from a solution of the Fourier law.

Two different approaches have been generally adopted for thermal conductivity measurements, a steady state (stationary) and a time dependent (transient) one. This distinction provides the basis for the classification of the techniques used in the determination of the thermal conductivity of fluids that is the subject of the next two Sections. In the last Section of this

Chapter, an evaluation of the various methods will be attempted, and their errors and disadvantages in relation to the transient hot wire technique will be shown.

1.1. STATIONARY METHODS

In the stationary methods the principle of measurements is relative straightforward. The medium to be investigated is placed in a vessel of known geometry and a heat flux is introduced. As a consequence of this, the temperature of the medium rises and after a certain time equilibrium is reached and a stationary temperature difference is established in the medium. The thermal conductivity is thus calculated as a function of the heat flux , the temperature gradient, the properties of the medium and the geometry of the vessel.

There are three basic categories of stationary methods; the double plate methods, concentric spheres and concentric cylinders methods.

1.1.1. DOUBLE PLATE METHODS

The double plate technique is the oldest experimental method and was first used in the early 1800's by Nicholson [1], Murray[2] and Rumford [3] who used a vertical column of fluid contained between horizontal flat plates, heated from above so as to reduce convective effects. The thermal conductivity is obtained from the steady state solution of the Fourier law as :-

$$Q = -\lambda \cdot (A/d) \cdot \Delta T \qquad (1.2)$$

where, Q is the heat transferred across plates of area A separated by a distance d and held in a constant temperature difference ΔT. Quantitative measurements were made following Biot's [4] formulation of a law of conduction, by Depretz [5], Weber [6] and others.

An important improvement to the original design was the addition of guard rings to ensure a one-dimensional heat flux and thus eliminate edge effects. These devices were probably first used by Berget [7]. In 1933, Bates [8]argued in favour of increasing the small separation between the plates which had formerly been used,

as it was difficult to measure the gap to the required accuracy. Later Sokiades and Coates [9,10] also suggested an increase of the plate separation and attempted to show that radiation and convection were negligible. Subsequently, Michels and Botzen [11], described a double plate method for measuring thermal conductivity of gases up to 3000 Atmospheres. This was improved by Michels, Sengers and Van der Gulick [12] in 1962, and used extensively for measurements on gases over a wide range of pressures and temperatures. Their apparatus, probably the best of its kind, consists of two plates (see Fig. 1), an upper U and a lower L kept apart 1.4mm, both containing a spiral winding used as a heater and a resistance thermometer for the temperature measurement. The upper plate being surrounded by a ring plate G, was kept at the same temperature with it and both were placed in an insulation cap C. Finally, an insulating film F was also used in an attempt to compensate for edge effects.

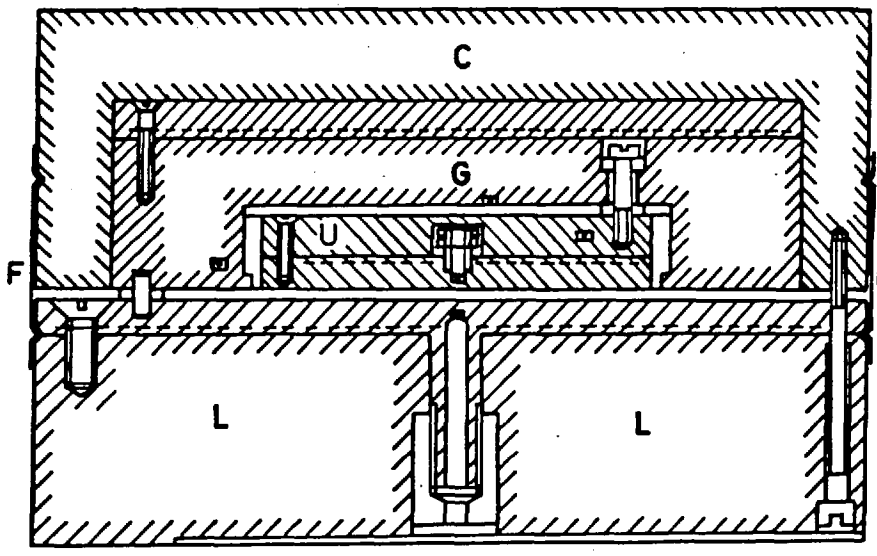

Figure 1. Michels et al. double plate.

A similar arrangement was also used by Fritz and Poltz [13] in an attempt to investigate the effects of convection and radiation.

1.1.2. CONCENTRIC SPHERES METHODS

In an attempt to avoid problems created by the edges of the plates, a concentric sphere arrangement was suggested. According to this technique, the medium to be investigated is placed between two concentric spheres of radii r_1 and r_2. The inner sphere is heated while the outer is kept at a constant temperature. Thus, a temperature difference, ΔT, is established between the two

spheres. The thermal conductivity of the fluid can be calculated from the steady state solution of the Fourier law as :-

$$Q = \lambda \left(\frac{4\pi r_1 r_2}{r_2 - r_1}\right) \cdot \Delta T \qquad (1.3)$$

where Q is the heat loss from the inner sphere.

In 1951, Riedel [14] constructed a succesful spherical cell by using a 28mm diameter copper sphere containing a heater supported in another vacuum tight sealed spherical cell. Centering was achieved by various micrometer measurements and the results that he obtained seemed to agree to an accuracy of 1% with his results using both flat plates and concentric cylinders.

Richter and Sage [15] used a similar arrangement for methane and nitrogen dioxide up to a pressure of 300 Atmospheres with a layer thickness of about 0.5mm. However, they observed that the temperature distribution over the outer sphere was not uniform indicating the presence of natural convective currents.

1.1.3. CONCENTRIC CYLINDERS METHODS

In an attempt to avoid the complications that arose in the double plate methods with the introduction of the guard rings and the magnitude of the plate separation, Bridgmann [16], in 1923, used a concentric cylinder arrangement. In his original design the inner cylinder which was partially immersed in the test fluid was heated, and the outer one was in good thermal contact with the pressure vessel in its oil bath. Convective effects were reduced by using a very small temperature difference ΔT across the liquid layer. The thermal conductivity was obtained from the steady state solution of the Fourier law as :-

$$Q = \lambda \left(2\pi \ln\left(\frac{r_1}{r_2}\right)\right) \cdot \Delta T \qquad (1.4)$$

where, Q is the heat dissipation per unit length of the inner cylinder and r_1 and r_2 are the radii of the cylinders. However, his results were considered to be rather high and Riedel [17] showed that this could be largely accounted for by the inadequate compensation of conduction through the ends of the cylinders.

Bridgman's arrangement was improved later in 1932 by Schmidt and Seleshop [18], by surrounding the inner cylinder completely

by the fluid and compensating mathematically for convective flow patterns at the edges. Seleshop, later introduced guards on the inner cylinder in the form of heated end sections, to reduce heat loss by axial conduction.

In 1935, Schmidt and Milveston [19] published correlations for the convective heat transfer, in terms of the Rayleigh number but no definite absolute criteria for the detection of the presence of convection was suggested.

More recently the concentric cylinder method was used by Misic and Thodos [20] in 1966. In an attempt to reduce convective effects the gap was kept to a minimum, while at the same time the length of the cylinders was greatly increased so as to produce an 'infinite' cylinder with a one-dimensional radial heat flux.

A special case of the concentric cylinders method is the 'hot-wire' in which the inner cylinder takes the form of a wire which is electrically heated, and acts also as a thermometer. This was probably first used by Schliermacher [21] in 1888, who sought to eliminate end effects by considering only the middle section of the wire.

Recently Cecil and Munch [22] used a platinum wire of 58μm diameter held in tension by a small spring in a glass tube, with potential leads attached to its middle section so that only a segment of the wire (with no ends) is employed in the measurements. A similar arrangement was also described by Taylor and Johnston [23] and Johnston and Grilly [24] in their measurements of the thermal conductivity of gases. Corrections for axial heat transfer were made and conduction losses along the potential leads were estimated. Radiation effects were also accounted for by measurements in vacuum.

1.2. NON-STATIONARY METHODS

The transient hot wire technique is the only non-stationary method which has been given serious consideration. It was introduced in an attempt to eliminate convective currents which, are almost certainly, the basic source of errors in all stationary methods. In its ideal form this method employs a very thin wire 'infinitely long', suspended in an 'infinite' medium. A heat flux ,q , is initiated electrically in the wire at time t=0,and

the temperature rise in the medium is measured at different times. The thermal conductivity is obtained from the time dependent solution of the Fourier law as :-

$$\Delta T = \frac{q}{4\pi\lambda} \ln\left(\frac{4k_d t}{a^2 C}\right) \qquad (1.5)$$

where, a is the wire radius, k_d the thermal diffusivity of the fluid and C a known constant. The thermal conductivity can thus be obtained from the measured temperature rise as a function of time. The advantage of this method is, that provided the times involved are very small (less than 2 sec approximately) convection does not significantly offset the measurements due to the inertia of the fluid.

This method known as the transient hot wire method, was first used by Stahlane and Pyk [37] at 1930 to measure the thermal conductivity of powders. After 1945 , the method was tested and used as a means of measuring the thermal conductivity of liquids by Van der Held and his coworkers (Van der Held and Van Drunen [25] , Van Drunen [26], Hardebal and Kalshoven [27]). They used a 0.3 mm diameter Manganine wire W (see Fig. 2) as the heating wire placed together with a thermocouple T in a capillary tube dipped in a glass vessel filled with the liquid to be investigated L .This in turn was placed in a Dewar flask filled with water. Times of 5sec were used. A similar apparatus was used by de Vries [28] and Buettner [29] in investigating the influence of humidity in the thermal conductivity of granulated materials and by Gillan [30] and Grassman [31] .

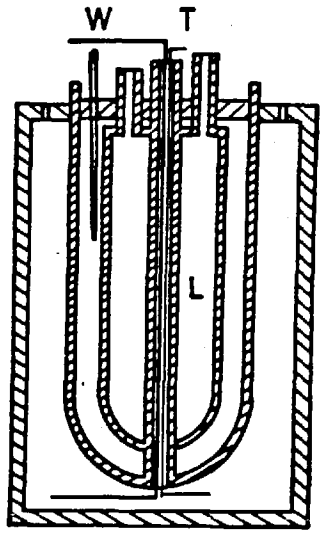

Figure 2 .Van der Held Transient hot wire

Weber [41] and later McLaughlin [32] used a platinum wire (see Fig. 3) and tried to correct for end effects due to axial conduction, by placing potential leads across a central section and thus actually using it as a four terminal resistance. Times of about 30sec were used. The same idea was adopted by Pittman[33]

and Mani [34] in measuring the thermal conductivity of liquids and Vos [35] for gases.

In 1969, Haarman [36] introduced electronic counters and considerably improved the method. Instead of measuring the temperature rise, he used an automatic bridge to measure the time taken for the resistance of the wire to reach certain predetermined values. From the resistance of the wire, the temperature rise of the medium is obtained and thus the thermal conductivity derived as before. Following his work, Castro and Wakeham [38] applied the technique to liquids, while de Groot, Kestin and Sookiazian [39] applied it to gases.

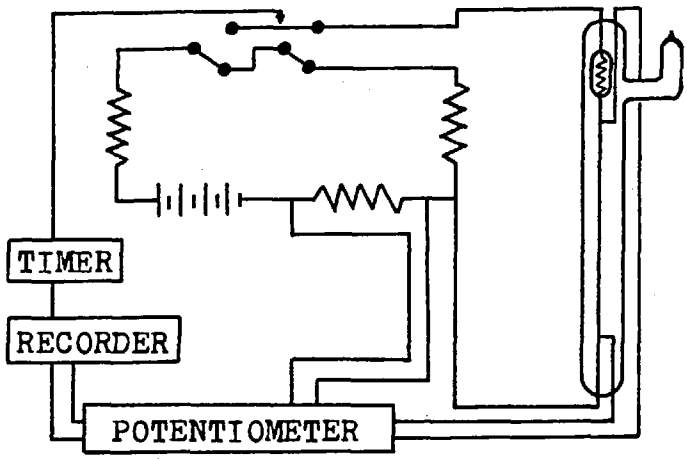

Figure 3 . McLaughlin's apparatus

These preliminary investigations have shown that measurements of fluid thermal conductivity of high precision are possible with this technique, although some problems remain before high accuracy can be also achieved.

This work will describe the final modifications to the hot wire technique that brought the absolute uncertainty of the measurements to its expected value of 0.2%.

1.3. EVALUATION OF THE ACCURACY AND ERRORS OF THE VARIOUS METHODS

At this point it is necessary to make a digression and to discuss the concepts of precision and accuracy as these are the criteria by which one can examine the various quoted results. Precision characterises the imperfections of the instrument, whereas accuracy characterises the imperfection of the resulting measurement. Moreover, precision is a measure of the interval expected in a given instrument within which the result of a measurement must fall. Accuracy is a measure of the probable departure of the result obtained by the measurement in question from a hypothetical measurement free of all imperfections.

The viscosity of the monatomic gases has been measured with an estimated accuracy of ±0.2% near room temperature. Therefore, the accuracy of thermal conductivity measurements can be examined with reference to the corresponding viscosities with the aid of the well known Eucken factor relation for a monatomic gas defined as (§2.3.3.p.42) :-

$$Eu = \frac{\lambda^{\circ}(T) \cdot M}{C_v \cdot \eta^{\circ}(T) \cdot F(T)} = 2.5 \text{ (exact)} \qquad (1.6)$$

where, $\lambda^{\circ}(T)$ is the zero density thermal conductivity, $\eta^{\circ}(T)$ the zero density viscosity, C_v the molar heat capacity at constant volume, M the molecular weight and F(T) a known factor accounting for the high order corrections to the Chapman-Enskog expressions(§2.3.3.p.42).

Figure 4 displays Eucken factors deduced using the best viscosity data [60] and the results of thermal conductivity measurements by various techniques. Only selected results that do not differ by more than 4% from the expected value are displayed in the interest of clarity. Some values reported in literature depart by as much as 50% from the expected value of Eu=2.5, and in some extreme cases differ even by a factor of five as shown by Liley [59] . The advantages of the transient hot wire can easily be seen in relation to others as the results of the most recent measurements with this method [42] , lie within the mutual uncertainty band of ±0.4%.

The wide range of variations in the absolute values of the thermal conductivity obtained from a variety of experimental methods is primarely due to the inevitable presence of convective currents in almost all the steady state apparatii, arising either due to the earth's gravitational field or due to the pattern of heating. Furthermore, in the stationary methods it is very difficult to detect experimentally whether convection is taking place and to what extent. Even Michels' double plate apparatus [12] , produced results which now are known to be high - probably due to convection. This problem is not significant in the transient techniques as will be discussed in a later section (§3.2.1.p.61).

In addition to the presence of convective heat transfer, the steady state methods described earlier have the advantage that it is difficult to secure the necessary one-dimensional heat flux. In such circumstances either the working equation does not refer

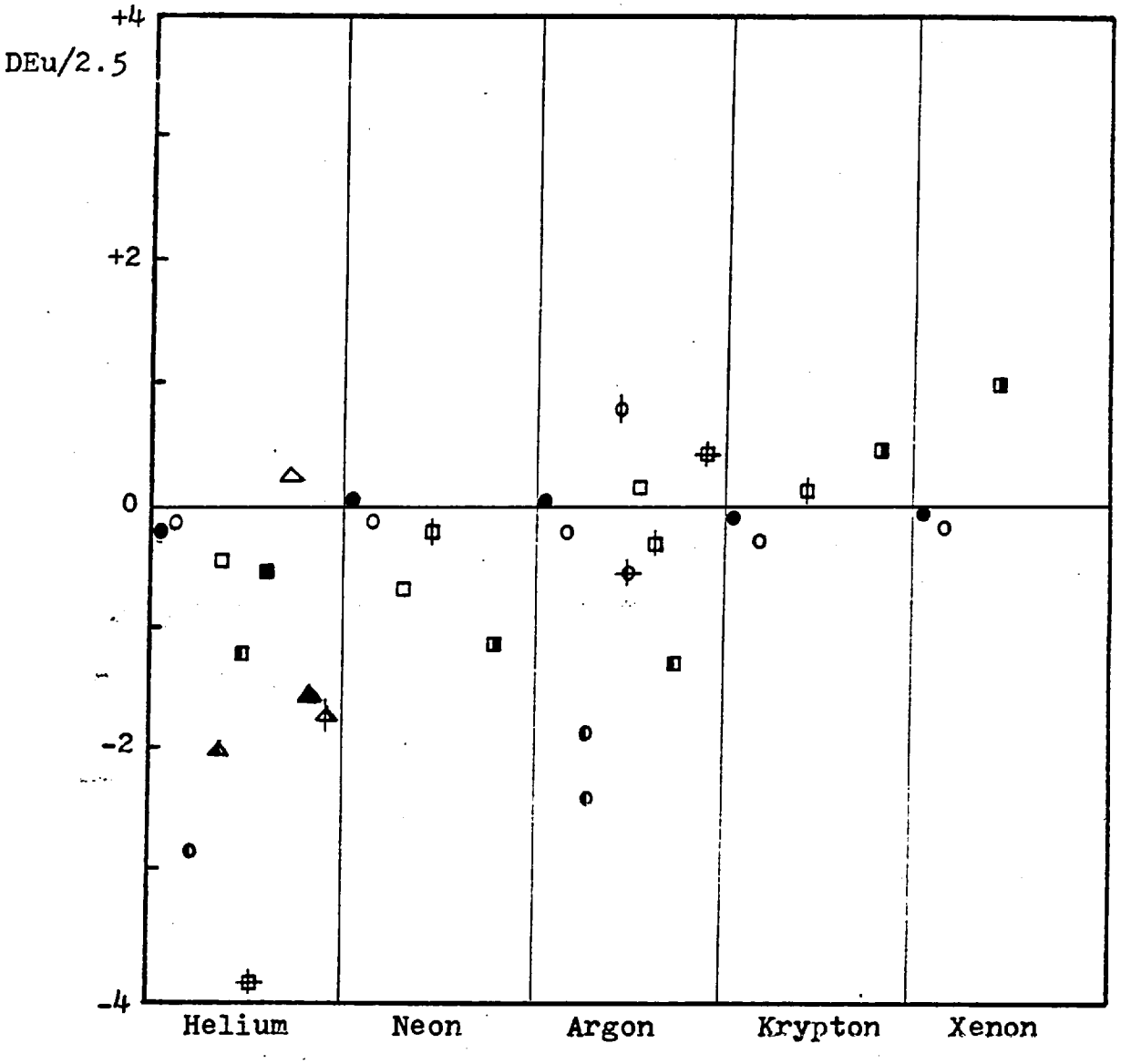

Figure 4 . Various Eucken factors for the monatomic gases (expressed as % of the theoretical value of 2.5)

●	Present Work		⌖	Keyes	(48)
o	Kestin et al.	(42)	■	Johnston et al.	(24)
o	Tufeu et al.	(43)	△	Dickins et al.	(49)
ϕ	Michels et al.	(44)	▲	Weber	(41)
⌖	Bailey et al.	(45)	⧋	Eucken	(50)
□	Van Dael et al.	(46)	▮	Tufeu	(56)
⌽	Haarman	(36)	▲	Kannuluik et al.	(57)
▮	Waelbroeck et al.	(47)			

to the experimental arrangements and so systematic errors are introduced, or the working equations have not been modified to account for such effects in a proper manner. Most often attempts have been made to modify the apparatus to ensure one-dimensional heat flow with a corresponding increase in its complexity. With the exception of the transient hot wire such modifications have not usually proved completely succesful.

Heat losses due to radiation may also be significant and owing to an incomplete knowledge of the emmissivities of the surfaces involved and the interaction of the radiant heat flux with the conductive heat flux, may be difficult to estimate. In the hot wire as the emitting area is very small, radiation effects can be neglected, at least in the case of gases.

All these considerations strongly suggest that the transient hot wire technique is the most suitable method for thermal conductivity measurements. It will be shown in this thesis that the transient hot wire technique can be used to perform thermal conductivity measurements on gases which have an associated uncertainty of only $\pm 0.2\%$.

• TWO

THE KINETIC THEORY OF GASES

2. HISTORICAL SUMMARY

In 1859, in a paper presented at a Conference of the British Association for the Advancement of Science, Maxwell [61] introduced the statistical approach to the molecular motion in gases that formed the basis of the Kinetic Theory of gases as it is presently understood. In this paper, the assumption made by all previous workers, that all molecules of a gas move with the same speed, was abandoned and the random character of molecular motion was recognised. In subsequent papers Maxwell derived the law of molecular velocities for a uniform gas in equilibrium -so called Maxwellian velocity distribution - and the law of equipartition of the mean molecular energy in a mixture of gases. In an attempt to give rigorous justification of the Maxwell assumption of the random character of molecular motion, Boltzmann [62] in 1872 established the H-Theorem, describing the irreversibility of physical processes. He then procceeded to derive an integro-differential equation, known as the Boltzmann equation, describing the evolution of the distribution function for molecular velocities in space and time and demonstrated that in equilibrium the velocity distribution function was just that obtained by Maxwell. Thus, the formal framework of the Kinetic Theory was established. However, from the investigations of Maxwell, Boltzmann [62,63] , Stephan [64], Langevin [64], Lorentz [65] and others it became apparent that solving the Boltzmann equation for a non-uniform gas was very complicated.

In 1910, the mathematician Hilbert [66] showed that for rigid spherical molecules Boltzmann's equation is equivalent to a linear integral equation of the second kind, for which a rigorous mathematical theory was available. Shortly after publication of the

Hilbert results, Chapman [67,68] and Enskog [69,70] independently both presented a suitable formulation for solving Boltzmann's equation. Both approaches although slightly different lead to the same expressions for the transport coefficients for dilute monatomic gases.

The Boltzmann equation describes the evolution of the velocity distribution function only for structurless molecules i.e. those that possess no internal energy. Thus it can not be applied to polyatomic gases which possess internal energy. A means of dealing with such polyatomic molecules was provided by Wang Chang,de Boer and Uhlenbeck [77,78] who reformulated the Boltzmann equation by treating each different internal energy state of the molecule as an independent species. They then treated the internal energy quantum mechanically and the translational energy classically leading to the so-called Semi-Classical Theory. Taxman [132] on the other hand developed an equivalent but entirely classical theory using the same ideas. Formal expressions for the transport coefficients were derived by Wang Chang and Uhlenbeck using essentially the Chapman-Enskog method.

The formal Uhlenbeck equations were put into a useful form by Mason and co-workers [79,80] yielding the thermal conductivity of dilute polyatomic gases and gas mixtures in terms of their viscosity and other measurable properties. These expressions made possible the evaluation of an Eucken factor for polyatomic gases that later was improved by Viehland, Mason and Sandler [84] to include the spin polarisation effect which the Semi-Classical theory neglects.

In relation to dense gases, Enskog [88] attempted to modify the Boltzmann equation to account for the finite volume of molecules which becomes significant at high densities. Enskog carried out this analysis for a rigid sphere model and consequently the results obtained were in poor agreement with experimental thermal conductivities at high densities. Consequently, in order to describe the experimental results Mason [89] and Wakeham [90] presented a semi-empirical scheme for calculating the thermal conductivity of polyatomic gas mixtures at high densities from that of their constituent gases.

In the following sections a more detailed examination of all

the various theories will be presented. On the one hand, these provide an introduction to the new extentions of the theory presented in this thesis, and on the other hand id provides a means whereby the limitations of present theories in some areas can be established and indicates the need for further developments.

2.1. THE BOLTZMANN EQUATION

Consider a gas mixture composed of structurless particles which interact through a spherically symmetric intermolecular pair potential $U_{ij}(r)$. Here i and j label two molecules of possibly different species. It is supposed that the number density of molecules in the gas is low enough such that only two molecules collide simultaneously, but high enough so that each molecule collides more frequently with others than it does with the walls of the containing vessel. Since it is clearly impossible to describe in a deterministic manner the motion of $\approx 10^{23}$ molecules in a gas by Classical Mechanics, we seek instead to describe the probable behaviour of a N molecule system. Because it has been assumed that only binary collisions occur, the position $\underline{r}$ and velocity $\underline{c}$ of a typical molecule are independent of the position and velocity of the other (N-1) particles in the system. Furthermore one may write a similar statement for all other molecules, so that an adequate description of the behaviour of the N molecules can be obtained (in this density range) by specifying the probable behaviour of a single molecule of each species in the gas mixture. Thus the analysis reduces to the search for a function $f_i(\underline{r},\underline{c},t)$ which is defined such that $f_i\, d\underline{r}\, d\underline{c}$ is the probable number of molecules of species i whose centres have at time t position coordinates in the range $\underline{r} \rightarrow \underline{r}+d\underline{r}$ and velocities in the range $\underline{c} \rightarrow \underline{c}+d\underline{c}$. It follows that from this definition of f_i that the number density n, mean velocity $\underline{v}$ and thermal kinetic energy u for the gas mixture are given by :-

$$n_i = \int f(\underline{r},\underline{c}_i,t)\cdot d^3c_i \qquad i=1,..,\nu \tag{2.1}$$

$$\rho\, \underline{v}(\underline{r},t) = \sum_{i=1}^{\nu} \int m_i \underline{c}_i f(\underline{r},\underline{c}_i,t)\cdot d^3c_i \tag{2.2}$$

$$\rho\, u(\underline{r},t) = \sum_{i=1}^{\nu} \int \tfrac{1}{2} m_i C_i^2 f(\underline{r},\underline{c}_i,t)\cdot d^3c_i \tag{2.3}$$

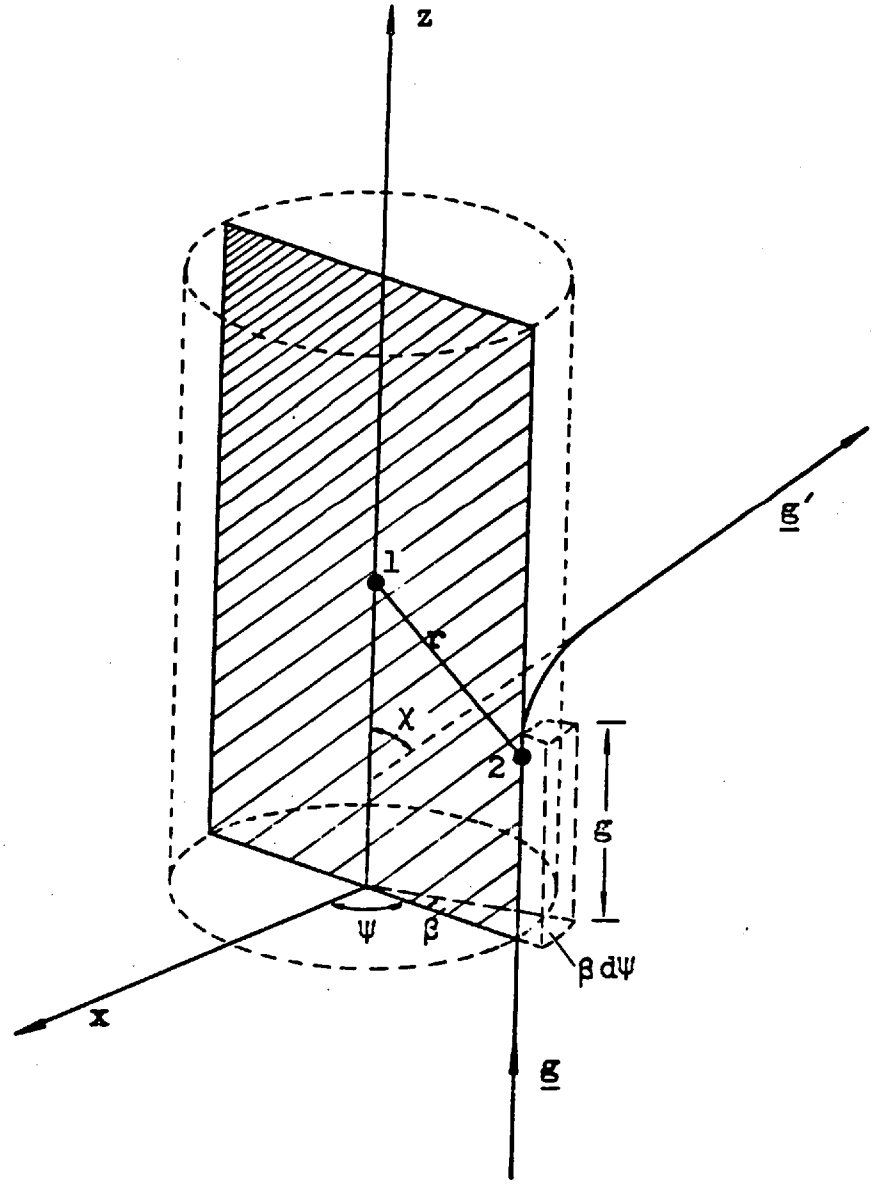

Figure 5 . Direct Collision of two molecules. Molecule 1 is at rest, angle χ is the angle of deflection of the relative velocity of molecule 2, $\underline{g}$ and $\underline{g}'$ are in the plane defined by the angle Ψ .

where $\underline{C}_i$ is the peculiar velocity of species i , given by $\underline{C}_i = \underline{c}_i - \underline{v}$

For a gas mixture whose molecules are not subjected to external forces, the only way in which a molecule can change its velocity is by collisions with other molecules. These changes in velocity on collision must influence the evolution of the function $f(\underline{r}, \underline{c}, t)$

with time as the molecules change their velocities and molecules enter or leave a particular region of configuration and velocity space. It may easily be shown, following this argument, that the equation of change of f_i can be written in the form [71] :-

$$\mathcal{D} f_i = \frac{\partial f_i}{\partial t} + \underline{c}_i \cdot \nabla_r f_i = \left(\frac{\partial f_i}{\partial t}\right)_{coll} \qquad (2.4)$$

where $(\partial f_i/\partial t)_{coll}$ denotes the rate of change in the function f_i by virtue of binary collisions with other molecules of its own and different kind.

By considering a single binary collision between a molecule of species i initially with a velocity $\underline{c}_i$ and a molecule of species j with velocity $\underline{c}_j$ (see Fig. 5) it may be shown that $(\partial f_i/\partial t)_{coll}$ is equal to :-

$$\left(\frac{\partial f_i}{\partial t}\right)_{coll} = \sum_{j=1}^{\nu} \int_0^\infty d\underline{c}_j \int_0^\infty \beta d\beta \int_0^{2\pi} d\psi \cdot g_{ij} \left\{ f(\underline{r}, \underline{c}_i', t) f(\underline{r}, \underline{c}_j', t) - f(\underline{r}, \underline{c}_i, t) f(\underline{r}, \underline{c}_j, t) \right\}$$

$$= \sum_{j=1}^{\nu} \int_0^\infty d\underline{c}_j \int_0^\infty \beta d\beta \int_0^{2\pi} d\psi \cdot g_{ij} \left\{ f_i' f_j' - f_i f_j \right\} = \sum_{j=1}^{\nu} J(f_i f_j) \qquad (2.5)$$

Here, β is the impact parameter for the collision, ψ specifies the orientation of the plane of collision in space and g_{ij} is the relative velocity of the two molecules before collision. In addition $\underline{c}_i'$ and $\underline{c}_j'$ represents velocities after collision.

In essence, the term $(\partial f_i/\partial t)_{coll}$ introduces the effect of all possible binary collisions between a molecule of species i and all other molecules in the gas at all impact parameters and spatial orientations upon the distribution function f_i . It should be noted that in formulating the collision term it has been assumed that the probable number of molecules in $d\underline{r}$ with velocities near $d\underline{c}$ is independent of the position and velocities of all other molecules. This is the statistical assumption of Molecular Chaos which will be examined later in the contest of gases at moderate densities.

Combining equations (2.4) and (2.5), the equation of change for f_i can be written in a compact form for a ν-component mixture as:-

$$\mathcal{D} f_i = \sum_{j=1}^{\nu} J(f_i f_j) \qquad (2.6)$$

This equation is known as the Boltzmann equation.
In order to obtain macroscopic equations of state for the number

density of species i , the momentum and the energy of the gas, the definition of the function f indicates that one should merely multiply both sides of equation (2.6) by 1 , $m\underline{c}_i$ and $\frac{1}{2}m_i C_i^2$ and integrate over all velocities $\underline{c}_i$ and sum over all components of the mixture to obtain the conservation equations:-

$$\frac{1}{\rho_i}\frac{d\rho_i}{dt} = -\nabla\cdot\underline{v} - \sum_{j=0}^{\infty}\nabla\cdot\underline{V}_i - \sum_{j=0}^{\infty}\underline{V}_i\cdot\frac{1}{\rho_i}\cdot\nabla\rho_i \qquad i=1,..,\nu \tag{2.7}$$

$$\rho\frac{d\underline{v}}{dt} = -\sum_{j=0}^{\infty}\nabla\cdot\underline{P} \tag{2.8}$$

$$\rho\frac{du}{dt} = -\sum_{j=0}^{\infty}\nabla\cdot\underline{q} - \sum_{j=0}^{\infty}\underline{P} : \nabla\underline{v} \tag{2.9}$$

where $d/dt = \partial/\partial t + \underline{v}\cdot\nabla_r$ and $\underline{V}_i$, $\underline{P}$ and $\underline{q}$ are the diffusion velocity vector of species i , the pressure tensor and the heat flux vector for the mixture respectively, defined by :-

$$n_i\underline{V}_i = \int\underline{C}_i f_i d^3c_i \tag{2.10}$$

$$\underline{P} = \sum_{i=1}^{\nu}\int m_i\underline{C}_i\underline{C}_i f_i d^3c_i \tag{2.11}$$

$$\underline{q} = \sum_{i=1}^{\nu}\int\frac{1}{2}m_i C_i^2\underline{C}_i f_i d^3c_i \tag{2.12}$$

Here, the fact that the collusion term $J(f_i f_j)$ automatically conserves molecules, momentum and energy, has been used.

2.1.1. THE EQUILIBRIUM SOLUTION

For a gas in equilibrium a solution to equation (2.6) is straightforward. Since the parameters of state for a gas do not change with position or time, the solution of the equation is not a function of $\underline{r}$ or t but only of $\underline{c}$. In this case the equilibrium solution for f_i , f_i^E , is obtained from the set of equations :-

$$\sum_{j=1}^{\nu}J(f_i^E f_j^E) = 0 \tag{2.13}$$

Examination of equations (2.13) show that a sufficient† condition for this equality is that :-

$$f_i^E\cdot f_j^E = f_i^E\cdot f_j^E \tag{2.14}$$

---

†It may also be shown that this a necessary condition [71] .

or,

$$\ln f_i^E + \ln f_j^E = \ln f_i^E + \ln f_j^E \qquad (2.15)$$

Thus $\ln f_i^E$ is conserved in a binary collision, it may therefore only be a function of quantities conserved in such a collision, the number density, momentum and mean kinetic energy, and thus the equilibrium solution for f_i^E reads :-

$$f_i^E = n_i \cdot \left(\frac{m_i}{2\pi kT}\right)^{3/2} \cdot \exp\left(-\frac{m_i C_i^2}{2kT}\right) \qquad (2.16)$$

2.2. THE CHAPMAN - ENSKOG SOLUTION

For a gas not in equilibrium, where the parameters of state maybe functions of position and time, no such simple solution of the Boltzmann equation is possible. However, Chapman and Enskog independently developed an iterative procedure whereby the solution for f_i in a non-uniform gas could be obtained to any desired order of accuracy. The starting point for the Chapman - Enskog solution is the recognition that in a non-equilibrium gas, the approach to equilibrium takes place via molecular collisions. Furthermore on a macroscopic time scale $>10^{-4}$ sec, the details of individual collisions are not important to the solution for f_i . Consequently, Chapman and Enskog sought a solution for f_i in which its explicit dependence on $\underline{r}$ and t was replaced by an implicit dependence through the dependence of n, $\underline{v}$ and T on these quantities. That is, it was supposed that if collisions occurred sufficiently rapidly compared to a macroscopic time scale the gas would be in 'local equilibrium' where $f(\underline{r},\underline{c}_i,t)$ is characteristic of the local value of $\underline{r}$, $\underline{c}$ and t over a small region of space. The approach to equilibrium is then obtained by the rate at which the local equilibrium relaxes to global equilibrium. The other postulate of the Chapman-Enskog method of solution is that the departures from local equilibrium can be characterised by a parameter ξ where $1/\xi$ measures the collision frequency in the gas mixture. With these assumptions they supposed that the non-equilibrium solution for f_i could be written as :-

$$f_i = f_i^{(0)} + \xi f_i^{(1)} + \xi^2 f_i^{(2)} + \ldots\ldots \qquad (2.17)$$

where it is anticipated that $f_i^{(0)}$ will be the local equilibrium solution corresponding to an infinite collision frequency. The use of the parameter ξ to alter the collision frequency in the gas requires modification of the collision term in the Boltzmann equation so that it now reads [71] :-

$$\mathcal{D} f_i = \frac{1}{\xi} \sum_{j=1}^{\nu} J(f_i f_j) \tag{2.18}$$

An expansion in powers of ξ is applied to the left hand side of the modified Boltzmann equation and the variables $n(\underline{r},t)$, $\underline{v}(\underline{r},t)$ and $u(\underline{r},t)$ are introduced in place of the explicit $\underline{r}$ and t dependencies. Then, the expansion of f_i, equation (2.17) is substituted into the modified Boltzmann equation and a series expansion in ξ is obtained on both sides. Since, the parameter ξ was arbitrary chosen, both sides of the resulting equation must be equal for all powers of ξ , so that coefficients of different powers of ξ can be equated to yield the following set of equations :-

for ξ^{-1}

$$\sum_{j=1}^{\nu} J(f_i^{(0)} f_j^{(0)}) = 0 \tag{2.19}$$

for ξ^{0}

$$\sum_{j=1}^{\nu} J(f_i^{(0)} f_j^{(1)}) + \sum_{j=1}^{\nu} J(f_i^{(1)} f_j^{(0)}) = \mathcal{D} f_i^{(0)} \tag{2.20}$$

where,

$$\mathcal{D} f_i^{(0)} = f_i^{(0)} \left\{ \frac{n}{n_i} \underline{C}_i \cdot \underline{d}_i + \left(\frac{m_i C_i^2}{2kT} - \frac{5}{2} \right) \underline{C}_i \cdot \nabla \ln T + \frac{m_i}{kT} \left(\underline{C}_i \underline{C}_i - \frac{1}{3} C_i^2 \underline{I} \right) : \nabla \underline{v} \right\} \tag{2.21}$$

and

$$\underline{d}_i = \nabla \left(\frac{n_i}{n} \right) + \left(\frac{n_i}{n} + \frac{\rho_i}{\rho} \right) \cdot \nabla \ln (nkT) \tag{2.22}$$

It will be noted that once the set of equations (2.19) is solved for $f_i^{(0)}$, equations (2.20) - (2.22) can be solved for $f_i^{(1)}$ which is the only unknown.

Corresponding macroscopic conservation equations for each order of approximation to f_i , can also be written by means of the process employed earlier to the full Boltzmann equation.

2.2.1. THE ZERO ORDER SOLUTION

The zeroth order solutions $f_i^{(0)}$ are obtained from equations (2.19) exactly as the equilibrium solution was obtained and

they read :-

$$f_i^{(0)} = n_i(\underline{r},t)\left(\frac{m_i}{2\pi kT(\underline{r},t)}\right)^{3/2}\exp\left(-\frac{m_i C_i^2}{2kT(\underline{r},t)}\right) \qquad (2.23)$$

$$i = 1,\ldots,\nu$$

where, $\underline{C}_i = \underline{c}_i - \underline{v}$

It is noted here, that the zeroth order solution (2.23) for f_i does indeed correspond to that for local equilibrium and that the approach to this state is via collisions since the collision term $J(f_i^{(0)} f_j^{(0)})$ is involved in its solution.

Using now, $f_i^{(0)}$ to evaluate the diffusion velocity vector of species i, $\underline{V}_i$, the pressure tensor $\underline{P}$ and the heat flux $\underline{q}$ via equations (2.10) - (2.12), one obtains :-

$$\underline{V}^{(0)} = 0 \qquad (2.24)$$

$$\underline{P}^{(0)} = p\,\underline{I} \quad \text{and} \quad p = nkT \qquad (2.25)$$

$$\underline{q}^{(0)} = 0 \qquad (2.26)$$

With these results the macroscopic conservation equations (2.7)-(2.9) read :-

$$\frac{1}{\rho_i}\frac{d\rho_i}{dt} = -\nabla\cdot\underline{v} \qquad i = 1,..,\nu \qquad (2.27)$$

$$\rho\frac{d\underline{v}}{dt} = -\nabla p = -\nabla nkT \qquad (2.28)$$

$$\frac{d}{dt}(\rho T^{-3/2}) = 0 \qquad (2.29)$$

These are the Euler's equations of hydrodynamics for a perfect gas.

2.2.2. THE FIRST ORDER SOLUTION

In order to derive the first order solution $f_i^{(1)}$ we define $f_i^{(1)} = f_i^{(0)}\,\phi_i^{(1)}$ and use this together with the zeroth order solution $f_i^{(0)}$ in equations (2.20) - (2.22). This substitution leads to the set of integral equations for $\phi_i^{(1)}$:-

$$\sum_{j=1}^{\nu} n_i n_j I_{ij}(\phi^{(1)}) = -f_i^{(0)}\left\{\frac{n}{n_i}\underline{C}_i\cdot\underline{d}_i + \left(\frac{m_i C_i^2}{2kT} - \frac{5}{2}\right)\underline{C}_i\cdot\nabla\ln T + \frac{m_i}{kT}\left(\underline{C}_i\underline{C}_i - \frac{1}{3}C_i^2\,\underline{I}\right):\nabla\underline{v}\right\} \qquad (2.30)$$

The integral operator I is defined as :-

$$I_{ij}(\phi^{(1)}) = \frac{1}{n_i n_j}\iiiint f_i^E f_j^E (\phi_i^{(1)} + \phi_j^{(1)} - \phi_i^{(1)} - \phi_j^{(1)}) g_{ij} \beta \, d\beta d\psi d^3 c_j \qquad (2.31)$$

The solution for $\phi_i^{(1)}$ is of the form :-

$$\phi_i^{(1)} = -\frac{1}{n}\sum_j \underline{D}_i^j \cdot \underline{d}_j - \frac{1}{n}\underline{A}_i \cdot \nabla \ln T - \frac{1}{n}\underline{B}_i : \nabla \underline{u} \qquad (2.32)$$

Here, the quantities $\underline{D}_i^j$ and $\underline{A}_i$ are vector functions of $\underline{C}_i$ and $\underline{B}_i$ is a traceless tensor function of $\underline{C}_i$ of the form :-

$$\underline{D}_i^j = D_i^j (C_i) \underline{C}_i \qquad (2.33)$$

$$\underline{A}_i = A_i (C_i) \underline{C}_i \qquad (2.34)$$

$$\underline{B}_i = B_i (C_i) (\underline{C}_i \underline{C}_i - \tfrac{1}{3} C_i^2 \underline{I}) \qquad (2.35)$$

By substituting the equation for $\phi_i^{(1)}$,(2.32), in equation (2.30) and comparing the coefficients of corresponding macroscopic gradients on both sides one obtains :-

$$\sum_j \frac{n_i n_j}{n^2} I_{ij}(\underline{D}_i^k) = \frac{1}{n_i} f_i^{(0)} (\delta_{ik} - \frac{\rho_i}{\rho}) \underline{C}_i \qquad i,k = 1,..,\nu \qquad (2.36)$$

$$\sum_j \frac{n_i n_j}{n^2} I_{ij}(\underline{A}_i) = \frac{1}{n} f_i^{(0)} (\frac{m_i C_i^2}{2kT} - \frac{5}{2}) \underline{C}_i \qquad i = 1,..,\nu \qquad (2.37)$$

$$\sum_j \frac{n_i n_j}{n^2} I_{ij}(\underline{B}_i) = \frac{m_i}{nkT} f_i^{(0)} (\underline{C}_i \underline{C}_i - \tfrac{1}{3} C_i^2 \underline{I}) \qquad i = 1,..,\nu \qquad (2.38)$$

where δ_{ik} is the Kronecker delta.

By multiplying the above equations by $\underline{D}^\ell$, $\underline{A}$ and $\underline{B}$ respectively, integrating over all velocities $\underline{c}_i$ and summing over all components i one obtains the following results :-

$$[\underline{D}^k, \underline{D}^\ell] = \frac{1}{n_k}\int f_k^{(0)} \cdot \underline{D}_k^\ell \cdot \underline{C}_k \, d^3 c_k - \frac{1}{\rho}\sum_i m_i \int f_i^{(0)} \cdot \underline{D}_i^\ell \cdot \underline{C}_i \, d^3 c_i \qquad (2.39)$$

$$[\underline{A}, \underline{A}] = \frac{1}{n}\sum_i \int f_i^{(0)} (\frac{m_i C_i^2}{2kT} - \frac{5}{2}) \underline{A} \cdot \underline{C}_i \, d^3 c_i \qquad (2.40)$$

$$[\underline{B}, \underline{B}] = \frac{1}{nkT}\sum_i m_i \int f_i^{(0)} (\underline{C}_i \underline{C}_i - \tfrac{1}{3} C_i^2 \underline{I}) : \underline{B} \, d^3 c_i \qquad (2.41)$$

Here, we have introduced the so-called 'bracket integral' which represent the integral :-

$$[F,G] = \frac{1}{4n^2}\sum_{ij}\iiiint f_i^E f_j^E (F_i + F_j - F_i' - F_j')(G_i + G_j - G_i' - G_j') g \beta \, d\beta d\psi d^3 c_i \, d^3 c_j \qquad (2.42)$$

For convenience it is useful to separate the bracket integral into two partial bracket integrals, one of the first kind $[F,G]'_{ij}$ and one of the second kind $[F,G]''_{ij}$ as :-

$$[F,G] = \sum_{ij} \frac{n_i n_j}{n^2} \left([F,G]'_{ij} + [F,G]''_{ij} \right) \tag{2.43}$$

These, are in turn defined as :-

$$[F,G]'_{ij} = \frac{1}{2n_i n_j} \iiiii f_i^E f_j^E (G_i - G_i')(F_i - F_i') g\beta d\beta d\Psi d^3c_i\, d^3c_j \tag{2.44}$$

and,

$$[F,G]''_{ij} = \frac{1}{2n_i n_j} \iiiii f_i^E f_j^E (G_i - G_i')(F_j - F_j') g\beta d\beta d\Psi d^3c_i\, d^3c_j \tag{2.45}$$

and obey the symmetry relations

$$[F,G]'_{ij} = [G,F]'_{ij} \qquad [F,G]''_{ij} = [G,F]''_{ji} \tag{2.46}$$

By defining ,

$$D_{ij} = \frac{1}{3n} [\underline{D}^i, \underline{D}^j] \tag{2.47}$$

and

$$D_{Ti} = \frac{1}{3n} [\underline{D}^i, \underline{A}] \tag{2.48}$$

and substituting the first order solution for $f_i^{(1)} = f_i^{(0)}(1+\xi\phi_i^{(1)})$ from equation (2.32), in the relation for the diffusion velocity $\underline{V}_i$ (2.10), the diffusion velocity for the molecules of species may be written as :-

$$\underline{V}_i = -\sum_j D_{ij}\, \underline{d}_j - D_{Ti} \nabla \ln T \tag{2.49}$$

The coefficients D_{ij} and D_{Ti} are thus identified with the multicomponent diffusion coefficients and the multicomponent thermal diffusion coefficients, respectively.

At this stage it is convenient to introduce the thermal diffusion ratio K_{Ti} as :-

$$\sum_j D_{ij}\, K_{Tj} = D_{Ti} \qquad i = 1, \ldots, \nu \tag{2.50}$$

with

$$\sum_i K_{Ti} = 0 \tag{2.51}$$

Using again the first order solution for $f_i^{(1)} = f_i^{(0)}(1+\xi\phi_i^{(1)})$ the expression for the heat flux vector $\underline{q}^{(1)}$, read :-

$$\underline{q}^{(1)} = -\frac{1}{3} k \left[\underline{A},\underline{A}\right] \nabla T - p \sum_i D_{Ti}\underline{d}_i + \frac{5}{2} k T \sum_i n_i \underline{V}_i \qquad (2.52)$$

The first term in this expression represents the heat flux due to the temperature gradient directly. However in a gas mixture a temperature gradient leads to a concentration gradient via thermal diffusion. The flux of heat associated with the maintenance of this partial separation is represented by the second term. The third term corresponds to the flux of enthalpy due to the diffusion of molecules in the coordinate system which moves with the hydrodynamic velocity $\underline{v}$. Equation (2.52) can be rewritten as :-

$$\underline{q}^{(1)} = -\lambda' \cdot \nabla T - p \sum_i D_{Ti}\,\underline{d}_i - \frac{5}{2} k T \sum_i n_i \underline{V}_i \qquad (2.53)$$

Here, λ' is the partial thermal conductivity of the gas mixture -which is the thermal conductivity which would be measured in a hypothetical experiment with no concentration gradient ($\underline{d}_i = \underline{0}$). In practice a diffusion driving force will always exist in the mixture and the total thermal conductivity of the gas mixture is defined by the equation :-

$$\underline{q}^{(1)} = -\lambda \nabla T + p \sum_i \left(K_{Ti} + \frac{5}{2}\frac{n_i}{n}\right) \underline{V}_i \qquad (2.54)$$

where

$$\lambda = \lambda' - n k \sum_i K_{Ti} D_{Ti} \qquad (2.55)$$

In terms of bracket integrals one may write using equations (2.48) and (2.53) :-

$$\lambda = \frac{1}{3} k \left[\underline{A},\underline{A}\right] - \frac{1}{3} k \sum_i K_{Ti}\left[\underline{D}^i,\underline{A}\right] \qquad (2.56)$$

with K_{Ti} given by the solution of the equations

$$\sum_j \left[\underline{D}^i,\underline{D}^j\right] K_{Tj} = \left[\underline{D}^j,\underline{A}\right] \qquad (2.57)$$

It can be seen therefore, that in order to obtain an expression for the thermal conductivity of a multicomponent gas mixture,

first one must evaluate the associated bracket integrals $[\underline{A},\underline{A}]$, $[\underline{D}^i,\underline{A}]$, $[\underline{D}^i,\underline{D}^j]$ and $[\underline{D}^j,\underline{A}]$.

Because in this thesis we are concerned with the thermal conductivity of gases, we omit the corresponding expressions for the viscosity of a multicomponent mixture [71].

2.2.3. EVALUATION OF THE MULTICOMPONENT THERMAL CONDUCTIVITY

In order to evaluate the bracket integrals which enter the expression for the multicomponent thermal conductivity it is necessary to seek a solution through successive approximations. For this purpose each of the coefficients $\underline{A}_i$ and $\underline{D}_i^k$ is expanded in an infinite series of polynomials called Sonine polynomials as :-

$$\underline{A}_i(\underline{C}) = A_i(C_i)\underline{C}_i = -\left(\frac{m_i}{2kT}\right)^{1/2} \sum_{p=0}^{\infty} a_{i,p} S_{3/2}^{(p)}(\mathfrak{C}_i^2)\underline{\mathfrak{C}}_i \qquad (2.58)$$

and

$$\underline{D}_i^k = D_i^k(C_i)\underline{C}_i = \left(\frac{m_i}{2kT}\right)^{1/2} \sum_{p=0}^{\infty} d_{i,p}^k S_{3/2}^{(p)}(\mathfrak{C}_i^2)\underline{\mathfrak{C}}_i \qquad (2.59)$$

where the dimensionless velocity variable $\underline{\mathfrak{C}}$ is given by :-

$$\underline{\mathfrak{C}}_i = \left(\frac{m_i}{2kT}\right)^{1/2} \underline{C}_i \qquad (2.60)$$

When the above equations are employed in equations (2.39) and (2.40) and the orthogonality properties of the Sonine polynomials are used together with the solution for $f_i^{(0)}$ one obtains two infinite sets of algebraic equations for the coefficients $a_{i,p}$ and $d_{i,p}^k$ of the Sonine polynomials of the forms :-

$$\sum_{j=1}^{\nu}\sum_{q=0}^{\infty} \Lambda_{ij}^{pq} a_{j,q} = \frac{4}{5k}\frac{n_i}{n}\delta_{p1} \qquad \begin{matrix} i=1,..,\nu \\ p=0,..,\infty \end{matrix} \qquad (2.61)$$

and

$$\sum_{j=1}^{\nu}\sum_{q=0}^{\infty} \Lambda_{ij}^{pq} d_{j,q}^k = \frac{8}{25k}\left(\delta_{ik} - \frac{\rho_i}{\rho}\right)\delta_{p,0} \qquad \begin{matrix} i=1,..,\nu \\ p=0,..,\infty \end{matrix} \qquad (2.62)$$

For $p=0$ both sets of equations (2.61) and (2.62) are linearly dependent and thus they must be supplemented by one more equation each, reading :-

$$\sum_i (\rho_i/\rho)\, a_{i,0} = 0 \qquad (2.63)$$

and

$$\sum_i (\rho_i/\rho)\, d_{i,0}^k = 0 \qquad (2.64)$$

In these equations (2.61) and (2.62) the coefficients Λ_{ij}^{pq} used are related to the partial bracket integrals as [71] :-

$$\Lambda_{ij}^{pq} = \frac{8 m_i^{1/2} m_j^{1/2}}{75 k^2 T}\left\{\delta_{ij}\sum_h \frac{n_i n_h}{n^2}\left[S_{3/2}^{(p)}(\mathcal{C}^2)\underline{\mathcal{C}}, S_{3/2}^{(q)}(\mathcal{C}^2)\underline{\mathcal{C}}\right]'_{ih} + \frac{n_i n_j}{n^2}\left[S_{3/2}^{(p)}(\mathcal{C}^2)\underline{\mathcal{C}}, S_{3/2}^{(q)}(\mathcal{C}^2)\underline{\mathcal{C}}\right]''_{ij}\right\} \tag{2.65}$$

From the symmetry properties (2.46) of the partial bracket integrals and from the principle of conservation of momentum one finds that :-

$$\Lambda_{ij}^{pq} = \Lambda_{ji}^{qp} \tag{2.66}$$

$$\sum_i \Lambda_{ij}^{p0} = 0 \qquad \sum_i \Lambda_{ij}^{0q} = 0 \tag{2.67}$$

Thus, if the bracket integrals are known, Λ_{ij}^{pq} can be calculated and used in equations (2.61) - (2.64) to obtain the coefficients $a_{j,q}$ and $d_{j,q}^k$, $\underline{A}_i(C)$ and $\underline{D}_i^k$ (2.58)-(2.59) and thus the thermal conductivity of a multicomponent mixture via equation (2.56).

In order to obtain approximate solution to these infinite sets of equations, Chapman and Cowling [137] suggested that the Sonine polynomial expressions should be truncated after a finite number of terms and the resulting finite set of equations solved for the appropriate values of the coefficients. The solution of this truncated set of equations are supposed to be approximations to the exact values of the coefficients [71] . Here the convention of Ferziger and Kaper [71] is adopted that the first-order approximation to a given transport coefficient is the first non-vanishing approximation. Consequently we retain in the Sonine polynomials expressions sufficient terms to ensure this. This convection differs from that of Muckenfuss and Curtis [121] who denoted a nth approximation as that for which n terms were retained in the Sonine polynomials expansion.

We denote a nth order approximation to any quantity by the symbol $_n$ which is to be distinguished from n which represents the number density.

Thus to summarize, a $_\eta$th order approximation to the thermal conductivity of a gas mixture is obtained from the equations:-

$$[\lambda]_n = [\lambda']_n - n k \sum_{i=1}^{\nu} [K_{Ti}]_n [D_{Ti}]_n \tag{2.68}$$

where,

$$[\lambda']_n = \frac{5}{4} k \sum_{i=1}^{\nu} \left(\frac{n_i}{n}\right) a_{i,1}^{(n)} \tag{2.69}$$

$$[D_{Ti}]_n = -\frac{1}{2n} a_{i,0}^{(n)} \tag{2.70}$$

and

$$\sum_{j=1}^{\nu} d_{j,0}^{i(n+1)} [K_{Tj}]_n = -\frac{5}{2} \sum_{j=1}^{\nu} \left(\frac{n_j}{n}\right) d_{j,1}^{i(n+1)} \qquad i = 1,..,\nu \tag{2.71}$$

with

$$\sum_{i=1}^{\nu} [K_{Ti}]_n = 0 \tag{2.72}$$

Here, the coefficients $a_{i,1}^{(n)}$, $a_{i,0}^{(n)}$, $d_{j,0}^{i(n)}$ and $d_{j,1}^{i(n)}$ can be obtained from the following sets of equations :-

$$\sum_{j=1}^{\nu} \sum_{q=0}^{n} \Lambda_{ij}^{pq} a_{j,p}^{(n)} = \frac{4}{5k} \left(\frac{n_i}{n}\right) \delta_{p1} \qquad \begin{matrix} i = 1,..,\nu \\ p = 0,..,n-1 \end{matrix} \tag{2.73}$$

with

$$\sum_{i=1}^{\nu} (\rho_i/\rho) a_{i,0}^{(n)} = 0 \qquad \text{for} \quad p=0 \tag{2.74}$$

and

$$\sum_{j=1}^{\nu} \sum_{q=0}^{n-1} \Lambda_{ij}^{pq} d_{j,q}^{k(n)} = \frac{8}{25k} \left(\delta_{ik} - \frac{\rho_i}{\rho}\right) \delta_{p0} \qquad \begin{matrix} i = 1,..,\nu \\ p = 0,..,n-1 \end{matrix} \tag{2.75}$$

with

$$\sum_{i=1}^{\nu} (\rho_i/\rho) d_{i,0}^{k(n)} = 0 \qquad \text{for} \quad p=0 \tag{2.76}$$

Equations (2.68) - (2.72) together with equations (2.73) - (2.76) provide a consistent scheme for calculating the thermal conductivity of a multicomponent mixture provided the bracket integrals and thus the coefficients Λ_{ij}^{pq} are known.

Muckenfuss and Curtis [121] have obtained an explicit solution to these equations for a first order approximation to the thermal conductivity of a multicomponent gas mixture. However the accuracy of the measurements described later in this thesis makes it necessary to obtain higher order approximations in order to secure sufficient accuracy in the theoretical expressions for a comparison with experimental results. Some of the partial bracket integrals involving Sonine polynomials necessary for the evaluation of the thermal conductivity have been evaluated by Ferziger and Kaper [171] . However, it has been necessary to derive further bracket integrals in order to make possible the evaluation of higher order approximations. In the next Section a brief description

of the method whereby the partial bracket integrals have been evaluated is given. Subsequently, the new results for higher order approximation to the thermal conductivity of a multicomponent mixture will be given in a form suitable for numerical evaluation.

2.2.4. EVALUATION OF THE BRACKET INTEGRALS

In this Section the method for the reduction of the partial bracket integrals of the previous section to combinations of the familiar collision integrals of Kinetic Theory will be presented. It can be shown [71] that the partial bracket integrals of the first and second kind can be evaluated from the following set of equations :-

$$\left[S_{3/2}^{(p)}(\mathcal{C}^2)\underline{\mathcal{C}}, S_{3/2}^{(q)}(\mathcal{C}^2)\underline{\mathcal{C}} \right]''_{ij} = 8\mu_j^{p+1/2}\mu_i^{q+1/2} \sum_{\ell,r=0}^{\infty} A_{pq\ell r}\, \Omega_{ij}^{(\ell,r)} \qquad (2.77)$$

and

$$\left[S_{3/2}^{(p)}(\mathcal{C}^2)\underline{\mathcal{C}}, S_{3/2}^{(q)}(\mathcal{C}^2)\underline{\mathcal{C}} \right]'_{ij} = 8 \sum_{\ell,r=0}^{\infty} A'_{pq\ell r}\, \Omega_{ij}^{(\ell,r)} \qquad (2.78)$$

where,

$$\Omega_{ij}^{(\ell,r)} = \left(\frac{kT(m_i+m_j)}{2\pi m_i m_j}\right)^{1/2} \int_0^{\infty} \exp(-g^2)\, g^{2r+3} \left\{ 2\pi \int_0^{\infty} (1-\cos^{\ell}\chi(\beta,g))\beta d\beta \right\} dg \qquad (2.79)$$

where the scattering angle $\chi(\beta,g)$, the collision parameter β and the relative velocity of the molecules g upon collision have been defined earlier (see Fig. 5 ,p.16).

The coefficients $A_{pq\ell r}$ themselves can be obtained from the following set of equations [71] :-

$$\pi^{-3/2}(\mu_i\mu_j)^{-1/2}(1-s)^{-5/2}(1-t)^{-5/2} H_{ij}(\chi) = \exp(-g^2) \sum_{pq\ell r=0}^{\infty} A_{pq\ell r}(\mu_j s)^p (\mu_i t)^q g^{2r} \cos^{\ell}\chi \qquad (2.80)$$

with

$$H_{ij}(\chi) = \pi^{3/2}(\mu_i\mu_j)^{1/2} \exp(-\gamma g^2)\, \alpha^{-5/2} \left\{ \frac{3}{2} + g^2(1-\gamma-\cos\chi) \right\} \qquad (2.81)$$

and

$$\alpha = 1 + \frac{\mu_i s}{1-s} + \frac{\mu_i t}{1-t} \qquad (2.82)$$

$$\gamma = \frac{1 - 2\mu_i\mu_j st(1-\cos\chi)}{1-\mu_j s - \mu_i t} \qquad (2.83)$$

and $\mu_i = m_i / (m_i + m_j)$

and a corresponding set of equations for $A'_{pq\ell r}$ [71].

The coefficients $A_{pq\ell r}$ could be derived from equations (2.80) -(2.83) by expansion of the left hand side in powers of s and t and equating coefficients of various powers on both sides. However it is slightly simpler, althoughstill very complicated, to adopt a different method. In this method expressions (2.80)-(2.83) were differentiated p times with respect to s and q times with respect to t and subsequently s and t are set equal to zero.Finally by equating coefficients of equal powers of $g^{2r}\cos^{\ell}\chi$ the required coefficients are obtained.

At this point we should examine the expressions for the thermal conductivity of a multicomponent monatomic gas mixture (2.68) to (2.76). As these produce the thermal conductivity in the form of successive approximations the 'correct' value will correspond to the infinite order approximation. For obvious reasons however, we can only have a finite order of approximation, the constraint being always the evaluation of the bracket integrals or equivalently the coefficients $A_{pq\ell r}$ and $A'_{pq\ell r}$ in the previous expressions. The highest order of approximation for which explicit expressions have so far been given are those for the first order. Not only are higher order approximations unavailable, but the rate of convergence of the successive approximations is unknown, so that , the accuracy of the first order formulae is not known. Because the new experimental results described in this thesis have an uncertainty of only $\pm 0.2\%$, it is essential to develop theoretical formulae which are at least that accurate.

Equations (2.68) - (2.76) show that for a third order of approximation to the thermal conductivity elements Λ_{ij}^{pq} need to be evaluated for $p,q=0,..,3$. According to the previous discussion the evaluation of both partial bracket integrals, to calculate the coefficients $A_{pq\ell r}$ and $A'_{pq\ell r}$ for $p,q = 0,1,2,3$, requires three successive differentiations with respect to s and three more times differentiation with respect to t. By inspection of the equations involved one may see that the final solution will be composed of about ten thousand terms ! Furthermore it is unfortunate that no real check of the answer as such exists except the requirement that when $i = j$ the sums of the partial bracket integrals reduces to these for a pure gas which have been calculated to third order [71] .

Table 1 .

The partial bracket integrals $\left[S^{(p)}_{3/2}(\mathcal{C}^2)\underline{\mathcal{C}}, S^{(q)}_{3/2}(\mathcal{C}^2)\underline{\mathcal{C}}\right]'_{ij}$ for p=3,q=0,1,2,3

	$\left[S^{(p)}_{3/2}(\mathcal{C}^2)\underline{\mathcal{C}}, S^{(q)}_{3/2}(\mathcal{C}^2)\underline{\mathcal{C}}\right]'_{ij}$
p=3,q=0	$8\mu_j^4\left\{ \frac{315}{48}\Omega_{ij}^{(1,1)} - \frac{189}{24}\Omega_{ij}^{(1,2)} + \frac{27}{12}\Omega_{ij}^{(1,3)} - \frac{1}{6}\Omega_{ij}^{(1,4)} \right\}$
p=3,q=1	$8\mu_j^3\left\{ (\frac{525}{32}\mu_j^2 + \frac{945}{16}\mu_i^2)\Omega_{ij}^{(1,1)} - (\frac{105}{4}\mu_j^2 + \frac{189}{4}\mu_i^2)\Omega_{ij}^{(1,2)} + (\frac{27}{2}\mu_j^2 + \frac{27}{4}\mu_i^2)\Omega_{ij}^{(1,3)} - \frac{8}{3}\mu_j^2\Omega_{ij}^{(1,4)} + \frac{1}{6}\mu_j^2\Omega_{ij}^{(1,5)} + \frac{63}{4}\mu_i\mu_j\Omega_{ij}^{(2,2)} - 9\mu_i\mu_j\Omega_{ij}^{(2,3)} + \mu_i\mu_j\Omega_{ij}^{(2,4)} \right\}$
p=3,q=2	$8\mu_j^2\left\{ (\frac{4725}{48}\mu_i^4 + \frac{39690}{192}\mu_i^2\mu_j^2 + \frac{11025}{384}\mu_j^4)\Omega_{ij}^{(1,1)} - (\frac{945}{24}\mu_i^4 + \frac{11907}{48}\mu_i^2\mu_j^2 + \frac{11025}{192}\mu_j^4)\Omega_{ij}^{(1,2)} + (\frac{4050}{48}\mu_i^2\mu_j^2 + \frac{1953}{48}\mu_j^4)\Omega_{ij}^{(1,3)} - (\frac{198}{24}\mu_i^2\mu_j^2 + \frac{301}{24}\mu_j^4)\Omega_{ij}^{(1,4)} + \frac{41}{24}\mu_j^4\Omega_{ij}^{(1,5)} - \frac{1}{12}\mu_j^4\Omega_{ij}^{(1,6)} + (\frac{1323}{24}\mu_i\mu_j^3 + 63\mu_i^3\mu_j)\Omega_{ij}^{(2,2)} - (\frac{567}{12}\mu_i\mu_j^3 + 18\mu_i^3\mu_j)\Omega_{ij}^{(2,3)} + \frac{150}{12}\mu_i\mu_j^3\Omega_{ij}^{(2,4)} - \mu_i\mu_j^3\Omega_{ij}^{(2,5)} + 9\mu_i^2\mu_j^2\Omega_{ij}^{(3,2)} - 2\mu_i^2\mu_j^2\Omega_{ij}^{(3,4)} \right\}$
p=3,q=3	$8\left\{ (\frac{535815}{1152}\mu_i^2\mu_j^5 + \frac{127575}{288}\mu_i^4\mu_j^3 + \frac{6615}{144}\mu_i^6\mu_j + \frac{99225}{2304}\mu_j^7)\Omega_{ij}^{(1,1)} - (\frac{25515}{72}\mu_i^4\mu_j^3 + \frac{107163}{144}\mu_i^2\mu_j^5 + \frac{119070}{1152}\mu_j^7)\Omega_{ij}^{(1,2)} + (\frac{52731}{576}\mu_j^7 + \frac{54675}{144}\mu_i^2\mu_j^5 + \frac{4455}{72}\mu_i^4\mu_j^3)\Omega_{ij}^{(1,3)} - (\frac{2673}{36}\mu_i^2\mu_j^5 + \frac{2709}{72}\mu_j^7)\Omega_{ij}^{(1,4)} + (\frac{351}{72}\mu_i^2\mu_j^5 + \frac{1107}{144}\mu_j^7)\Omega_{ij}^{(1,5)} - \frac{3}{4}\mu_j^7\Omega_{ij}^{(1,6)} + \frac{1}{36}\mu_j^7\Omega_{ij}^{(1,7)} + (\frac{567}{2}\mu_i^3\mu_j^4 + \frac{1701}{36}\mu_i^5\mu_j^2 + \frac{35721}{288}\mu_i\mu_j^6)\Omega_{ij}^{(2,2)} - (\frac{5103}{36}\mu_i\mu_j^6 + \frac{5832}{36}\mu_i^3\mu_j^4)\Omega_{ij}^{(2,3)} + (22\mu_i^3\mu_j^4 + \frac{225}{4}\mu_i\mu_j^6)\Omega_{ij}^{(2,4)} - 9\mu_i\mu_j^6\Omega_{ij}^{(2,5)} + \frac{1}{2}\mu_i\mu_j^6\Omega_{ij}^{(2,6)} + (15\mu_i^4\mu_j^3 + \frac{81}{2}\mu_i^2\mu_j^5)\Omega_{ij}^{(3,3)} - 18\mu_i^2\mu_j^5\Omega_{ij}^{(3,4)} + 2\mu_i^2\mu_j^5\Omega_{ij}^{(3,5)} + \frac{12}{9}\mu_i^3\mu_j^4\Omega_{ij}^{(4,4)} \right\}$

Table 2 .

The partial bracket integrals $\left[S^{(p)}_{3/2}(\mathcal{C}^2)\underline{e}, S^{(q)}_{3/2}(\mathcal{C}^2)\underline{e}\right]''_{ij}$ for p=3,q=0,1,2,3

	$\left[S^{(p)}_{3/2}(\mathcal{C}^2)\underline{e}, S^{(q)}_{3/2}(\mathcal{C}^2)\underline{e}\right]''_{ij}$
p=3,q=0	$-8\mu_i^{1/2}\mu_j^{7/2}\left\{ \frac{315}{48}\Omega^{(1,1)}_{ij} - \frac{189}{24}\Omega^{(1,2)}_{ij} + \frac{27}{12}\Omega^{(1,3)}_{ij} - \frac{1}{6}\Omega^{(1,4)}_{ij}\right\}$
p=3,q=1	$-8\mu_i^{3/2}\mu_j^{7/2}\left\{ \frac{7245}{96}\Omega^{(1,1)}_{ij} - \frac{441}{6}\Omega^{(1,2)}_{ij} + \frac{81}{4}\Omega^{(1,3)}_{ij} - \frac{8}{3}\Omega^{(1,4)}_{ij} + \frac{1}{6}\Omega^{(1,5)}_{ij} - \frac{189}{12}\Omega^{(2,2)}_{ij} + 9\Omega^{(2,3)}_{ij} - \Omega^{(2,4)}_{ij}\right\}$
p=3,q=2	$-8\mu_i^{5/2}\mu_j^{7/2}\left\{ \frac{128205}{384}\Omega^{(1,1)}_{ij} - \frac{66213}{192}\Omega^{(1,2)}_{ij} + \frac{6003}{48}\Omega^{(1,3)}_{ij} - \frac{499}{24}\Omega^{(1,4)}_{ij} + \frac{41}{24}\Omega^{(1,5)}_{ij} - \frac{1}{12}\Omega^{(1,6)}_{ij} - \frac{2835}{24}\Omega^{(2,2)}_{ij} + \frac{783}{12}\Omega^{(2,3)}_{ij} - \frac{150}{12}\Omega^{(2,4)}_{ij} + \Omega^{(2,5)}_{ij} + 9\Omega^{(3,3)}_{ij} - 2\Omega^{(3,4)}_{ij}\right\}$
p=3,q=3	$-8\mu_i^{7/2}\mu_j^{7/2}\left\{ \frac{2297295}{2304}\Omega^{(1,1)}_{ij} - \frac{76923}{64}\Omega^{(1,2)}_{ij} + \frac{34119}{64}\Omega^{(1,3)}_{ij} - \frac{895}{8}\Omega^{(1,4)}_{ij} + \frac{201}{16}\Omega^{(1,5)}_{ij} - \frac{3}{4}\Omega^{(1,6)}_{ij} + \frac{1}{36}\Omega^{(1,7)}_{ij} - \frac{14553}{32}\Omega^{(2,2)}_{ij} + \frac{1215}{4}\Omega^{(2,3)}_{ij} - \frac{313}{4}\Omega^{(2,4)}_{ij} + 9\Omega^{(2,5)}_{ij} - \frac{1}{2}\Omega^{(2,6)}_{ij} + \frac{111}{2}\Omega^{(3,3)}_{ij} - 18\Omega^{(3,4)}_{ij} + 2\Omega^{(3,5)}_{ij} - \frac{12}{9}\Omega^{(4,4)}_{ij}\right\}$

Nevertheless the differentiation has been carried out and fortunately many terms cancel so that the sixth differentiation involves only nine hundred terms. The differentiations were repeated twice so that the results obtained could be confirmed. The results satisfied the symmetry requirements for the equations (2.66) and (2.67).

In Tables 1 and 2, only the extra expressions for $p=3$, $q=0,1,2,3$ are given since the lower order bracket integrals have been derived by Ferziger and Kaper [71]. For reasons of convenience we have retained their nomenclature.

In the following section we use these results to obtain expressions for the second and third approximations to the thermal conductivity of a multicomponent monatomic gas mixture.

2.3. EXPLICIT FORMULAE FOR THE MULTICOMPONENT THERMAL CONDUCTIVITY

2.3.1. FIRST ORDER APPROXIMATION

A first order approximation can be obtained by putting $n=1$ in equations (2.72) - (2.76), and solving for the coefficients $a_{ij}^{(1)}$ and $d_{iq}^{(1)}$ explicitly. Consequently the thermal conductivity of a ν-component monatomic gas mixture may be written to first order as a ratio of determinents reading :-

$$[\lambda]_1 = - \frac{\begin{vmatrix} L_{11}^{11} & \cdots & L_{1\nu}^{11} & x_1 \\ \vdots & & \vdots & \vdots \\ L_{\nu 1}^{11} & \cdots & L_{\nu\nu}^{11} & x_\nu \\ x_1 & \cdots & x_\nu & 0 \end{vmatrix}}{\begin{vmatrix} L_{11}^{11} & \cdots & L_{1\nu}^{11} \\ \vdots & & \vdots \\ L_{\nu 1}^{11} & \cdots & L_{\nu\nu}^{11} \end{vmatrix}} \qquad (2.84)$$

where x_i is the mole fraction of component i in the mixture and the elements L_{ij}^{11} are listed in Table 3, p.36-38.

Equation (2.84) for a pure gas reduces to :-

$$[\lambda]_1 = \frac{75}{64} \left(\frac{k^3 T}{m \pi}\right)^{1/2} \frac{1}{\sigma^2 \Omega^{(2,2)*}} \qquad (2.85)$$

A similar equation for the viscosity of the pure gas to a first order approximation [71] reads :-

$$[\eta]_1 = \frac{5}{16}\left(\frac{mkT}{\pi}\right)^{1/2}\frac{1}{\sigma^2\,\Omega^{(2,2)*}} \tag{2.86}$$

In relation to binary mixtures, it is also convenient to define the so-called 'interaction' thermal conductivity and viscosity as :-

$$[\lambda_{ij}]_1 = \frac{75}{64}\left(\frac{k^3T(m_i+m_j)}{2m_im_j\pi}\right)^{1/2}\frac{1}{\sigma_{ij}^2\;\Omega_{ij}^{(2,2)*}} \tag{2.87}$$

$$[\eta_{ij}]_1 = \frac{5}{16}\left(\frac{2m_im_jkT}{(m_i+m_j)\pi}\right)^{1/2}\frac{1}{\sigma_{ij}^2\;\Omega_{ij}^{(2,2)*}} \tag{2.88}$$

These, correspond to the thermal conductivity and viscosity of a hypothetical gas of molecules with a mass equal to twice the reduced mass of the two species in the mixture whose intermolecular potential is $U_{ij}(r)$.

In the case of $i=j$ equations (2.87) - (2.88) reduce to the ones for pure gases (2.85) - (2.86).

2.3.2. n^{th} ORDER APPROXIMATION

We will now procceed to give explicit formulae to a n^{th} order approximation for the individual contributions to the thermal conductivity. Thus solution of (2.68) - (2.76) in a determinent form produces the following results :-

$$[\lambda']_n = -\frac{\begin{vmatrix} L^{00} & L^{01} & L^{02} & \cdots & L^{0n} & 0 \\ L^{10} & L^{11} & L^{12} & \cdots & L^{1n} & X \\ L^{20} & L^{21} & L^{22} & \cdots & L^{2n} & 0 \\ \vdots & \vdots & \vdots & & \vdots & \vdots \\ L^{n0} & L^{n1} & L^{n2} & \cdots & L^{nn} & 0 \\ 0 & X & 0 & \cdots & 0 & 0 \end{vmatrix}}{D} \tag{2.89}$$

where,

$$D = \begin{vmatrix} L^{00} & L^{01} & L^{02} & \cdots & L^{0n} \\ L^{10} & L^{11} & L^{12} & \cdots & L^{1n} \\ \vdots & \vdots & \vdots & & \vdots \\ L^{n0} & L^{n1} & L^{n2} & \cdots & L^{nn} \end{vmatrix} \tag{2.90}$$

In these determinents L^{pq} represent the array :-

$$L^{pq} = \begin{matrix} L_{11}^{pq} \cdots L_{1\nu}^{pq} \\ \vdots \qquad \vdots \\ L_{\nu 1}^{pq} \cdots L_{\nu\nu}^{pq} \end{matrix} \tag{2.91}$$

In addition X represents the array $X = x_1\ x_2 \ldots\ x_\nu$ of the mole fractions. The symbol 0 represents a horizontal or vertical array of ν zeros.

The multicomponent diffusion coefficients $[D_{Ti}]_n$ can be obtained by solving equations (2.73) and (2.74) for $a_{i,0}^{(1)}$ and thus via equation (2.70) to be :-

$$[D_{Ti}]_n = \frac{2}{5kn} \frac{\begin{vmatrix} L^{00} & L^{01} & L^{02} \cdots & L^{0n} & 0 \\ L^{10} & L^{11} & L^{12} \cdots & L^{1n} & X \\ L^{20} & L^{21} & L^{22} \cdots & L^{2n} & 0 \\ \vdots & \vdots & \vdots & \vdots & \vdots \\ L^{n0} & L^{n1} & L^{n2} \cdots & L^{nn} & 0 \\ \delta_i & 0 & 0 \cdots & 0 & 0 \end{vmatrix}}{D} \tag{2.92}$$

where δ_i denotes the horizontal array of Kronecker's delta

$$\delta_i = \delta_{i1}\ \delta_{i2}\ \delta_{i3} \cdots \delta_{i\nu} \tag{2.93}$$

Finally, by solving equations (2.75) and (2.76) for the coefficients $d_{j,0}^{i(n+1)}$ and $d_{j,1}^{i(n+1)}$ one obtains via equations (2.71) and (2.72) the multicomponent diffusion ratios as :-

$$[K_{Ti}]_n = -\frac{\begin{vmatrix} D_{11}^{(n+1)} & D_{12}^{(n+1)} \cdots D_{1\nu}^{(n+1)} & S_1^{(n+1)} \\ D_{21}^{(n+1)} & D_{22}^{(n+1)} \cdots D_{2\nu}^{(n+1)} & S_2^{(n+1)} \\ \vdots & \vdots & \vdots \\ D_{\nu 1}^{(n+1)} & D_{\nu 2}^{(n+1)} \cdots D_{\nu\nu}^{(n+1)} & S_\nu^{(n+1)} \\ \delta_{i1} & \delta_{i2} \cdots \delta_{i\nu} & 0 \end{vmatrix}}{\begin{vmatrix} D_{11}^{(n+1)} & D_{12}^{(n+1)} \cdots D_{1\nu}^{(n+1)} \\ D_{21}^{(n+1)} & D_{22}^{(n+1)} \cdots D_{2\nu}^{(n+1)} \\ \vdots & \vdots \\ D_{\nu 1}^{(n+1)} & D_{\nu 2}^{(n+1)} \cdots D_{\nu\nu}^{(n+1)} \end{vmatrix}} \tag{2.94}$$

The elements $D_{k\ell}^{(n+1)}$ are defined by the following relations :-

$$D_{kk}^{(n+1)} = 0 \qquad \text{for} \quad k=1,2,\ldots,\nu \tag{2.95}$$

$$D_{k\ell}^{(n+1)} = d_{\ell 0}^{k(n+1)} - d_{\ell 0}^{k(n+1)} \quad \text{for} \quad k\neq\ell \quad \text{and} \quad k,\ell=1,2,\ldots,\nu \tag{2.96}$$

The quantities $d_{k0}^{k(n+1)}$ are given in turn, by the equations :-

$$d_{k0}^{k(n+1)} = -\frac{8}{25k}\frac{\begin{vmatrix} L^{00} & L^{01} & L^{02} & \cdots & L^{0n} & \Delta_k \\ L^{10} & L^{11} & L^{12} & \cdots & L^{1n} & 0 \\ L^{20} & L^{21} & L^{22} & \cdots & L^{2n} & 0 \\ \vdots & \vdots & \vdots & & \vdots & \vdots \\ L^{n0} & L^{n1} & L^{n2} & \cdots & L^{nn} & 0 \\ \delta_k & 0 & 0 & \cdots & 0 & 0 \end{vmatrix}}{D} \tag{2.97}$$

$$k=1,2,\ldots,\nu$$

with Δ_k defined as a vertical array of ν elements as :-

$$\Delta_k = \left(\delta_{1k} - \frac{\rho_1}{\rho}\right)\left(\delta_{2k} - \frac{\rho_2}{\rho}\right) \cdots\cdots \left(\delta_{\nu k} - \frac{\rho_\nu}{\rho}\right) \quad k=1,2,\ldots,\nu \tag{2.98}$$

Furthermore D is defined by (2.90) and δ_k by (2.94).

Finally the elements $S_j^{(n+1)}$ of equation (2.90) are defined as:-

$$S_j^{(n+1)} = \frac{4}{5k}\frac{\begin{vmatrix} L^{00} & L^{01} & L^{02} & \cdots & L^{0n} & \Delta_j \\ L^{10} & L^{11} & L^{12} & \cdots & L^{1n} & 0 \\ L^{20} & L^{21} & L^{22} & \cdots & L^{2n} & 0 \\ \vdots & \vdots & \vdots & & \vdots & \vdots \\ L^{n0} & L^{n1} & L^{n2} & \cdots & L^{nn} & 0 \\ 0 & X & 0 & \cdots & 0 & 0 \end{vmatrix}}{D} \tag{2.99}$$

Equations (2.89) - (2.99) provide the first explicit consistent calculation scheme for the thermal conductivity of a dilute multi-component gas mixture of monatomic components for any order of approximation, provided the elements L_{ij}^{pq} are known.

The elements L_{ij}^{pq} can be defined in terms of the earlier

Table 3 .

Elements L_{ij}^{pq} & L_{ij}^{pq} .

$$L_{ij}^{00} = -\frac{x_i x_j}{2A_{ij}^{*}[\lambda_{ij}]_1} - \sum \frac{x_i x_k M_j}{2A_{ik}^{*}[\lambda_{ik}]_1 M_i}$$

$$L_{ij}^{01} = \frac{x_i x_j}{4A_{ij}^{*}[\lambda_{ij}]_1 (M_i+M_j)} \left\{ 6C_{ij}^{*} - 5 \right\}$$

$$L_{ij}^{02} = -\frac{x_i x_j M_i^2}{4A_{ij}^{*}[\lambda_{ij}]_1 (M_i+M_j)^2} \left\{ \frac{35}{4} - 3B_{ij}^{*} - 6C_{ij}^{*} \right\}$$

$$L_{ij}^{03} = -\frac{x_i x_j M_i^3}{2A_{ij}^{*}[\lambda_{ij}]_1 (M_i+M_j)^3} \left\{ \frac{315}{48} + \frac{81}{8} C_{ij}^{*} - \frac{27}{4} B_{ij}^{*} - 10G_{ij}^{*} \right\}$$

$$L_{ij}^{11} = -\frac{x_i x_j M_i M_j}{2A_{ij}^{*}[\lambda_{ij}]_1 (M_i+M_j)^2} \left\{ \frac{55}{4} - 3B_{ij}^{*} - 4A_{ij}^{*} \right\}$$

$$L_{ij}^{12} = -\frac{x_i x_j M_i^2 M_j}{2A_{ij}^{*}[\lambda_{ij}]_1 (M_i+M_j)^3} \left\{ \frac{595}{16} + \frac{3}{8} C_{ij}^{*} - \frac{57}{4} B_{ij}^{*} - 30G_{ij}^{*} - 2(7-8E_{ij}^{*}) A_{ij}^{*} \right\}$$

$$L_{ij}^{13} = -\frac{x_i x_j M_i^3 M_j}{2A_{ij}^{*}[\lambda_{ij}]_1 (M_i+M_j)^4} \left\{ \frac{2415}{32} + \frac{333}{4} C_{ij}^{*} - \frac{243}{4} B_{ij}^{*} - 160G_{ij}^{*} + 60I_{ij}^{*} - (\frac{63}{2} - 72E_{ij}^{*} + 40H_{ij}^{*}) A_{ij}^{*} \right\}$$

$$L_{ij}^{22} = -\frac{x_i x_j M_i^2 M_j^2}{2A_{ij}^{*}[\lambda_{ij}]_1 (M_i+M_j)^4} \left\{ \frac{8505}{64} + \frac{558}{4} C_{ij}^{*} - \frac{723}{8} B_{ij}^{*} - 210G_{ij}^{*} + 90I_{ij}^{*} + 24F_{ij}^{*} - (77 - 112E_{ij}^{*} + 80H_{ij}^{*}) A_{ij}^{*} \right\}$$

$$L_{ij}^{23} = \frac{x_i x_j M_i^3 M_j^2}{2A_{ij}^{*}[\lambda_{ij}]_1 (M_i+M_j)^5} \left\{ \frac{42735}{128} + \frac{53847}{64} C_{ij}^{*} - \frac{6003}{16} B_{ij}^{*} + 108F_{ij}^{*} - 120Q_{ij}^{*} - \frac{2495}{2} G_{ij}^{*} + 615I_{ij}^{*} - 210K_{ij}^{*} - (\frac{945}{4} - 522E_{ij}^{*} + 500H_{ij}^{*} - 240J_{ij}^{*}) A_{ij}^{*} \right\}$$

$$L_{ij}^{33} = -\frac{x_i x_j M_i^3 M_j^3}{2A_{ij}^{*}[\lambda_{ij}]_1 (M_i+M_j)^6} \left\{ \frac{255255}{256} + \frac{35127}{8} C_{ij}^{*} - \frac{102357}{64} B_{ij}^{*} - \frac{123425}{2} G_{ij}^{*} + \frac{9045}{2} I_{ij}^{*} - 1890K_{ij}^{*} + 666F_{ij}^{*} - 1080Q_{ij}^{*} + 490V_{ij}^{*} + 720W_{ij}^{*} - (\frac{14553}{16} - 2430E_{ij}^{*} + 3130H_{ij}^{*} - 2160J_{ij}^{*} - 64U_{ij}^{*}) A_{ij}^{*} \right\}$$

$$L_{ii}^{00} = 0.0$$

$$L_{ii}^{01} = \sum \frac{x_i x_k}{4A_{ik}^{*}[\lambda_{ik}]_1} \frac{M_k}{(M_i+M_k)} \left\{5-6C_{ik}^{*}\right\}$$

$$L_{ii}^{02} = \sum \frac{x_i x_k}{4A_{ik}^{*}[\lambda_{ik}]_1} \frac{M_k^2}{(M_i+M_k)^2} \left\{\frac{35}{4}-3B_{ik}^{*}-6C_{ik}^{*}\right\}$$

$$L_{ii}^{03} = \sum \frac{x_i x_k}{2A_{ik}^{*}[\lambda_{ik}]_1} \frac{M_k^3}{(M_i+M_k)^3} \left\{\frac{315}{48}+\frac{81}{8}C_{ik}^{*}-\frac{27}{4}B_{ik}^{*}-10G_{ik}^{*}\right\}$$

$$L_{ii}^{11} = \sum \frac{x_i x_k}{2A_{ik}^{*}[\lambda_{ik}]_1 (M_i+M_k)^2} \left\{\frac{15}{2}M_i^2+\frac{25}{4}M_k^2-3M_k^2B_{ik}^{*}+4M_iM_kA_{ik}^{*}\right\} + \frac{x_i^2}{[\lambda_i]_1}$$

$$L_{ii}^{12} = \sum \frac{x_i x_k}{2A_{ik}^{*}[\lambda_{ik}]_1} \frac{M_k}{(M_i+M_k)^3} \left\{M_i^2\left(\frac{105}{4}-\frac{63}{2}C_{ik}^{*}\right)+M_k^2\left(\frac{175}{16}+\frac{255}{8}C_{ik}^{*}-\frac{57}{4}B_{ik}^{*}-30G_{ik}^{*}\right)+2M_iM_k(7-8E_{ik}^{*})A_{ik}^{*}\right\} + \frac{x_i^2(7-8E_{ii}^{*})}{4[\lambda_i]_1}$$

$$L_{ii}^{13} = \sum \frac{x_i x_k}{2A_{ik}^{*}[\lambda_{ik}]_1} \frac{M_k^2}{(M_i+M_k)^4} \left\{M_k^2\left(\frac{525}{32}+\frac{495}{4}C_{ik}^{*}-\frac{81}{2}B_{ik}^{*}-150G_{ik}^{*}+60I_{ik}^{*}\right)+M_i^2\left(\frac{945}{16}+\frac{243}{4}C_{ik}^{*}-\frac{81}{2}B_{ik}^{*}\right)+M_iM_k\left(\frac{63}{2}-72E_{ik}^{*}+40H_{ik}^{*}\right)A_{ik}^{*}\right\} + \frac{x_i^2}{4[\lambda_i]_1}\left(\frac{63}{8}-18E_{ii}^{*}+10H_{ii}^{*}\right)$$

$$L_{ii}^{22} = \sum \frac{x_i x_k}{2A_{ik}^{*}[\lambda_{ik}]_1} \frac{}{(M_i+M_k)^4} \left\{M_i^4\frac{175}{8}+M_k^2\left(\frac{1225}{64}+\frac{315}{2}C_{ik}^{*}-\frac{399}{8}B_{ik}^{*}-210G_{ik}^{*}+90I_{ik}^{*}\right)+M_i^2M_k^2\left(\frac{735}{8}-18C_{ik}^{*}-\frac{81}{2}B_{ik}^{*}+24F_{ik}^{*}\right)+28M_i^3M_kA_{ik}^{*}+M_iM_k^3(49-112E_{ik}^{*}+80H_{ik}^{*})A_{ik}^{*}\right\} + \frac{x_i^2}{[\lambda_i]_1}\left(\frac{77}{16}-7E_{ii}^{*}+5H_{ii}^{*}\right)$$

$$L_{ii}^{23} = \sum \frac{x_i x_k}{2A_{ik}^{*}[\lambda_{ik}]_1} \frac{M_k}{(M_i+M_k)^5} \left\{M_i^4\left(\frac{1575}{16}-\frac{945}{8}C_{ik}^{*}\right)+M_k^4\left(\frac{675}{128}+\frac{28035}{64}C_{ik}^{*}-\frac{1953}{16}B_{ik}^{*}-\frac{1505}{2}G_{ik}^{*}+615I_{ik}^{*}-210K_{ik}^{*}\right)+M_i^2M_k^2\left(\frac{6615}{32}+\frac{8343}{16}C_{ik}^{*}-\frac{2025}{8}B_{ik}^{*}-495G_{ik}^{*}+108F_{ik}^{*}-120Q_{ik}^{*}\right)+M_iM_k^3\left(\frac{441}{4}-370E_{ik}^{*}+500H_{ik}^{*}-240J_{ik}^{*}\right)A_{ik}^{*}+M_i^3M_k(126-144E_{ik}^{*})A_{ik}^{*}\right\} + \frac{x}{4[\lambda_i]_1}\left(\frac{945}{32}-\frac{261}{4}E_{ii}^{*}+\frac{125}{2}H_{ii}^{*}-30J_{ii}^{*}\right)$$

$$L_{ii}^{33} = \sum \frac{x_i x_k}{2A_{ik}^{*}[\lambda_{ik}]_1} \frac{}{(M_i+M_k)^6} \left\{M_k^6\left(\frac{99225}{2304}+\frac{25515}{24}C_{ik}^{*}-\frac{52731}{32}B_{ik}^{*}-\frac{4515}{2}G_{ik}^{*}+\frac{5535}{2}I_{ik}^{*}-1890K_{ik}^{*}+560V_{ik}^{*}\right)+M_i^6\frac{6615}{144}+M_i^2M_k^4\left(\frac{178605}{384}+\frac{13851}{4}C_{ik}^{*}-\frac{18225}{16}B_{ik}^{*}-4455G_{ik}^{*}+1755I_{ik}^{*}+486F_{ik}^{*}-1080Q_{ik}^{*}+720W_{ik}^{*}\right)+M_i^4M_k^2\left(\frac{14175}{32}-135C_{ik}^{*}-\frac{1485}{8}B_{ik}^{*}+180F_{ik}^{*}\right)+M_i^3M_k^3(567-1296E_{ik}^{*}+880H_{ik}^{*}+64U_{ik}^{*})A_{ik}^{*}+\frac{189}{2}M_i^5M_k+M_iM_k^5\left(\frac{3969}{16}-1134E_{ik}^{*}+2250H_{ik}^{*}-2160J_{ik}^{*}+840S_{ik}^{*}\right)A_{ik}^{*}+180M_i^4M_k^2F_{ik}^{*}\right\} + \frac{x_i^2}{4[\lambda_i]_1}\left(\frac{14553}{256}-\frac{1215}{8}E_{ii}^{*}+\frac{1565}{8}H_{ii}^{*}-135J_{ii}^{*}+\frac{105}{2}S_{ii}^{*}+4U_{ii}^{*}\right)$$

The following definitions of collision integral ratios have been employed in the elements L_{ii}^{pq} and L_{ij}^{pq} :-

$$A_{ij}^{*} = \Omega_{ij}^{(2,2)*}/\Omega_{ij}^{(1,1)*} \qquad B_{ij}^{*} = \left\{5\,\Omega_{ij}^{(1,2)*} - 4\,\Omega_{ij}^{(1,3)*}\right\}/\Omega_{ij}^{(1,1)*}$$

$$C_{ij}^{*} = \Omega_{ij}^{(1,2)*}/\Omega_{ij}^{(1,1)*} \qquad E_{ij}^{*} = \Omega_{ij}^{(2,3)*}/\Omega_{ij}^{(2,2)*}$$

$$F_{ij}^{*} = \Omega_{ij}^{(3,3)*}/\Omega_{ij}^{(1,1)*} \qquad G_{ij}^{*} = \Omega_{ij}^{(1,4)*}/\Omega_{ij}^{(1,1)*}$$

$$H_{ij}^{*} = \Omega_{ij}^{(2,4)*}/\Omega_{ij}^{(2,2)*} \qquad I_{ij}^{*} = \Omega_{ij}^{(1,5)*}/\Omega_{ij}^{(1,1)*}$$

$$J_{ij}^{*} = \Omega_{ij}^{(2,5)*}/\Omega_{ij}^{(2,2)*} \qquad K_{ij}^{*} = \Omega_{ij}^{(1,6)*}/\Omega_{ij}^{(1,1)*}$$

$$Q_{ij}^{*} = \Omega_{ij}^{(3,4)*}/\Omega_{ij}^{(1,1)*} \qquad S_{ij}^{*} = \Omega_{ij}^{(2,6)*}/\Omega_{ij}^{(2,2)*}$$

$$U_{ij}^{*} = \Omega_{ij}^{(4,4)*}/\Omega_{ij}^{(2,2)*} \qquad V_{ij}^{*} = \Omega_{ij}^{(1,7)*}/\Omega_{ij}^{(1,1)*}$$

$$W_{ij}^{*} = \Omega_{ij}^{(3,5)*}/\Omega_{ij}^{(1,1)*}$$

In addition, the following definitions for the first approximation to the thermal conductivity of pure gas i and the so-called interaction conductivity, have been employed :-

$$[\lambda_i]_1 = \frac{75}{64}\left\{\frac{N_A k^3 T}{\pi M_i}\right\}^{1/2}\frac{1}{\sigma_{ii}^2\Omega_{ii}^{(2,2)*}} \qquad [\lambda_{ij}]_1 = \frac{75}{64}\left\{\frac{N_A k^3 T(M_i+M_j)}{2\pi M_i M_j}\right\}^{1/2}\frac{1}{\sigma_{ij}^2\Omega_{ij}^{(2,2)*}}$$

Furthermore:-

$$\sum \longrightarrow \sum_{\substack{k=1 \\ k\neq i}}^{\nu}$$

introduced quantities Λ_{ij}^{pq} as :-

$$L_{ij}^{pq} = (1 - \delta_{ij}\delta_{p0}\delta_{q0})(\Lambda_{ij}^{pq} - \delta_{p0}\delta_{q0}\frac{m_i}{m_i}\frac{x_i}{x_i}\Lambda_{ii}^{00}) \qquad \begin{matrix} i,j = 1,2,\ldots,\nu \\ p,q = 0,1,\ldots,n \end{matrix} \qquad (2.100)$$

Thus, they themselves satisfy the symmetry relations :-

$$L_{ij}^{pq} = L_{ji}^{qp} \qquad \begin{matrix} p,q = 0,1,..,n \\ i,j = 1,2,..,\nu \end{matrix} \quad \text{except } p = q = 0,\ i \neq j \qquad (2.101)$$

and

$$\sum_{i=1}^{\nu} L_{ij}^{p0} = 0 \ , \quad \sum_{i=1}^{\nu} L_{ij}^{0q} = 0 \qquad \begin{matrix} p,q = 0,1,..,n \\ j = 1,2,..,\nu \end{matrix} \qquad (2.102)$$

The elements L_{ij}^{pq} are presented in Table 3 , p.36-38. These have been obtained from the elements Λ_{ij}^{pq} via equation (2.100) which in turn has been derived from the newly calculated partial bracket integrals. Sufficient elements are presented for a third order ($n=3$) calculation of the thermal conductivity of a multicomponent dilute monatomic gas mixture. Inaddition we have formulated in Table 3,p.36-38,the elements L_{ij}^{pq} in terms of the commonly employed reduced collision integrals $\Omega_{ij}^{(\ell,s)*}$ for the interaction of species i and j defined by Hirschfelder et al. [76] and Ferziger and Kaper [71] as :-

$$\Omega_{ij}^{(\ell,s)*} = \frac{\Omega_{ij}^{(\ell,s)}}{[\Omega_{ij}^{(\ell,s)}]_{r.s.}} = \Omega_{ij}^{(\ell,s)} \left(\frac{\pi m}{k T}\right)^{1/2} \frac{2}{(s+1)!}\left[1 - \frac{1 + (-1)^{\ell}}{2(\ell+1)}\right]^{-1} \frac{1}{\pi\sigma_{ij}^2} \qquad (2.103)$$

with $\qquad m_{ij}^{-1} = m_i^{-1} + m_j^{-1}$

and we have introduced a number of symbols for the commonly occuring combinations of reduced collision integrals. Thus expressions (2.89) - (2.99) together with Table 3 , provide a schemefor calculating the thermal conductivity to a third order approximation.

We then proceed to define a function $f_{mix}^{(n)}$ which relates the first order thermal conductivity of a mixture to the n^{th} order approximation by the equation :-

$$[\lambda]_n = [\lambda]_1 \cdot f_{mix}^{(n)} \qquad (2.104)$$

Due to the complexity of the equations used to derive the thermal conductivity of a mixture to a n^{th} order approximation we are unable to derive an explicit formulation for $f_{mix}^{(n)}$. Nevertheless, for specific systems, $f_{mix}^{(n)}$ can be calculated by computing the mixture

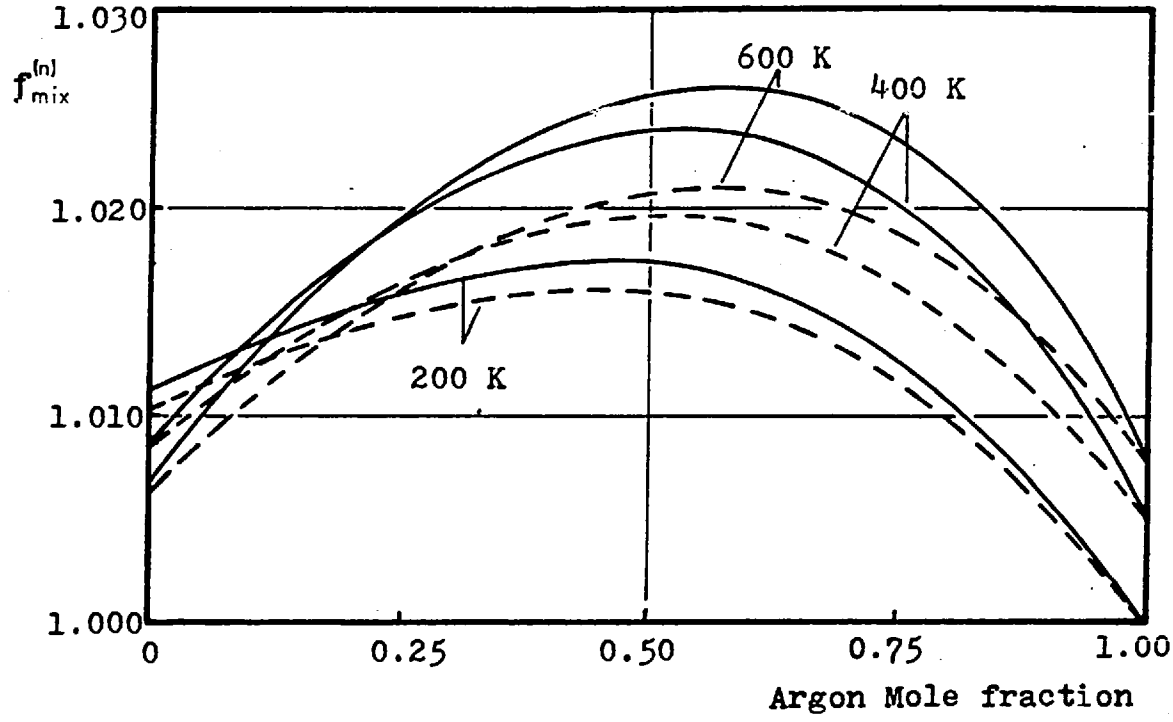

Figure 6 . Higher order correction factor for the thermal conductivity of mixture of Argon and Helium ——— $f_{mix}^{(3)}$, - - - - $f_{mix}^{(2)}$

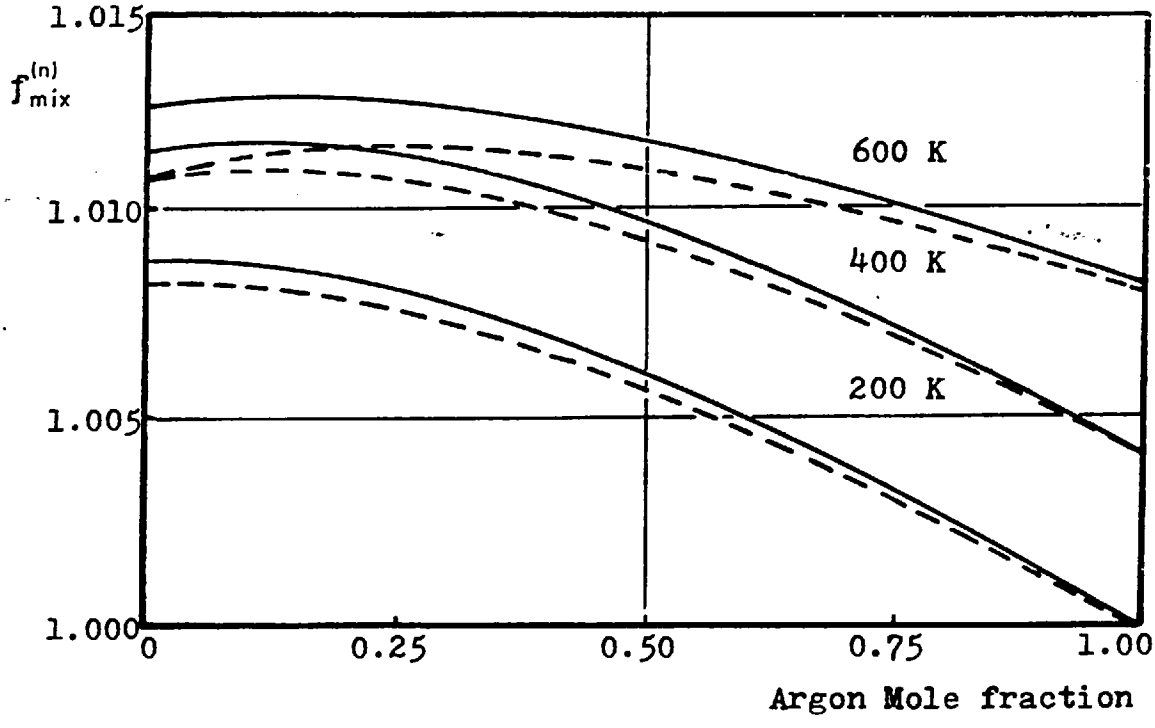

Figure 7 . Higher order correction factor for the thermal conductivity of mixture of Argon and Neon ——— $f_{mix}^{(3)}$, - - - - $f_{mix}^{(2)}$

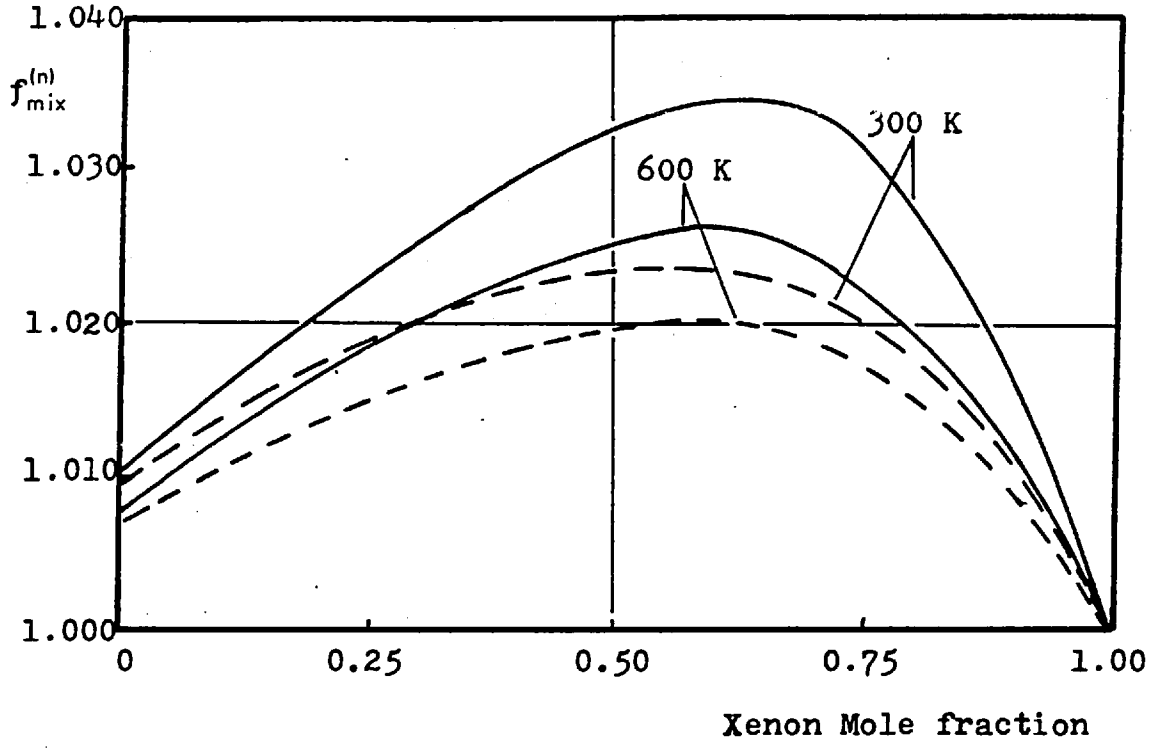

Figure 8 . Higher order correction factor for the thermal conductivity of mixture of Xenon and Helium ——— $f^{(3)}_{mix}$, ---- $f^{(2)}_{mix}$

thermal conductivity in the first, second and third order approximation according to equations (2.89) - (2.99). In order to illustrate the magnitude of the higher order approximations we have carried out such calculations for three binary mixtures of monatomic species.

We have chosen the binary systems Neon-Argon, Helium-Argon and Helium-Xenon, as they have approximate mass ratios of the constituent species of two, ten and thirtythree respectively and thus we cover a wide range of mass ratios . In order to compute the reduced collision integrals for the various pair interactions we have employed a Universal potential obtained from $\Omega^{(2,2)*}$ and $\Omega^{(1,1)*}$ determined from accurate viscosity and diffusion coefficient measurements [58,60] by an inversion procedure outlined by Smith and co-workers [122,123,124] . The thermal conductivity of the three binary mixtures to a first, second and third order of approximation was then computed and thus the functions $f^{(2)}_{mix}$ and $f^{(3)}_{mix}$

were calculated from equation (2.104) for different temperatures displayed in Figures 6 , 7 p.40 and 8 p.41 . From the three Figures it is clear that the magnitude of the correction factor for either order of approximation increases as the mass ratio of the two species is increased. In the extreme case of Xenon-Helium the second order correction factor $f_{mix}^{(2)}$ contributes as much as 2.6% to the mixture thermal conductivity whereas the third order correction factor $f_{mix}^{(3)}$ adds a further 0.7% in the worst case. A third order approximation is therefore essential for the description of accurate thermal conductivity data for mixtures of high mass ratios.

2.3.3. EUCKEN FACTOR - MONATOMIC GASES

To a third order approximation the Chapman-Enskog theory produces the following result for the Eucken factor of pure dilute monatomic gases :-

$$Eu = \frac{\lambda^\circ(T) \cdot M}{C_v^\circ \cdot \eta^\circ(T) \cdot F(T)} = 2.5 \text{ (exact)} \qquad (2.105)$$

where $\lambda^\circ(T)$ and $\eta^\circ(T)$ are the zero density thermal conductivity and viscosity of the pure gas , M the molecular weight and C_v° the molar heat capacity at constant volume. In this expression $F(T)$ accounts for the higher order corrections and is given by :-

$$F(T) = \frac{f_\lambda^{(3)}}{f_\eta^{(3)}} \qquad (2.106)$$

The factors $f_\lambda^{(3)}$ and $f_\eta^{(3)}$ for pure gases have been given by Ferziger and Kaper [71] in terms of the collision integrals $\Omega^{(\ell,s)*}$. The results presented here for the third order mixture thermal conductivity reduce identically to those for the pure gases when either $i=j$ or $x_i = 1$.

The Eucken relationship provides an important criterion for establishing the thermodynamic consistency of viscosity and thermal conductivity measurements for monatomic gases.

In the cases of gas mixtures there is no equivalent relationship between the mixture viscosity and thermal conductivity. However an analogous relationship does exist between the interaction viscosity and thermal conductivity (§2.3.1.p33) that reads:-

$$Eu = \frac{[\lambda_{ij}]_1 2\, m_i m_j}{(m_i+m_j)\, C_v^\circ [\eta_{ij}]_1} = 2.5 \text{ (exact)} \qquad (2.107)$$

2.4. DILUTE POLYATOMIC GASES

The Chapman-Enskog theory presented in the previous section is remarkably succesful in providing a derivation of the equations of fluid mechanics and in relating the transport properties of gases to the forces between molecules. It is unfortunate however, that the theory possesses important limitations that greatly reduce its usefulness. Most of these restrictions are actually inherent in the Boltzmann equation itself ; the most important one being that it is only applicable to monatomic molecules at low density.

Polyatomic gases possess two features that do not appear in the treatment of monatomic gases . Firstly they have internal degrees of freedom with which energy may be associated. Secondly, they may have various shapes and consequently, the molecular interaction is, in general, not spherically symetric. It is clear that for polyatomic molecules even at low density a new theory is required having as its starting point an equivalent Boltzmann equation generalised to account for the internal states of the molecules. Because the internal energy of a molecule are quantized a quantum mechanical treatment is strictly necessary. However this is very complicated and does not exist in a form suitable for calculations. Consequently almost all work on transport coefficients of polyatomic gases has been carried out with other, less rigorous theories. Fortunately, the numerical consequences of using these less rigorous theories are not large although the present measurements are sufficiently accurate that some account of quantum effects must be taken. A discussion of these effects is postponned until a later section (§2.4.4.p50).

2.4.1. WANG CHANG, DE BOER AND UHLENBECK

The most frequently employed theory is the quasi-classical approach of Wang Chang, de Boer and Uhlenbeck [77] . For a pure polyatomic gas the basic assumption of this theory is that the molecules may have only certain 'discrete' internal energy states, labelled with an index. Essentially, in a similar way to Boltzmann a local distribution function $f(\underline{c},i;\underline{r},t)$ is defined in such a way that $f(\underline{c},i)d^3c$ is the number density of molecules having velocity $\underline{c}$ in the element d^3c about $\underline{c}$ in the velocity space

and having an internal state specified by the set of quantum number i , while the variables $\underline{r}$ and t occur only as parameters . Each internal quantum state is treated as an independent chemical species, thus for a pure polyatomic gas, in parallel to the monatomic mixture , equations (2.1) - (2.3), the following equations can be written, for the number density n , the mean velocity $\underline{v}$ and the mean kinetic energy u as:-

$$n = \sum_i \int f(\underline{c},i)\, d^3c_i \tag{2.108}$$

$$\rho \underline{v} = \sum_i \int m_i \underline{c}_i f(\underline{c},i)\, d^3c_i \tag{2.109}$$

$$\rho u = \sum_i \int (\tfrac{1}{2}mC_i^2 + E_i)\, f(\underline{c},i)\, d^3c_i \tag{2.110}$$

where $\underline{C}_i$ is the peculiar velocity of a molecule defined as previously $\underline{C}_i = \underline{c}_i - \underline{v}$, and E_i is the energy associated with the internal state i .The derivation of the Boltzmann equation for these functions follows the derivation of the Boltzmann equation for a mixture very closely. The essential difference arises from the existence of inelastic collisions i.e., collisions in which the internal state of one or both molecules is changed. Thus generalised differential collision cross-sections are introduced $\sigma_{ij}^{k\ell}(g,\chi,\Psi)$ for scattering molecules in internal states i and j with relative velocity g , such that, after the encounter the molecules have internal states k and ℓ respectively. Furthermore the relative velocity (whose magnitude is no longer constant) is rotated through a polar angle χ and azimuthal angle Ψ (see Fig. 5 ,p.16) ; the cross section depending on Ψ as the molecules are no longer spherically symmetric.Following then a very similar analysis to that described for the monatomic case we obtain the corresponding Boltzmann equation for a polyatomic gas as :-

$$\mathcal{D} f_i = \sum_{jk\ell} J_{ij}^{k\ell}(ff) \tag{2.111}$$

with

$$J_{ij}^{k\ell} = \iint (f_k' f_\ell' - f_i f_j) g \sigma_{ij}^{k\ell}(g,\chi,\Psi) d^2\Omega d^3c_j \tag{2.112}$$

with $\mathcal{D}f_i$ still defined by (2.4).

This is known as the Wang Chang and Uhlenbeck equations and it was established in the 1940's independently by Wang Chang, de

Boer and Uhlenbeck.

Applying now, the same analysis as for the monatomic case, we again obtain as in (2.13) for the zeroth order $f_i^{(0)}$:-

$$\sum_{jk\ell} J_{ij}^{k\ell}(f^{(0)}f^{(0)}) = 0 \qquad (2.113)$$

and again as $\log f_i$ must be a summational invariant it can be derived by analogy with equation (2.23) that :-

$$f_i^{(0)} = n_i\left(\frac{m_i}{2\ kT}\right)^{3/2} \frac{\exp[-(m_i C_i^2/2kT) - (E_i/kT)]}{\sum_i \exp(-E_i/kT)} \qquad (2.114)$$

The only difference is due to the energy E_i associated with the internal energy in equation (2.110). The factor

$$Z_{INT} = \sum_i \exp(-E_i/kT) \qquad (2.115)$$

can be recognised as the statistical mechanical partition function for the internal degrees of freedom.

The analysis then procceeds in a similar way as before but is more complicated because the bracket integrals involved are now eightfold integrals as well as sums over all internal states. The final results for the thermal conductivity of a polyatomic gas mixture derived by Wang Chang and Uhlenbeck produce the thermal conductivity λ as a summation of a translational contribution λ_{tr} and an internal contribution λ_{int} as :-

$$\lambda = \lambda_{tr} + \lambda_{int} \qquad (2.116)$$

with

$$\lambda_{tr} = \frac{75k^2T}{8m\,a_{11}} \frac{1-(3/5)(a_{12}/a_{22})\,c_{v,int}/(3k/2m)}{1 - a_{12}^2/a_{11}a_{22}} \qquad (2.117)$$

$$\lambda_{int} = \frac{9\,k\,T}{4\,a_{22}} \frac{c_{v,int}^2}{3k/2m} \frac{1-(5/3)(a_{12}/a_{11})(3k/2m)/c_{v,int}}{1 - a_{12}^2/a_{11}\,a_{22}} \qquad (2.118)$$

where,

$$a_{11} = 4\left(\frac{kT}{m}\right)^{1/2} Z_{INT}^{-2} \sum_{ijk\ell} e^{-(\varepsilon_i+\varepsilon_j)} \iint e^{-g^2} g^3 \left\{ g^4 \sin^2\chi - \frac{1}{2}(\Delta\varepsilon)^2 \sin^2\chi + \frac{11}{8}(\Delta\varepsilon)^2 \right\} \sigma_{ij}^{k\ell}\, d^2\Omega\, dg \qquad (2.119)$$

$$a_{12} = -\frac{5}{2}\left(\frac{kT}{m}\right)^{1/2} Z_{INT}^{-2} \sum_{ijk\ell} e^{-(\varepsilon_i+\varepsilon_j)} \iint e^{-g^2} g^3 (\Delta\varepsilon)^2 \sigma_{ij}^{k\ell}\, d^2\Omega\, dg \qquad (2.120)$$

$$a_{22} = \left(\frac{kT}{m}\right)^{1/2} Z_{INT}^{-2} \sum_{ijk\ell} e^{-(\varepsilon_i+\varepsilon_j)} \iint e^{-g^2} g^3 \left\{ (g(\varepsilon_i-\varepsilon_j) - g'(\varepsilon_k-\varepsilon_\ell))^2 + \frac{3}{2}(\Delta\varepsilon)^2 \right\} \sigma_{ij}^{k\ell}\, d^2\Omega\, dg \qquad (2.121)$$

and

$$\varepsilon_i = E_i/kT \quad , \quad \Delta\varepsilon = \varepsilon_k + \varepsilon_\ell - \varepsilon_i - \varepsilon_j = g - g' \qquad (2.122)$$

If there is no internal energy then these reduce formally to the results for a monatomic gas to a first order approximation reading :-

$$\lambda_{tr} = 75\, k^2 T / 32 m \Omega^{(2,2)} \qquad (2.123)$$

$$\lambda_{int} = 0 \qquad (2.124)$$

For pure polyatomic gases it has not yet been possible to evaluate any of these expressions exactly for any intermolecular potential because of the complicated collision dynamics concerned with inelastic collisions in a non-spherical symmetric intermolecular potential, although work in this area is in progress [127]. However it has been possible to relate the thermal conductivity of a pure polyatomic gas to other measurable properties of the gas.

Monchick, Pereira and Mason [79,80] have shown that without introducing any other approximations beyond those implicit in Wang Chang and Uhlenbeck theory, the thermal conductivity and the viscosity of a pure polyatomic gas possessing only rotational intermolecular energy, can be related by the equivalent of a first order Chapman-Cowling approximation expression as :-

$$\frac{m[\lambda]_1}{k[\eta]_1} = \frac{5}{2}\left(\frac{C_{v,tr}}{k} - \Delta\right) + \frac{\rho D_{int}}{[\eta]_1}\left(\frac{C_{v,int}}{k} + \Delta\right) \qquad (2.125)$$

where

$$\Delta = \left(\frac{2C_{v,int}}{\pi k \zeta}\right)\left(\frac{5}{2} - \frac{\rho D_{int}}{[\eta]_1}\right)\left\{1 + \frac{2}{\pi\zeta}\left(\frac{5C_{v,int}}{3k} + \frac{\rho D_{int}}{[\eta]_1}\right)\right\}^{-1} \qquad (2.126)$$

which contains only experimentally accessible quantities.

In these expressions m denotes the mass of a molecule, $C_{v,tr}$ and $C_{v,int}$ the translational and internal contributions to the molar heat capacity at constant volume, while D_{int} denotes the diffusion coefficient for internal energy in the pure gas. ζ may be thought of as the number of collisions required for equilibrium of rotational and translational energy in the gas. No higher order approximations for this relationship are known.

In the case of $\zeta \to \infty$, equations (2.125) and (2.126) reduce to the following result , known as the Modified Eucken

relation, reading :-

$$\frac{m\,[\lambda]_1}{k\,[\eta]_1} = \frac{5}{2}\left(\frac{C_{v,tr}}{k}\right) + \frac{\rho D_{int}\, C_{v,int}}{[\eta]_1\, k} \qquad (2.127)$$

If the viscosity and the thermal conductivity are available from accurate measurements and the rotational collision number ζ can be obtained from experiment or estimation procedures, equations (2.125) and (2.126) may be employed to determine D_{int} which is not available from any other source. In cases where one of the transport coefficients, viscosity or thermal conductivity, are not available, equations (2.125) and (2.126) may be used to estimate the missing quantity.

2.4.2. MASON - MONCHICK APPROXIMATION

No exact calculations of individual transport coefficients according to Wang-Chang and Uhlenbeck theory for realistic intermolecular pair potentials have been carried out. However, Mason and Monchick [79,80] have been able to derive approximate expressions from those of Wang Chang and Uhlenbeck which are amenable to direct evaluation. They have shown that to a high order of approximation the viscosity and diffusion coefficient of a polyatomic gas, or the interaction viscosity for two such gases, are independent of the occurence of inelastic collisions. Thus for polyatomic gases :-

$$[\eta]_1 = \frac{5}{16}\,\frac{(mkT)^{1/2}}{\langle\Omega^{(2,2)}\rangle} \qquad (2.128)$$

and

$$[\eta_{ij}]_1 = \frac{5}{16}\left(\frac{2m_i m_j kT}{m_i+m_j}\right)^{1/2}\frac{1}{\langle\Omega_{ij}^{(2,2)}\rangle} \qquad (2.129)$$

These expressions are formally identical to those for a monatomic gas. However, the collision integrals which enter are different because of the non-spherical nature of the interaction potential. The collision dynamics for non-spherical molecular interactions are extremely complicated, and it is only recently that methods for treating them founded on well characterised approximations, have been developed [128] . These new methods turn out to be the quantum mechanical equivalent of a heuristic method of calculation proposed by Monchick and Mason [129] . According to their method the collision integral for a non-spherical interaction is obtained from the formula :-

$$<\Omega^{(2,2)}> = \frac{1}{8\pi}\int \Omega_{\omega}^{(2,2)}\, d\underline{\omega} \qquad (2.130)$$

where $\underline{\omega}$ defines the relative orientation of the two molecules and $\Omega_{\omega}^{(2,2)}$ is the collision integral for the molecules which interact through the central potential specific to the orientation $\underline{\omega}$. That is, the collision integrals are obtained as uniformly weighted averages of collision integrals evaluated at fixed relative orientations.

In a companion paper, Monchick, Yun and Mason [79] extended the Wang Chang and Uhlenbeck equations to polyatomic gas mixtures. Although they did not made any additional assumptions, the expressions derived were not amenable to calculations. Monchick, Pereira and Mason subsequently introduced physically measurable approximations to the rigorous formulae in order to make calculations possible. In particular in addition to the collision integrals for non-spherical interaction obtained by Monchick and Mason [129], they assumed that 'complex collisions', involving jumps of more than one quantum of internal energy, were unimportant. Furthermore they assumed that there is no correlation between internal energy states and relative velocities, or in other words they assumed uncorrelated internal and translational motions.Finally, they tried to account for inelastic collisions.

Their results, which represent a first order approximation in the Chapman Cowling sense to the Wang Chang and Uhlenbeck equations for polyatomic , ν-component, gas mixture at low density can be written :-

$$\lambda_{mix} = \lambda_{HE} + \Delta\lambda \qquad (2.131)$$

where

$$\lambda_{HE} = \lambda_{mix,tr} + \sum_{i}^{\nu}(\lambda_i - \lambda_{i,tr})\Big(1 + \sum_{j\neq i}^{\nu}\frac{x_j D_{i\,int,i}}{x_i D_{i\,int,j}}\Big)^{-1} \qquad (2.132)$$

Here, λ_{HE} is the Hirschfelder-Eucken result [81] adjusted to reproduce the experimentally obtained thermal conductivity of the pure ends and $\Delta\lambda$ represents a correction term incorporating explisit effects due to inelastic collisions and is given by :-

$$\Delta\lambda = 4\sum_{i}\Big\{x_i\sum_{\alpha}\Lambda_{i\alpha}\sum_{\beta}(\Delta\mathcal{L}_{\alpha\beta}^{10,10})\Big(\sum_{\gamma}\Lambda_{\beta\gamma}x_\gamma\Big) - 2\Big(\frac{x_i}{\mathcal{L}_{ii}^{01,01}}\Big)\sum_{\alpha}(\Delta\mathcal{L}_{i\alpha}^{10,01})\Big(\sum_{\beta}\Lambda_{\alpha\beta}x_\beta\Big) -$$
$$\Big(\frac{x_i^2}{\mathcal{L}_{ii}^{01,01}}\Big)\Big[\Big(\frac{\rho_{ii}^{01,01}}{\rho_{ii}^{10,10}}\Big)\Big(\frac{\Delta\rho_{ii}^{10,10}}{\rho_{ii}^{10,10}}\Big) + 2\Big(\frac{\Delta\rho_{ii}^{10,01}}{\rho_{ii}^{10,10}}\Big) + \Big(\frac{\Delta\rho_{ii}^{01,01}}{\rho_{ii}^{01,01}}\Big) - \Big(\frac{\Delta\mathcal{L}_{ii}^{01,01}}{\mathcal{L}_{ii}^{01,01}}\Big)\Big]\Big\} \qquad (2.133)$$

where

$$\ell^{rs,r's'} = \lim_{x_i \to 1} \mathcal{L}_{ii}^{rs,r's'} \qquad (2.134)$$

In these equations x_i represents the mole fraction of species i in the mixture. The symbol $\lambda_{mix,tr}$ is the translational contribution to the thermal conductivity of the mixture, $\lambda_{i,tr}$ is the translational contribution to the thermal conductivity of the pure gas i. The symbols $D_{i\,int,i}$ and $D_{i\,int,j}$ represent the diffusion coefficients for internal energy of species i through species i and j respectively. Finally the elements in the last term $\Delta\lambda$ may be written as :-

$$\Lambda_{\alpha\beta} = \frac{\begin{vmatrix} \mathcal{L}_{11}^{10,10} & \cdots & \mathcal{L}_{1\beta}^{10,10} & \cdots & \mathcal{L}_{1\gamma}^{10,10} & 0 \\ \vdots & & \vdots & & \vdots & \vdots \\ \mathcal{L}_{\alpha 1}^{10,10} & \cdots & \mathcal{L}_{\alpha\beta}^{10,10} & \cdots & \mathcal{L}_{\alpha\gamma}^{10,10} & 1 \\ \vdots & & \vdots & & \vdots & \vdots \\ \mathcal{L}_{\gamma 1}^{10,10} & \cdots & \mathcal{L}_{\gamma\beta}^{10,10} & \cdots & \mathcal{L}_{\gamma\gamma}^{10,10} & 0 \\ 0 & \cdots & 1 & \cdots & 0 & 0 \end{vmatrix}}{\begin{vmatrix} \mathcal{L}_{11}^{10,10} & \cdots & \mathcal{L}_{1\gamma}^{10,10} \\ \vdots & & \vdots \\ \mathcal{L}_{\gamma 1}^{10,10} & \cdots & \mathcal{L}_{\gamma\gamma}^{10,10} \end{vmatrix}} \qquad (2.135)$$

where,

$$\mathcal{L}_{ii}^{10,10} = -\frac{16}{15}\left(\frac{x_i^2 m_i}{n_i k}\right) - \frac{16}{25}\sum_{j\neq i}^{\nu}\left\{x_i x_j T/pD_{ij}(m_i+m_j)^2\right\}\left\{\frac{15}{2}m_i^2+\left(\frac{25}{4}-3B_{ij}^*\right)m_j^2+4m_i m_j A_{ij}^*\right\} \qquad (2.136)$$

$$\mathcal{L}_{ij}^{10,10} = \frac{16}{15}\frac{x_i x_j T\, m_i m_j}{p\, D_{ij}\,(m_i+m_j)^2}\left\{\frac{55}{4}-3B_{ij}^*-4A_{ij}^*\right\} \qquad i \neq j \qquad (2.137)$$

In addition, the other elements can be written as :-

$$\mathcal{L}_{ii}^{01,01} = -\frac{4kT}{p\, D_{i\,int,i}\, C_{i\,int}}\left\{x_i^2 + \sum_{j\neq i}^{\nu} x_i x_j \frac{D_{i\,int,i}}{D_{i\,int,j}}\right\} \qquad (2.138)$$

$$\Delta\mathcal{L}_{ii}^{10,10} = -\frac{32}{9\pi}\frac{x_i^2 m_i C_{i,rot}}{k^2 \eta_i \zeta_{ii}} - \frac{64}{15\pi}\sum_{j\neq i}^{\nu}\frac{x_i x_j T\, A_{ij}^*\, m_i m_j}{p\, D_{ij}(m_i+m_j)^2}\left\{\frac{C_{i,rot}}{k\,\zeta_{ij}} + \frac{C_{j,rot}}{k\,\zeta_{ji}}\right\} \qquad (2.139)$$

$$\Delta\mathcal{L}_{ij}^{10,10} = -\frac{64}{15\pi}\frac{x_i x_j T\, A_{ij}^*\, m_i m_j}{p\, D_{ij}(m_i+m_j)^2}\left\{\frac{C_{i,rot}}{k\,\zeta_{ij}} + \frac{C_{j,rot}}{k\,\zeta_{ji}}\right\} \qquad i \neq j \qquad (2.140)$$

$$\Delta\mathcal{L}_{ii}^{01,01} = -\frac{8\,k}{\pi C_{i,int}^2}\left\{\frac{x_i^2 m_i C_{i,rot}}{k\,\eta_i\,\zeta_{ii}} + \frac{6}{5}\sum_{j\neq i}^{\nu} x_i x_j \frac{m_i}{m_j}\frac{T\,A_{ij}^{*}\,C_{i,rot}}{p\,D_{ij}\,\zeta_{ii}}\right\} \qquad (2.141)$$

$$\Delta\mathcal{L}_{ii}^{10,01} = \frac{16}{15\pi C_{i,int}}\left\{\frac{5x_i^2 m_i C_{i,rot}}{k\,\eta_i\,\zeta_{ii}} + 6\sum_{j\neq i}^{\nu}\frac{x_i x_j T\,A_{ij}^{*}\,m_i C_{i,rot}}{p\,D_{ij}(m_i+m_j)\,\zeta_{ij}}\right\} \qquad (2.142)$$

$$\Delta\mathcal{L}_{ij}^{10,01} = \frac{32}{5\pi}\frac{x_i x_j T\,A_{ij}^{*}\,m_i C_{j,rot}}{C_{j,int}\;p\,D_{ij}(m_i+m_j)\,\zeta_{ij}} \qquad (2.143)$$

and

$$p = n\,k\,T \qquad (2.144)$$

In the above equations $C_{i,int}$ and $C_{i,rot}$ are the internal and rotational heat capacity of species i, and ζ_{ij} is the collision number for equilibration of rotational energy of species i by collisions with species j.

2.4.3. QUANTUM MECHANICAL EFFECTS

All theories described so far were either Classical (Chapman-Enskog) or Semi-Classical (Uhlenbeck, Mason-Monchick) and thus they are deficient in at least two respects. Firstly, they employ without justification, quantum mechanical cross sections in an essentially classical equation. Secondly, in solving the Boltzmann equation the possibility that the zero order approximation to the distribution function might depend on another summational invarient - the molecular angular momentum - was overlooked. Furthermore, Waldman [87] pointed that strictly the Wang Chang and Uhlenbeck equation should not be applicable to molecules with rotational energies as such states are degenerate. Alternatively, a quantum mechanically correct equation analogous to the Boltzmann equation has been derived known as the Waldmann-Snider equation [86], and expressions for some of the transport coefficients have been given. These expressions are very complicated and no calculations have been performed using them as yet [127].

Failure of the semi-classical theory to account for angular momentum conservation has small but significant effect on the transport coefficients for a polyatomic gas, which will be discussed in the next section.

2.4.4. SPIN POLARISATION EFFECTS

In 1930, Senftleben et al. [133] observed that the transport

properties of a paramagnetic gas were affected by the application of a magnetic field. However, no great significance was given to this effect until Beenakker and his collaborators [134,135] began a systematic study of it in the early 1960's. They noticed that the imposition of a velocity or temperature gradient in a gas produces a prefferential alignment of the angular momentum vectors of non-spherically symmetric molecules through binary collisions. If a molecule possesses a permanent magnetic dipole moment then application of a magnetic field to the gas causes the magnetic moment to precess about the field direction. This precession partially destroys the preferential alignment of molecules established by the coupling between the macroscopic gradients and molecular collisions. The extent of this destruction of the polarization, depends upon how fast the molecule precesses relative to the time between collisions in the gas which tends to re-establish the alignment. For large values of the precession frequency and the time between collisions, the spin polarization is completely destroyed and further increase of the field produces no further effect. This represents a saturation and corresponds to compete splitting of the digenerate rotational energy states of the molecule by the applied field. A further point that ought to be made here, is that the orientation of the magnetic field relative to the gradient of temperature or velocity, influences the value of the transport coefficients.

According to the foregoing analysis, one would expect the Wang Chang and Uhlenbeck theory to be appropriate when saturation of the field effect is reached because of the destruction of the spin polarization for which it does not account. Thus qualitatively at least, the magnitude of the magnitude of the magnetic field effect of saturation is a measure of the difference between the Wang Chang and Uhlenbeck result for the transport coefficients and the full quantum mechanical result.

Viehland, Mason and Sandler [84] showed with the aid of the existing quantum mechanical kinetic theory for diatomic molecules that an improved relation to equation (2.125), between the viscosity and thermal conductivity of such a gas reads :-

$$\frac{m[\lambda]_1}{k[\eta]_1} = \frac{m[\lambda_{tr}]_1}{k[\eta]_1} + \frac{m[\lambda_{int}]_1}{k[\eta]_1} \qquad (2.145)$$

and

$$\frac{m\,[\lambda_{tr}]_1}{k\,[\eta]_1} = \frac{5}{2}\left(\frac{3}{2} - \Delta\right) \tag{2.146}$$

$$\frac{m\,[\lambda_{int}]_1}{k\,[\eta]_1} = \frac{\rho D_{int}}{[\eta]_1}\left(\frac{C_{int}}{k} + \Delta\right)\left\{1 - \frac{5}{3}\left(1 + \frac{[\lambda_{tr}]_1}{[\lambda_{int}]_1}\right)\left(\frac{\Delta\lambda_{\parallel}}{\lambda}\right)_{sat}\right\} \tag{2.147}$$

where Δ is given by equation (2.126). Here, $(\Delta\lambda_{\parallel}/\lambda)_{sat}$ is the fractional change in the thermal conductivity measured parallel to a magnetic field at saturation, an experimentally accessible quantity.

The correction is restricted in its validity to systems where the rotational energy level spacing is small compared to kT .

2.5. DENSE GASES - THE ENSKOG THEORY

A first attempt towards a kinetic theory of dense gases is due to Enskog [88] . It is an ad hoc extension of the kinetic theory of dilute monatomic gases for rigid spherical molecules only. The advantage of the rigid sphere model in this connection is that collisions are instantaneous and the probability of multiple simultaneous encounters is negligible. Enskog's extension involves the introduction of corrections that account for the fact that the molecular diameter is no longer small compared with the average intermolecular distance. A major consequence of this is that a mechanism of momentum and energy transfer which is negligible at normal densities becomes important - i.e, during a collision momentum and energy are transferred over a distance equal to the separation of the molecules.

Although Enskog's theory is valid for rigid spheres only, its results may be applied to real gases with considerable success if an appropriately chosen effective collision diameter is used.

In a similar way to that employed for the dilute gas Boltzmann equation, Enskog derived an integro-differential equation for the velocity distribution function. In the case of a dense gas, the collision term is deficient firstly because of the finite size of the molecules, as the centres of two colliding molecules can not be at the same point and this ought to be taken into account in $f(\underline{r},\underline{c},t)$. Secondly, in a dense gas the volume in which any one of the molecules can lie (i.e.'free volume') is reduced and thus the probability of collision is increased. The latter effect

is accounted for by increasing the collision frequency by a factor χ known as the pseudo-radial distribution function, which may be a function of the number density and therefore of position and time and evaluated at the point of contact of the two colliding molecules.

An appropriate expression for the increase in the collision frequency can be obtained by the following argument. When two molecules collide, the distance between their centres is σ, thus the volume which cannot be occupied by the centre of a molecule is approximately the whole volume of the associated spheres, that is $(4/3)\pi n\sigma^3$ per unit volume. Hence the volume in which the centre of a molecule can lie is reduced to $(1-2bn)$ where b is the Van der Waals co-volume for rigid spheres of diameter σ. Thus, the probability of molecular collisions is increased by $1/(1-2bn)$. A second factor that ought to be taken into account is the shielding of one molecule by another. This has been found by Chapman and Cowling (Chapter 16, [73]) to decrease the pseudo-radial distribution function χ by $(1-(11/8)bn)$. Thus an approximate value for χ to a first order in bn reads :-

$$\chi = (1 - \tfrac{11}{8}bn)/(1 - 2bn) = 1+\tfrac{5}{8}bn \qquad (2.148)$$

An identical expression for the pseudo-radial distribution function χ may be derived from the equation of state for rigid spheres [71].

By a similar method to that employed for the dilute gas case, it is possible to obtain an expression for the kinetic flux of any molecular property. Furthermore, by considering the transfer of this property upon collisions in the dense gas it is possible to evaluate the 'collisional' transport of, for example, energy in the gas.

These two kinetic and 'collisional' contributions to the energy flux are added to yield the total heat flux [71] which to a first order of Chapman-Cowling approximation reads :-

$$\underline{q} = -\left\{\frac{2}{5}\pi n\sigma^3(1+\frac{2}{5}\pi n\sigma^3\chi)^2\lambda^\circ + \tilde{c}_{vi}n^2\eta^\circ b^2\chi\right\}\nabla T \qquad (2.149)$$

where η° and λ° are the zero density viscosity and thermal conductivity of the gas. The thermal conductivity of the pure gas at elevated densities can thus be obtained as :-

$$\lambda_i(n,T) = \frac{1}{\chi_i}\left(1 + \frac{3}{5}b_i n \chi_i\right)^2 \lambda_i^\circ + \tilde{c}_{vi} n^2 \eta_i b_i^2 \chi_i \qquad (2.150)$$

and if we define,

$$\gamma_i = \frac{6}{5} b_i \qquad (2.151)$$

expression (2.150) becomes :-

$$\lambda_i(n,T) = \frac{1}{\chi_i}\left(1 + \frac{1}{2}\gamma_i \chi_i n\right)^2 \lambda_i^\circ + \frac{25}{36}\gamma_i^2 n^2 \eta_i^\circ \tilde{c}_{vi} \chi_i \qquad (2.152)$$

Note that for rigid sphere gases :-

$$\lambda_i^\circ = \frac{5}{2} \tilde{c}_{vi}\, \eta_i^\circ \qquad (2.153)$$

and

$$\tilde{c}_{vi} = \frac{3}{2}\frac{k}{m_i} \qquad (2.154)$$

Thorne [95] generalised the Enskog theory to binary mixtures whereas Tham and Gubbins [96] completed the development for multicomponent mixtures. In the form in which these results were originally given, they were inconsistent with the Onsager[91,92,93] reciprocal relations of irreversible thermodynamics. This defect was subsequently corrected by Van Beijeren and Ernst [130] .

Real molecules are not rigid spheres and so comparison of experimental results with the predictions of the Enskog theory are not entirely satisfactory. In an attempt to improve the agreement between the Enskog theory and experimental data for real gases, Enskog suggested that the intermolecular forces between real gases could be accounted for by using a suitable definition of an effective rigid sphere diameter for the molecules. He proposed that the definition :-

$$\gamma_i = \frac{6}{5} b_i = \frac{6}{5}\left\{ B_{ii} + T\left(\frac{dB_{ii}}{dT}\right) \right\} \qquad (2.155)$$

where B_{ii} is the second virial coefficient of the pure gas, should be employed. This procedure has been demonstrated by Hanley [131] to result in substantially better agreement with experimental data, although its basis is insecure [172] .

2.5.1. MASON - WAKEHAM APPROXIMATION

In the case of a pure polyatomic gas, account must also be taken of the internal energy transport. Mason et al. [89] presented

a method according to which the thermal conductivity of a pure dense polyatomic gas is taken to be composed of two distinct contributions, a translational and an internal, as can be done rigorously for the low density gas (§2.4.2.p.47) as :-

$$\lambda_i = \lambda_{i,tr} + \lambda_{i,int} \qquad (2.156)$$

The translational contribution can be obtained from equation (2.152) using the zero density viscosity η°, that is :-

$$\lambda_{i,tr} = \frac{5}{2}\left(\frac{3k}{2m_i}\right)\eta_i \left(1 + \frac{1}{2}\gamma_i \chi_i n\right)\frac{1}{\chi_i} + \frac{25}{36}\left(\frac{3k}{2m_i}\right)n^2 \eta_i^\circ \gamma_i^2 \chi_i \qquad (2.157)$$

to calculate the internal contribution $\lambda_{i,int}$ to the thermal conductivity of a pure dense polyatomic gas, Mason et al. postulated that internal energy is transported by a diffusive mechanism, with an associated diffusion coefficient D_{int}. However, for practical calculations, they proposed that it is sufficiently accurate to equate D_{int} to the self diffusion coefficient of the gas D_{ii}. Thus, the expression for the internal contribution $\lambda_{i,int}$ reads :-

$$\lambda_{i,int} = n\, m_i D_{ii} \tilde{c}_{v,int} = n\, m_i D_{ii}^\circ \tilde{c}_{v,int} \frac{1}{\chi_i} \qquad (2.158)$$

where D_{ii}° is the zero density self-diffusion coefficient, while,

$$\tilde{c}_{v,int} = \tilde{c}_v - \frac{3}{2}\left(\frac{k}{m}\right) \qquad (2.159)$$

is the internal specific heat capacity per unit mass.

Mason et al. then attempted to derive relations for polyatomic gas mixtures at elevated densities. Since a rigorous theory of polyatomic gas mixtures at elevated densities is not available, they preferred to derive an interpolation formula according to which if the pure gas thermal conductivities are known the mixture thermal conductivity at high density can be obtained using only information about the mixture thermal conductivity at low density. This interpolation formula is based on the Thorne-Enskog hard sphere theory extended to apply to any molecular interaction with the additional restriction that inelastic effects are neglected. The expressions are written in such way that the pure gas thermal conductivities are exactly reproduced. As in the case of

the pure gas, the thermal conductivity of a ν-component mixture is written as the summation of two contributions, the translational or monatomic and the internal parts. The final expressions read :-

$$\lambda_{mix} = \lambda_{mix,tr} + \lambda_{mix,int} \tag{2.160}$$

where the translational contribution $\lambda_{mix,tr}$ is given by :-

$$\lambda_{mix,tr} = -\frac{\begin{vmatrix} H_{11} & \cdots & H_{1\nu} & y_1 \\ \vdots & & \vdots & \vdots \\ H_{\nu 1} & \cdots & H_{\nu\nu} & y_\nu \\ y_1 & \cdots & y_\nu & 0 \end{vmatrix}}{\begin{vmatrix} H_{11} & \cdots & H_{1\nu} \\ \vdots & & \vdots \\ H_{\nu 1} & \cdots & H_{\nu\nu} \end{vmatrix}} + K_{mix} \tag{2.161}$$

with

$$y_i = x_i \left\{ 1 + \sum_{j=1}^{\nu} \frac{2m_i m_j}{(m_i+m_j)^2} x_i \gamma_{ij} \chi_{ij} n \right\} \tag{2.162}$$

$$H_{ii} = \frac{x_i^2 \chi_{ii}}{\lambda_i^\circ} + \sum_{\substack{j=1 \\ j\neq i}}^{\nu} \frac{x_i x_j \chi_{ij}}{2\lambda_{ij}^\circ A_{ij}^* (m_i+m_j)^2} \left\{ \frac{15}{2} m_i^2 + \frac{25}{4} m_j^2 - 3m_j^2 B_{ij}^* + 4m_i m_j A_{ij}^* \right\} \tag{2.163}$$

$$H_{ij} = -\frac{m_i m_j x_i x_j \chi_{ij}}{2\lambda_{ij}^\circ A_{ij}^* (m_i+m_j)^2} \left\{ \frac{55}{4} - 3B_{ij}^* - 4A_{ij}^* \right\} \tag{2.164}$$

$$K_{mix} = \frac{10}{9} n^2 \sum_{i,j=1}^{\nu} \frac{x_i x_j m_i m_j}{(m_i+m_j)^2} \lambda_{ij}^\circ \gamma_{ij}^2 \chi_{ij} \tag{2.165}$$

while the internal contribution is given by :-

$$\lambda_{mix,int} = \sum_{i=1}^{\nu} \left(\frac{\lambda_i^\circ - \lambda_{i,tr}^\circ}{\chi_{ii}} \right) \left(1 + \sum_{\substack{j=1 \\ j\neq i}}^{\nu} \frac{x_j \lambda_{i,tr}^\circ \chi_{ij}}{x_i \lambda_{ij,tr}^\circ \chi_{ii}} \right)^{-1} \tag{2.166}$$

here x_i and x_j are molefractions and λ_{ij}° is the low density interaction thermal conductivity of the binary mixture, defined previously by equation (2.87). The γ_{ij} are corrections for the free path shortening in an i-j collision in the dense gas given by [79] :-

$$\gamma_{ij} = \frac{6}{5} \left(B_{ij} + T\left(\frac{dB_{ij}}{dT} \right) \right) \tag{2.167}$$

where B_{ij} is the interaction second virial coefficient of the mixture. When values of B_{ij} are not available, an empirical combination rule can be used, reading :-

$$\gamma_{ij} = \frac{1}{8}\left(\gamma_{ij}^{1/3} + \gamma_{ij}^{1/3}\right)^3 \qquad (2.168)$$

The practical implemantation of the calculation scheme begins with the evaluation of the pseudo-radial distribution function for the pure gases χ_i . This is obtained from equation (2.157) so that automatic reproduction of the thermal conductivities of the pure components is ensurred :-

$$\chi_i(n,T) = \frac{18}{19}\left\{\frac{\lambda_i - n\,\gamma_i\,\lambda^{\circ}_{i,tr}}{n^2\,\gamma_i^2\,\lambda^{\circ}_{i,tr}}\right\} - \frac{36}{19}\left\{\left[\frac{\lambda_i - n\,\gamma_i\,\lambda^{\circ}_{i,tr}}{2n^2\,\gamma_i^2\,\lambda^{\circ}_{i,tr}}\right]^2 - \frac{19\,\lambda_i^{\circ}}{36\,n^2\gamma_i^2\,\lambda^{\circ}_{i,tr}}\right\}^{1/2} \qquad (2.169)$$

The pseudo-radial distribution function in the mixture , χ_{ij} , is obtained as suggested by Wakeham et al. [90] with the aid of a combination rule derivable from the Percus Yevick [97] integral equations for hard spheres as :-

$$\chi_{ij}(n,T) = 1 + \left(\frac{2}{5}\right)\sum_{k=1}^{\nu}\left\{\chi_k(\chi_k - 1) + \frac{6}{5}\,\frac{(\chi_k - 1)^{1/3}(\chi_j - 1)^{1/3}\sum_{k=1}^{\nu}\chi_k(\chi_k - 1)^{2/3}}{(\chi_k - 1)^{1/3} + (\chi_j - 1)^{1/3}}\right\} \qquad (2.170)$$

These results together with equations (2.160) - (2.168) and available experimental data for the thermal conductivity of the pure ends and the interaction thermal conductivity provide a consistent scheme for the calculation of the thermal conductivity of a dense polyatomic gas mixture. In view of the semi-empirical nature of the final equations, care must be taken in the selection of the molecular size parameters for the pure gases. This is because certain values can lead to physically unreasonable behaviour for the pseudo-radial distribution functions in the gas at high densities. This limitation of the Modified Enskog theory has been discussed by Sandler and Fiszdon [98] who proposed a scheme, whereby, the parameters γ_{ij} and thus the pseudo-radial distribution functions can be calculated from experimental measurements of the viscosity and then used to evaluate the thermal conductivity.

2.5.2. THE DENSITY EXPANSION

A complete, rigorous kinetic theory of dense gases would require a new Boltzmann equation for dense gases, which does not make use of the restrictive Molecular Chaos assumption. Attempts at theories of this kind, have been reviewed by Dorfman and Beijeren [136] . The principal conclusion of such work so far is that the transport coefficients of a dense gas are not simple polynomial expansions but rather of the form :-

$$\frac{\lambda(n)}{\lambda(0)} = 1 + c_1(nd^3) + c_2'(nd^3)^2 \log(nd^3) + c_2''(nd^3)^2 + .. \quad (2.171)$$

with a similar expansion for the viscosity. The logarithmic term in this density expansion arises essentially from correlations in the velocities of colliding particles over the distance of a mean free path which are specifically not included in the Enskog theory, as these correlations correspond to a breakdown of the Molecular Chaos assumption. There is no convincing experimental evidence for the existence of the logarithmic term, although molecular dynamics calculations support its inclusion.

The first correction to the low density thermal conductivity contains contributions from collisional momentum transfer in binary collisions and from the effects of three-body encounters in the gas which may include correlated binary collisions as well as genuine three-body collisions where three molecules collide simultaneously. However the calculation of the coefficients of the density expansion have not yet been carried out for realistic intermolecular potentials.

Olmsted and Curtiss have however, performed calculations [163] for a Lennard-Jones (12-6) potential, for the first density coefficient of the thermal conductivity of the monatomic gases. A comparison of their results with the experimental values obtained here, is given in a later section (§6.1.2.,p.157).

•THREE

THE THEORY OF THE TRANSIENT HOT WIRE METHOD

3. INTRODUCTION

In the previous Chapter the need for accurate measurements of the thermal conductivity was emphasized. It will also be shown in a latter section (§4.5. ,p101) that the measurements described in this thesis -obtained by the transient hot wire technique- enjoy a high degree of precision and accuracy. We thus procceed to present the theory of the transient hot wire technique.

3.1. IDEAL SOLUTION

In the transient hot wire technique a thin, straight platinum wire immersed in an isotropic gas and initially at equilibrium with it, is subjected at time t=0 to a step change in the voltage applied to it . Following this change, the wire appears as a line source of heat with a constant magnitude, q, per unit length and the time evolution of the temperature of the wire is determined by the thermal conductivity of the fluid. Thus, the thermal conductivity of the gas can be calculated from the time taken for the temperature of the wire to rise to a certain predetermined value, the properties of the wire and gas and the geometry of the wire enclosure.

In the ideal situation, an infinite, thin and long platinum wire of zero specific heat and infinite thermal conductivity is immersed in, and initially at equilibrium with, a gas of infinite extent at a temperature T_0 . The temperature field around the wire following the initiation of a constant heat dissipation in it, at time t=0 , is described by the line source solution of the Fourier heat conduction equation :-

$$\frac{\partial T}{\partial t} = k_d \cdot \nabla^2 T \qquad (3.1)$$

Here, $k_d = \lambda/\rho c_p$, is the thermal diffusivity of the medium and is assumed to be temperature independent. The boundary conditions of the solution of this equation for the transient hot wire in the ideal case read :-

i) @ $t \leq 0$ & any r $\quad \Delta T(r,t) = 0$ (3.2)

ii) @ $r = 0$ & any $t \geq 0$ $\quad \lim_{r\to 0}(r\frac{\partial T}{\partial t}) = -\frac{q}{2\pi\lambda}$ (3.3)

iii) @ $r = \infty$ & any $t \geq 0$ $\quad \lim_{r\to\infty}(\Delta T(r,t)) = 0$ (3.4)

The problem is a standard one and its solution is [73] :-

$$\Delta T_{id}(r,t) = T(r,t) - T_o = (-\frac{q}{4\pi\lambda})\, Ei(-\frac{r^2}{4k_d T}) \qquad (3.5)$$

where,

$$Ei(x) = \int_x^{\infty} \frac{e^{-x}}{x}\, dx = -\ln C - \ln x + x + O(x^2) \qquad (3.6)$$

and $C = \exp(-\gamma) = 1.78107...$ where γ is the Euler constant.

At a fixed distance $r=a$ (surface of the wire) and for small values of x (typically 10^{-6}, in practice) equation (3.5) reads:-

$$\Delta T_{id}(a,t) = T(a,t) - T_o = (\frac{q}{4\pi\lambda}) \ln(\frac{4k_d t}{a^2 C}) + \ldots \qquad (3.7)$$

Thus, the temperature rise at the surface of the wire $\Delta T_{id}(a,t)$ in the time interval t_1 to t_2 may be represented as :-

$$\Delta T_{id}(a,t) = T(a,t_2) - T(a,t_1) = \frac{q}{4\pi\lambda} \ln(\frac{t_2}{t_1}) \qquad (3.8)$$

Therefore, the thermal conductivity can be obtained from the slope of a ΔT_{id} versus $\ln t$ line.

This, however, represents the ideal model. In practice because the conditions employed are different from ideal, corrections have to be made to real experimental data to adjust them so that they can be described by the simple working equation of the ideal model (3.8) . That is, the philosophy adopted is that corrections can be applied to real experimental data so that they refer to the ideal arrangement discussed above. To simplify the following analysis of the assumptions and corrections employed, the discussion is separated into three main categories. Firstly, corrections that are eliminated entirely will be discussed. Such corrections,

are eliminated due to the careful design and mode of operation of the equipment. Secondly, corrections that are rendered negligible will be presented. By 'rendered negligible' it is implied that each particular effect constitutes a correction to ΔT_{id} which is not more than 0.01%. Finally, the remaining corrections will be discussed.

Summarising, the format of this Chapter is :-

A. Effects eliminated entirely
   i) Convection

B. Corrections rendered negligible
   i) Finite diameter of the wire
   ii) Knudsen effect
   iii) Radiation
   iv) Viscous heating
   v) Compression work

C. Remaining corrections
   i) End effects
   ii) Finite heat capacity of the wire
   iii) Outer boundary correction
   iv) Variable fluid properties

The following analysis will presuppose that the temperature rise of a finite portion of an infinite wire as a function of time is available from experiments. The method whereby these measurements are made will then be discussed in the following Chapter.

3.2. EFFECTS ELIMINATED ENTIRELY

3.2.1. CONVECTION

Convection, which is the major source of errors in most other methods (§1.3. p 9), ought to be examined very carefully for this method. Strictly, one must distinguish between two types of convective currents. One type, is due to temperature gradients along the vessel created if the upper regions of the wire enclosures are warmer than lower regions. This type of convection can, however, be avoided by ensuring that the top of the wire enclosures is at a slightly higher temperature than its bottom part.

The second type of convection starts due to the heat dissipation in the wire. Consider Fig. 9 . The current in the wire induces a heat flow in the gas such that temperatures T_1 and T_2 are higher than T_1' and T_2' . However, this results in temperature T_2 being higher than T_1' and thus the conditions for the onset of convection are established. However, the experimental conditions can be so arranged that the characteristic time required for the boyancy forces to accelerate the gas and thus appreciably affect the rate of heat loss from the wire, is higher than the experimental times employed. The foregoing discussion indicates that experimental times can be chosen to eliminate convective heat transfer entirely. However, the transient hot wire has the additional advantage that should convection occur it can

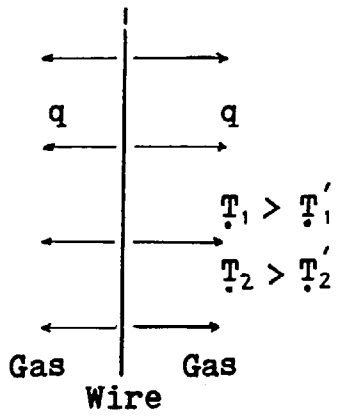

Figure 9 . Convection

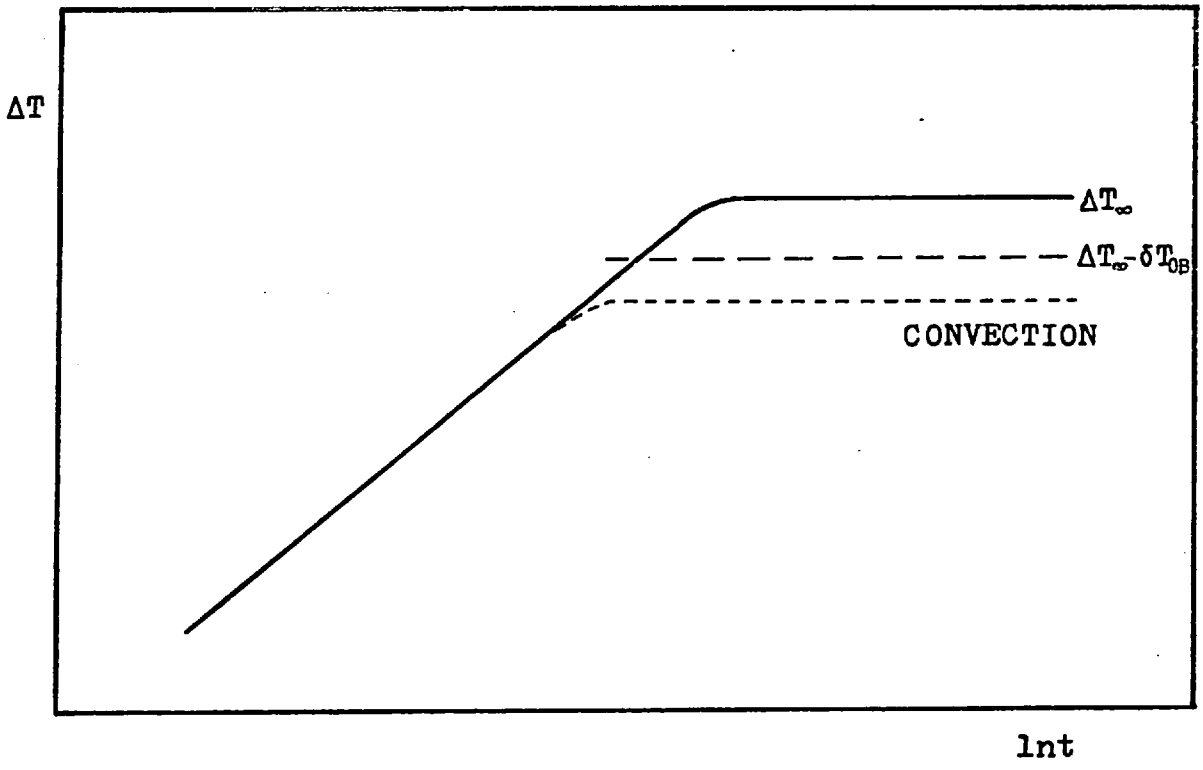

Figure 10 . Effect of convection on the temperature rise ΔT .

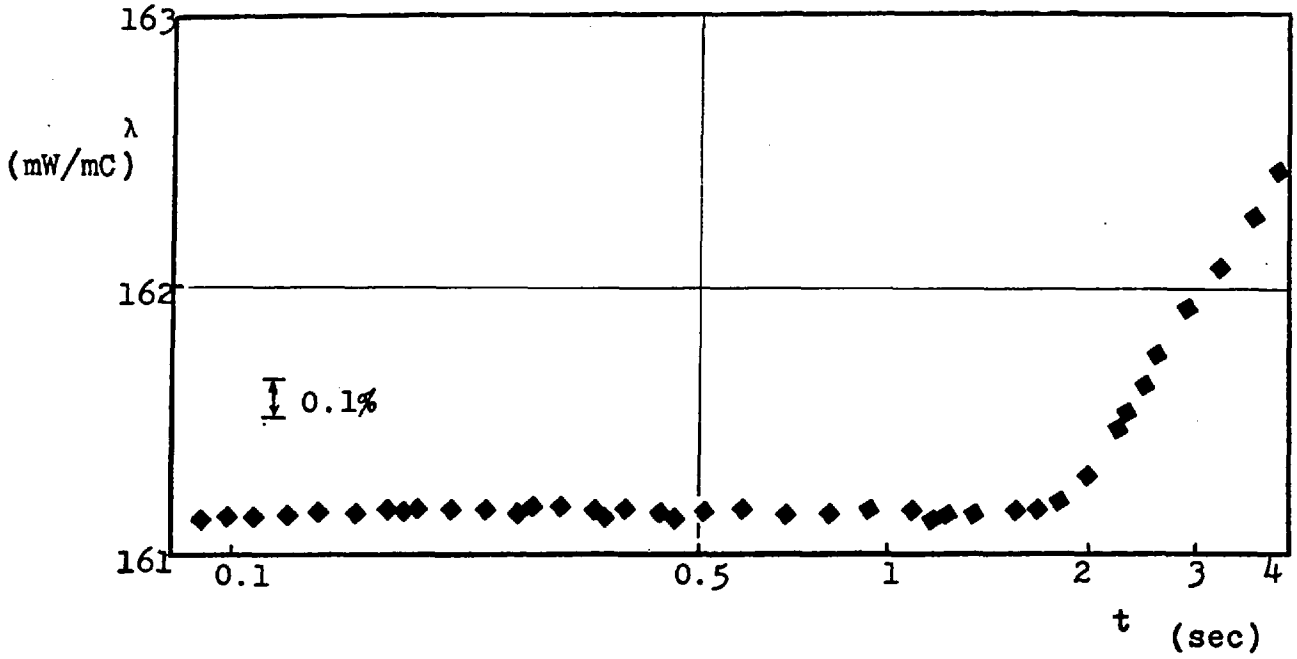

Figure 11 . Effect of convection on the thermal conductivity of Helium @ 7.13 MPa 35 °C

be immediately detected according to the following analysis. Consider Fig. 10 , a significant influence from convection causes the wire temperature to increase less rapidly owing to this new mechanism of heat transfer and leads to an appreciably lower plateau than $\Delta T_\infty - \delta T_{OB}$ (δT_{OB} represents the outer boundary correction , §3.4.3.p 68). Furthermore, this effect results in a sudden increase in the apparent value of the thermal conductivity as shown in Fig. 11 .

Another point that ought to be made here, is that convection can also result if the wires are not absolutely vertical [38] .

3.3. CORRECTIONS RENDERED NEGLIGIBLE

3.3.1. FINITE DIAMETER OF THE WIRE

Evidently in any real experiment the wire employed as the heat source must be of a finite radius a . Thus the previous boundary condition (3.3) has to be modified to :-

$$@ \quad r = a \quad \& \quad \text{any} \quad t \geq 0 \qquad \frac{\partial T}{\partial r} = -\frac{q}{2\pi\lambda a} \qquad (3.9)$$

The solution of the conduction equation under these circumstances (page 338 of [73]) reads :-

$$\Delta T\,(r,t) = -\frac{q}{\pi^2 a\lambda}\int_0^{\infty}(1-e^{-k_d u^2 t})\left\{\frac{J_0(ur)\cdot Y_1(ua) - Y_0(ur)\cdot J_1(ua)}{u^2(J_1^2(ua) - Y_1^2(ua))}\right\}du \qquad (3.10)$$

It is remarkable however that for small values of $(r^2/4k_d t)$ the ideal solution is recovered as :-

$$\Delta T\,(r,t) = \frac{q}{4\pi\lambda}\ln\left(\frac{4k_d t}{Cr^2}\right) + \mathcal{O}(a^2/k_d t) \qquad (3.11)$$

The effect of the last terms can be made small (0.01%) by employing a wire of small radius (typically 3.5 μm). Thus the first term remains which is identical with the ideal solution (3.7)@r=a.

3.3.2. KNUDSEN EFFECTS

The previous discussion (as well as that of further corrections) indicates that very thin wires ought to be used. This however introduces another problem, because at low densities, the mean free path in the gas becomes of the same order of magnitude as the wire diameter, resulting in a temperature jump at the wire surface. That is, the temperature of the gas at r=a is not necessarily equal to that of the wire at r=a. This temperature jump is described by the Smoluchowski equation [101,102] as :-

$$T_w(a,t) - T(a,t) = -g'\left(\frac{\partial T}{\partial r}\right)_{r=a} \qquad (3.12)$$

where, $T_w(a,t)$ is the wire temperature, $T(a,t)$ is the temperature of the adjacent gas and g' is an empirical factor proportional to the mean free path (no reliable measurements or correlations for g are available).

The presence of this temperature jump modifies the boundary condition (3.3) to :-

$$@\ r = a\ \ \&\ \ \text{any}\ \ t \geq 0 \qquad -2\pi a\lambda\left(\frac{\partial T}{\partial r}\right)_{r=a} = q \qquad (3.13)$$

so that the temperature rise according to the analysis of Healy [100] to a first order approximation reads :-

$$\Delta T\,(a,t) = \frac{q}{4\pi\lambda}\ln\frac{4k_d t}{a^2 C} + \frac{q}{4\pi\lambda}\frac{2g'}{a} = \Delta T_{id} + \delta T_K \qquad (3.14)$$

This result demonstrates that because δT_K is time independent to a first order, Knudsen effects produce only a shift of the ΔT

versus lnt line and not a change in slope. Because the thermal conductivity is obtained from the slope of the line, this correction to a first order approximation can therefore be neglected.

To second order approximation, however, Knudsen effects give rise to a change of slope.However, it has been shown [100] that if measurements are restricted to densities greater than :-

$$\rho \geq 3 \cdot 10^{2} q \left(2 N \sigma^{2} \lambda a T \right)^{-1} \qquad (3.15)$$

where, N is the Avogadro number and σ is the rigid sphere diameter of the gas molecules,the second order effect is entirely negligible (< 0.01% of the temperature rise).

3.3.3. RADIATION

The ideal solution of the Fourier law assumes that all energy is conducted into the fluid from the wire. In practice however, some of it can also be radiated, and thus reduce the actual amount conducted. The radiated energy maybe partly absorbed by the gas and partly absorbed and re-emitted by the outer cylinder @ r=b. These effects could modify the temperature history of the wire.

Fortunately, owing to the very small circumferential area of the wire, the very small temperature difference between the wire and the enclosure (about 5 'C) and the weak absorption of most gases, there is no need to perform a detailed analysis of this process as for gases an approximate treatment is all that is necessary.

Assuming that the gas is transparent and that all surfaces involved are black, the amount of energy radiated per unit length can be written as :-

$$q_{rad} = 2 \pi a \sigma_{B} \left(T_{W}^{4} - T_{o}^{4} \right) \simeq 8 \pi a \sigma T_{o}^{3} \Delta T \qquad (3.16)$$

where σ_B is the Stefan-Boltzmann constant. The radiation loss modifies q in equation (3.5) and is equivalent to a reduction in ΔT (a,t) by the amount :-

$$\delta T_{R} = \frac{q_{rad}}{q} \Delta T \ (a,t) = \left(8 \pi a \sigma_{B} T_{o}^{3} / q \right) \left[\Delta T \ (a,t) \right]^{2} \qquad (3.17)$$

Typically for monatomic gases this produces a correction to

ΔT (a,t) of the order of 0.005 %.

For absorbing fluids, the full integro-partial differential equations governing the simultaneous radiation and conduction problem must be solved. A recent treatment of the full problem has been solved and applied [104] to liquids where radiation can amount up to 2% of the total heat transferred in similar experiments.

3.3.4. VISCOUS HEATING

As stated previously (§3.2.1.p.61), the temperature gradient in the gas inevitably gives rise to a velocity field. This velocity field in turn can cause viscous dissipation in the gas leading to local temperature increases and a consequent reduction in the heat loss from the wire.

Healy [100] showed by solving the energy balance equation that an approximate formula for the effect of viscous heating on the temperature rise of the wire is :-

$$\delta T_v = \frac{q}{4\pi\lambda} \frac{Pr\, g^2\, t}{2\, T_o^2\, c_p} \qquad (3.18)$$

where g is the gravitational constant and Pr is the Prandtl number. This effect however, was found to be of the order of 0.01 % of the measured temperature rise and thus can be neglected.

3.3.5. COMPRESSION WORK

In the ideal model, the outer radius b , as well as the axial length L, of the cell are assumed to be infinite. However, in practice , the hot wire is accomodated in a cylinder of finite dimensions (constant volume $V=\pi b^2 L$, and constant mass m) and the fact that heat is fed into it causes even the pressure P to change with time. Thus elementary cylindrical expansion waves spreading outwards with the speed of sound result in essentially constant pressure in space but which changes with time.

In order to account for this expansion process, the energy equation involving only terms due to compression work, coupled with an integral condition of constant mass and the perfect gas law, need to be solved. This produces a correction to the tempe-

rature rise of the wire as :-

$$\delta T_{cw} = \frac{q \; R \; t}{\rho \; c_p \; c_v \; \pi \; b^2} \qquad (3.18)$$

where R is the Universal gas constant. This , in real terms, results in a correction of 0.01% to the temperature rise of the wire and according to our previous discussion can be neglected.

3.4. REMAINING CORRECTIONS

3.4.1. END EFFECTS

Clearly in the real experiment the wire must be supported and provided with electric contacts. These connections provide departures from ideality known as end effects. Haarman [99] and Healy [100] , have provided different, approximate analyses of these end effects. Both analyses indicate that such effects are best eliminated experimentally. This may be accomplished by using two hot wires identical, except for length, both of which are surrounded by the same fluid and both of which are subjected to the same heat dissipation per unit length. It may be shown that if the resistance of each wire is used as a measure of its temperature then the difference of the resistance of the two wires measures the temperature of a wire which acts as a finite segment of an infinitely long wire. That is, the end effects in the two wires cancel exactly.

Of course this argument rests upon the assumption that the two wires differ only in length. However, it is impossible to obtain two samples of wire of identical diameter. Consequently, this ideal compensation can not be achieved. However, the description of this effect properly belongs with the working equations for the experimental installation and so it is postponned until a later Chapter (Chapter 4,§4.3.3.p.93). For now it is assumed that it is possible to experimentally determine the temperature rise of a finite segment of a wire free from end effects.

3.4.2. FINITE HEAT CAPACITY OF THE WIRES

Here we take into account the finite radius ,a , of the wire, its finite conductivity λ_w and its proper heat capacity $(\rho c_p)_w$ per unit volume. The following two coupled Fourier equations can

be written, for the wire and the gas respectively :-

$$(\rho\ c_p)_w\ \frac{\partial T_w}{\partial t} = \lambda_w\ \nabla^2 T_w - \frac{q}{\pi a^2} \qquad 0 \le r \le a \qquad (3.19)$$

and

$$\rho\ c_p\ \frac{\partial T}{\partial t} = \lambda\ \nabla^2 T \qquad r > a \qquad (3.20)$$

The continuity condition can also be used reading :-

$$T_w(a,t) = T(a,t) \qquad \& \qquad \lambda_w \left(\frac{\partial T_w}{\partial r}\right)_{r=a} = \lambda \left(\frac{\partial T}{\partial r}\right)_{r=a} \qquad (3.21)$$

This is a standard problem (p.397 of [73]) whose solution for large values of $4k_d t/r^2$ reads :-

$$\Delta T(r,t) = \frac{q}{4\pi\lambda}\left\{\left[1 - a^2 \frac{((\rho c_p)_w - \rho c_p)}{2\lambda t}\right] \ln\left(\frac{4k\ t}{r^2 C}\right) + \frac{a^2}{2k_d t} - \frac{a^2}{8k_w t}\right\} + \frac{q}{4\pi\lambda}\left(1 - \frac{r^2}{a^2}\right)\left(1 - \frac{a^2 \lambda_w \lambda}{4k_w}\ t\right) \qquad (3.22)$$

The actual temperature measured (Chapter 4, §4.3.3.p.93) corresponds to an integral average of equation (3.22) over the radial coordinate of the wire, so that :-

$$\Delta T(t) = \frac{q}{4\pi\lambda}\left\{\left[1 - a^2 \frac{((\rho c_p)_w - \rho c_p)}{2\lambda t}\right] \ln\left(\frac{4k\ t}{a^2 C}\right) + \frac{a^2}{2k_d t} - \frac{a^2}{4k_w t} + \frac{\lambda}{2\lambda_w}\right\} \qquad (3.23)$$

Therefore the finite heat capacity correction constitutes a correction given by :-

$$\delta T_{HC} = + a^2 \frac{((\rho c_p)_w - \rho c_p)}{2\lambda t}\ \Delta T - \frac{q}{4\pi\lambda}\ \frac{a^2}{4k_d t}\left(2 - \frac{k_d}{k_w}\right) \qquad (3.24)$$

Usually only the first term is considered because the second term constitutes a correction to ΔT of the order of 0.001%.

It can be seen that the effects of this correction will be larger at small times.

3.4.3. OUTER BOUNDARY CORRECTION

The ideal solution presupposes an infinite outer boundary to the heat wave. However, the need to contain the heat fluid in a finite vessel means that at large times the thermal wave spreading out from the wire will reach the outer boundary of the cell @r=b and thus modify the temperature history of the wire. It should be expected however, that the correction will be small as $b/a \approx 1500$

and negligible at small times.

To account for this effect the boundary condition (3.4) must be modified to read :-

$$@ \quad r = b \quad \& \quad \text{any} \quad t \geq 0 \qquad \Delta T(r,t) = 0 \qquad (3.25)$$

which in effect implies that the temperature of the outer wall does not change. For $b/a \gg 1$, Fischer [106] derived an approximate solution for the temperature rise of the wire reading :-

$$\Delta T(a,t) = \Delta T_{id} - \frac{q}{4\pi\lambda}\left\{\ln\left(\frac{4k_d t}{b^2 C}\right) + \sum_{v=1}^{\infty} \exp(-g_v^2 k_d t/b^2)\,(\pi Y_0(g_v))^2\right\} \qquad (3.26)$$

where g_v are the consecutive roots of $J_0(g_v)=0$. It can be seen that the ideal solution can again be recovered if we employ an outer boundary correction reading :-

$$\delta T_{0B} = -\frac{q}{4\pi\lambda}\left\{\ln\left(\frac{4k_d t}{b^2 C}\right) + \sum_{v=1}^{\infty} \exp(-g_v^2 k_d t/b^2)\,(\pi Y_0(g_v))^2\right\} \qquad (3.27)$$

This correction in contrast to the specific capacity correction has a larger effect at large times and it is also more emphasized at the lower density regions. However it never constitutes more than 1 % of the temperature rise of the wires, in practice.

3.4.4. VARIABLE FLUID PROPERTIES

The fact that the density and the thermal conductivity of the gas vary with temperature, introduces a further correction. This can however, most conveniently viewed, as a correction to the temperature with which the thermal conductivity obtained from the plot of ΔT versus $\ln t$, is identified.

In the present work, the slope of ΔT versus $\ln t$, is usually obtained for the range $\Delta T(t_1)$ to $\Delta T(t_2)$. The change of the gas thermal conductivity over a small range of, say five degrees, is in the region of 1%. Thus it is possible to adopt the analysis given by Healy *et al.* [100] . This analysis indicates that if the temperature of the fluid at equilibrium is T_o , the temperature to which the observed thermal conductivity refers is T_r given :-

$$T_r = T_o + \frac{1}{2}\left(\Delta T(t_1) + \Delta T(t_2)\right) \qquad (3.28)$$

The error involved in this approximation is negligible.

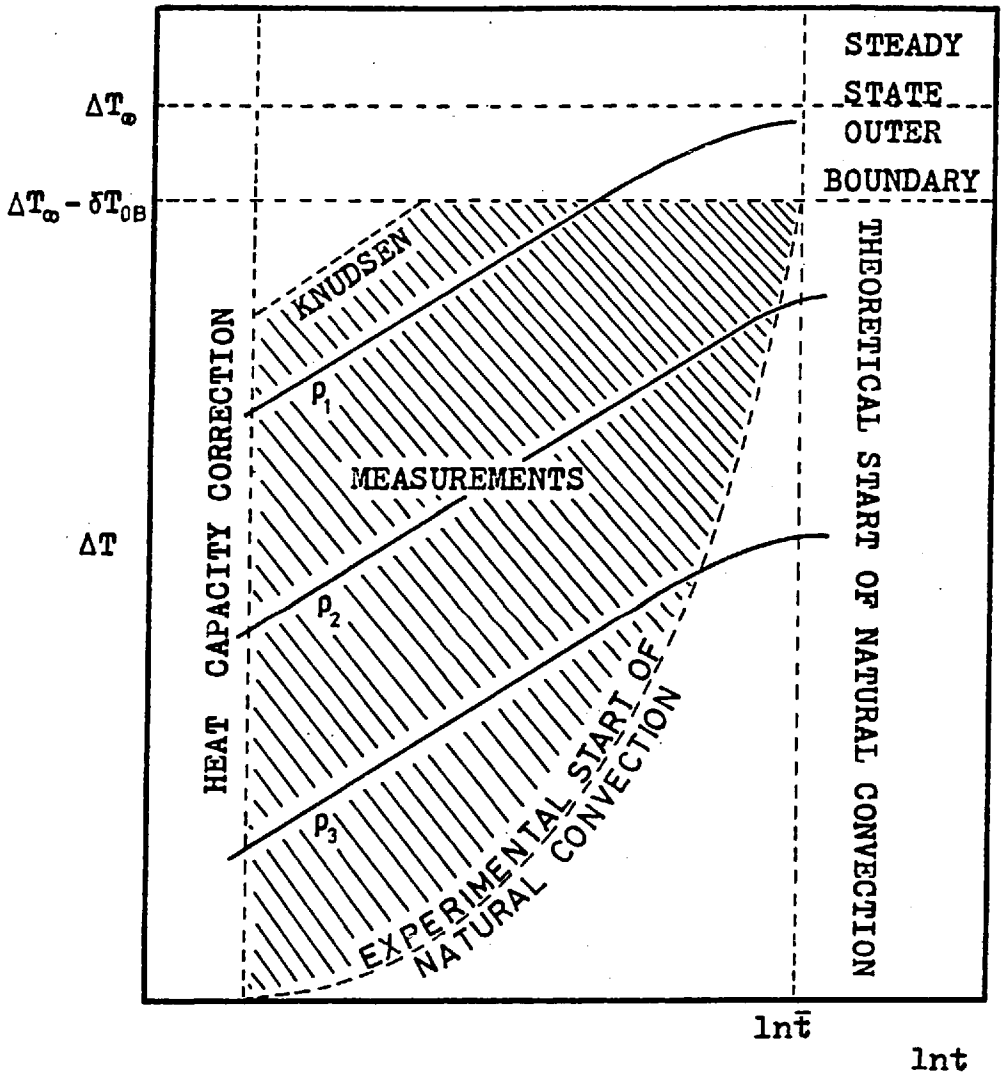

Figure 12 . Experimental region of measurements

In the case of gas mixtures (§2.2.3,p.25) the theoretical discussion of the thermal conductivity has indicated that in the presence of thermal diffusion fluxes,the thermal conductivity coefficient is different from that in the absence of such fluxes. That is, λ' in eq.(2.68),p.26, represents the thermal conductivity in a gas mixture of uniform composition (at zero time in our measurement system) whereas λ represents the thermal conductivity in the non-uniform gas mixture corresponding to the steady state. It is therefore essential to establish which of these thermal conductivities is measured in a transient hot wire apparatus. An analysis of this problem has been given by Khalifa et al. [173]. They have shown that the transient hot

wire method always determines the steady state thermal conductivity. In essence this is because at the wire/fluid boundary there can be no diffusive flux of mass.

3.5. SUMMARY

The thermal conductivity is obtained from the slope of the ΔT versus $\ln t$ plot according to the equation :-

$$\Delta T_{id} = \frac{q}{4\pi\lambda_r} \ln \frac{4(\lambda_o/\rho_o c_p)t}{a^2 C} \qquad (3.29)$$

where, subscript o refers to the initial equilibrium conditions whereas subscript r at the reference conditions. Here,

$$\Delta T_{id} = \Delta T\ (t) \quad + \quad \delta T_{0B} \quad + \quad \delta T_{HC} \qquad (3.30)$$

where

$$\delta T_{HC} = \quad + \quad a^2 \frac{((\rho c_p)_w \ - \ \rho c_p)}{2\lambda t} \ \Delta T \qquad (3.31)$$

and

$$\delta T_{0B} = - \frac{q}{4\pi\lambda} \left\{ \ln\left(\frac{4k_d t}{b^2 C}\right) \quad + \quad \sum_{v=1}^{\infty} \exp\left(-\frac{g_v^2 k_d t}{b^2}\right) (\pi Y_o(g_v))^2 \right\} \qquad (3.32)$$

The thermal conductivity obtained is refered to a reference temperature T_r obtained from :-

$$T_r = T_o + \frac{1}{2}(\Delta T(t_1) + \Delta T(t_2)) \qquad (3.33)$$

• FOUR

DESIGN OF THE APPARATUS EXPERIMENTAL PROCEDURE

4. INTRODUCTION

In the previous Chapters the theory and the advantages of the transient hot wire were presented.We now proceed to describe the equipment used in this work, the consequent derivation of the working equations and the experimental procedure adopted.

4.1. APPARATUS DESIGN

In this section the apparatus used for the measurements of the thermal conductivity coefficient of gases will be described. The geometric, mechanical and electrical characteristics of the equipment were selected after a careful design study based upon the previous theoretical analysis. That is, the various conflicting requirements for accurate measurements were balanced so as to lead to an instrument whose precision is one of ± 0.1%. Consequently the parameters of the equipment described below must be understood to be a result of such a study rather than an arbitrary choice.

4.1.1. INITIAL DESIGN OF THE CELLS

The design of the present cells evolved through experience gained with an earlier set of cells. In order to provide the foundation for the present design the earlier one is described first. This will prove of value when the suggestions for future work are described in a later Chapter.

The initial design is shown in Figure 13 ,p.74 . In order to minimise the corrections outlined in the third Chapter, a 5μm diameter, Wollaston process platinum wire is used for the hot wire. For the same reasons two cells are employed which are identical except for their length. The outer wall ⑧ is made from

stainless steel (SS304), inside diameter 1cm, and it has viewing slots ⑥ milled in it. A concentric quartz tube ⑦ , is placed inside the stainless steel tube. The 5μm platinum wire is supported between two thick (0.5mm outside diameter) platinum tubes ④ which in turn are spot welded to two threaded stainless steel pins ③ . The stainless steel pins are electrically insulated from the tube by means of pyrophilite bushes ② . Nuts ① provide the vertical adjustments and the stainless steel pins the electrical contacts. The assembly was performed in the following way. The platinum wire was cut to length and its ends were crimped in the platinum tube. The top tube was then spot welded to the top stainless steel pins. In order to remove the silver coating from the wire, the wire ends were covered by black wax and the whole wire held by the top pyrophilite bush was lowered into successive baths of dilute nitric acid to remove the silver, and finally carbon tetrachloride to remove the wax. The wire was then lowered into the cell and the bottom platinum tube was spot welded to the bottom stainless steel pin. The wire was then tightened until no deflection from the vertical was observed when a bar magnet was brought near the wire and a small d.c. current was flowing in the wire.

One disadvantage of the above procedure, is that owing to the way in which the Wollaston wire is made some silver always diffuses into the wire. Thus the temperature coefficient of resistance of the wire is not identical to that of pure platinum. Furthermore it is very difficult to ensure that the silver is completely removed from the surface of the wire. Any remaining silver contributes to non-uniformities in the wire radius. However, the most important disadvantage of this design is that during an experimental run the wires increase in temperature. Because the wire is supported between two fixed points and is taut at room temperature during a run it necessarily expands and becomes slack.This slackness implies a sideways motion of the wire through the gas, leading to convective cooling superimposed on any conductive transfer. Measurements with cells of this design were found always to reveal the presence of convective effects.

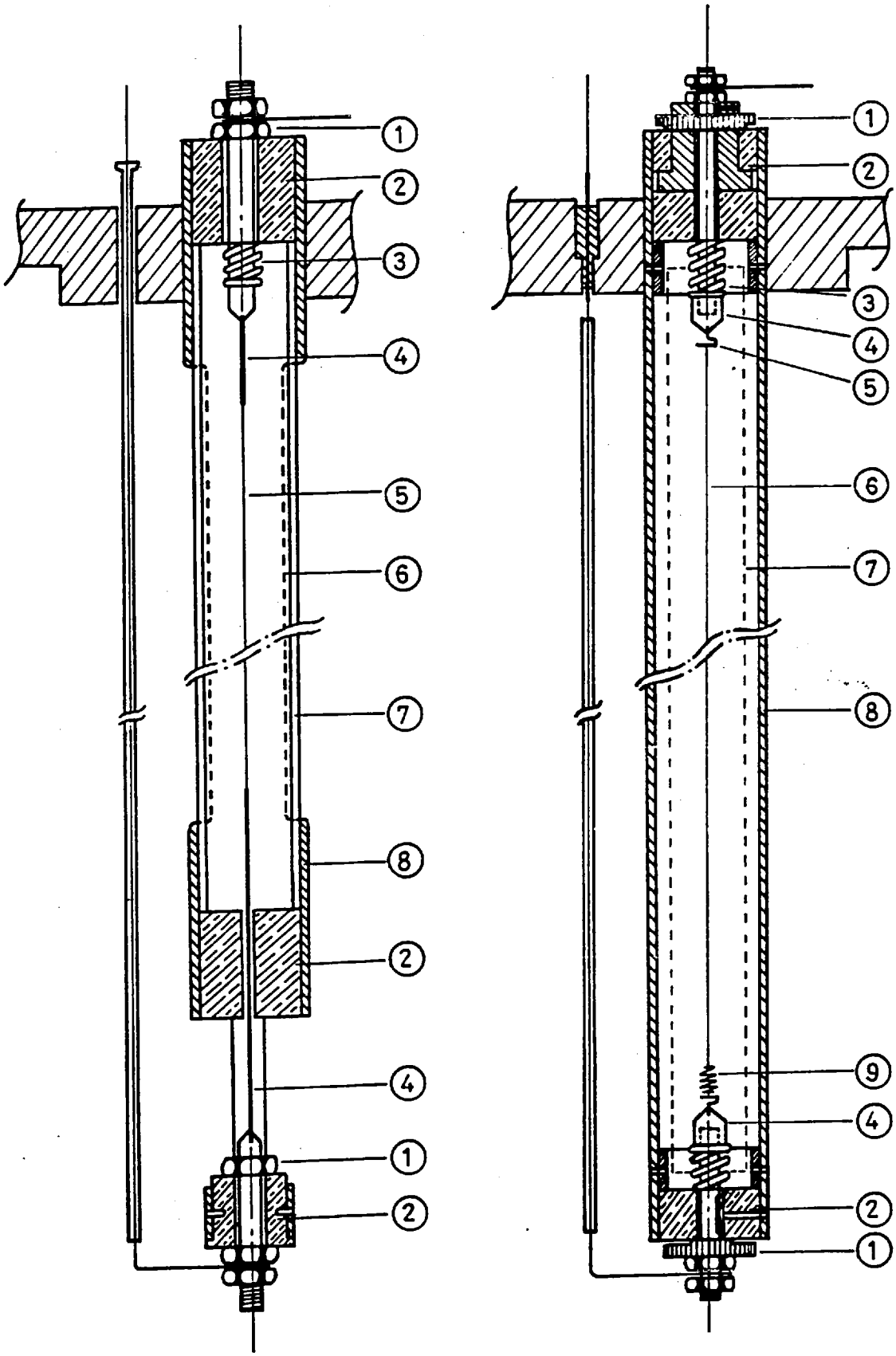

Figure 13 . Previous cell design (left)
Present cell design (right)

4.1.2. PRESENT CELL DESIGN

In order to obviate the difficulties discussed above a new design for the cells was adopted. To the constraints already imposed on the design of the cells it was thought desirable to ensure that the wires would not be touched by hand. Furthermore, because the original cells required about ten to fifteen days to prepare, the new design aimed to incorporate ease of assembly.

In the present cells a 7μm bare platinum wire is used as the hot wire. As well as its freedom from the silver coating, the wire was appreciably more uniform than the Wollaston process wire. The problem associated with the thermal expansion of the wire during transient heating was solved by means of a tensioning spring. Further features of the present cells are the ability to use longer wires and more flexible adjustments. The present cell design is shown in Figure 13, p.74 and Figure 14, p.76 .

The cell body ⑧ consists of a stainless steel tube (SS304) of internal diameter 11mm and external 13mm. A longitudinal slot milled in the central section ⑦ provides access to the interior. A matching hemicylindrical cover for the window manufactured from the same material, ensures the necessary cylindrical internal surface when placed in position. Electrical insulation of the platinum wire is provided at either end of the cell through non-porous glass ceramic bushings (MGC9658) ② , that also provide the support for the stainless steel pins ③ . The upper pin is equipped with an adjusting mechanism ① that allows either rotation of the pin or vertical movement. This is achieved by means of a set-screw at the top of the hollow cylinder ① - if the set-screw is loose the pin can rotate; if the set-screw is tightened the pin is fixed to the hollow cylinder and the only vertical movement can be achieved with the knurled nut. The thread of this nut is callibrated so that the vertical movement resulting from its rotation is known. A coarse adjustment is also provided for the bottom pin. At the upper end the wire is sldered with gold to a platinum hook ⑤ made from 0.5mm diameter wire. At the lower end the wire is fixed to a helical spring ⑨ made from 0.25mm gold wire, which is also connected to another platinum hook with a silver alloy solder. The two platinum hooks are mounted in threaded stainless steel cones ④ with the same silver alloy solder and a stainless steel flux. Finally the two pins are screwed into the

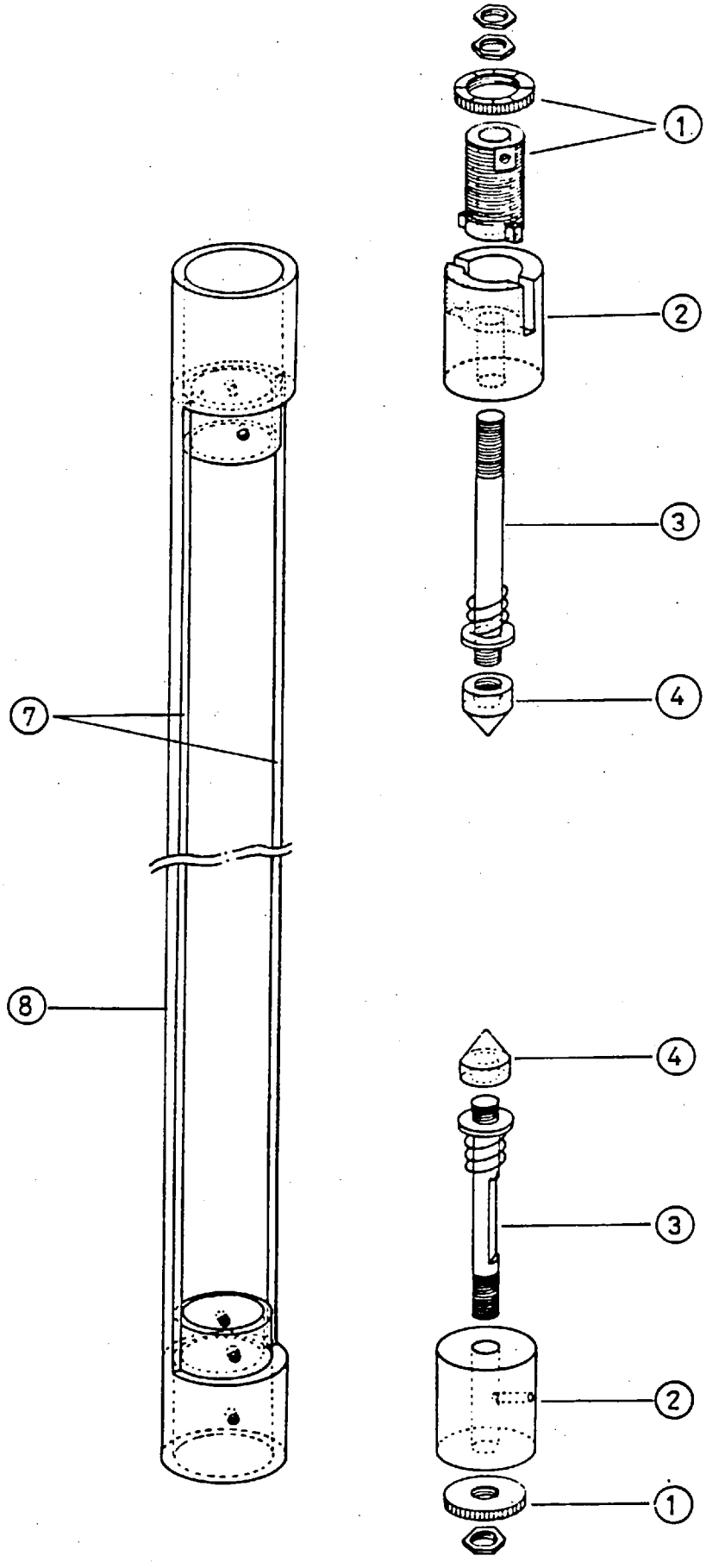

Figure 14 . Present cell

cones.

In order to assemble the cells the following procedure is adopted. First the platinum hooks are soldered to the cones and the cones are mounted in a jig. The spring is then prepared and soldered to the lower hook. A length of the 7μm platinum wire is placed over the hooks and soldered in position. The jig is then inserted in the cell and placed so that the cones are immediately next to the stainless steel pins. The pins are then screwed into the cones and a nut is placed on each pin to ensure it does not move. The small set-screw in the top hollow cylinder is then tightened and the jig is carefully removed. The platinum wire is then annealed by direct Ohmic dissipation for about an hour at approximately 85 W/m. At the end of this period the heating current is decreased slowly. The wire is then tightened until no movement is observed when a bar magnet is brought close while a small current (about 5mA) is passing through the wire. The wire is then adjusted laterally to make it coincident with the cylindrical axis of the cell. The final step in the preparation of the cells is the imposition of a small, known tension in the wires. In view of its importance to the measurements this is described in a separate section below.

4.1.3. WIRE TENSION

The purpose of tensioning the wires in the thermal conductivity cells is to ensure that the wires remain taut during the measurements. The choice of wire tension is therefore a compromise between the need to keep the wires taut and not causing them to creep or break. Furthermore, since the tension in the wires will vary throughout the transient heating of the wire, its value under equilibrium conditions must be known.

The tensioning springs (see Fig. 13 ,p. 74) were manufactured by wrapping a predetermined number of turns of gold wire (0.25mm diameter) around a thin rod (3mm diameter). One such spring was suspended in the field of view of a cathetometer and a 1gr weight was attached of its bottom. An extension, e , of 0.04mm/turn was observed. This was repeated several times with weights up to 2g . The extension per turn was found to be proportional to the mass applied. Thus denoting by N_t the number of turns in a spring, and by F the imposed force, the spring constant K_s is given by:-

$$K_s = \frac{F}{e\ N_t} = \frac{245.3}{N_t}\ \text{N/m/turn} \qquad (4.1)$$

The gold wire has a much larger diameter than the platinum wire, thus the limiting yield stress is that for the platinum wire, which is 14×10^6 N/m^2 (annealed) [108,109] . This corresponds for the platinum wires to a maximum weight of about 650mg .

In the present cells, the stress imposed on the platinum wires was chosen to be about 30% of the yield stress. Therefore it is necessary to establish for each wire, the number of turns in the spring and the extension associated with the imposition of this stress. We start by arbitrarily choosing the number of turns of the spring to be such that given a certain tension, 60% of the extension will be taken by the spring and 40% by the wire. Furthermore, if Y is the Young Modulus of platinum (15×10^{10} N/m^2, [109]), A the cross-sectional area of the wire and ℓ the length of any wire, then :-

$$\text{Platinum wire extension} = \frac{1}{Y}\frac{F}{A}\ell \qquad (4.2)$$

and

$$\text{Gold spring extension} = \frac{F}{K_s N_t} \qquad (4.3)$$

and using the above choice of the extension ratio of 3/2 of the spring to the wire, one obtains :-

$$K_s = \frac{2}{3}\frac{A\ Y}{\ell\ N_t} \qquad (4.4)$$

For specified wire lengths, equation (4.4) can be equated to equation (4.1) and thus for each wire the corresponding number of turns of the helical spring may be found. For the present cells the two springs were constructed with 4 ¼ and 9 ¼ turns for the short and long wire respectively.

After the wires and the springs were assembled and annealed the following procedure was adopted to tension the wires. The total extension of the wire and spring in series corresponding to a given tension can be obtained as the summation of equations (4.2) and (4.3). Thus a knowledge of the total extension of the wire-spring assembly serves to determine the imposed tension. The cell design allows vertical extension of the wire-spring assembly by means of the adjusting knurled nut ① of Figure 14 , p. 76, whose thread is callibrated. Consequently rotation of the nut corresponds to known vertical movement of the upper stainless

steel pin ③ and so the nut is rotated by a calculated amount so as to impose the required tension (30% of the yield stress) in the platinum wire.

4.1.4. WIRE CALIBRATION

The calibration of the cells to determine the temperature coefficient of resistance of the 7μm platinum wire was carried out with the wires slack, that is, under constant, zero tension. The cells mounted in an air filled enclosure were placed in a well-stirred thermostat bath. The temperature of the bath was measured with an NPL calibrated platinum resistance thermometer (±1 mK) and the resistance of the wires was measured with a 30Hz a.c.bridge (Automatic Systems Laboratories) to ±2 10^{-4} Ohms. The resistances of the wire and the NPL calibrated resistance thermometer were determined at three temperatures. Table 4 contains the resistance ratios for both the wire and the thermometer taking the lowest

Bath temp.	Resistances			Ratios		
	NPL thermometer	Long wire	Short wire	NPL thermometer	Long wire	Short wire
°C	Ohm	Ohm	Ohm	-	-	-
35.30	29.3472	452.9672	190.0153	1.00000	1.00000	1.00000
45.45	30.3651	468.6722	196.5746	1.03468	1.03467	1.03452
50.54	30.8880	476.8148	200.0012	1.05250	1.05264	1.05253

Table 4 .

temperature as a standard. It can be seen that within the overall experimental error (0.01%) the resistance ratios are identical. This was expected because in contrast to the previously used Wollaston process wire, the present 7μm wire was of 99.99% purity platinum. Thus for the change of resistance of the wires with temperature we have employed the recommended correlation for pure platinum of the International Practical Temperature Scale of 1968 [138] which reads :-

$$\frac{R(T)}{R(273.15)} = 1 + \alpha^{*}\left(1 + \frac{\delta^{*}}{G}\right)(T-273.15) - \alpha^{*}\delta^{*}G^{-2}(T-273.15)^{2} \qquad (4.5)$$

where, $\alpha^{*} = 3.9250668\times10^{-3}\ K^{-1}$ and $\delta^{*} = 1.496334$, $G = 100$ K

Rewritting equation (4.5) in a more convenient form:-

$$\frac{R(T)}{R(273.15)} = 1 + A\,(T - 273.15) + B\,(T - 273.15)^2 \qquad (4.6)$$

where, $A = 3.98471\times10^{-3}\ K^{-1}$ and $B = 5.874557\times10^{-7}\ K^{-2}$
This correlation for the temperature range concerned is insignificantly different from that of the International Practical Temperature Scale of 1976 [139] but it is very much simpler to use.

The average radius of the platinum wire was determined from several electron microscopic photographs of different wire segments. It was found to be $3.89 \pm 0.01\ \mu m$. It should he noted that because the wire radius is not constant, small differences between the resistances per unit length of different wire samples should be expected.

4.1.5. THE PRESSURE VESSEL

Having discussed the way the cells are made and assembled we nowdescribe the pressure vessel employed to contain them and the sample gas.

The pressure vessel in which the cells are enclosed, is a cylinrical vessel made from stainless steel (EN58B) designed for pressures up to 150 Atmospheres (see Fig.15 ,p.81). The flanged cap ④ of the pressure vessel is sealed by a gold wire '0' ring (0.5mm diameter). The cap itself is equipped with a gas/vacuum port ① also sealed with a gold '0' ring and feeds-through for electrical connections ② .The feeds-through are constructed from copper wire embedded in Araldite and sealed by the double coned PTFE plug ③ .The sealing pressure is provided by the stainless steel flange bolted to the top cap. This arrangement has been found to be the most suitable for the work described in this thesis near ambient conditions.

Holes are drilled in the top and bottom of the vessel ⑨ , for two calibrated Degussa platinum resistance thermometers used to measure the temperature of the vessel and copper/constantin thermocouples which act as sensors for the temperature control system.

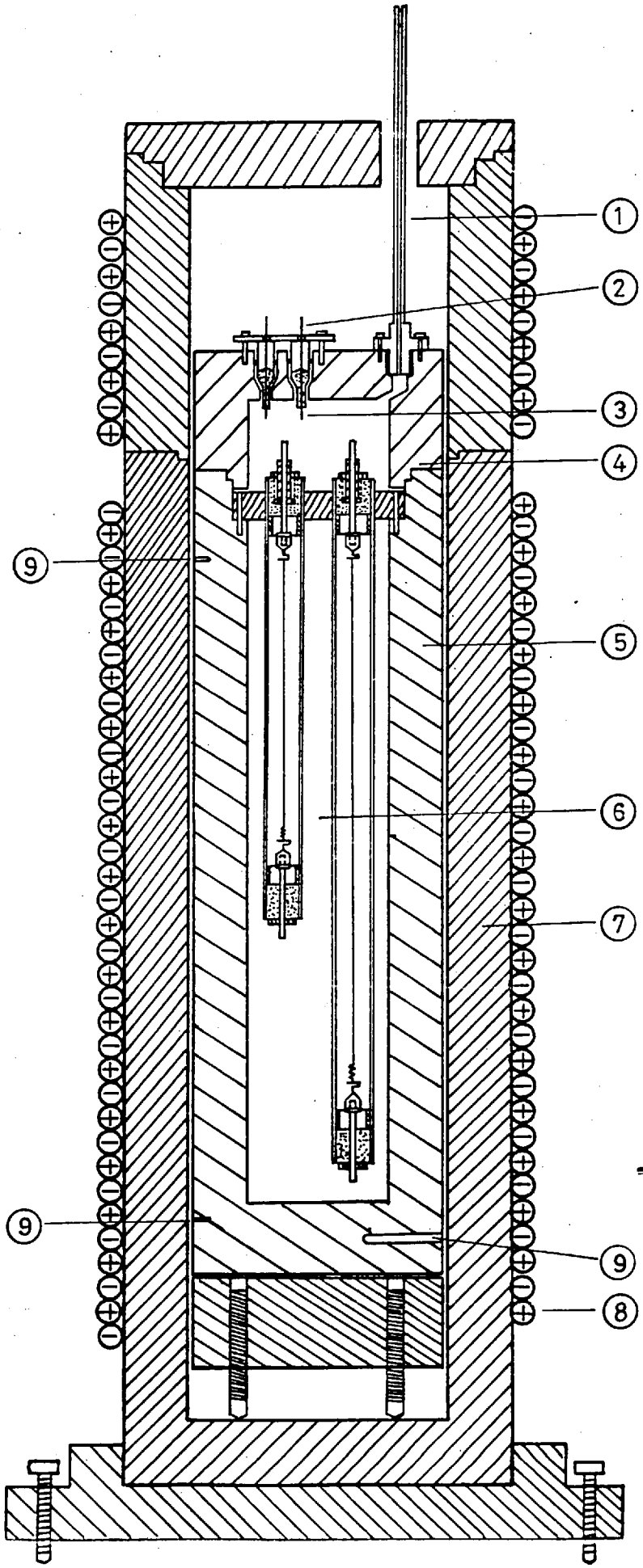

Figure 15 .

Pressure Vessel Assembly

4.1.6. THE TEMPERATURE CONTROL UNIT

The pressure vessel is mounted in a massive copper cylindrical vessel ⑦ (see Fig. 15,p.81). This external vessel is surrounded by heating wire and cooling coils and is used to provide an isothermal enclosure around the pressure vessel. The heating wire ⑧ is wound in a bifilar fashion so as to ensure the absence of a magnetic field. Furthermore, the top part of the enclosure is separately wired so as to allow control of the temperature gradient between top and bottom of the vessel. Both heating wires - top part and bottom- are connected to independent 30V d.c. power supplies, which are regulated with two PID temperature control units using as sensors thermocouples embedded in the pressure vessel. The maximum fluctuation observed in the temperature of the wires over a period of hours is $\pm 1 \cdot 10^{-2}$ K approximately.† The absolute temperature of the vessel is taken as the average of the results for the two Degussa thermometers. Usually a half degree temperature difference is maintained along the vessel, with the top hotter than the bottom, so as to eliminate gravitationally induced convective effects. The two Degussa thermometers were calibrated against the NPL calibrated standard Tinsley platinum resistance thermometer. For this purpose both Degussa thermometers and the standard were placed in a copper block immersed in a fluid bath to ensure good thermal contact. Resistance measurements were performed using a Smith Bridge No 3,type 41623, Tinsley & Co. for the Degussa thermometers, and a Precision a.c. Double Bridge, Automatic Systems Laboratories, for the NPL thermometer. In operation the resistances of the Degussa thermometers were measured with a Smith Difference Bridge, Cambridge Instruments Co., to ±0.0005 Ohm. Taken together with the calibration, the overall uncertainty in the temperature measured with the Degussa thermometers is ±0.01 K.

4.1.7. THE GAS SYSTEM

The pressure vessel within the isothermal enclosure, is connected to the Gas system shown in Figure 16 ,p.83 . The Gas system

---

†The change in the bath temperature observed in the first Result Tables is due to changes in the reference ice point used for the thermocouples.

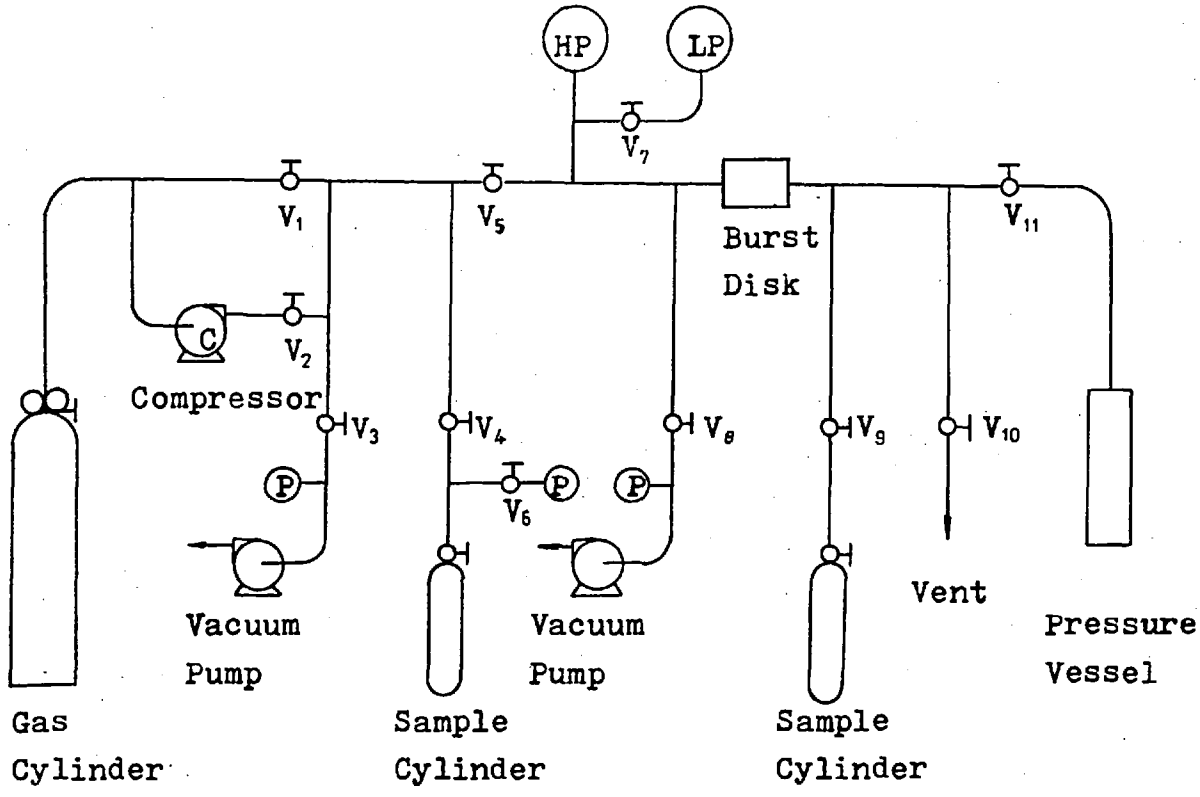

Figure 16. The Gas System

is equipped with two Edwards Vacuum Products pumps and a Stansted Fluids Power compressor. All high pressure connections are made with Hoke or Aminco fittings whereas the vacuum lines employ Edwards Vacuum Products fittings. The pressure gauges are supplied by Bernet Instruments and have been calibrated against a standard pressure balance by the manufacturers; one gauge reads 0 - 1000psig and the other 0 - 2000psig.

Once the pressure vessel is connected, the system is evacuated to less then 10^{-2} Torr, recorded on the Pirani gauges P . Subsequent closure of valves V_3 , V_6 and V_8 isolate the vacuum lines and gas from the cylinder can be allowed to enter the pressure vessel to the required pressure using the compressor C .

4.2. ELECTRONIC COMPONENTS

The purpose of the electronic components of the apparatus is ultimately to determine the temperature rise of the platinum wire in the thermal conductivity cells as a function of the time during their transient heating. The next sections describe in detail the various components and the manner in which these measurements were accomplished.

4.2.1. THE BRIDGE CIRCUIT

Consider the circuit diagram shown in Figure 17 ,p. 85 . The resistances of the long and short wire mounted in the cells as described previously are denoted by R_ℓ and R_s respectively. Resistances R1, R2 and RX are decade resistance boxes, while R3,R4,R9 and R10 are all equal in value (designated hereafter as R). Relay switches S2,S5,S6,S7,S8 and S9 are all high speed reed relays, S1 is a mercury wetted reed relay, S10 a low contact resistance manual switch and S12 a single pole manual switch.

Two constant d.c. voltage units (Hewllet Packard 6112A) supply the power, arranged so that point A in the bridge is close to earth potential, so as to keep noise to a minimum. Voltage polarity changes are detected between points A and F, by a high-impedance electronic comparator.

The principle of the bridge operation is as follows. Prior to a measurement it is arranged so that in the 'reset' position the upper right hand arm resistance is slightly in excess of that required for balance with all parallel resistors connected. RX is adjusted to be approximately equal to the sum of the two wire resistances in order to avoid a significant jump in the load upon switching S1 to position Y.

Switching S1 to position Y, a measurement cycle is initiated by sending a pulse through S2 and C from the current flowing in the wires. This pulse is used to open gates between six electronic counters and a crystal-controlled clock, and thus initiating the timing sequence. Relay switch S2 is then opened again.

The current flowing through the wires causes heat dissipation, their temperature is therefore increased as are their resistances R_ℓ and R_s . As the resistance of the wires increases with that of the long wire increasing more, the bridge approaches balance

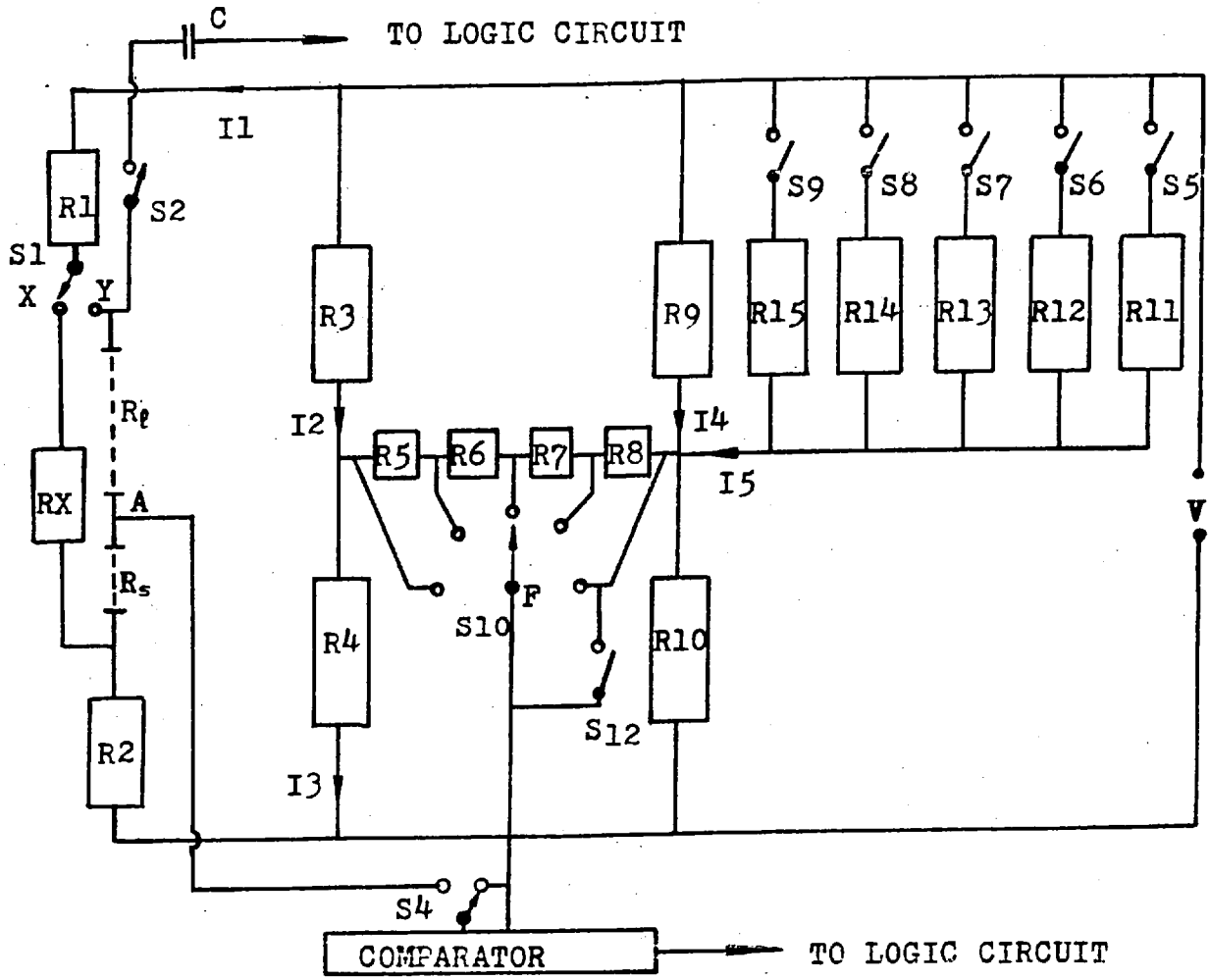

Figure17. The bridge circuit

BRIDGE RESISTANCE	TYPE/MAKE	RANGE (Ohms)	TOL.%
R1,R2	VISHAY 1304	0.01 - 1,000	0.005
R3,R4,R9,R10	VISHAY HA412	2,000	0.001
R5	VISHAY HA412	1,000	0.001
R6	VISHAY HA412	2,000	0.001
R7	VISHAY HA412	4,000	0.001
R8	VISHAY HA412	8,000	0.001
RX	MUIRHEAD D825K	10 x 100	0.010
		10 x 10	0.050
		10 x 1	0.100
		10 x 0.1	0.500
R11,R12,R13,R14,R15	MUIRHEAD D805E	10 x 1,000	0.002
	MUIRHEAD D805F	10 x 10,000	0.001
	MUIRHEAD D805G/1	10 x100,000	0.001

section P_1 to E_1 of Figure 18, which contains the potential difference across the bridge as a function of time. Eventually a point is reached when the polarity of the signal between points A and F (E_1) is changed (see also Fig.17 ,p. 85),indicating that a balance point of the bridge is reached at the particular time t_1. This polarity reversal causes the first electronic counter to be stopped, as well as switch S5 to be opened . This action increases the resistance of the upper right hand arm and the potential difference across the bridge rises to P_2 .Subsequently owing to the continuous resistance increase of the wires, the potential difference decays again towards a new balance point E_2 which occurs at time t_2 which is used to stop a second counter. Relay S6 is then opened increasing the upper right hand arm resistance. This process is repeated until all six counters are stopped. Thus six times are recorded, with the last time taken with switches S5 to S9 open. A single measurement therefore yields six time readings at which the bridge was balanced. It will be shown later how this information can be used to obtain the difference of the wire resistances at each of these times.

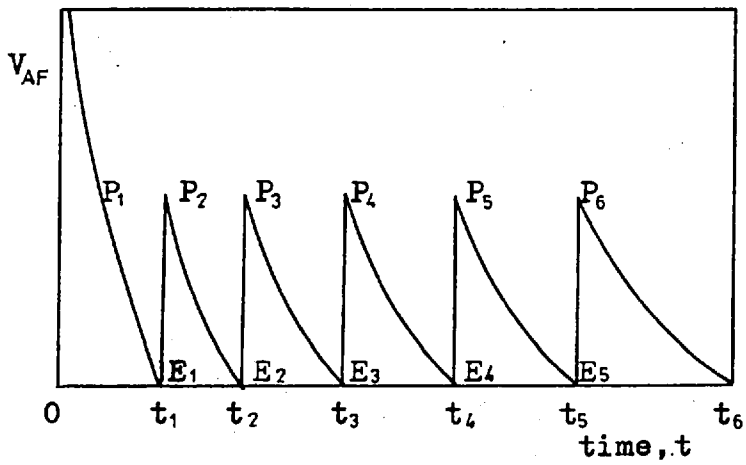

Figure 18 . Potential difference V_{AF} across the bridge as a function of time

To increase the number of balance points, a Selector and a Mode switch are installed. The Selector switch, which is indicated by S10, simply alters the bridge configuration so that different wire resistances R_ℓ and R_s are required for balance. In this way a total of thirty times can now be obtained. The Mode switch alters the way the parallel arm resistances are switched. In one mode, they are all in the circuit and one at a time is removed (Mode A, described above) whereas in the other mode one resistance is replaced by another successively (Mode B). Further more switch S12 produces two more combinations and thus the total number of

readings can amount to hundred twenty. Moreover, by changing the values of the parallel resistances, even more balance points can be obtained. In this way for a single measurement (at a particular thermodynamic state) a sufficient number of points of balance can be recorded (in practice about 36) so as to produce a good distribution of points along the ΔT versus lnt line. It may be noted that as the last reading is always carried out with resistance R9 only in the upper right hand arm, irrespective of the Mode and Selector positions, the condition for bridge balance is always identical.

4.2.2. THE COMPARATOR

The bridge is connected to a comparator which serves as a bridge balance detector. It consists of two input buffer amplifiers (Analog devices type 43K). These are in a balanced crosscoupled mode so as to achieve a very high input impedence (greater than 10^{11} Ohms) and a common mode rejection ratio greater than 80 db.

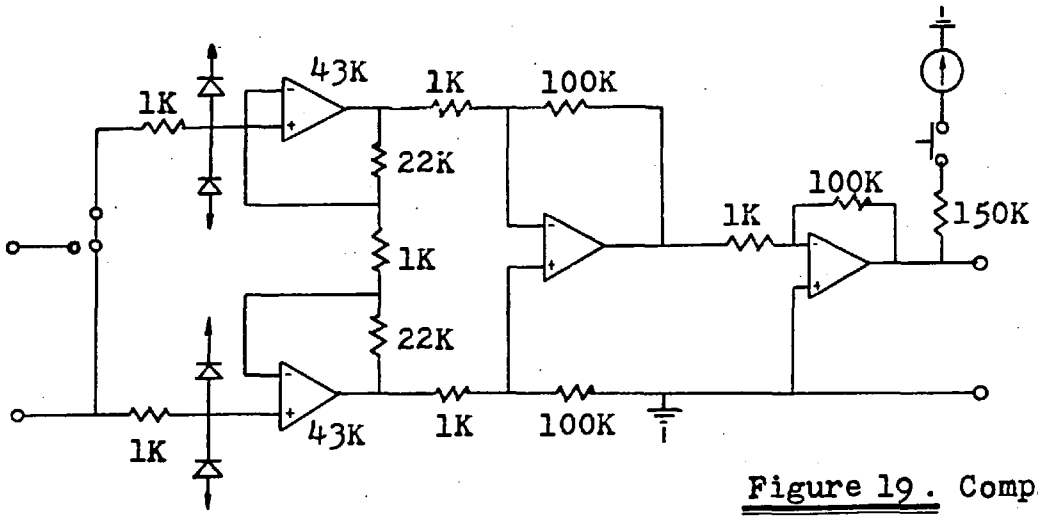

Figure 19. Comparator

The cross coupling ensures that common mode signals are passed at unity gain while differential signals are amplified. The outputs of the two buffers are connected to a conventional differential circuit, that is equipped with a zero-set control and a meter to allow offset adjustments. The complete circuit has a band width of a 100KHz, a high gain of $4 \cdot 10^6$ and a peak to peak noise level of approximately 20μV .

4.2.3. THE CONTROL LOGIC

The control logic is responsible for the automatic sequencing of the bridge operation and the gating of the counters (see Figure 20 ,p.89). Sequencing is accomplished by the six-stage shift register (SN74174) which is clocked by the comparator through a 2ms monostable. The monostable ensures that only one pulse is passed to the register for each bridge balance point and effectively marks the comparator output during the bridge registor switching operation. The shift register outputs are connected to two sets of gates. The first set selects for activation the appropriate buffer transistor from a group which drives the high speed reed relays of the bridge. The second set feeds the corresponding counters from a 100MHz master clock (NEON type MC105-TM). The system is provided with an interlock to the counter unit in order to minimise the risk of accidental triggering or resetting. This is accomplished by means of a 'reset' button that must be pressed before the 'arm' and 'start' operations become active.

To commence a run, the 'reset' and 'arm' buttons are deppressed sequentially. The 'reset' button loads all stages to logic state '1' and resets all counters. In this state all counters are gated off and all relays de-energised. The 'arm' command enables the trigger monostable 2 and the monostable 3. Depression of the 'start' button fires the 30ms monostable 3, which in turn energises the start relay S1 and thus the wires connect to the bridge. The current in the bridge produces a pulse through the capacitor C (see Fig.17 ,p.85) which is fed to the trigger monostable 2. A 2ms pulse is then passed to the clear input of the shift register setting the outputs of all elements to logic state '0', thereby energizing relays S5 to S9 (Mode A). The 2ms pulse holds the shift register clear while the relays and comparator settle. In the case of no pulse returning through the capacitor C after 30ms since the monostable 3 has fired, relay S1 is de-energised and then the wires disconnected.

Following the first polarity reversal detected by the comparator a logic state '1' is shifted into the first element of the shift register. The first counter is therby stopped, and relay S9 is de-energised. While this is performed the comparator is disconnected from the bridge by relay S2 so that it does not experience oscillatory inputs due to the bouncing of relay S9. The

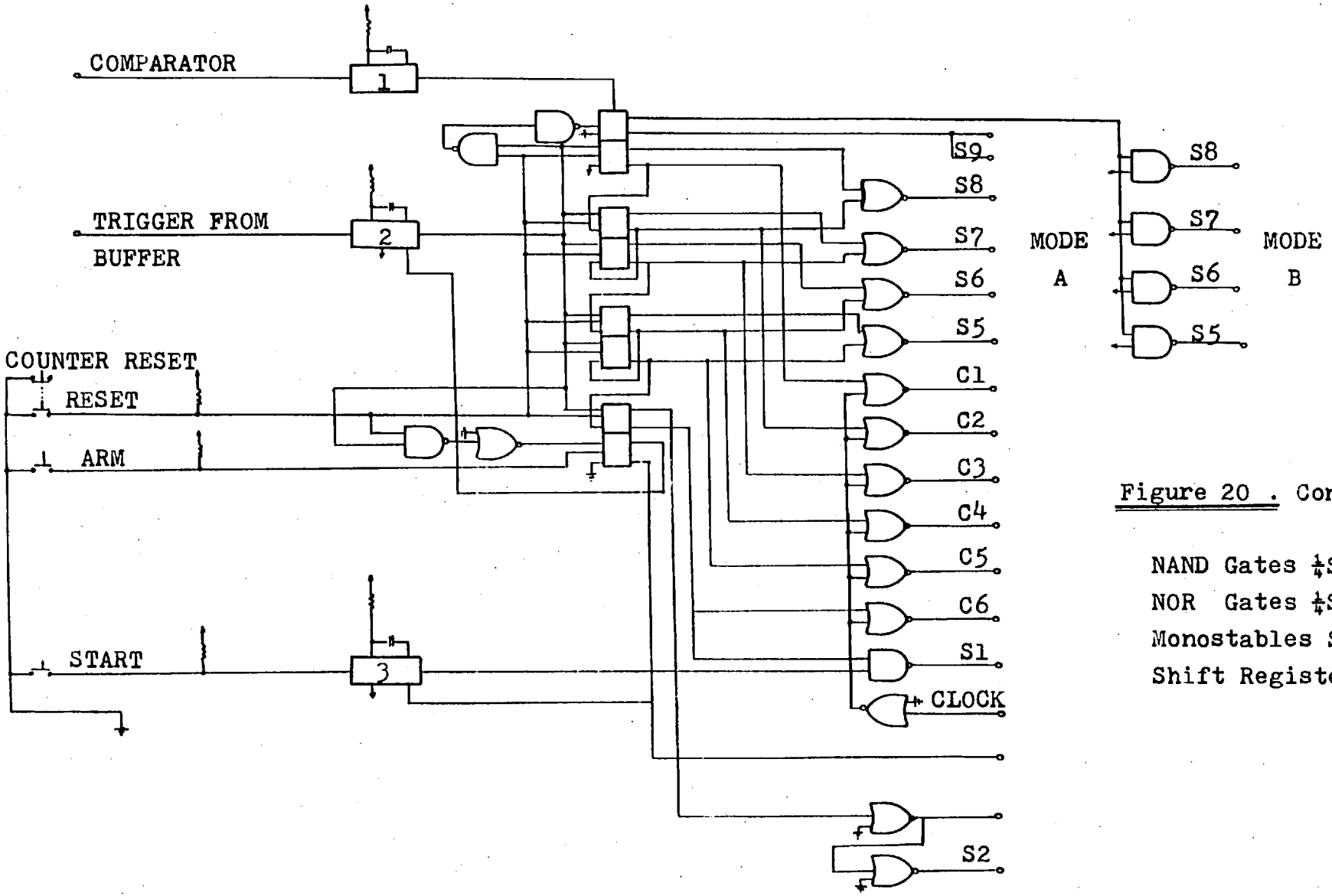

Figure 20 . Control Logic

NAND Gates ¼SN7400
NOR Gates ¼SN7402
Monostables SN74121
Shift Register SN74174

The duration of this disconnection is set at 3ms. A similar process is initiated by each successive polarity reversal of the bridge until all counters stopped. The logic elements used throughout are '74' series TTL.

The sequence described above corresponds to the position A of the Mode switch. In this case the gates controlling relays S5 to S9 are NOR gates. In Mode B the NOR gates are replaced in the circuit by NAND gates to achieve the desired switching pattern. However in other respects the principle of operation is similar to that described above.

Relay S2 is used to switch the comparator in circuit upon depression of the 'start' button. Finally, the counting unit consists of six counters each of six decades (type SN7490) with separate clock inputs and a common reset line.

4.3. WORKING EQUATIONS

4.3.1. THE BRIDGE BALANCE EQUATIONS

To formulate the balance conditions of the bridge (see Fig. 17, p. 85) we consider the case of switch S12 being in the open position and conditions of polarity reversal between A and F.

Applying Kirchoff's law to the circuit we obtain:-

$$V = I1\cdot(R1 + R_\ell + R_s + R2) \qquad (4.7)$$

$$V = I2\cdot R3 + I3\cdot R4 \qquad (4.8)$$

$$V = I4\cdot R9 + (I2 - I3 + I4 + I5)\cdot R10 \qquad (4.9)$$

$$I4\cdot R9 = I2\cdot R3 + (I2 - I3)\cdot R' \qquad (4.10)$$

$$I4\cdot R9 = I5\cdot RS \qquad (4.11)$$

where RS is the total value of the parallel resistors in circuit in the upper right hand arm of the bridge at the time of polarity change and R' is the sum of R5,R6,R7 and R8.

If now β is the fraction of R' in the circuit, for polarity reversal $V_{AF} = 0$. Thus the following relations can be easily obtained from equations (4.7) to (4.11) :-

$$R_\ell - R_s = \frac{C1\cdot R2 - R1}{(R_\ell/R_s) - 1}\left(\frac{R_\ell}{R_s} - 1\right) \qquad (4.12)$$

where,

$$C1 = \frac{1 - (B + 1)/D}{(1 + B/D)} \tag{4.13}$$

$$B = \beta R'/R \tag{4.14}$$

and

$$D = \left\{2\left(\frac{RS}{R}\right) + 1\right\}\left(1 + \frac{R'}{R}\right) \tag{4.15}$$

Thus, the difference of the resistances of the two wires at any balance point may be obtained from a knowledge of the resistances of the bridge. Similar relations can be easily obtained for all configurations. We note that in order to calculate the required resistance difference of the wires ($R_\ell - R_s$) the ratio R_ℓ/R_s should be known. However, as will be shown later, to a very good zero approximation,

$$\frac{R_\ell}{R_s} \simeq \frac{R_\ell(0)}{R_s(0)} \tag{4.16}$$

where, $R_\ell(0)$ and $R_s(0)$ denote the resistances of the two wires at equilibrium condition prior to measurements, which may be measured directly.

4.3.2. THE TEMPERATURE COEFFICIENT OF RESISTANCE

It was shown in the previous section how the difference in the resistances of the wires ($R_\ell - R_s$) can be obtained during an experimental run. In the following section we will obtain from this resistance difference the actual temperature rise of the middle portion of one wire which acts as a finite segment of an infinitely long wire. For this purpose it is necessary to use the resistance-temperature characteristics of the wires and it is convenient to use a pseudo-linear-temperature coefficient of resistance for any wire; defined by the equation :-

$$R(T) = R(T_\circ)\left\{1 + \alpha'(T, T_\circ)(T - T_\circ)\right\} \tag{4.17}$$

where, $R(T)$ is the resistance of the wire at a temperature T and $T_\circ$ refers to the equilibrium bath temperature prior to a measurement. The advantage of this definition is that we have substituted the full quadratic expression for the resistance of a wire given by equation (4.6) by a linear relation.

From equation (4.6) and (4.17) we can obtain an expression for this pseudo-linear-temperature coefficient of resistance as:-

$$\alpha'(T,T_o) = \frac{A + B(2(T - 273.15) + (T - T_o))}{1 + A(T - 273.15) + B(T - 273.15)^2} \qquad (4.18)$$

This expression refers to the situation of constant, zero tension in the wire. However, under the experimental conditions the wires are subjected to a variable tension (§4.1.3.,p.77).The effect of this variable tension is to actually lower the temperature coefficient of resistance. Thus, under the experimental conditions of varying stress, we can write the effective temperature coefficient of resistance as :-

$$\alpha(T_o) = \frac{1}{R(0)}\left[\frac{dR}{dT}\right]_e = \underbrace{\frac{1}{R(0)}\left[\frac{\partial R}{\partial T}\right]_{\tau=0}}_{\alpha'(T,T_o)} + \frac{1}{R(0)}\left[\frac{\partial R}{\partial \tau}\right]_T\left[\frac{\partial \tau}{\partial T}\right]_e \qquad (4.19)$$

where the subscript e denotes the experimental conditions. The first term on the right hand side of equation (4.19) is the pseudo-temperature coefficient of resistance whereas the second term can be evaluated to a good approximation as follows :-

$$\frac{1}{R(0)}\left[\frac{\partial R}{\partial \tau}\right]_T = \frac{(1 + 2\tilde{\nu})}{YA} \qquad (4.20)$$

and

$$\left[\frac{\partial \tau}{\partial T}\right]_e = -\beta' \cdot \left(\frac{1}{YA} + \frac{1}{\ell \cdot K_s}\right)^{-1} \qquad (4.21)$$

In these expressions $\tilde{\nu}$ and Y denote Poisson's ratio and Young's modulus of elasticity for platinum respectively while A is the cross-sectional area of the wire, ℓ its length, β' the linear expansion coefficient of platinum and K_s the elasticity constant of the spring. Substituting equations (4.20) and (4.21) in equation (4.19) one obtains the effective temperature coefficient of resistance as :-

$$\alpha(T_o) = \alpha'(T,T_o)\,(1 - \varepsilon_1) \qquad (4.22)$$

where,

$$\varepsilon_1 = \frac{\beta'(1 + 2\tilde{\nu})}{\alpha'(T,T_o)(1 + AY/\ell K_s)} \qquad (4.23)$$

For the present cells ε_1 has a value of 0.001 .

4.3.3. THE TEMPERATURE RISE EQUATIONS

The purpose of using two wires in the opposite arms of the automatic bridge is to eliminate the effects of axial heat transfer in them, which occur at their connections to the cell terminals. In the ideal case when the two wires and their supports are identical except for their length, this compensation works exactly and it is possible from the resistance difference of the two wires to calculate the temperature rise of a central section of one of them directly [100] . However, inevitable nonuniformities in the radius of the platinum wire make the two wires slightly different. Consequently a different approach to the calculation of the temperature rise of the wire must be adopted.

We first ascribe to each wire a different average radius and heat flux per unit length, denoted by a_ℓ and q_ℓ for the long wire and a_s and q_s for the short wire respectively. Then, if each wire behaved as a finite portion of an infinitely long wire, the temperature rise of each wire reads :-

$$(\Delta T)_\ell = \frac{q_\ell}{4\pi\lambda} \ln\left(\frac{4k_d \cdot t}{a_\ell^2 \cdot C}\right) \qquad (4.24)$$

and

$$(\Delta T)_s = \frac{q_s}{4\pi\lambda} \ln\left(\frac{4k_d \cdot t}{a_s^2 \cdot C}\right) \qquad (4.25)$$

We ignore all corrections due to the heat capacity (§3.4.2.,p. 67) and outer boundary (§3.4.3.,p. 68) for the purpose of this analysis, since we assume that the effects we are discussing are small and so their coupling to other small effects is one order smaller.

Experimentally we infer the temperature rise for the wire from its resistance change. Let us describe an 'experimental' temperature rise for the long wire, $\overline{\Delta T_\ell}$, defined by the equation :-

$$R_\ell - R_\ell(0) = \alpha(T_\circ) \cdot R_\ell(0) \cdot \overline{\Delta T_\ell} \qquad (4.26)$$

and for the short wire:-

$$R_s - R_s(0) = \alpha(T_\circ) \cdot R_s(0) \cdot \overline{\Delta T_s} \qquad (4.27)$$

Here, R_ℓ and R_s represent as before the resistances of the long and short wire at a time t , whereas $R_\ell(0)$ and $R_s(0)$ the resistances of the long and short wire at time t=0 (i.e. at the

bath temperature prior to the initiation of the current, that is $R_\ell(0) = R_\ell(T_\circ)$).

The 'experimental' temperature rise $\overline{\Delta T}_\ell$ differs from the ideal temperature rise $(\Delta T)_\ell$ by an amount dependent on the axial heat conduction at the ends of the wire. Therefore we can write:-

$$\overline{\Delta T}_\ell = (\Delta T)_\ell - \frac{q_\ell}{\ell_\ell} \mathcal{F}_\ell(G_\ell, a_\ell, t, k_d, \lambda_w) \tag{4.28}$$

and for the short wire,

$$\overline{\Delta T}_s = (\Delta T)_s - \frac{q_s}{\ell_s} \mathcal{F}_s(G_s, a_s, t, k_d, \lambda_w) \tag{4.29}$$

where G is a function of the geometry of the ends of the wires.

We now define a further temperature rise $\Delta T'$ such that :-

$$\Delta T' = \frac{(R_\ell - R_s) - (R_\ell(0) - R_s(0))}{\alpha(T_\circ)(R_\ell(0) - R_s(0))} \tag{4.30}$$

Substituting now equations(4.26) to (4.29) in equation (4.30) we derive :-

$$\Delta T' = (\Delta T)_\ell \left[1 + \frac{R_s(0)}{R_\ell(0)-R_s(0)}\left(1-\frac{(\Delta T)_s}{(\Delta T)_\ell}\right) - \frac{1}{R_\ell(0)-R_s(0)}(q_\ell \bar{\sigma}_\ell \mathcal{F}_\ell - q_s \bar{\sigma}_s \mathcal{F}_s)\right] \tag{4.31}$$

where,

$$\bar{\sigma}_\ell = R_\ell(0)/\ell_\ell \quad \& \quad \bar{\sigma}_s = R_s(0)/\ell_s \tag{4.32}$$

It can be seen that if the radii of the two wires were exactly the same, their resistances per unit length would have been equal and so would the heat dissipation within them and the temperature rise in each wire. In this case equation (4.31) reads:-

$$\Delta T' = (\Delta T)_\ell \tag{4.33}$$

The first term in equation (4.31) accounts for the difference in the temperature rise of each wire. The second term represents the consequent incomplete cancellation of the end effects of the two wires.Because, however, the end effects for each wire constitute only about 2% of the temperature rise, the difference between them can usually be neglected [105] .

Therfore, the temperature rise of a portion of the long wire acting as a segment of an infinitely long wire may be obtained from the temperature rise $\Delta T'$ as :-

$$(\Delta T)_\ell = \Delta T' \left\{ 1 + \frac{R_s(0)}{R_\ell(0) - R_s(0)} \left(1 - \frac{(\Delta T)_s}{(\Delta T)_\ell} \right) \right\}^{-1} \qquad (4.34)$$

By further manipulation of equation (4.34) together with equations (4.24) to (4.30), one can show that the required temperature rise $(\Delta T)_\ell$ can be obtained from entirely experimental parameters by the following equations :-

$$(\Delta T)_\ell = \frac{\Delta T'}{1 + \varepsilon_2} \qquad (4.35)$$

where $\Delta T'$ is given by the equation (4.30) and,

$$\varepsilon_3 = \frac{R_s(0)}{(R_\ell(0) - R_s(0))} \varepsilon_2 \qquad (4.36)$$

$$\varepsilon_2 = \varepsilon \left(1 + \ln \left(\frac{4 k_d \cdot t}{a_s^2 \cdot C} \right) \right) \qquad (4.37)$$

and

$$\varepsilon = 1 - \bar{\sigma}_s / \bar{\sigma}_\ell \qquad (4.38)$$

The difference $(R_\ell - R_s)$ in equation (4.30) is obtained from the bridge balance equations (§4.3.1.,p.90). There it was stated that to zeroth order the ratio R_ℓ/R_s which is required for the evaluation, may be equated to $R_\ell(0)/R_s(0)$. A more rigorous approach is to calculate the corrected value of R_ℓ/R_s with the aid of the following relationship :-

$$\begin{aligned} \frac{R_\ell}{R_s} &= \frac{R_\ell(0)}{R_s(0)} \left\{ 1 + \alpha(T_o) \left[(\Delta T)_\ell - (\Delta T)_s \right] \right\} \\ &= \frac{R_\ell(0)}{R_s(0)} \left\{ 1 + \alpha(T_o) \cdot (\Delta T)_\ell \cdot \varepsilon_2 \right\} \end{aligned} \qquad (4.39)$$

with ε_2 given by equation (4.37) and $\alpha(T_o)$ is the effective temperature coefficient of resistance of the platinum wire given by the equation (4.22). An approximate value for $(\Delta T)_\ell$ may be obtained from the zeroth order approximation $R_\ell/R_s = R_\ell(0)/R_s(0)$, which can then be used in equation (4.39) to generate a better estimate of R_ℓ/R_s which can be returned to the bridge balance equations for a better estimate of $(\Delta T)_\ell$. Normally one iteration of this type is sufficient.

4.3.4. THE HEAT FLUX EQUATIONS

The bridge arrangement of Figure 17 ,p.85 , ensures that equal currents flow in both wires. However, this alone does not imply an equal rate of heat dissipation per unit length in the wires as has already been discussed.

By a similar analysis to that in the previous section one can derive [105] , the following equations for the heat flux per unit length of the middle portion of the long wire, q, written in terms of experimental quantities as :-

$$q = \frac{q^*}{(1-\varepsilon_4)^2(1+\varepsilon_5)} \qquad (4.40)$$

where,

$$q^* = \frac{V^2(R_\ell - R_s)/(\ell_\ell - \ell_s)}{\{R1 + R2 + (R_\ell - R_s)(\ell_\ell + \ell_s)/(\ell_\ell - \ell_s)\}^2} \qquad (4.41)$$

and

$$\varepsilon_4 = \frac{2\sigma_\ell \cdot \varepsilon \cdot \ell_\ell \ell_s}{(\ell_\ell - \ell_s)(R_\ell + R_s) + (R_\ell - R_s)(\ell_\ell + \ell_s)} \qquad (4.42)$$

$$\varepsilon_5 = \frac{\ell_s \varepsilon}{\ell_\ell - \ell_s} \qquad (4.43)$$

where, V is the applied voltage to the bridge, while R1 and R2 are bridge resistances defined previously (§4.2.1.,p.84).

4.3.5. SUMMARY & ALGORITHM FOR ANALYSIS

The foregoing analysis has shown that the temperature rise of a finite section of the long wire acting as a part of an infinite wire can be deduced from the measurements carried out by the automatic bridge. This temperature rise, $(\Delta T)_\ell$ cannot yet be identified with the ΔT_{id} of section 3.1. (Ideal solution), because the latter refers to the temperature rise of a wire of negligible heat capacity in an infinite fluid of constant physical properties, whereas the former refers to the real wire. In order to deduce ΔT_{id} from $(\Delta T)_\ell$ it is necessary to correct the latter with the heat capacity (§3.4.2.,p. 67) and outer boundary corrections (§3.4.3.,p. 68). This is accomplished by the equation:-

$$\Delta T_{id} = (\Delta T)_\ell + \delta T_{HC} + \delta T_{OB} \qquad (4.44)$$

It was shown in Chapter 3 that these two corrections to the temperature rise were the only significant ones ($> 0.01\%$).

The values of ΔT_{id} derived from the experimental data in this way together with the corresponding times are all that is necessary to derive the thermal conductivity of the fluid $\lambda(\rho_r, T_r)$ from the equation,

$$\Delta T_{id} = \frac{q_\ell}{4\pi\lambda(\rho_r, T_r)} \ln\left(\frac{4k_d \cdot t}{a^2 \cdot C}\right) \qquad (4.45)$$

by linear regression. The reference temperature is defined by the equation,

$$T_r = T_o + \frac{1}{2}(\Delta T(t_1) + \Delta T(t_2)) \qquad (4.46)$$

and,

$$\rho_r = \rho(P, T_r) \qquad (4.47)$$

In order to present a concise summary of the analysis of the experimental data we conclude this section with an algorithm describing a computer program written to carry it out.

- 1. Solve the bridge equations (§4.3.1., p.90)(4.12) assuming $R_\ell/R_s = R_\ell(0)/R_s(0)$. Thus $(R_\ell - R_s)$ is obtained.
- 2. Calculate $\Delta T'$ from equation (4.30) assuming the effective temperature coefficient of resistance α is temperature independent.
- 3. Calculate the $(\Delta T)_\ell$ from equation (4.35).
- 4. Calculate a new effective temperature coefficient of resistance from equation (4.22) using the $(\Delta T)_\ell$ value obtained in Step 3 and the R_ℓ/R_s ratio from equation (4.39).
- 5. Repeat Steps 2 to 3 until the value of $(\Delta T)_\ell$ has converged to the required accuracy ($\pm$ 0.01%).
- 6. Compute the heat flux from equation (4.40).
- 7. Correct the temperature rise for the specific heat capacity and outer boundary and evaluate the reference temperature.
- 8. Determine the slope of the final temperature rise versus lnt values line and thus the thermal conductivity from equation (4.45).

4.4. EXPERIMENTAL PROCEDURE

4.4.1. PURE GASES

The system is evacuated to 10^{-2} Torr and the pure gas is introduced into the pressure vessel directly from the gas cylinder until a pressure of about 20 Atmospheres. The compressor is then switched on and the system is pressurised to 100 Atmospheres. The temperature control unit is turned on and the system is left for 24 hours to reach equilibrium of pressure and temperature. The bath temperature , T_o, is taken as an average of the two Degussa thermometers (top and bottom) usually kept at a temperature difference of 0.5 'C(top hotter). The pressure is then read. Resistances in the bridge are adjusted to give a good distribution in Int and about six transient heating runs performed. Finally the difference of the resistance of the wires and the resistance of each wire is recorded with the bridge operating at a steady state mode. These measurements are performed for several different bridge voltages and the resistance at zero voltage (i.e. at bath temperature) is obtained by extrapolating the measured resistances against input power to zero voltage. These plots were always found to be linear so that the extrapolation introduces negligible additional uncertainty.

The density of the gases at equilibrium and reference temperature has been computed from experimental P-V-T data [110-117] .

The constant pressure heat capacity of the gases has been deduced from standard tabulations of the zero density values [108,109] [130] , combined with an estimate of the density effect. This latter estimate has been based on the equations :-

$$c_p - c_p^o = \left\{(B - B_1)^2 - (C - C_1) - \frac{C_2}{2}\right\}\cdot\rho^2 - B_2\cdot\rho \qquad (4.48)$$

where,

$$B_1 = T\cdot\left(\frac{\partial B}{\partial T}\right) , \quad B_2 = T\cdot\left(\frac{\partial B_1}{\partial T}\right) \qquad (4.49)$$

and

$$C_1 = T\cdot\left(\frac{\partial C}{\partial T}\right) , \quad C_2 = T\cdot\left(\frac{\partial C_1}{\partial T}\right) \qquad (4.50)$$

For the second virial coefficient, B, and the third, C, experimental data have been employed [110-117].

4.4.2. MIXTURES

In the case of mixtures additional problems arise because there are few available data for the density of the mixture as a function of the pressure and temperature at different molefractions. For this reason the density associated with each particular measurement had to be measured directly. Two sample cylinders (330ml nominal volume)were thoroughly evacuated and weighed. They were then filled with Argon at 70 Atmospheres, and their pressure was recorded with a standard dead weight tester. The temperature was also measured by means of a thermocouple. The cylinders were then weighed and thus(as their mass, pressure and temperature were known) from accurate P-V-T data [110] the volume of the two sample cylinders was found. Table 5 presents the results for the mass and volume of the two sample cylinders.

Cylinder name	Red	White
Evacuated mass (Kg)	1.09077+0.0004%	1.08925+0.0004%
Volume @ 35 'C(m)	$3.3235 \cdot 10^{-4}$+0.03%	$3.2988 \cdot 10^{-4}$+0.03%

Table 5 .

The mixtures were prepared gravimetrically in the sample cylinders. First the one component is introduced and weighed and then the second. Molefractions were thus computed with a typical associated uncertainty of ± 0.0005

The mixture is left for two days in order to attain thermodynamic equilibrium and was then introduced into the pressure vessel. During measurement, the sample cylinder was kept at a temperature very near the nominal temperature of 35'C and following every measurement the pressure vessel was isolated and the sample cylinder was removed and weighed. Thus the associated density of the gas for each measurement was obtained. Small corrections to this density which were sometimes necessary were performed using approximate P-V-T data for particular mixtures

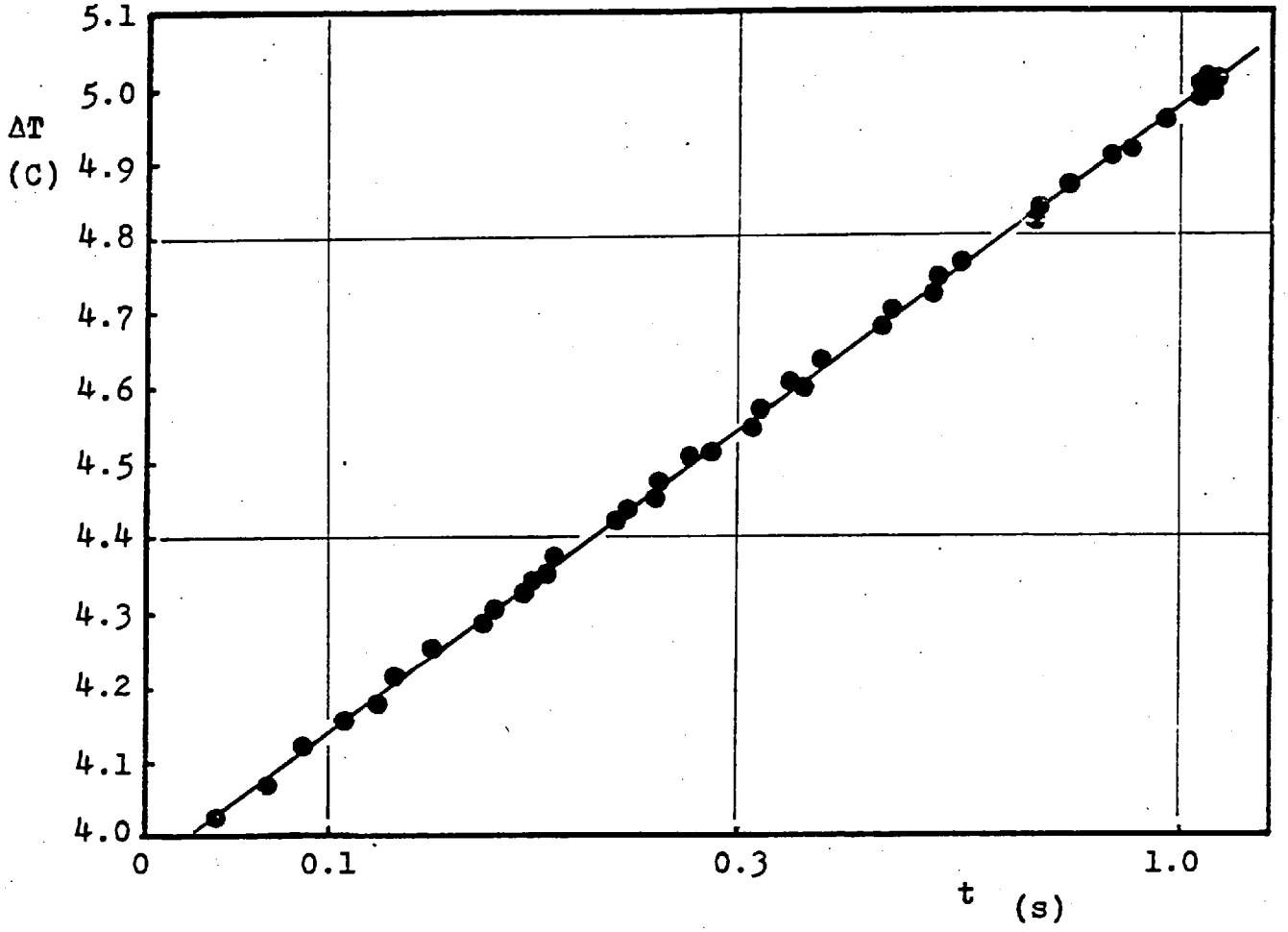

Figure 21 . Temperature rise as a function of time
(Helium 5.71 MPa, 35 'C)

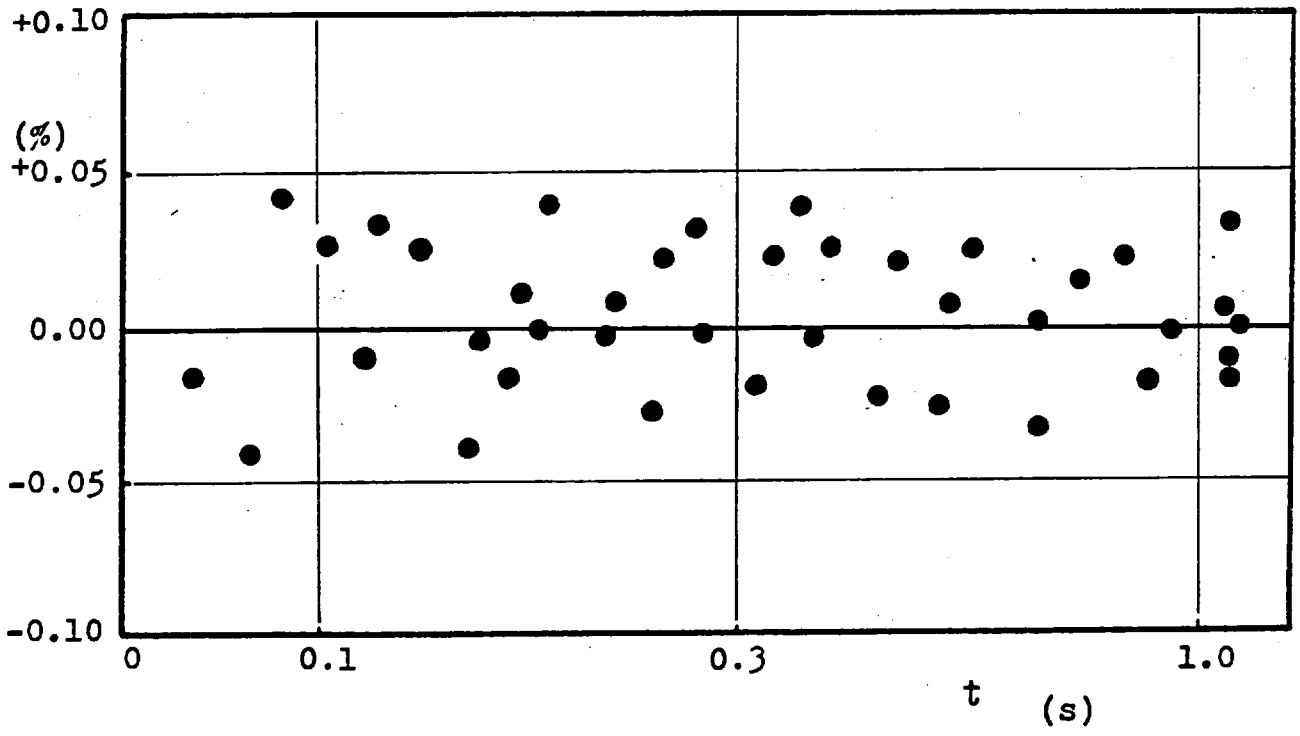

Figure 22 , Deviations from the ΔT versus lnt straight line
(Helium 5.71 MPa, 35 'C)

4.5. EQUIPMENT PERFORMANCE

The earlier discussion of the working equations has demonstrated that if the apparatus conforms exactly to the mathematical model of its operation the experimental values of the $\Delta T_{;d}$ vs lnt for a particular run should lie on a straight line. Since the mathematical description of the apparatus neglects entirely any convective heat transfer from the wire, the observation of the predicted linearity serves to establish that the experimental measurements are free from such effects. The overall, random error in the measured temperature rise of the wire owing to the bridge resolution and the accuracy of the bridge resistors is estimated to be $\pm$ 0.1% . Thus, it is expected that the deviations of the experimental points from a straight line should be randomnly distributed and should not exceed $\pm$ 0.1%. Figure 21 ,p.100 , shows a direct plot of the corrected temperature rise $\Delta T_{;d}$ against lnt for a typical experimental run in Helium at 35 °C and a pressure of 5.71 MPa in order to illustrate the straightness of the line. In this Figure, the deviations of the points from the least-squares fitted straight line have been multiplied by a factor of twenty to make them visible. Figure 22 , shows a deviation plot for the same results and it is seen that the deviations are indeed randomly distributed with a maximum deviation of only $\pm$ 0.05%. This is taken as conclusive evidence for the correct operation of our equipment.

It is estimated that the random error in the thermal conductivity of the gas, derived from straight lines such as that of Figure 21 , is $\pm$ 0.1%. Including a possible error in the temperature coefficient of resistance of the platinum wires to which the reported thermal conductivities are proportional, the overall accuracy of the thermal conductivity is estimated as $\pm$ 0.2%.

Occasionally measurements on Helium and Argon were repeated as a check on the continued satisfactory performance of the instrument. Such measurements produced results that did not deviate from the original ones by more than $\pm$ 0.15% (see Figure 38,p.141). Furthermore, measurements performed on Helium with a completely different set of wires yielded results which differed by not more than $\pm$ 0.25%. Thus, the overall accuracy of the reported thermal conductivity values is believed to be $\pm$ 0.2%.

• FIVE

RESULTS

5. INTRODUCTION

In the previous Chapters it has been demostrated how the equipment described in this thesis can be used to perform accurate measurements of the thermal conductivity of gases . In this Chapter results for the thermal conductivity of nine pure gases and eighteen binary mixtures at 35 'C and within the pressure range 1 - 10 MPa will be presented. In the interests of clarity a discussion of the interpretation of the results in terms of the theories presented in Chapter 2,is given in the next Chapter.

5.1. RESULTS

The nine pure gases studied in this work and their purity are listed in Table 6 ,p.102, while the eighteen binary mixtures in Table 7 ,p.103 . The measurements have been carried out at 35'C and up to a pressure of 10 MPa. The lowest pressure at which measurements have been performed has been set by the need to avoid significant Knudsen temperature jump effects (§3.3.2.,p.64).

Table 6 .

Gas	Purity %	Supplier
Helium	99.9992	B.O.C.
Neon	99.9995	B.O.C.
Argon	99.9997	B.O.C.
Krypton	99.97	B.O.C.
Xenon	99.997	B.O.C.
Hydrogen	99.999	B.O.C.
Methane	99.99	B.O.C.
Nitrogen	99.9992	B.O.C.
Carbon Monoxide	99.995	Matheson

Table 8 ,p.103,presents the characteristics of the thermal conductivity cells used to perform these measurements. The results for the thermal conductivity of the

Table 7 .

Mixture	Molefraction
He/Ne	$x_{He} = 0.2172$
	$x_{He} = 0.4662$
	$x_{He} = 0.6823$
	$x_{He} = 0.7156$
Ar/Kr	$x_{Ar} = 0.4088$
	$x_{Ar} = 0.7059$
H_2/Ne	$x_{H_2} = 0.2699$
	$x_{H_2} = 0.5168$
	$x_{H_2} = 0.7182$
H_2/Ar	$x_{H_2} = 0.2614$
	$x_{H_2} = 0.4847$
	$x_{H_2} = 0.6402$
	$x_{H_2} = 0.7504$
H_2/Kr	$x_{H_2} = 0.4795$
	$x_{H_2} = 0.7312$
H_2/N_2	$x_{H_2} = 0.2136$
	$x_{H_2} = 0.4865$
	$x_{H_2} = 0.7338$

pure gases are contained in Tables 9 to 17 ,p.107 to 123 , and for the mixtures in Tables 18 to 27 ,p.125 to 139. Each Table is followed by a Figure showing the thermal conductivity of the particular gas as a function of the density. In every Table the initial conditions prior to a measurement, i.e. pressure P, temperature T_o, and density ρ_o, as well as the reference conditions, temperature T_r and density are reported. The thermal conductivity $\lambda(T_r)$ is then given at the reference temperature. In addition, the thermal conductivity corrected to a nominal temperature T_n = 35 °C is given $\lambda(T_n)$. The correction to the nominal temperature has been carried out with the aid of the following equation :-

$$\lambda(T_n,\rho_r) = \lambda(T_r,\rho_r) + \left(\frac{\partial\lambda}{\partial T}\right)_{\rho_r} (T_n - T_r) \qquad (5.1)$$

For the purpose of this correction it has been assumed that

Table 8 .

The characteristics of the thermal conductivity cells

Length of the long cell	230.0 mm
Length of the short cell	134.0 mm
Internal diameter of the cell	11.05±0.01 mm
Length of the long wire	158.96±0.02 mm
Length of the short wire	63.80±0.02 mm
Long wire resistance @ 35°C	423.928±0.005 Ohm
Short wire resistance @ 35°C	172.493±0.005 Ohm
Platinum wire radius	3.89 ±0.01 μm

the derivative $(\partial\lambda/\partial T)_{\rho_r}$ is independent of the density and equal to the derivative in the limit of zero density (this will be discussed later in this section). In the case of the pure monatomic gases the latter derivative has been obtained directly from the corresponding temperature derivative of the viscosity [60] . For pure polyatomic gases the Hirschfelder-Eucken relation (2.162) was used. For the binary mixtures of monatomic gases the derivative has been estimated from the appropriate kinetic theory formulae and the universal functionals of the extended principle of corresponding states [58] , while for binary polyatomic mixtures the Mason-Monchick approximation (§2.4.2.,p.47) was used. Since the corrections amount to no more than 0.5% in any case the additional uncertainty introduced to the reported thermal conductivity at the nominal temperature is negligible. The value of the derivative $(\partial\lambda/\partial T)_{\rho_r}$ is included at the foot of each Table.

The entire set of experimental thermal conductivity data for each gas at the nominal temperature has been subjected to a statistical analysis to determine the values of the coefficients and c_i's in the density expansion of the thermal conductivity:-

$$\lambda(\rho) = \lambda^{\circ} + c_1\cdot\rho + c_2\cdot\rho^2 + c_3\cdot\rho^3 + c_2'\cdot\rho^2\cdot\ln\rho + \ldots \qquad (5.2)$$

The first five data points starting from the low density region are fitted to a linear expression in density and the coefficients λ° and c_i , their variance and the standard deviation of the whole fit are recorded. The procedure is then repeated including one more data point and continued until the standard deviation of the fit passes through a stationary point. This provides us with the range of densities where the linear fit is applicable. The whole operation is repeated for a quadratic, a cubic and a logarithmic fit.

In this way we determine the values of the coefficients λ_o and c_i's for each order of density expansion. If the data points conform to such an expansion, the coefficients λ_o and c_i's should be identical within their variance, among the fits for various orders of expansion. The logarithmic term c_2' , was always found insignificant for the density range studied here and it is not considered further. The remaining coefficients are listed for each order of expansion in Tables 28 to 31 ,p.139 to 152 .

Figures 38 to 42 ,p.141 to 145 , contain the deviations of the

present experimental data from the expansion of equation (5.2) covering the entire density range. With the exception of Xenon the maximum deviation of the present experimental data from the expansion does not exceed ±0.2%. For Xenon, where the gas is relatively close to its critical point, so that both the thermal conductivity measurements and the determination of the density are more uncertain, the maximum deviation is ±0.3%. The above Figures include the results of the independent measurements of Kestin et al.[42,51] for the pure gases, carried out with a similar apparatus at 27.5°C with an estimated accuracy of ±0.2%. We specifically exclude the earlier relative measurements of de Groot et al. [39] owing to their small systematic error. The deviation between the two sets of results do not exceed 0.4%, which is equivalent to the combined uncertainty of the data. For Xenon up to a density of 180 Kg/m^3 this remains true, but above this density the measurements of Kestin et al. deviate systematically upwards. This can be seen more easily if one examines the behaviour of the excess thermal conductivity for Xenon compared with other gases.

In the correction of our experimental results for the pure gases to a nominal temperature it was assumed that the excess thermal conductivity $\Delta\lambda$ of a dense gas is independent of the density. That is ,

$$\Delta\lambda = \lambda(\rho) - \lambda(0) = f(\rho) \text{ only} \qquad (5.3)$$

In order to substantiate this hypothesis, at least over small temperature ranges, we have plotted in Figures 46 and 47 p.153to 154 the excess thermal conductivity for the pure gases determined in this work at 35 °C as a function of density. The same Figures include the experimental data of Kestin et al. at 27.5 °C [42,51] [52], and the NEL data at 38.0 °C, 70.0 °c and 113.0 °C [119,120]. This method of comparison has the advantage that small, residual systematic discrepancies between the two sets of measurements and the present results are removed. The Figures demonstrate that the excess thermal conductivity for all gases but Xenon is indeed independent of temperature. In the case of Xenon the temperature independence of the excess thermal conductivity is preserved up to a density of 180 Kg/m^3 above which the values at the lower temperature of Xenon increase significantly more rapidly. The critical temperature of Xenon is 16.6 °C and its critical density

is 1155 Kg/m^3 . The enhanced thermal conductivity at elevated densities for the lower temperature is therefore almost certainly due to that arising from the tail of the critical point enhancement[137].

Figures 38 to 42 also show that results of earlier work deviate from the present correlations by as much as 4%, with the exception of the results of Michels et al. [126] , Tufeu et al. [43,56] and Haarman [36] that generally lie within ±2% of the present data.

For the mixtures deviations of the experimental data points from the equation (5.2) are shown in Figures 43 to 45 ,p.146 to148. Comparisons, however, with other data are omitted because a direct comparison with the few earlier measurements is more difficult.

In conclusion, the present experimental data for the pure gases and the mixtures studied are to be preferred to the earlier results owing to their higher accuracy.

Table 9 .

Thermal Conductivity of Helium @ T_n = 35 'C

P MPa	T_o 'C	ρ_o Kg/m^3	T_r 'C	ρ_r Kg/m^3	$\lambda(T_r)$ mW/m/C	$\lambda(T_n)$ mW/m/C
3.51	33.28	5.42	37.91	5.34	160.87	159.85
4.17	32.95	6.43	37.62	6.34	160.96	160.05
4.91	32.70	7.56	37.46	7.45	160.97	160.10
5.64	32.55	8.67	37.07	8.54	161.28	160.56
6.32	31.72	9.70	36.23	9.56	161.35	160.92
7.13	33.33	10.86	37.74	10.71	162.10	161.14
7.84	32.71	11.91	37.16	11.75	162.14	161.38
8.45	31.46	12.93	35.91	12.76	162.16	161.84
9.38	31.26	14.24	34.82	14.08	162.10	162.16
10.06	30.98	15.23	34.50	15.06	162.03	162.20
10.73	30.14	16.24	33.69	15.98	162.27	162.73

$(\partial\lambda/\partial T)_{35\,^{\circ}C}$ = 0.350 mW/m/C^2

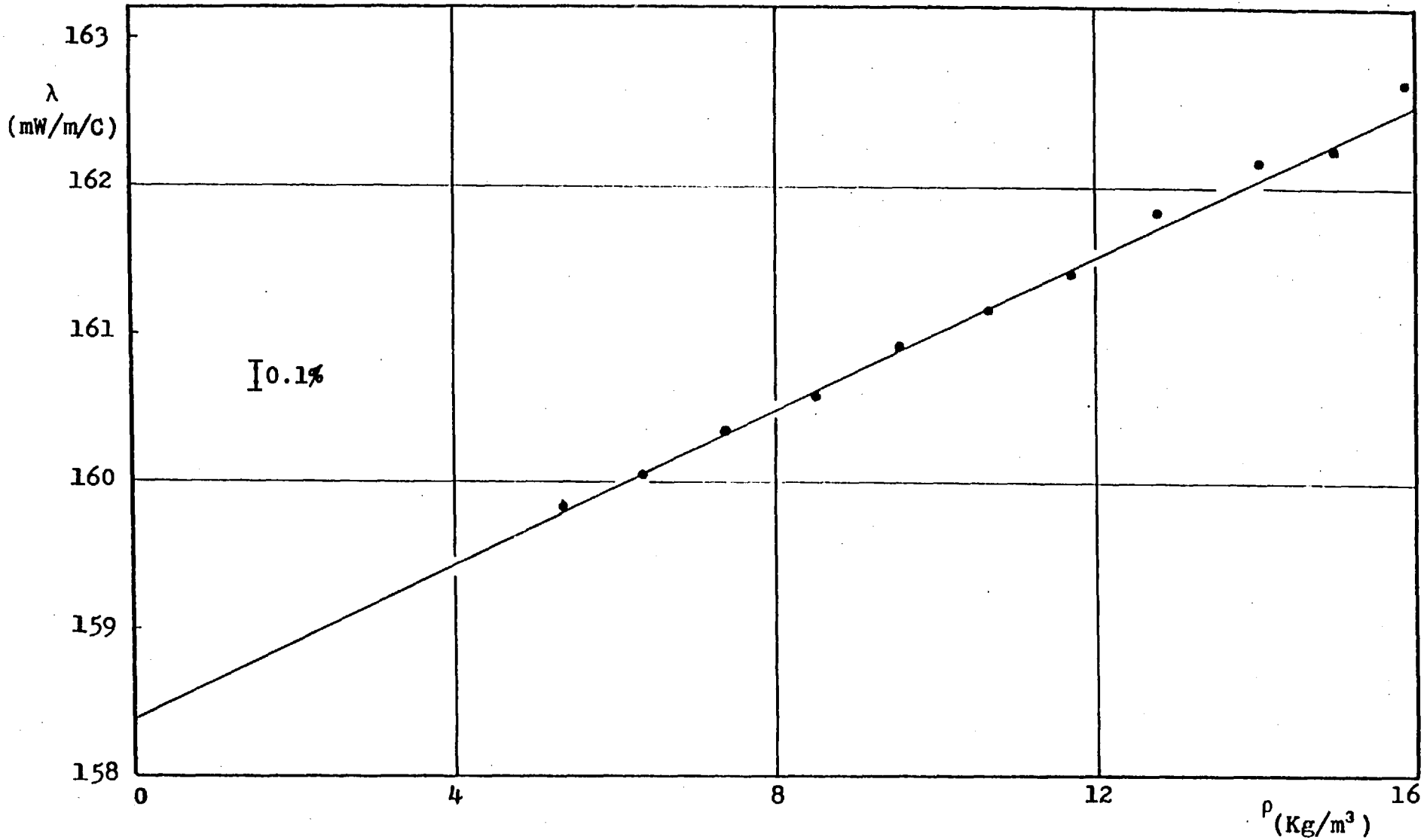

Figure 23 . Thermal Conductivity of Helium as a function of density at 35.0 °C

Table 10.

Thermal Conductivity of Neon @ T_n = 35 'C

P MPa	T_o 'C	ρ_o Kg/m^3	T_r 'C	ρ_r Kg/m^3	$\lambda(T_r)$ mW/m/C	$\lambda(T_n)$ mW/m/C
1.44	32.05	11.37	37.26	11.18	51.04	50.79
2.15	31.57	17.00	34.64	16.73	51.07	51.11
2.93	30.70	23.08	35.65	22.71	51.42	51.35
3.63	30.72	28.53	35.60	28.08	51.54	51.48
4.36	32.00	34.01	36.66	33.51	51.80	51.61
5.01	31.81	38.97	36.50	38.39	52.04	51.87
5.71	31.70	44.32	36.27	43.67	52.20	52.06
6.40	31.39	49.56	35.88	48.85	52.48	52.38
7.13	30.73	55.15	35.26	54.35	52.52	52.49
7.74	30.32	59.75	34.68	58.92	52.66	52.70
8.48	31.34	65.06	35.81	64.14	52.95	52.86
9.31	30.85	71.24	35.22	70.27	53.18	53.15
9.92	29.93	75.90	34.33	74.84	53.12	53.19
10.62	29.68	81.08	33.98	79.98	53.40	53.51

$(\partial\lambda/\partial T)_{35\cdot C}$ = 0.111 mW/m/C^2

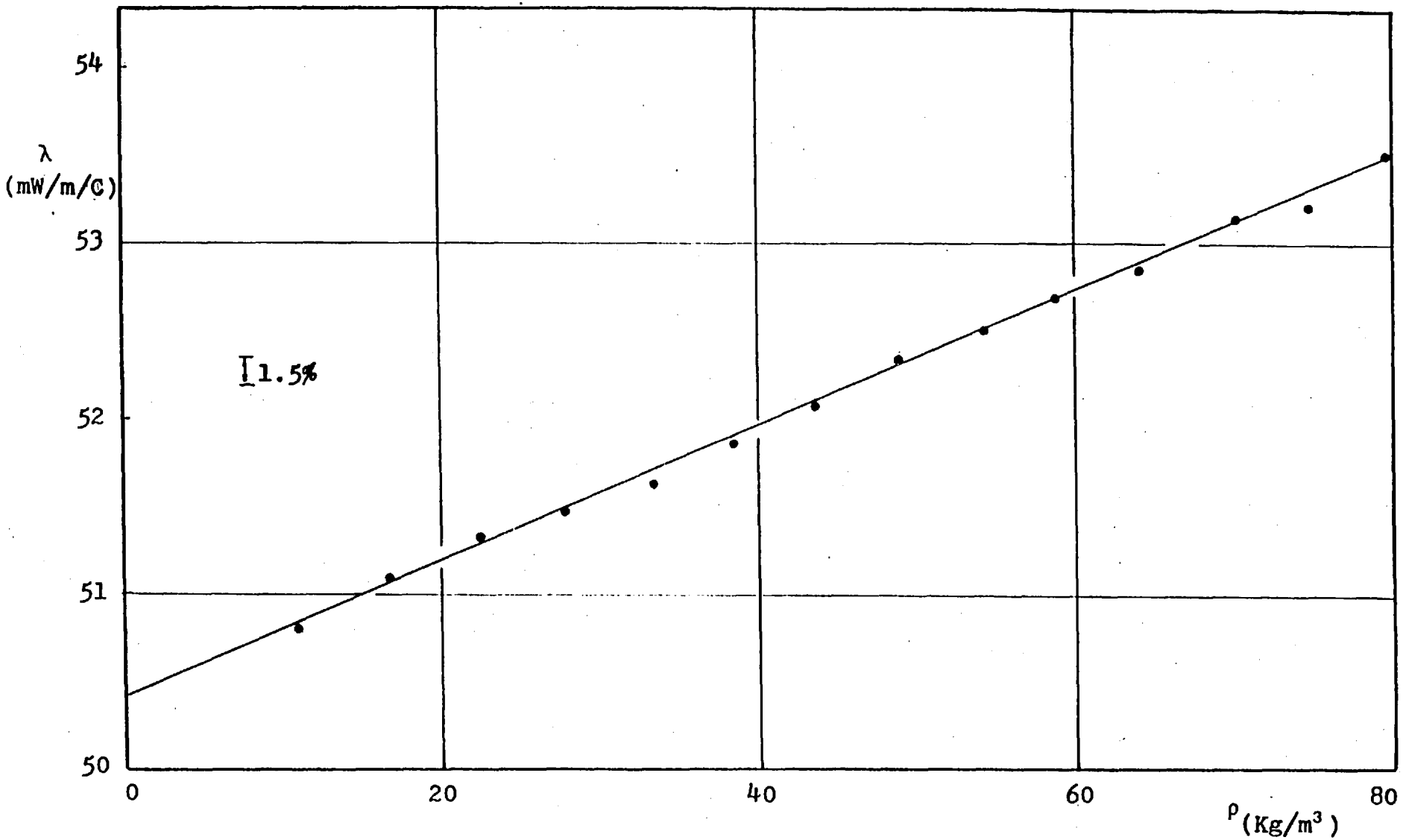

Figure 24 . Thermal Conductivity of Neon as a function of density at 35.0 °C

Table 11.

Thermal Conductivity of Argon @ T_n = 35 °C

P MPa	T_o °C	ρ_o Kg/m^3	T_r °C	ρ_r Kg/m^3	$\lambda(T_r)$ mW/m/C	$\lambda(T_n)$ mW/m/C
0.95	30.73	15.08	37.05	14.76	18.64	18.54
1.24	30.60	19.84	36.76	19.42	18.75	18.66
1.62	30.29	25.40	36.34	24.88	18.84	18.77
1.94	29.11	31.08	34.99	30.46	18.92	18.92
2.28	28.58	36.87	34.42	36.12	9.01	19.04
2.62	28.36	42.43	34.88	41.59	19.17	19.19
2.98	30.14	48.01	35.65	47.07	19.39	19.36
3.34	29.84	53.93	35.33	52.87	19.47	19.45
3.78	29.63	61.22	34.32	60.05	19.66	19.66
4.19	29.73	67.91	34.25	66.62	19.85	19.81
4.60	29.40	74.85	34.53	73.43	20.00	20.02
4.97	29.20	80.99	34.26	79.45	20.13	20.16
5.24	29.22	85.61	34.13	84.00	20.24	20.29
5.77	31.01	93.68	35.96	91.94	20.52	20.47
6.25	31.12	101.67	35.83	99.84	20.71	20.67
6.69	30.99	109.08	35.81	107.05	20.91	20.87
7.21	30.84	117.91	35.55	115.74	21.15	21.12
7.61	30.66	124.71	35.19	122.47	21.31	21.30
7.94	30.28	130.24	34.77	127.90	21.44	21.45
8.39	29.82	138.16	34.27	135.68	21.60	21.64
8.77	29.70	144.76	34.08	142.18	21.86	21.90
9.12	30.39	150.16	34.68	147.53	21.98	22.00
9.34	29.31	154.59	33.56	151.87	22.02	22.09
9.72	29.44	161.06	33.68	158.21	22.29	22.36
10.11	31.01	166.49	35.20	163.59	22.44	22.43
10.49	30.45	173.40	34.47	170.48	22.68	22.71
10.86	30.04	179.78	34.03	176.74	22.85	22.89

$(\partial\lambda/\partial T)_{35\,°C} = 0.050$ mW/m/C^2

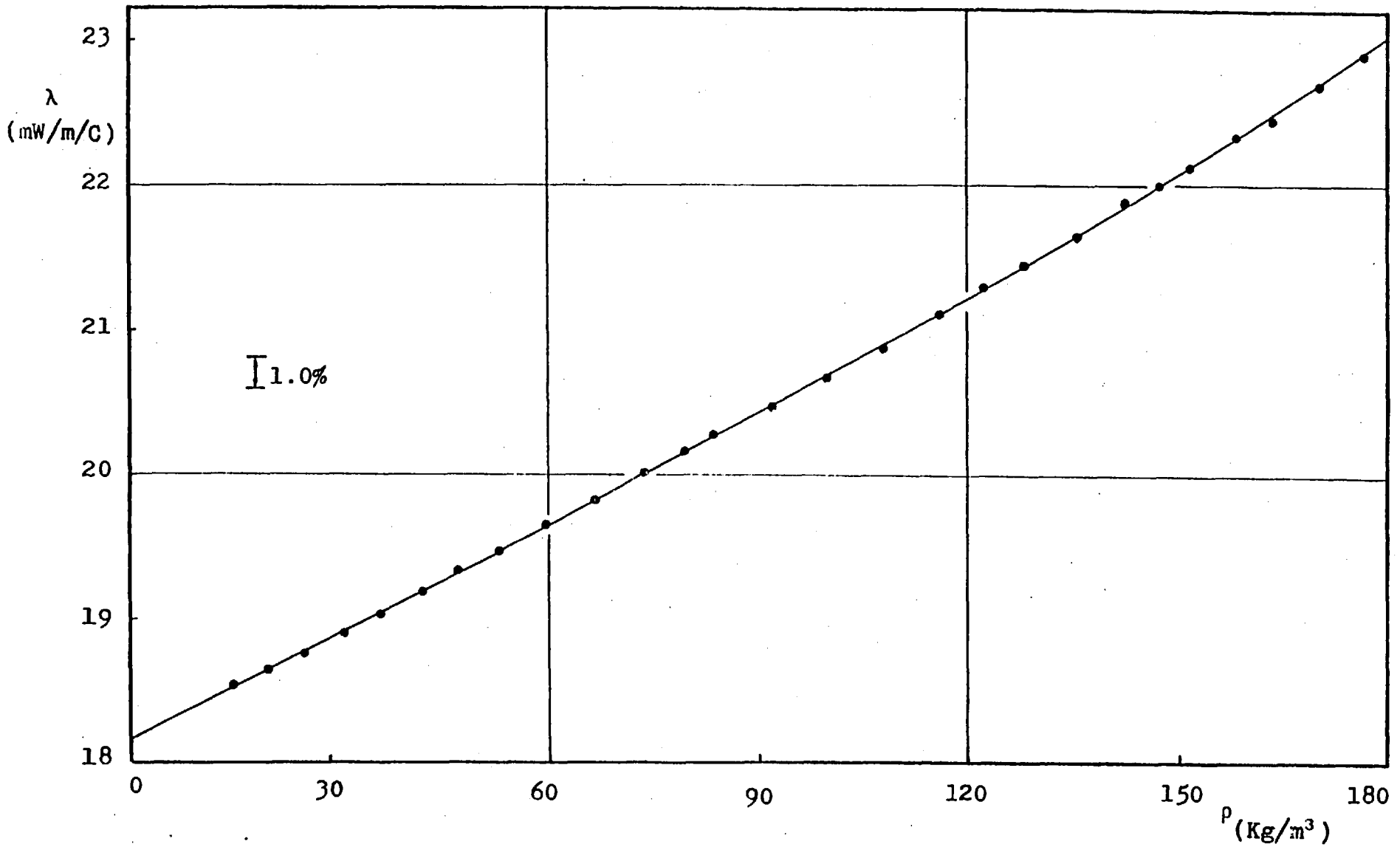

Figure 25 . Thermal Conductivity of Argon as a function of density at 35.0 °C

Table 12.

Thermal Conductivity of Krypton @ T_n = 35 'C

P MPa	T_o 'C	ρ_o Kg/m^3	T_r 'C	ρ_r Kg/m^3	$\lambda(T_r)$ mW/m/C	$\lambda(T_n)$ mW/m/C
1.01	29.35	34.37	35.68	33.63	10.03	10.04
1.46	29.27	50.30	35.31	49.23	10.20	10.19
1.94	29.40	68.96	35.17	67.51	10.37	10.37
2.46	29.41	86.02	34.87	84.25	10.58	10.55
2.97	29.37	104.98	34.71	102.79	10.69	10.70
3.39	29.32	121.18	34.47	118.68	10.96	10.91
3.96	29.29	143.05	34.27	140.08	11.16	11.18
4.44	29.62	161.88	34.45	158.52	11.35	11.36
4.93	29.18	181.65	33.87	177.87	11.57	11.60
5.52	29.32	205.96	33.82	201.68	11.82	11.86
6.03	29.50	227.25	33.83	222.56	12.04	12.07
6.55	29.30	249.71	33.50	244.54	12.30	12.35
7.07	29.25	272.78	33.33	267.10	12.57	12.62
7.62	29.20	297.27	33.12	291.12	12.90	12.96
8.24	34.51	316.28	38.30	309.91	13.22	13.13
8.69	34.31	337.03	37.93	330.32	13.56	13.48
9.48	33.52	374.63	36.97	367.19	13.99	13.93

$(\partial\lambda/\partial T)_{35\cdot C}$ = 0.028 mW/m/C^2

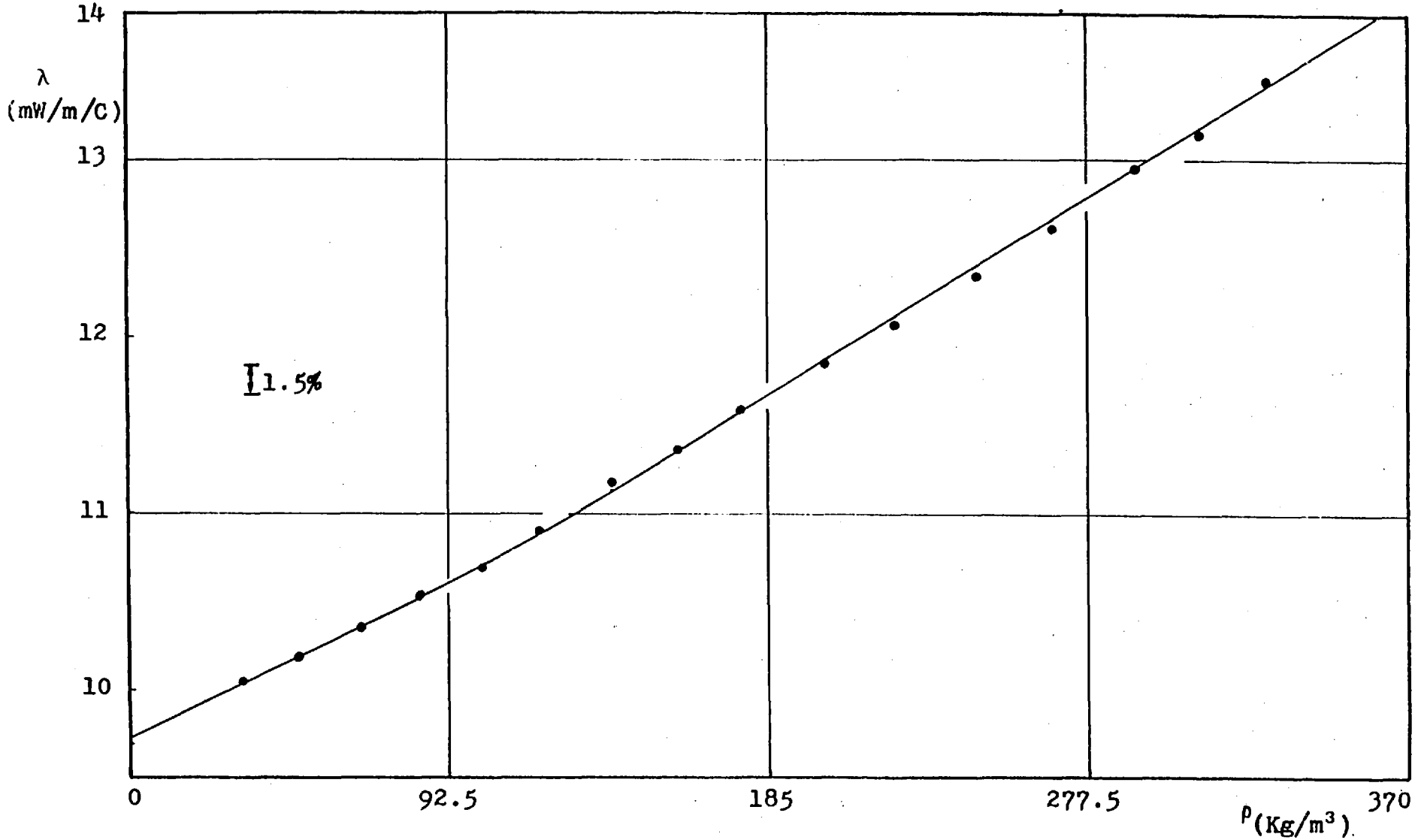

Figure 26 . Thermal Conductivity of Krypton as a function of density at 35.0 °C

Table 13.

Thermal Conductivity of Xenon @ T_n = 35 °C

P MPa	T_o °C	ρ_o Kg/m^3	T_r °C	ρ_r Kg/m^3	$\lambda(T_r)$ mW/m/C	$\lambda(T_n)$ mW/m/C
0.61	30.93	32.78	37.07	32.07	5.939	5.899
0.85	30.83	45.95	36.67	44.97	6.003	5.972
1.16	30.70	64.35	36.28	62.96	6.121	6.096
1.30	30.59	72.59	34.91	71.35	6.200	6.201
1.60	30.52	91.19	35.77	89.20	6.308	6.294
1.811	30.51	104.29	35.61	101.99	6.444	6.432
2.05	30.47	120.52	35.42	117.84	6.488	6.480
2.32	30.56	138.22	35.32	135.11	6.671	6.665
2.64	30.56	160.68	35.11	156.99	6.798	6.796
2.97	30.55	185.40	34.87	181.06	6.963	6.965
3.39	30.60	219.51	34.63	214.24	7.219	7.226
3.72	30.62	248.02	34.51	241.78	7.461	7.471
4.02	30.66	275.34	34.35	268.34	7.689	7.702
4.32	31.10	303.77	34.58	295.74	7.951	7.959
4.63	30.42	339.87	33.72	330.43	8.366	8.391

$(\partial\lambda/\partial T)_{35\,°C}$ = 0.019 mW/m/C^2

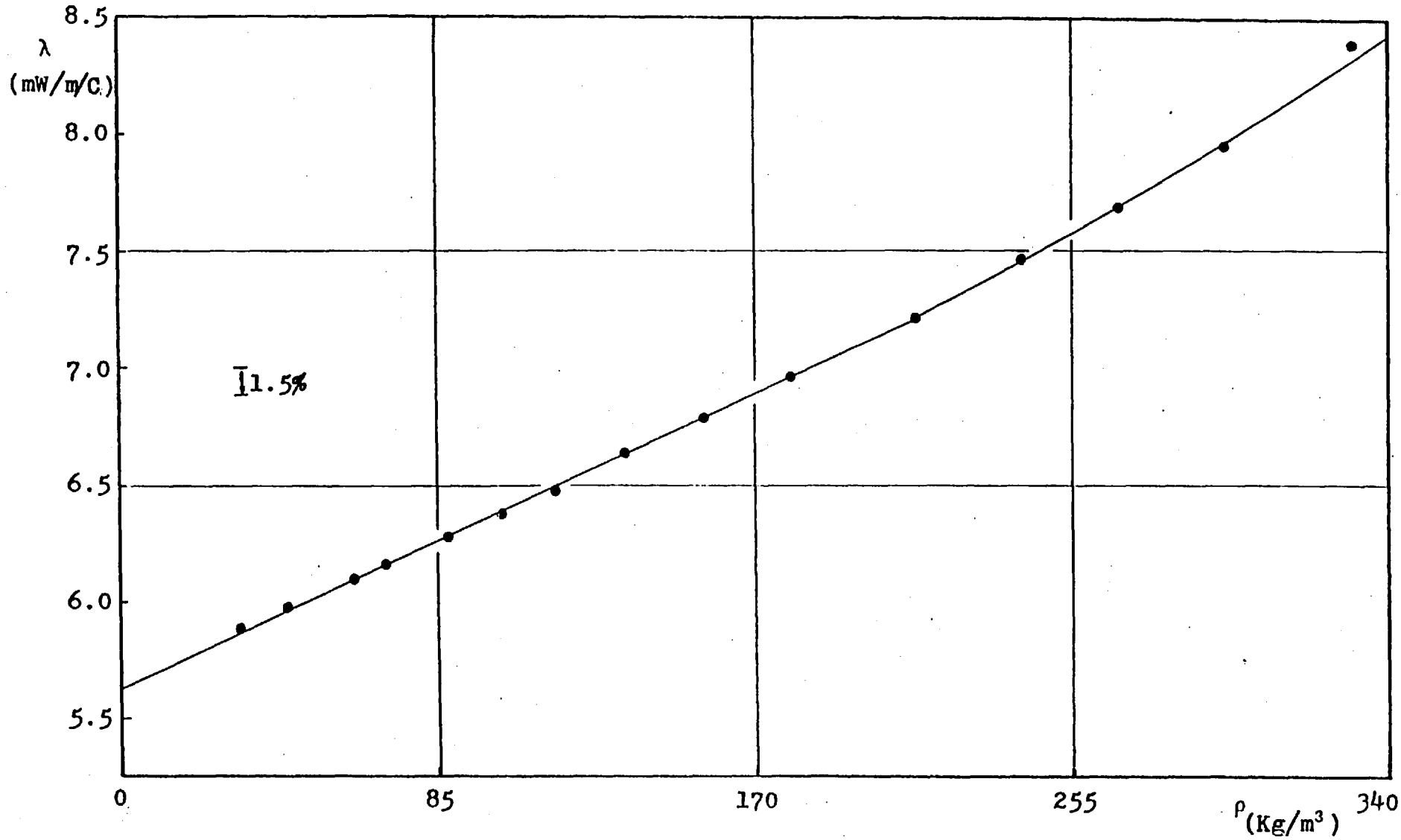

Figure 27 . Thermal Conductivity of Xenon as a function of density at 35.0 'C

Table 14.

Thermal Conductivity of Hydrogen @ T_n = 35 °C

P MPa	T_o °C	ρ_o Kg/m^3	T_r °C	ρ_r Kg/m^3	$\lambda(T_r)$ mW/m/C	$\lambda(T_n)$ mW/m/C
2.00	30.44	1.583	34.50	1.562	193.56	193.80
2.50	30.47	1.969	34.48	1.943	193.72	193.97
3.13	30.42	2.459	34.35	2.429	194.30	194.61
3.64	30.48	2.851	34.34	2.816	194.50	194.81
4.34	30.46	3.387	34.20	3.346	195.11	195.48
5.02	30.45	3.898	34.18	3.851	195.28	195.66
5.79	30.50	4.475	34.16	4.423	195.97	196.36
6.51	30.45	5.008	34.09	4.950	196.67	197.10
7.20	30.48	5.514	34.06	5.452	196.94	197.39
7.73	30.47	5.900	34.04	5.830	197.49	197.94
8.40	30.45	6.386	33.96	6.315	197.74	198.23
9.17	30.47	6.940	34.00	6.862	198.25	198.73

$(\partial\lambda/\partial T)_{35\,^\circ C}$ = 0.475 mW/m/C^2

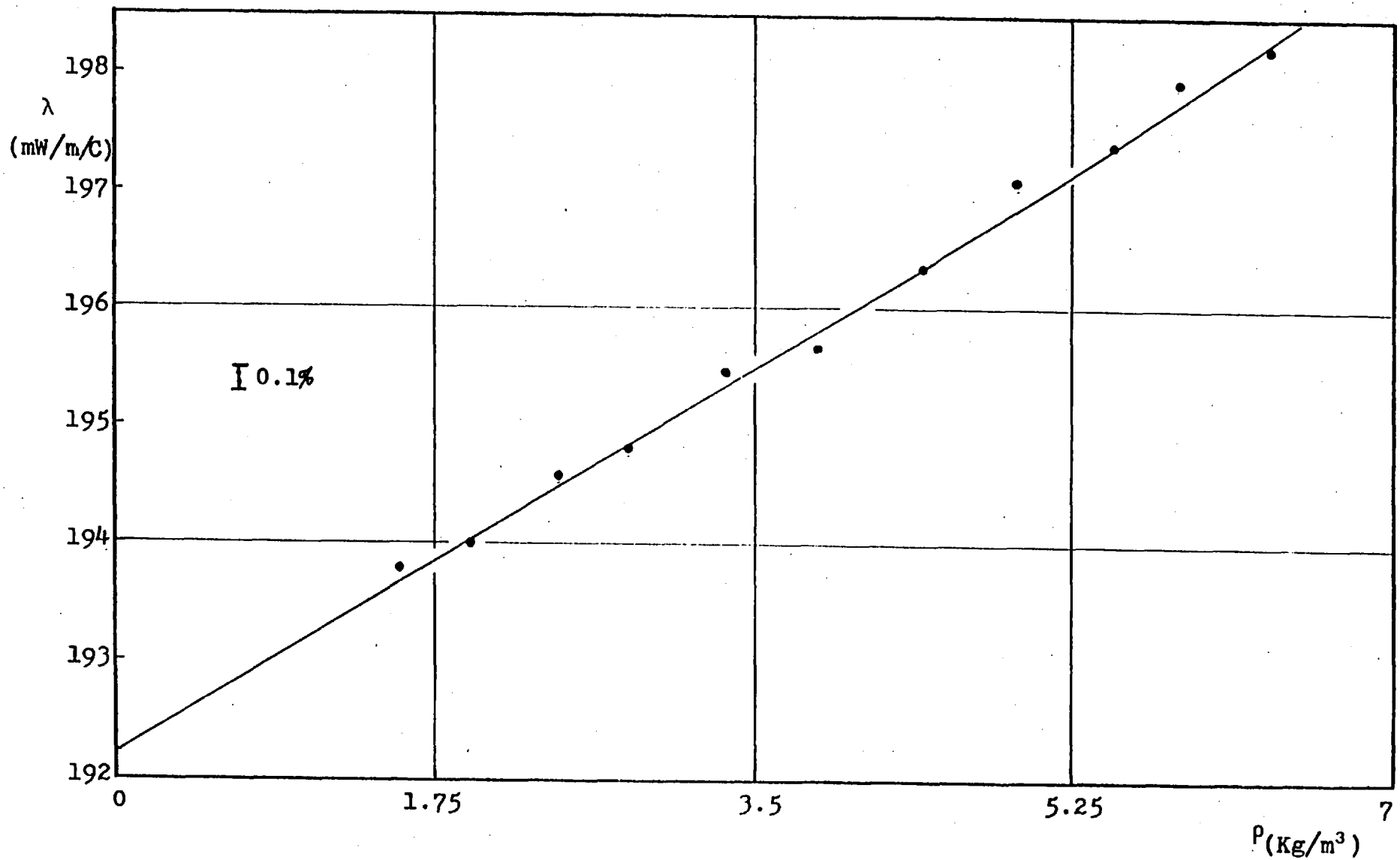

Figure 28 . Thermal Conductivity of Hydrogen as a function of density at 35.0 °C

Table 15.

Thermal Conductivity of Methane @ T_n = 35 °C

P MPa	T_o °C	ρ_o Kg/m^3	T_r °C	ρ_r Kg/m^3	$\lambda(T_r)$ mW/m/C	$\lambda(T_n)$ mW/m/C
1.84	30.43	12.05	34.33	11.88	36.45	36.51
2.60	30.41	17.24	34.12	17.00	37.01	37.09
3.31	30.43	22.25	34.00	21.94	37.62	37.71
3.93	30.41	26.68	33.88	26.30	38.09	38.19
4.48	30.41	30.68	33.81	30.25	38.62	38.73
5.06	30.40	34.96	33.67	34.47	39.22	39.35
5.79	30.41	40.44	33.58	39.87	39.99	40.12
6.48	30.41	45.71	33.47	45.06	40.78	40.92
7.12	30.42	50.62	33.42	49.89	41.53	41.68
7.81	30.41	56.04	33.72	65.86	42.71	42.74
8.36	30.42	60.42	33.58	59.16	43.39	43.43
8.79	30.42	63.85	33.51	62.51	44.00	44.04
9.27	30.41	67.74	33.37	66.35	44.65	44.71

$(\partial\lambda/\partial T)_{35\,^\circ C}$ = 0.092 mW/m/C^2

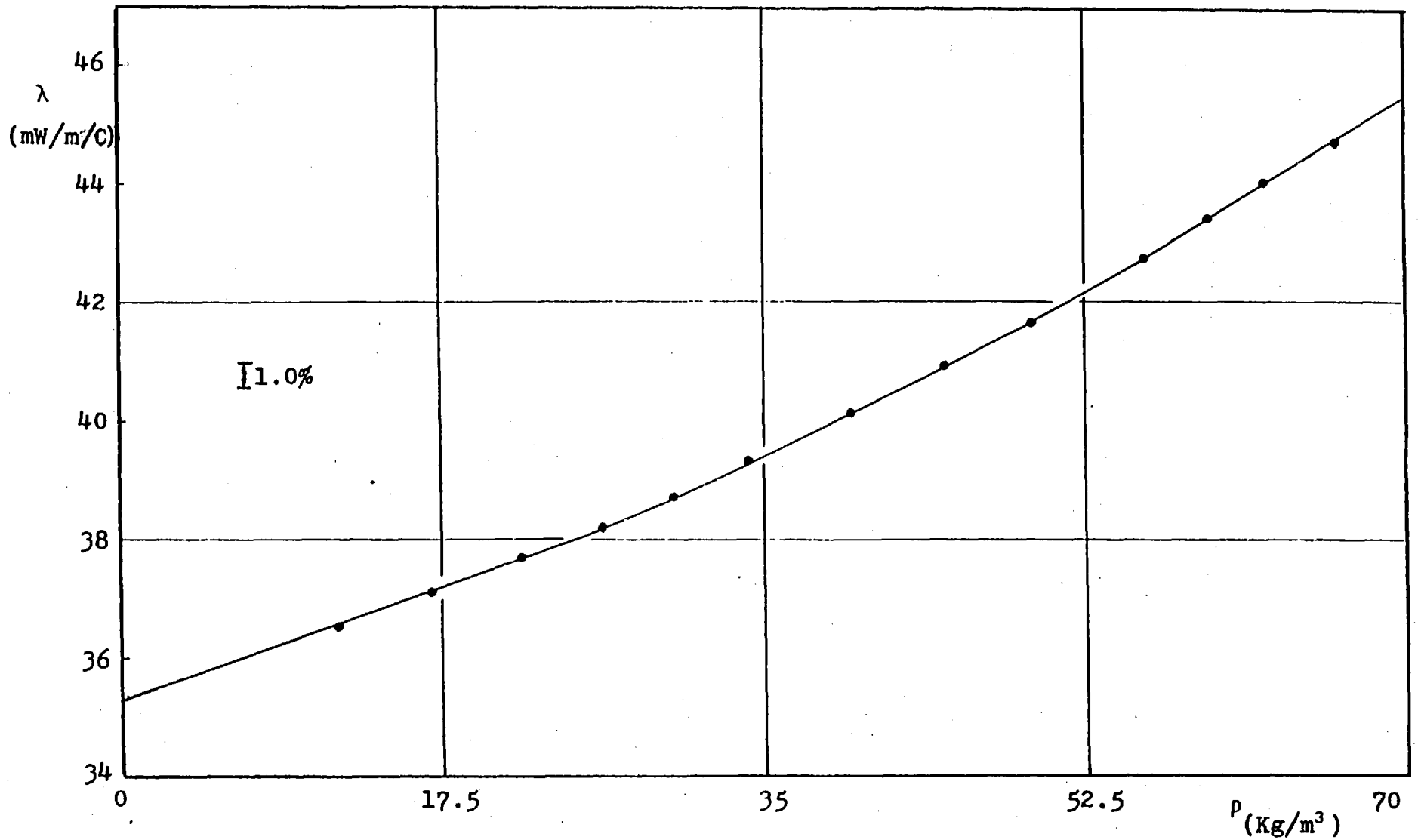

Figure 29 . Thermal Conductivity of Methane as a function of density at 35.0 'C

Table 16.

Thermal Conductivity of Nitrogen @ T_n = 35 °C

P MPa	T_o °C	ρ_o Kg/m^3	T_r °C	ρ_r Kg/m^3	$\lambda(T_r)$ mW/m/C	$\lambda(T_n)$ mW/m/C
1.07	30.46	11.85	36.02	11.64	26.96	26.90
1.55	30.48	17.30	35.84	16.99	27.09	27.04
2.00	30.49	22.21	35.69	21.83	27.21	27.16
2.58	30.49	28.75	35.51	28.25	27.49	27.52
3.15	30.47	35.04	35.38	34.45	27.74	27.72
3.64	30.45	40.57	35.21	39.90	28.02	28.01
4.19	30.44	46.71	35.14	45.94	28.24	28.23
4.76	30.43	52.99	35.01	52.13	28.58	28.58
5.35	30.47	59.57	34.82	58.64	28.78	28.79
5.92	30.51	65.81	34.93	64.77	29.14	29.15
6.45	30.45	71.62	34.67	70.52	29.35	29.37
6.98	30.47	77.53	34.63	76.35	29.66	29.69
7.41	30.43	82.24	34.51	81.01	29.87	29.90
7.84	30.42	86.94	34.45	85.64	30.14	30.18
8.32	30.44	92.20	34.40	90.84	30.42	30.46
8.76	30.43	97.01	34.33	95.60	30.65	30.69
9.03	30.43	100.00	34.32	98.55	30.84	30.88
9.31	30.41	103.00	34.23	101.53	30.97	31.02

$(\partial\lambda/\partial T)_{35\,^\circ C}$ = 0.063 mW/m/C^2

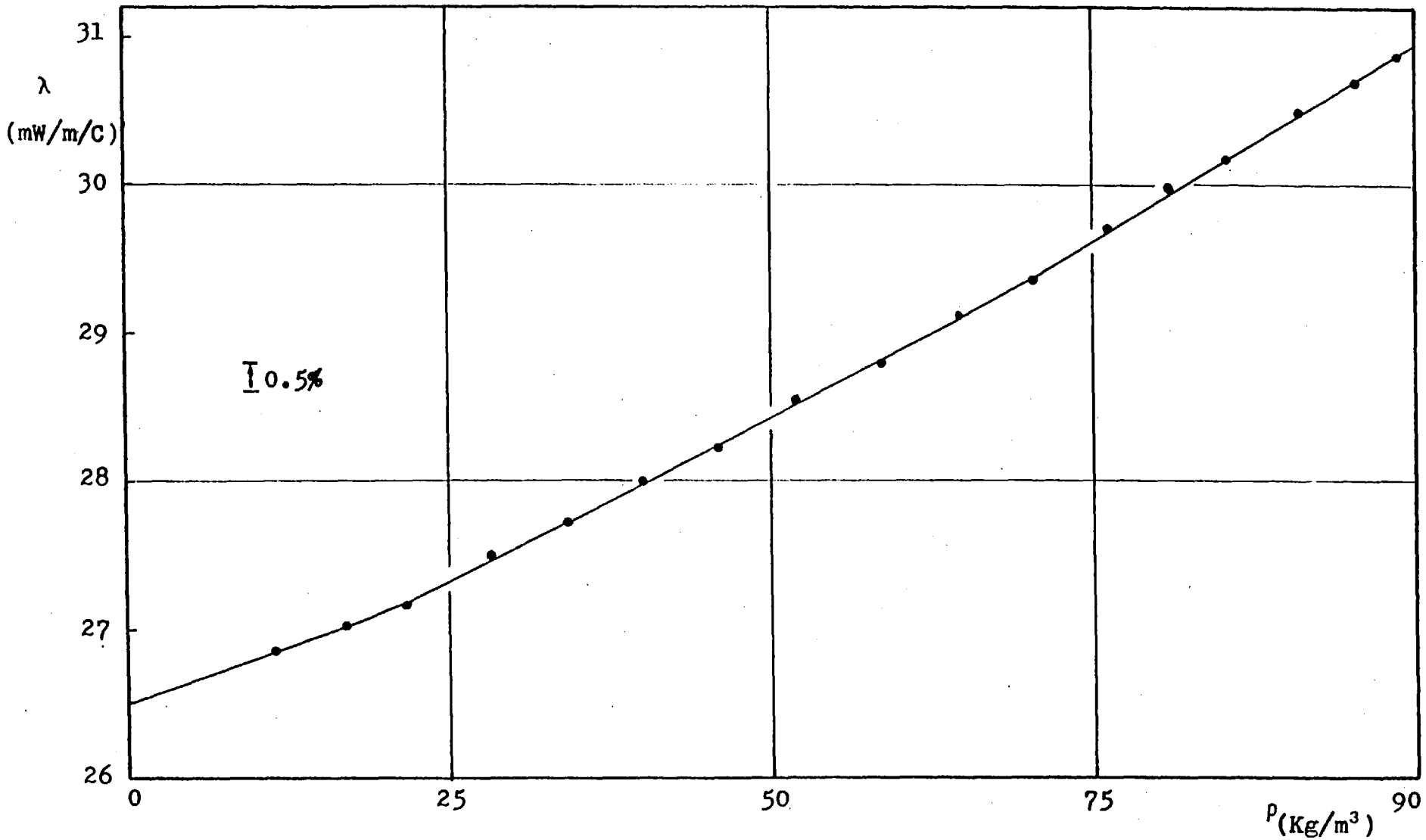

Figure 30 . Thermal Conductivity of Nitrogen as a function of density at 35.0 'C

Table 17 .

Thermal Conductivity of Carbon Monoxide @ T_n = 35 'C

P MPa	T_o 'C	ρ_o Kg/m^3	T_r 'C	ρ_r Kg/m^3	$\lambda(T_r)$ mW/m/C	$\lambda(T_n)$ mW/m/C
0.99	30.33	11.10	35.85	10.90	26 .21	26.16
1.68	30.34	18.73	35.52	18.40	26.45	26.42
2.28	30.34	25.44	35.36	25.01	26.72	26,70
3.31	30.33	37.04	35.10	36.42	27.12	27.12
4.42	30.32	49.42	34.89	48.61	27.67	27.68
5.01	30.31	56.07	34.89	55.17	27.90	27.92
5.78	30.30	64.72	34.62	63.69	28.37	28.39
6.46	30.29	72.27	34.52	71.14	28.61	28.64
7.27	30.29	81.34	34.40	80.08	29.02	29.06
8.00	30.26	89.45	34.28	88.09	29.44	29.48
8 75	30.29	97.68	34.16	96,21	29.84	29.89
9.43	30.19	105.26	34.05	103.69	30.11	30.17

$(\partial\lambda/\partial T)_{35\,^{\circ}C}$ = 0.060 mW/m/C^2

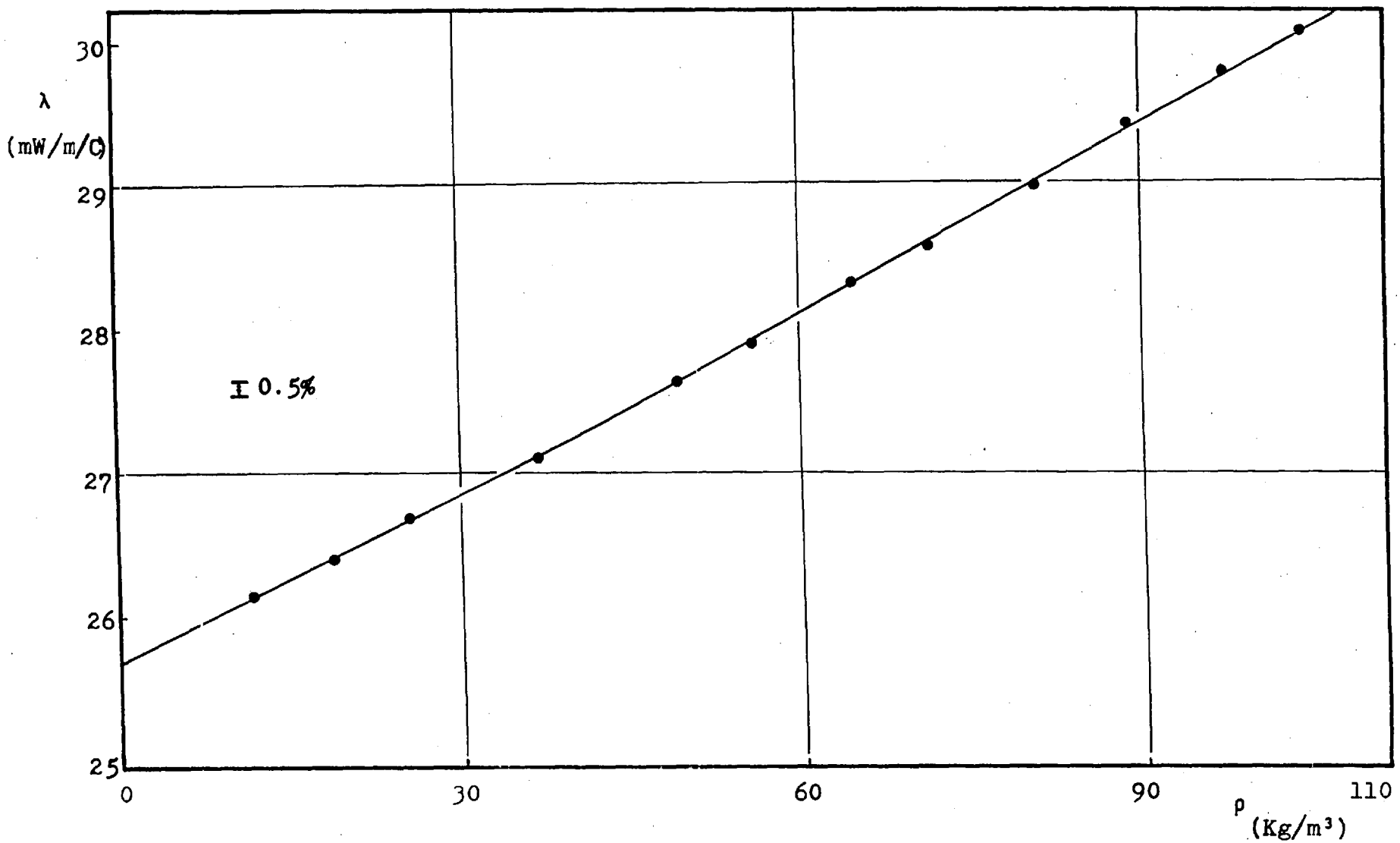

Figure 31 . Thermal Conductivity of Carbon Monoxide as a function of density at 35.0 °C

Table 18.

Thermal Conductivity of Helium/Neon @ T_n = 35 'C

P MPa	T_o 'C	ρ_o Kg/m^3	T_r 'C	ρ_r Kg/m^3	$\lambda(T_r)$ mW/m/C	$\lambda(T_n)$ mW/m/C
x_{He} = 0.2172						
1.53	30.39	9.77	36.17	9.60	63.90	63.72
2.02	30.37	12.83	36.03	12.61	63.82	63.67
2.71	30.40	17.46	35.93	17.15	64.07	63.93
3.33	30.39	21.51	35.84	21.14	64.23	64.11
3.63	30.44	24.60	35.76	24.19	64.12	64.00
4.43	30.42	28.15	35.71	27.68	64.58	64.47
5.02	30.41	32.06	35.61	31.54	64.60	64.51
5.74	30.41	36.32	35.55	35.73	64.78	64.70
6.55	30.37	41.39	35.45	40.72	64.91	64.84
7.53	30.33	47.45	35.34	46.71	65.51	65.46
					$(\partial\lambda/\partial T)_{35\,^{\circ}C}$ = 0.149 mW/m/C^2	
x_{He} = 0.4662						
2.03	30.44	9.18	35.47	9.04	83.72	83.63
2.29	30.41	11.17	35.39	10.99	83.64	83.56
2.60	30.34	12.84	35.27	12.64	83.88	83.82
3.22	30.41	15.75	35.25	15.51	83.89	83.84
3.91	30.49	18.97	35.24	18.69	83.90	83.86
4.44	30.50	21.56	35.88	21.20	84.33	84.15
5.05	30.46	24.37	35.80	23.96	84.60	84.43
5.75	30.45	27.65	35.70	27.19	84.45	84.32
6.53	30.43	31.43	35.58	30.92	84.81	84.69
7.49	30.41	36.03	35.49	35.45	84.87	84.77
					$(\partial\lambda/\partial T)_{35\,^{\circ}C}$ = 0.196 mW/m/C^2	

Table 19.

Thermal Conductivity of Helium/Neon @ T_n = 35 °C

P MPa	T_o °C	ρ_o Kg/m^3	T_r °C	ρ_r Kg/m^3	$\lambda(T_r)$ mW/m/C	$\lambda(T_n)$ mW/m/C
x_{He} = 0.6823						
2.11	30.48	7.57	34.93	7.46	107.49	107.51
2.43	30.38	8.80	34.82	8.67	107.54	107.59
2.78	30.08	9.98	34.47	9.84	107.42	107.69
3.16	29.74	11.36	34.09	11.20	107.57	107.80
3.59	29.70	13.03	33.99	12.85	107.65	107.91
4.14	29.84	14.88	34.09	14.68	107.62	107.85
4.76	29.85	17.09	34.03	16.87	107.81	108.06
5.53	29.84	19.79	33.99	19.53	108.08	108.33
6.94	29.83	22.24	33.88	21.96	108.22	108.50
7.49	29.96	26.69	33.95	26.36	108.85	109.12
					$(\partial\lambda/\partial T)_{35\,°C}$ = 0.256 mW/m/C^2	
x_{He} = 0.7156						
2.38	30.39	7.14	34.77	7.05	111.86	111.92
2.75	30.43	9.18	34.70	9.06	112.06	112.13
3.30	30.42	11.07	34.62	10.92	112.18	112.28
3.98	30.44	13.22	34.59	13.04	112.42	112.52
4.64	30.41	15.38	34.50	15.18	112.58	112.71
5.74	30.42	18.94	34.43	18.70	112.88	113.03
6.58	30.43	21.66	34.41	21.39	113.21	113.36
7.63	30.39	25.07	34.28	24.77	113.62	113.81
					$(\partial\lambda/\partial T)_{35\,°C}$ = 0.260 mW/m/C^2	

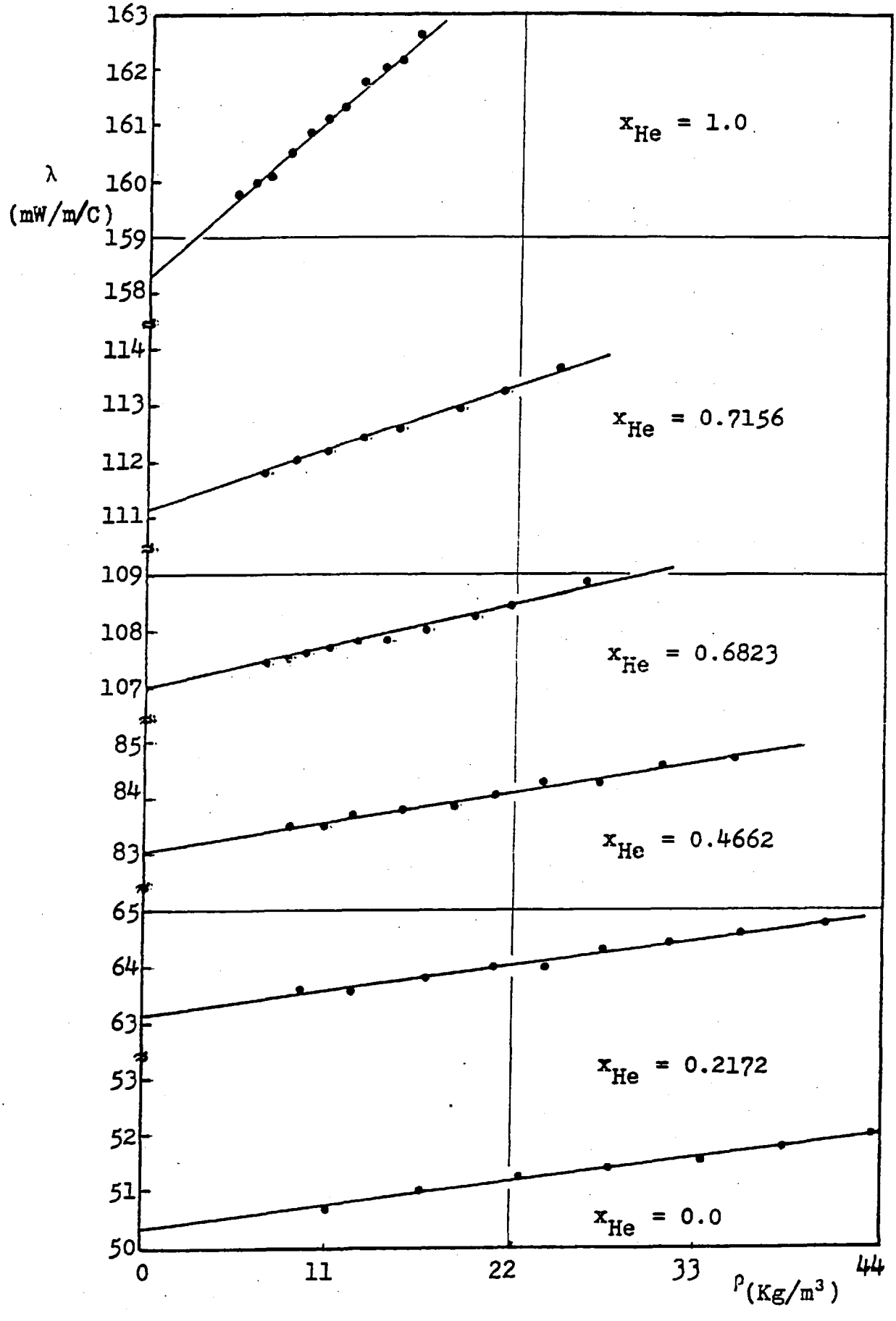

Figure 32. Thermal Conductivity of Helium/Neon mixture as a function of density at 35.0 'C

Table 20.

Thermal Conductivity of Argon/Krypton @ T_n = 35 °C

P MPa	T_o °C	ρ_o Kg/m^3	T_r °C	ρ_r Kg/m^3	$\lambda(T_r)$ mW/m/C	$\lambda(T_n)$ mW/m/C
x_{Ar} = 0.4088						
1.09	30.46	28.90	37.25	28.25	12.89	12.81
1.51	30.45	38.97	37.02	38.09	12.99	12.92
1.99	30.45	52.57	36.78	51.41	13.15	13.10
2.72	30.43	72.76	36.46	71.17	13.45	13.46
3.29	30.41	88.28	36.23	86.37	13.61	13.57
3.91	30.41	106.11	36.06	103.77	13.81	13.77
4.84	30.41	132.95	35.79	130.01	14.17	14.15
5.48	30.43	151.80	35.63	148.48	14.41	14.38
6.33	30.42	176.87	35.43	172.97	14.77	14.76
7.16	30.39	201.38	35.13	196.90	15.15	15.15
8.21	30.43	233.51	34.95	228.25	15.68	15.68
					$(\partial\lambda/\partial T)_{35\,°C}$ = 0.036	mW/m/C^2
x_{Ar} = 0.7059						
1.51	30.44	30.59	35.96	30.02	15.41	15.54
2.10	30.41	43.07	35.72	42.28	15.76	15.73
2.46	30.39	50.91	35.55	49.99	15.91	15.89
3.16	30.45	66.02	35.40	64.86	16.14	16.13
3.70	30.45	77.36	35.23	75.93	16.33	16.34
4.26	30.44	90.09	35.08	88.52	16.57	16.57
4.93	30.43	104.12	34.98	102.30	16.79	16.79
5.71	30.43	121.38	34.77	119.29	17.09	17.10
6.59	30.41	141.13	34.61	138.66	17.43	17.44
7.62	30.38	169.06	34.44	166.07	17.89	17.92
					$(\partial\lambda/\partial T)_{35\,°C}$ = 0.043	mW/m/C^2

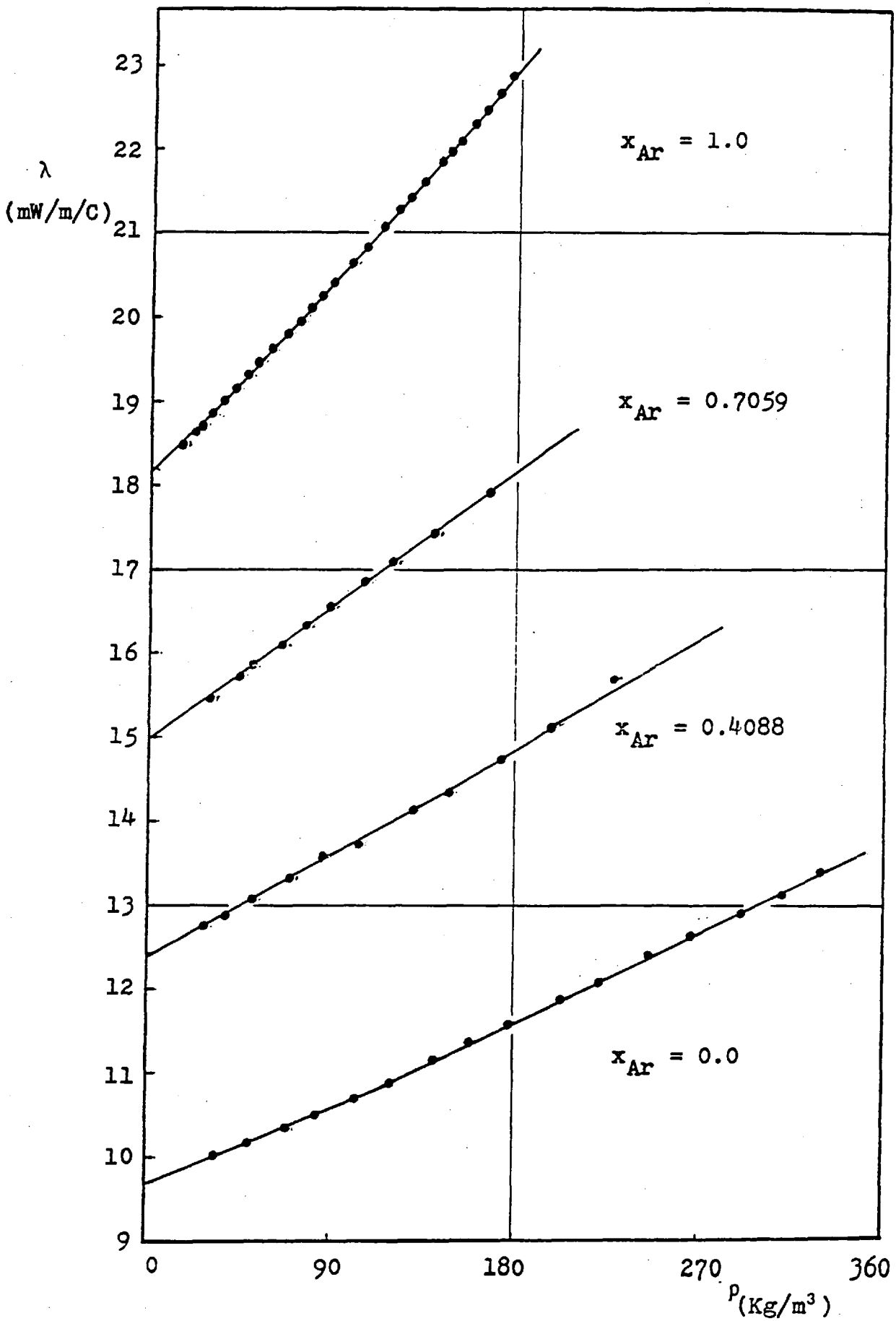

Figure 33 . Thermal Conductivity of Argon/Krypton mixture as a function of density at 35.0 °C

Table 21.

Thermal Conductivity of Hydrogen/Neon @ T_n = 35 °C

P MPa	T_o °C	ρ_o Kg/m³	T_r °C	ρ_r Kg/m³	$\lambda(T_r)$ mW/m/C	$\lambda(T_n)$ mW/m/C
x_{H_2} = 0.2699						
1.91	30.42	11.60	35.22	11.42	76.10	76.06
2.44	30.46	14.81	35.15	14.59	76.25	76.22
3.06	30.45	18.44	35.08	18.17	76.42	76.41
3.55	30.48	21.29	35.01	20.98	76.44	76.44
4.12	30.49	24.55	35.03	24.19	76.60	76.59
4.80	30.46	28.43	34.87	28.03	76.72	76.74
5.55	30.48	32.75	34.83	32.30	76.83	76.86
6.46	30.44	38.28	34.75	37.76	77.09	77.14
7.49	30.40	43.98	34.67	43.38	77.13	77.19
				$(\partial\lambda/\partial T)_{35\,°C}$ = 0.185 mW/m/C²		
x_{H_2} = 0.5168						
1.99	30.44	8.38	35.59	8.24	106.39	106.22
2.40	30.44	10.11	35.53	9.95	106.61	106.45
2.96	30.43	12.37	35.42	12.17	106.71	106.60
3.55	30.45	14.94	35.33	14.71	106.75	106.65
4.12	30.42	17.22	35.29	16.96	107.02	106.93
4.79	30.43	19.91	35.19	19.61	107.10	107.04
5.56	30.44	23.00	35.33	22.65	107.25	107.20
6.46	30.39	26.58	35.06	26.19	107.47	107.45
8.18	30.40	30.76	35.01	30.31	107.75	107.75
				$(\partial\lambda/\partial T)_{35\,°C}$ = 0.300 mW/m/C²		

Table 22.

Thermal Conductivity of Hydrogen/Neon @ T_n = 35 °C

P MPa	T_o °C	ρ_o Kg/m³	T_r °C	ρ_r Kg/m³	$\lambda(T_r)$ mW/m/C	$\lambda(T_n)$ mW/m/C
x_{H_2} =	0.7188					
2.20	30.48	5.975	34.98	5.890	138.07	138.08
2.79	30.48	7.632	34.89	7.526	138.11	138.15
3.33	30.47	9.135	34.82	9.010	138.30	138.37
3.89	30.50	10.53	34.73	10.39	138.40	138.49
4.51	30.48	12.24	34.75	12.07	138.54	138.64
5.24	30.51	14.15	34.72	13.96	138.71	138.81
6.10	30.50	16.33	34.67	16.11	139.11	139.23
7.11	30.48	18.92	34.58	18.68	139.39	139.55
8.12	30.47	21.20	34.48	20.93	139.60	139.80

$(\partial\lambda/\partial T)_{35\,°C}$ = 0.377 mW/m/C²

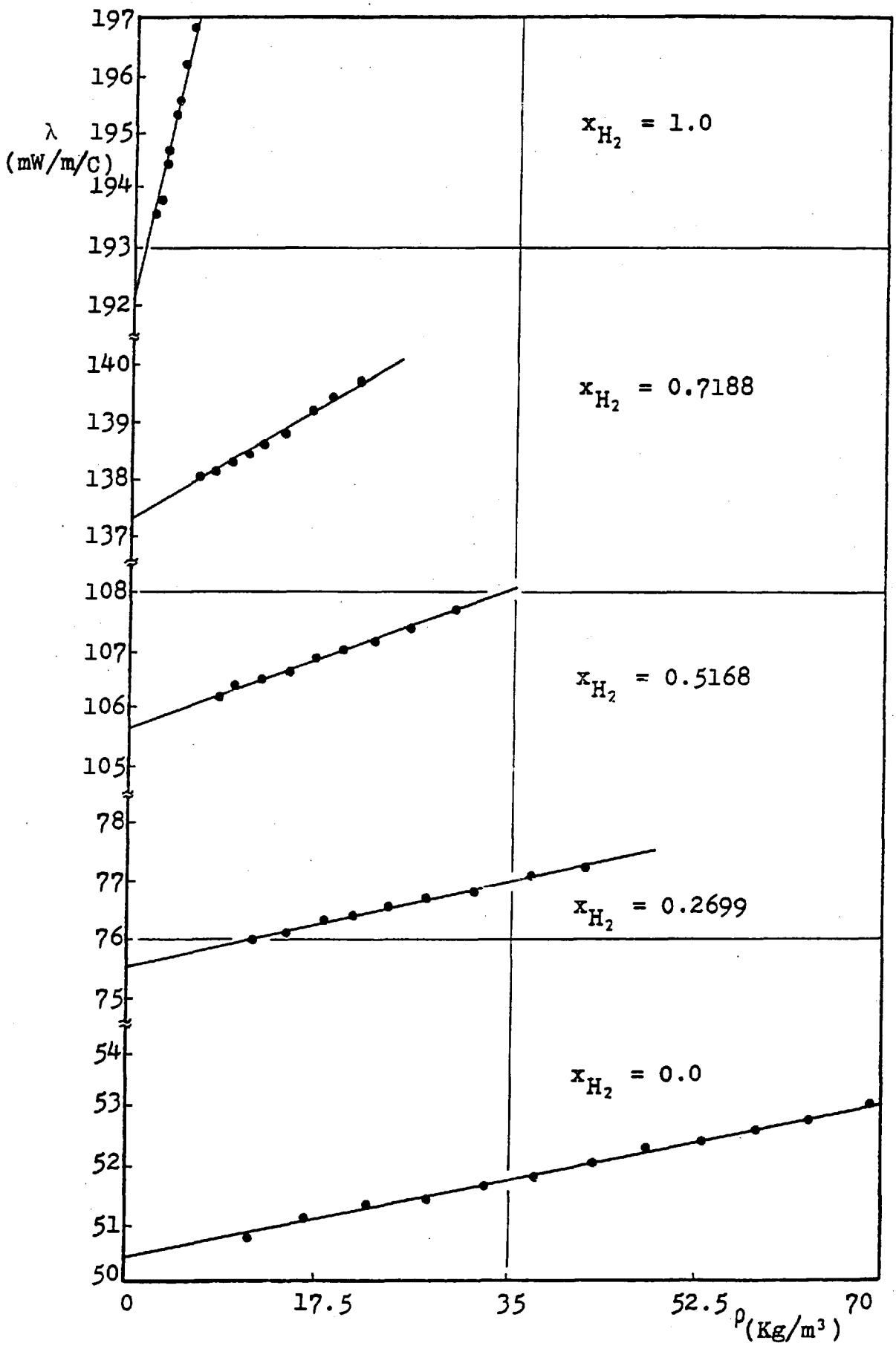

Figure 34 . Thermal Conductivity of Hydrogen/Neon mixture as a function of density at 35.0 °C

Table 23.

Thermal Conductivity of Hydrogen/Argon @ T_n = 35 °C

P MPa	T_o °C	ρ_o Kg/m^3	T_r °C	ρ_r Kg/m^3	$\lambda(T_r)$ mW/m/C	$\lambda(T_n)$ mW/m/C
x_{H_2} = 0.2614						
1.71	30.48	19.85	35.56	19.52	43.18	43.27
2.18	30.48	25.94	35.45	25.51	43.39	43.31
2.54	30.48	30.51	35.33	30.02	43.60	43.55
3.09	30.45	37.28	35.20	36.70	43.71	43.68
3.57	30.49	43.07	35.18	42.40	43.79	43.76
4.15	30.44	49.94	35.05	49.17	43.88	43.87
4.84	30.51	57.84	35.06	56.91	44.04	44.04
5.59	30.45	66.96	34.94	65.90	44.20	44.20
6.48	30.54	77.41	34.91	76.18	44.31	44.33
7.49	30.46	89.55	34.80	88.12	44.65	44.68
					$(\partial\lambda/\partial T)_{35\,°C}$ = 0.163 mW/m/C^2	
x_{H_2} = 0.4847						
2.20	30.50	18.24	34.84	17.98	72.02	72.06
2.47	30.51	21.14	34.76	20.84	72.01	72.08
2.90	30.49	24.53	34.71	24.19	72.21	72.28
3.34	30.52	28.44	34.67	28.05	79.19	72.28
3.89	30.48	32.87	34.56	32.43	72.39	72.50
4.51	30.46	38.11	34.66	37.57	72.47	72.59
5.23	30.49	44.15	34.45	43.56	72.50	72.64
6.06	30.47	51.01	34.43	50.34	72.98	73.13
7.05	30.50	58.96	33.79	58.30	72.79	73.10
8.06	30.61	65.13	33.82	64.42	73.23	73.53
					$(\partial\lambda/\partial T)_{35\,°C}$ = 0.256 mW/m/C^2	

Table 24.

Thermal Conductivity of Hydrogen/Argon @ T_n = 35 °C

P MPa	T_o °C	ρ_o Kg/m^3	T_r °C	ρ_r Kg/m^3	$\lambda(T_r)$ mW/m/C	$\lambda(T_n)$ mW/m/C
x_{H_2} = 0.6402						
1.88	30.47	11.51	34.88	11.34	97.71	97.75
2.21	30.52	13.31	34.87	13.12	97.79	97.83
2.68	30.48	16.42	34.78	16.19	97.84	97.91
3.30	30.52	20.04	34.71	19.76	97.85	98.15
4.00	30.49	24.23	34.62	23.91	98.13	98.25
4.64	30.48	27.94	34.53	27.57	98.12	98.27
5.37	30.48	32.35	34.50	31.92	98.43	98.59
6.23	30.50	37.36	34.40	36.88	98.50	98.70
7.24	30.49	43.32	34.34	42.76	98.70	98.90
					$(\partial\lambda/\partial T)_{35\,°C}$ = 0.322	mW/m/C^2
x_{H_2} = 0.7504						
1.96	30.49	8.67	35.00	8.54	120.94	120.94
2.57	30.49	13.36	34.94	11.20	121.18	121.20
3.05	30.52	13.38	35.00	13.18	121.28	121.28
3.52	30.50	15.48	34.85	15.26	121.42	121.47
4.15	30.53	18.13	34.87	17.88	121.59	121.64
4.84	30.50	20.95	34.73	20.65	121.76	121.86
5.62	30.51	24.17	34.70	23.84	122.11	122.22
6.51	30.49	27.94	34.66	27.57	122.36	122.49
7.60	30.47	31.70	34.55	31.58	122.63	122.79
					$(\partial\lambda/\partial T)_{35\,°C}$ = 0.369	mW/m/C^2

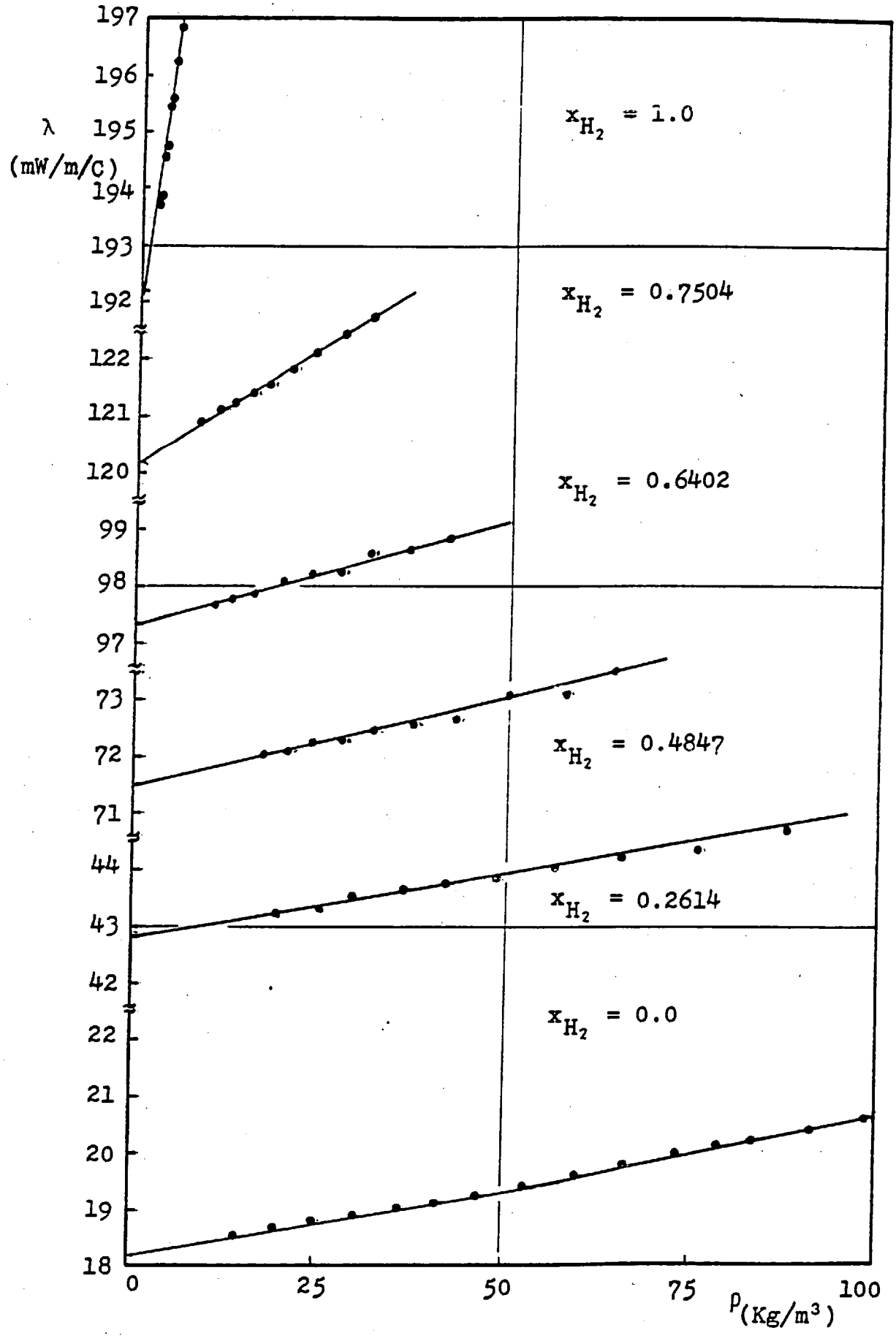

Figure 35 . Thermal Conductivity of Hydrogen/Argon mixture as a function of density at 35.0 °C

Table 25.

Thermal Conductivity of Hydrogen/Krypton @ T_n = 35°C

P MPa	T_o °C	ρ_o Kg/m³	T_r °C	ρ_r Kg/m³	$\lambda(T_r)$ mW/m/C	$\lambda(T_n)$ mW/m/C
x_{H_2} = 0.4795						
1.66	30.50	25.09	34.99	24.73	59.65	59.65
2.36	30.51	37.63	34.87	37.11	59.70	59.73
3.04	30.53	50.11	34.81	49.43	59.91	59.96
3.71	30.52	61.80	37.75	60.97	59.96	60.02
4.28	30.53	72.27	34.56	71.35	60.02	60.12
4.94	30.51	84.20	34.51	83.14	60.07	60.19
5.71	30.51	97.85	34.44	96.63	60.17	60.31
6.59	30.49	113.8	34.36	112.4	60.26	60.42
7.64	30.46	132.9	34.28	131.3	60.37	60.54
					$(\partial\lambda/\partial T)_{35\,°C}$ = 0.240	mW/m/C²
x_{H_2} = 0.7312						
2.02	30.45	18.75	34.99	18.48	106.80	106.80
2.53	30.40	23.72	34.87	23.39	106.98	107.03
2.94	30.45	27.44	34.83	27.06	106.98	107.04
3.56	30.43	33.41	34.78	32.95	107.14	107.22
4.14	30.43	38.61	34.67	38.09	107.20	107.33
4.83	30.44	44.67	34.64	44.08	107.49	107.63
5.60	30.41	51.67	34.52	50.99	107.69	107.86
6.50	30.42	59.64	34.46	58.88	107.74	107.94
7.51	30.39	69.00	34.37	68.14	108.01	108.24
					$(\partial\lambda/\partial T)_{35\,°C}$ = 0.360	mW/m/C²

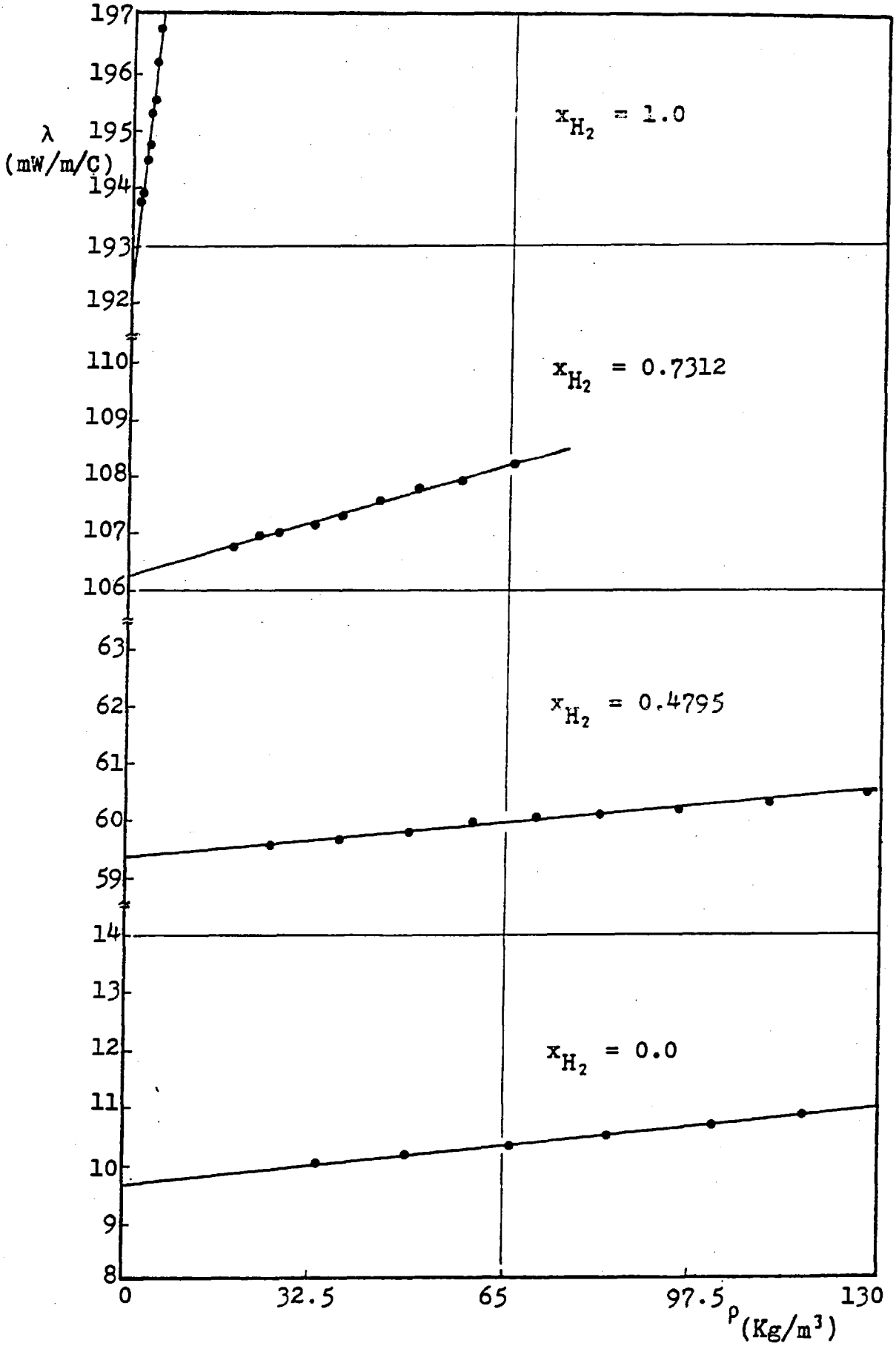

Figure 36 . Thermal Conductivity of Hydrogen/Krypton mixture as a function of density at 35.0 °C

Table 26 .

Thermal Conductivity of Hydrogen/Nitrogen @ T_n = 35 °C

P MPa	T_o °C	ρ_o Kg/m³	T_r °C	ρ_r Kg/m³	$\lambda(T_r)$ mW/m/C	$\lambda(T_n)$ mW/m/C
x_{H_2} = 0.2136						
2.02	30.51	18.13	35.24	17.85	44.72	44.68
2.72	30.46	24.67	35.06	24.31	44.99	44.98
3.33	30.50	29.99	35.01	29.56	45.17	45.16
3.88	30.50	34.84	34.95	34.35	45.22	45.23
4.68	30.47	41.89	34.83	41.31	45.52	45.54
5.41	30.51	48.25	34.78	47.59	45.73	45.76
6.28	30.46	55.88	34.62	55.13	46.06	46.12
7.31	30.49	64.71	34.60	63.86	46.35	46.41
					$(\partial\lambda/\partial T)_{35\,°C}$ = 0.150 mW/m/C²	
x_{H_2} = 0.4865						
1.66	30.50	10.54	35.42	10.37	74.80	74.69
2.13	30.46	13.23	35.22	13.03	74.83	74.77
2.46	30.51	16.55	35.25	16.30	74.98	74.91
3.26	30.54	20.14	35.12	19.84	74.99	74.96
3.92	30.52	24.12	35.09	23.77	75.08	75.05
4.58	30.58	28.01	35.07	27.61	75.13	75.11
5.30	30.52	32.39	34.89	31.94	75.31	75.34
6.14	30.55	37.34	34.87	36.83	75.49	75.53
7.16	30.48	43.20	34.70	42.62	75.71	75.78
					$(\partial\lambda/\partial T)_{35\,°C}$ = 0.260 mW/m/C²	

Table 27 .

Thermal Conductivity of Hydrogen/Nitrogen @ T_n = 35 'C

P MPa	T_o 'C	ρ_o Kg/m^3	T_r 'C	ρ_r Kg/m^3	$\lambda(T_r)$ mW/m/C	$\lambda(T_n)$ mW/m/C
x_{H_2} =	0.7338					
2.22	30.48	8.03	35.18	7.90	116.11	116.04
2.82	30.47	10.09	35.09	9.94	116.34	116.30
3.41	30.48	12.35	35.02	12.17	116.45	116.44
4.00	30.46	14.26	34.94	14.05	116.68	116.70
4.65	30.47	16.40	34.89	16.17	116.87	116.91
5.38	30.49	19.06	34.87	18.80	117.15	117.20
6.25	30.44	22.01	34.75	21.70	117.43	117.52
7.27	30.45	25.36	34.63	25.02	117.70	117.84

$(\partial\lambda/\partial T)_{35\,^{\circ}C}$ = 0.370 mW/m/C^2

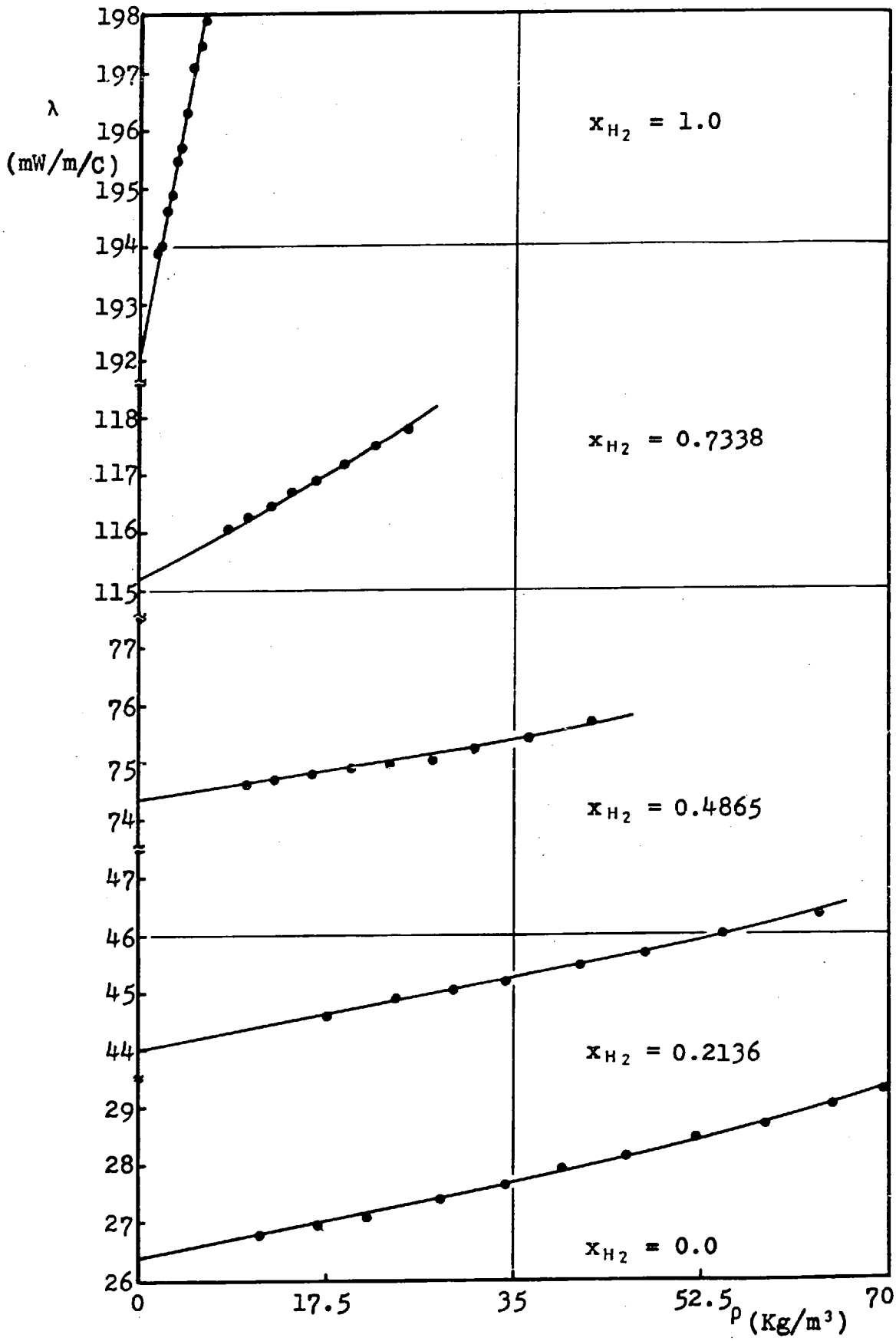

Figure 37 . Thermal Conductivity of Hydrogen/Nitrogen mixture as a function of density at 35.0 °C

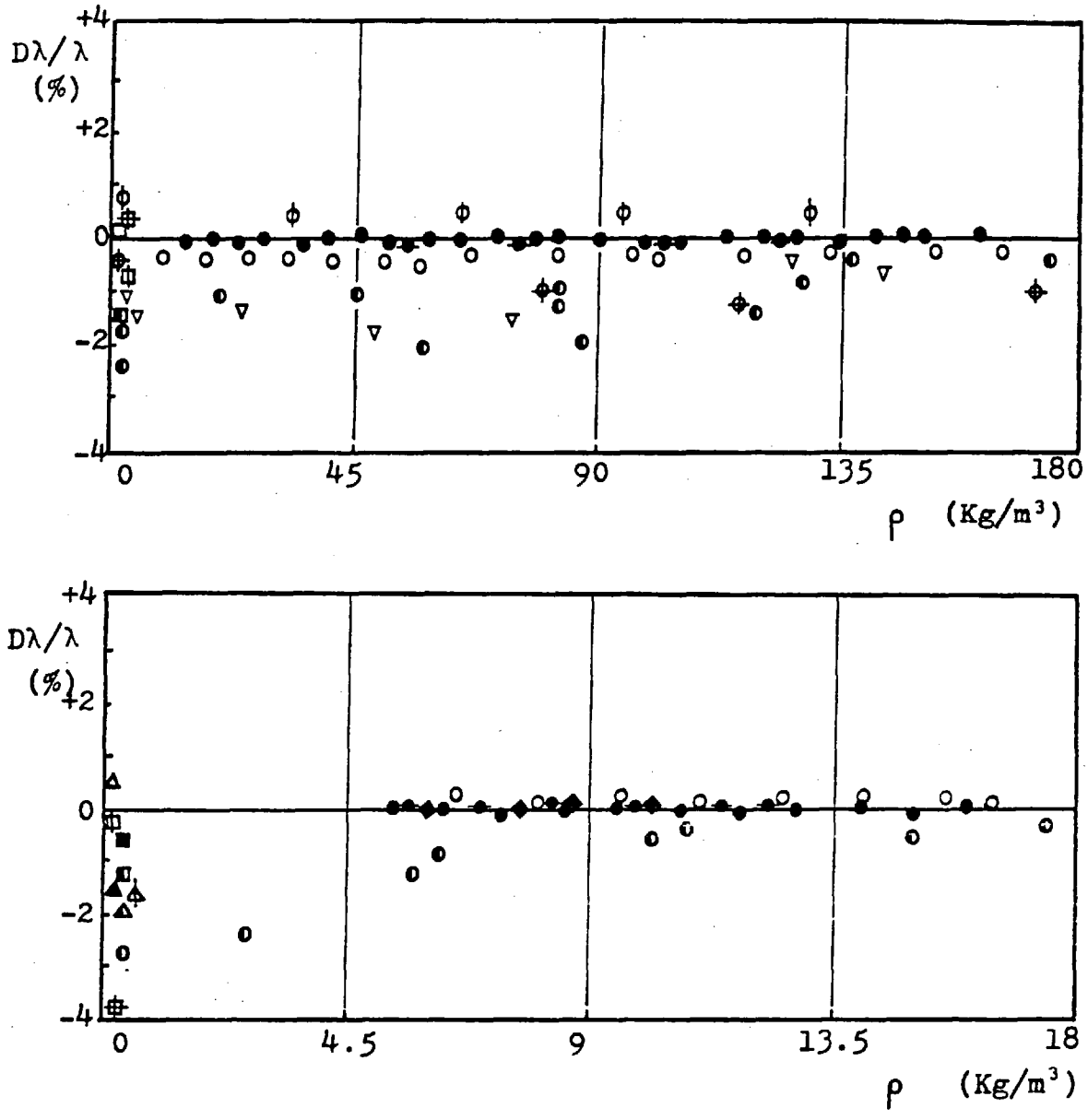

Figure 38 . Comparison of the Thermal Conductivity of Argon (above) and Helium (below) with other results, as a function of density at 35 °C

●	Present Work		▽	Michels et al.	(126)
◆	Remeasured values		◙	Waelbroeck et al.	(47)
o	Kestin et al.	(42)	⊕	Keyes	(48)
o	Tufeu et al.	(43)	■	Johnston et al.	(24)
ϕ	Michels et al.	(44)	△	Dickins	(49)
⊕	Bailey et al.	(45)	▲	Weber	(41)
□	Van Dael et al.	(46)	⋔	Eucken	(50)
⊡	Haarman	(36)	▲	Kannuluik et al.	(52)
◆	Remeasured(new wires)				

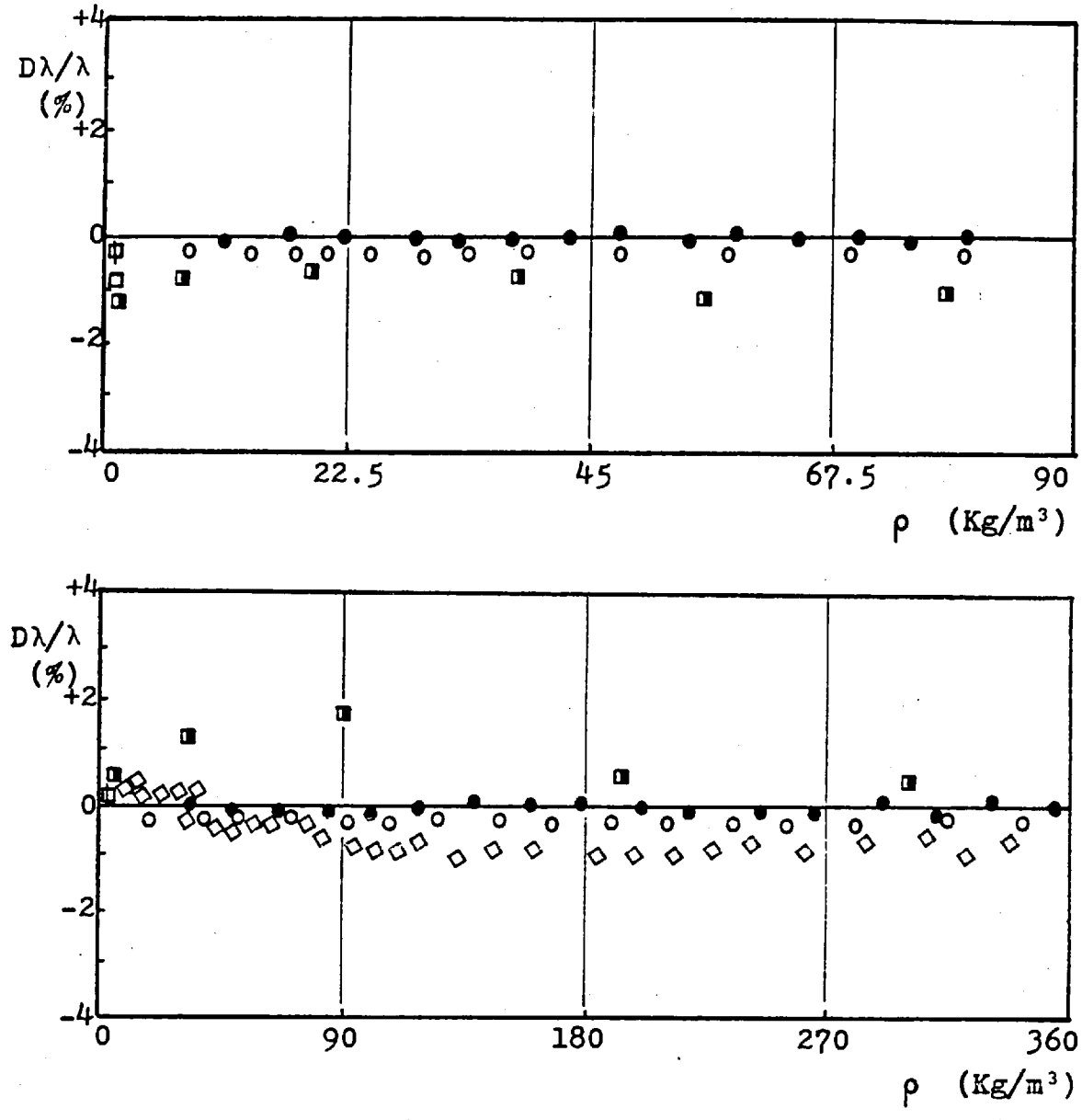

Figure 39. Comparison of the Thermal Conductivity of Neon (above) and Krypton (below) with other results, as a function of density at 35 °C

●	Present Work		⊕	Haarman	(36)
o	Kestin et al.	(42)	▪	Tufeu	(56)
□	Van Dael et al.	(46)	◇	Snel et al.	(167)

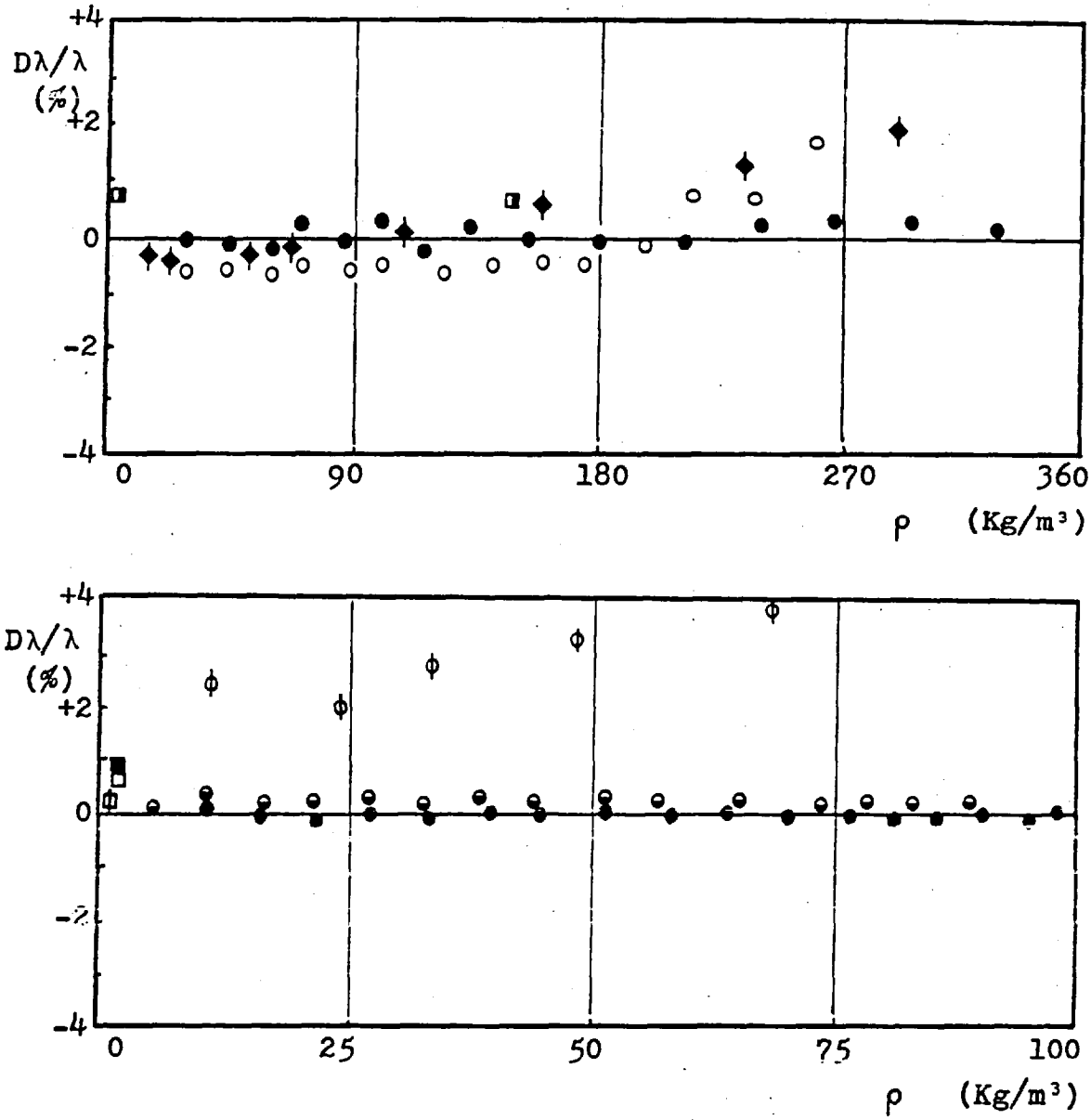

Figure 40. Comparison of the Thermal Conductivity of Xenon (above) and Nitrogen (below) with other results, as a function of density at 35 °C

●	Present Work		ϕ	Haarman	(36)
○	Kestin et al.	(51)	□	Van Dael et al.	(46)
ϕ	Michels et al.	(44)	■	Johnston et al.	(24)
♦	Van Oosten	(166)	▣	Tufeu	(56)

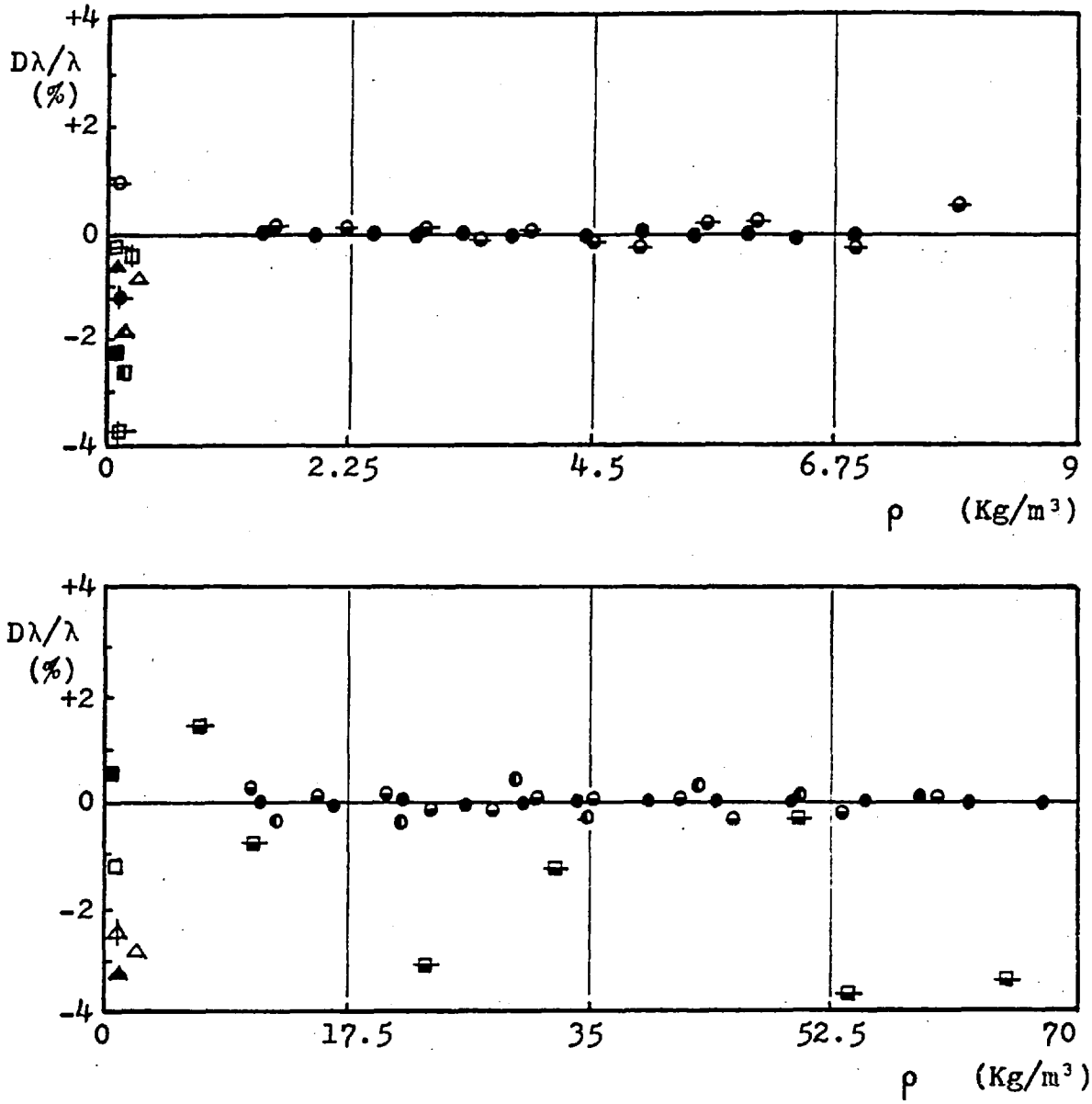

Figure 41. Comparison of the Thermal Conductivity of Hydrogen (above) and Methane (below) with other results, as a function of density at 35 °C

●	Present Work		⊕	Keyes	(48)
⊖	Clifford et al.	(52)	■	Waelbroeck et al.	(47)
✦	Gregory	(55)	⊟	Northdurft	(54)
⊖	Archer	(53)	⊕	Haarman	(36)
●	Kestin et al.	(51)	△	Dickins et al.	(49)
◐	Tufeu et al.	(43)	▲	Weber	(41)
■	Johnston et al.	(24)	▲	Kannuluik et al.	(57)
⊡	Misic et al.	(20)	□	Van Dael et al.	(46)
⏃	Eucken	(50)			

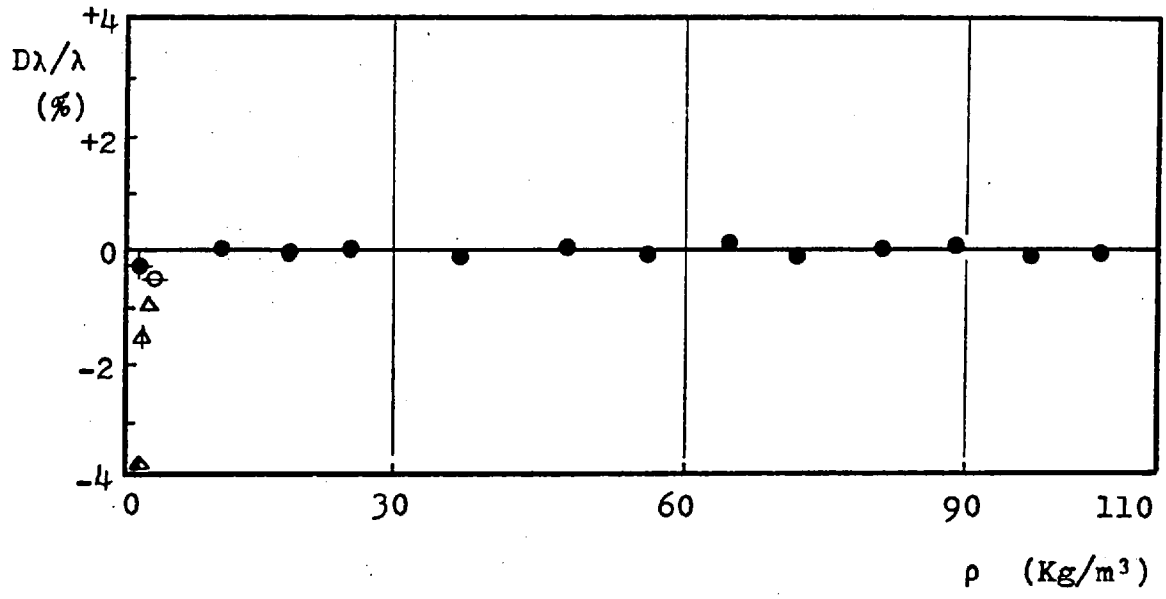

Figure 42 . Comparison of the Thermal Conductivity of Carbon Monoxide with other results, as a function of density at 35 'C

●	Present Work		△	Dickins et al.	(49)
⊖	Archer	(53)	⅄	Eucken	(50)
✦	Gregory et al.	(55)	▲	Kannuluik et al.	(57)

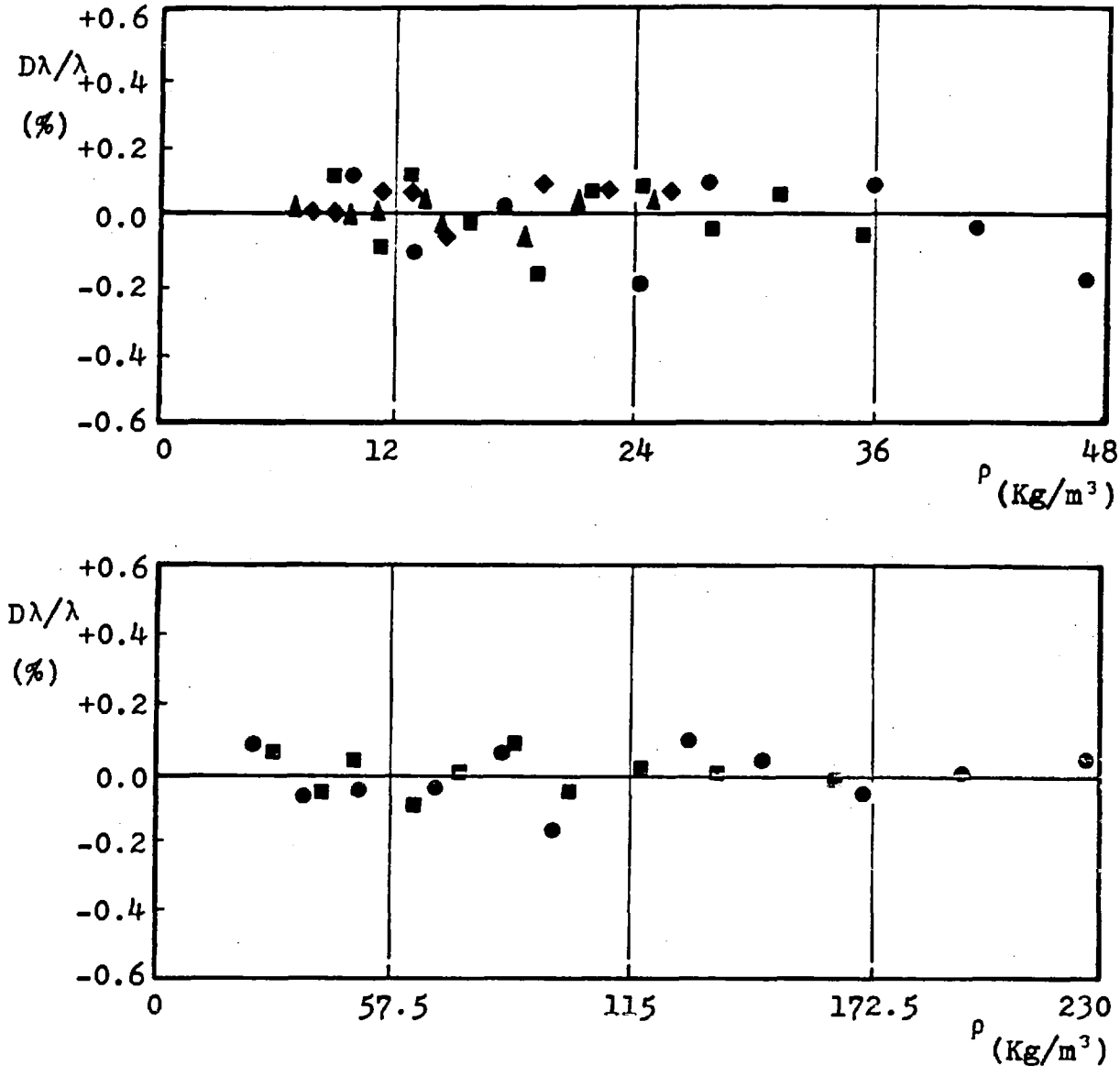

Figure 43 . The deviations of the experimental thermal conductivity data from the correlation of equation (5.2).

Above :- Helium/Neon mixture at 35 °C

● x_{He} = 0.2172 ■ x_{He} = 0.4662

◆ x_{He} = 0.6823

Below :- Argon/Krypton mixture at 35 °C

● x_{Ar} = 0.4082 ■ x_{Ar} = 0.7059

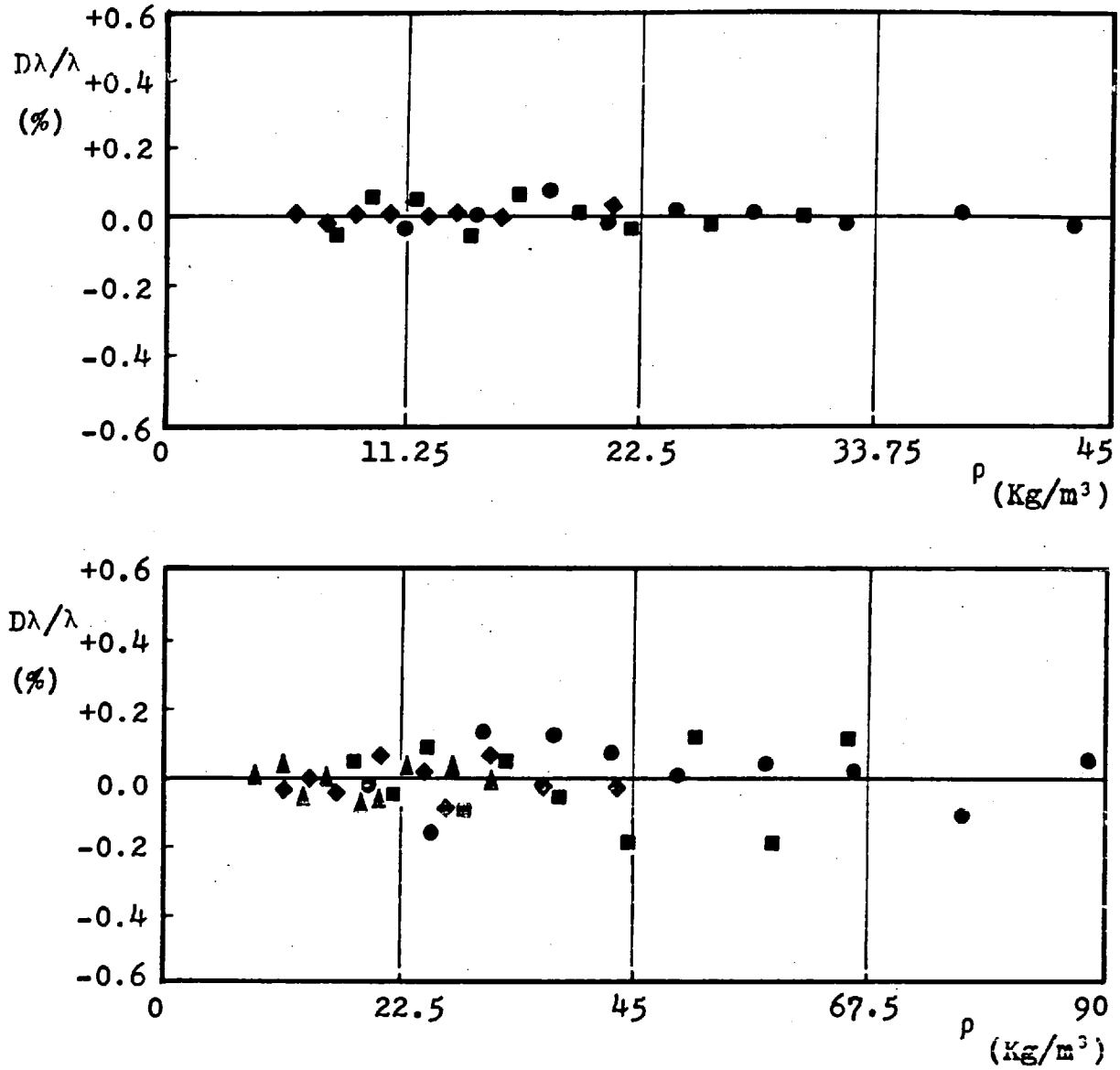

Figure 44 . The deviations of the experimental thermal conductivity data from the correlation of equation (5.2).

Above :- Hydrogen/Neon mixture at 35 °C

● x_{H_2} = 0.2691 ■ x_{H_2} = 0.5168

◆ x_{H_2} = 0.7188

Below :- Hydrogen/Argon mixture at 35 °C

● x_{H_2} = 0.2614 ■ x_{H_2} = 0.4847

◆ x_{H_2} = 0.6402 ▲ x_{H_2} = 0.7504

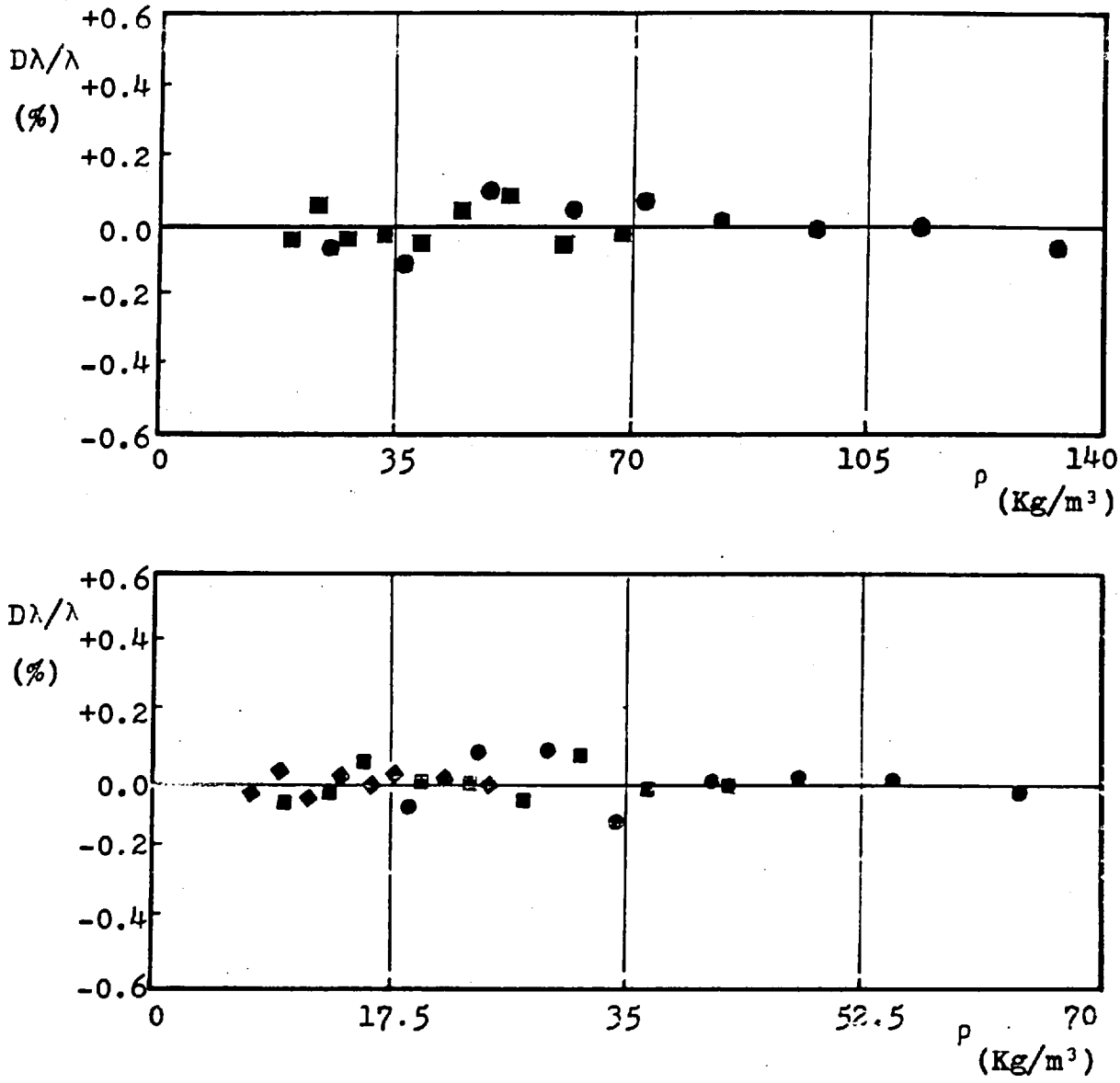

Figure 45 . The deviations of the experimental thermal conductivity data from the correlation of equation (5.2).

Above :- Hydrogen/Krypton mixture at 35 °C
● x_{H_2} = 0.4795 ■ x_{H_2} = 0.7312

Below :- Hydrogen/Nitrogen mixture at 35 °C
● x_{H_2} = 0.2136 ■ x_{H_2} = 0.4865
◆ x_{H_2} = 0.7338

Table 28 .

Statistical analysis of the experimental thermal conductivity values.
(Pure monatomic gases)

Gas	Highest density Kg/m^3	λ° mW/m/C	c_1 $\mu Wm^2/Kg/C$	c_2 $nWm^5/Kg^2/C$	c_3 $pWm^8/Kg^3/C$	Standard deviation %
He	16	158.40 ±0.10	256. ±9.	-	-	0.07
Ne	31	50.41 ±0.03	38.4±0.7	-	-	0.09
Ar	55	18.18 ±0.01	24.0±0.3	-	-	0.05
	85	18.20 ±0.01	22.0±0.7	33. ± 7.	-	0.05
	155	18.20 ±0.02	22.2±1.2	38. ±18.	-112.±82.	0.07
Kr	100	9.722±0.004	9.5±0.1	-	-	0.02
	370	9.708±0.020	9.5±0.3	5.4± 0.7	-	0.24
Xe	220	5.656±0.014	7.3±0.1	-	-	0.25
	250	5.676±0.027	6.8±0.4	2.1± 1.7	-	0.25
	340	5.609±0.034	8.8±0.7	-14. ±10.	40.± 9.	0.30

Table 29 .

Statistical analysis of the experimental thermal conductivity values.
(Pure polyatomic gases)

Gas	Highest density Kg/m^3	λ° $mW/m/C$	c_1 $\mu Wm^2/Kg/C$	c_2 $nWm^5/Kg^2/C$	c_3 $pWm^8/Kg^3/C$	Standard deviation %
H_2	5	192.21±0.01	951. ± 30.	-	-	0.06
	7	192.27±0.10	913. ±122.	5694.±1452.	-	0.06
CH_4	30	35.35±0.04	120. ± 1.8	-	-	0.06
	40	35.23±0.14	102.8± 14.0	412.± 33.	-	0.05
	65	35.23±0.11	104.4± 10.7	194.± 180.	6340.±2813.	0.07
N_2	40	26.45±0.06	37.5± 2.8	-	-	0.16
	105	26.43±0.03	34.5± 1.4	106.± 11.	-	0.12
CO	85	25.68±0.03	41.7± 0.6	-	-	0.16
	110	25.73±0.04	36.8± 1.8	61.± 13.	-	0.13

Table 30.

Statistical analysis of the experimental thermal conductivity values.
(Monatomic mixtures)

Gas	Mole fraction	Highest density Kg/m^3	λ° mW/m/C	c_1 $\mu Wm^2/Kg/C$	c_2 $nWm^5/Kg^2/C$	Standard deviation %
He/Ne	$x_{He} = 0.2172$	50	63.24±0.08	39.6±3.3	-	0.12
	$x_{He} = 0.4662$	35	83.13±0.08	47.5±3.9	-	0.09
	$x_{He} = 0.6823$	27	107.02±0.08	65.2±5.2	-	0.05
	$x_{He} = 0.7156$	22	111.22±0.03	98.4±2.0	-	0.02
Ar/Kr	$x_{Ar} = 0.4088$	130	12.43±0.01	13.1±0.1	-	0.09
		230	12.46±0.02	11.9±0.5	7.±2.	0.09
	$x_{Ar} = 0.7059$	170	15.00±0.01	17.6±0.1	-	0.06

Table 31 .

Statistical analysis of the experimental thermal conductivity values
(Hydrogen mixtures)

Gas	Mole fraction	Highest density Kg/m^3	λ° mW/m/C	c_1 $\mu Wm^2/Kg/C$	c_2 $pWm^5/Kg^2/C$	Standard deviation %
H_2/Ne	$x_{H_2} = 0.2699$	43	75.64±0.03	38.9±1.2	-	0.05
	$x_{H_2} = 0.5168$	32	105.74±0.04	65.9±2.3	-	0.04
	$x_{H_2} = 0.7188$	20	137.49±0.04	94.4±4.5	-	0.02
H_2/Ar	$x_{H_2} = 0.2614$	90	42.89±0.03	19.8±0.7	-	0.10
	$x_{H_2} = 0.4847$	55	71.50±0.11	30.1±1.6	-	0.06
	$x_{H_2} = 0.6402$	45	97.35±0.04	36.6±1.6	-	0.05
	$x_{H_2} = 0.7504$	34	120.24±0.03	80.7±0.02	-	0.03
H_2/Kr	$x_{H_2} = 0.4795$	135	59.48±0.03	8.3±0.4	-	0.07
	$x_{H_2} = 0.7312$	70	106.28±0.05	28.9±1.2	-	0.05
H_2/N_2	$x_{H_2} = 0.2136$	65	44.02±0.07	37.2±1.0	-	0.09
	$x_{H_2} = 0.4865$	45	74.33±0.04	32.3±1.0	-	0.04
	$x_{H_2} = 0.7338$	35	115.21±0.03	105.5±1.8	-	0.02

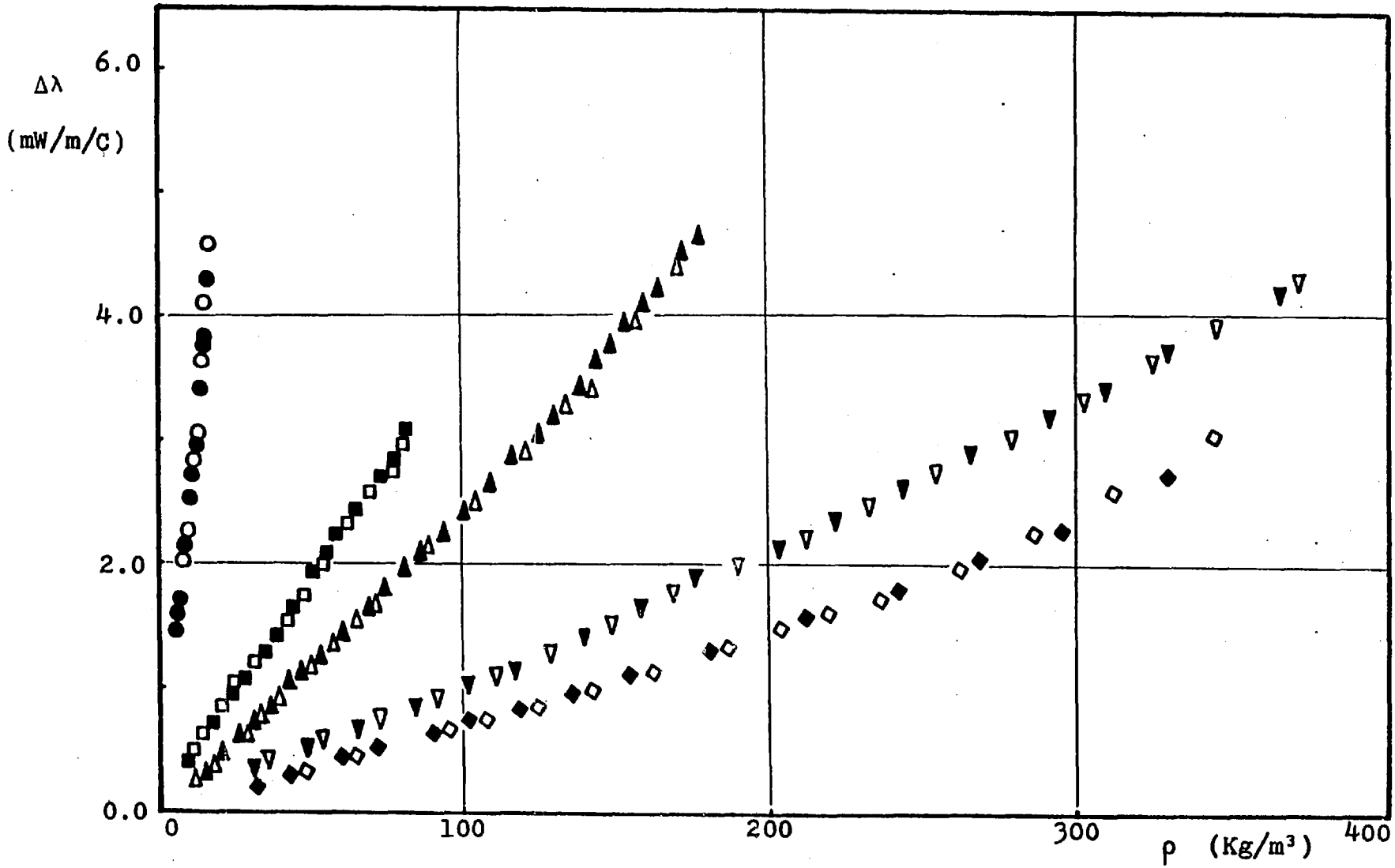

Figure 46 . Excess Thermal Conductivity of Monatomic Gases as a function of density
Present Work at 35.0 'C - ● He, ■ Ne, ▲ Ar, ▼ Kr, ◆ Xe
Kestin et al (42) at 27.5 'C - ○ He, □ Ne, Δ Ar, ▽ Kr, ◇ Xe

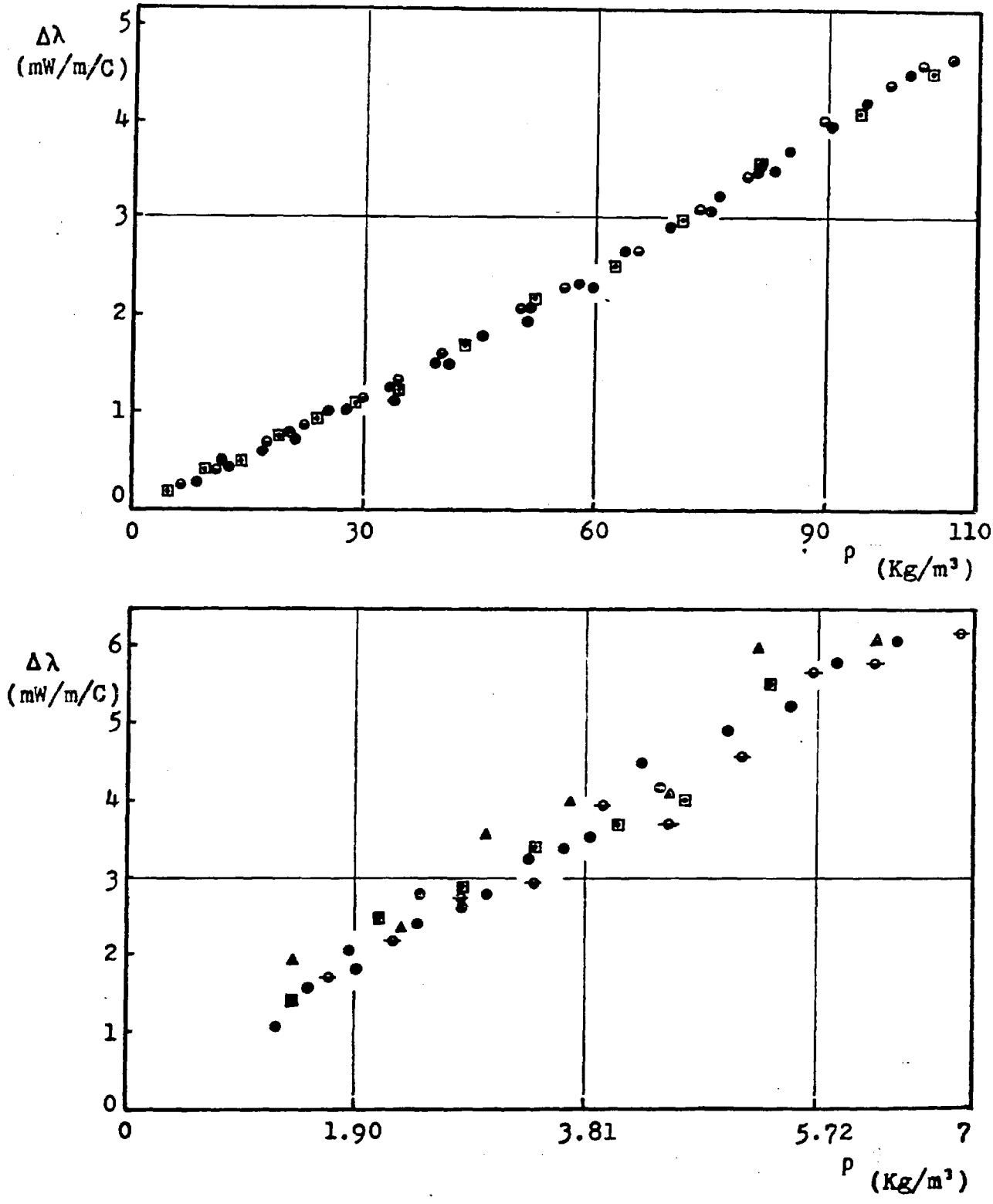

Figure 47. Excess Thermal Conductivity of Nitrogen(above) and Hydrogen (below) as a function of density.

- ● Present Work 35.0°C
- ○ Kestin et al 27.5°C (51)
- ◇ Kestin et al 27.5°C (52)
- ▲ NEL 38.0 °C (119)
- ▣ NEL 70.0 °C (120)
- ● NEL 113.0 °C (120)

SIX

DISCUSSION

6. INTRODUCTION

In this Chapter the results obtained by the transient hot wire technique described in this thesis, are analysed and compared with the most accurate kinetic theories available (Chapter 2).

For simplicity the analysis is separated into five sections, the pure monatomic gases, monatomic mixtures, pure polyatomic gases, hydrogen/monatomic mixtures and polyatomic mixtures.

6.1. PURE MONATOMIC GASES

6.1.1. THE ZERO DENSITY LIMIT

The statistical analysis of the experimental thermal conductivities as a function of density (§5.1. ,p.104) yields λ° , the zero density thermal conductivity of the gases (Table 28, p.149) which we may employ to confirm the accuracy of our thermal conductivity measurements. For the pure polyatomic gases this is made possible by the exact kinetic theory relationship for the Eucken factor (§2.3.3.,p.42) :-

$$Eu = \frac{\lambda^\circ(T) \cdot M}{C_v^\circ \cdot \eta^\circ(T) \cdot F(T^*)} = 2.5 \text{ (exact)} \qquad (6.1)$$

Kestin and his collaborators [60] have reported zero density viscosities η° , for the five pure monatomic gases with an estimated uncertainty of $\pm 0.1\%$. The correction factor $F(T^*)$ which accounts for the kinetic theory approximations above the first, was shown by Kestin and Mason [58] to be, to a good approximation independent of the intermolecular potential. They, therefore , proceeded to correlate this factor using the collision intergrals of the (11-6-8) potential model proposed by Hanley [151]. Their result for the factor $F(T^*)$reads :-

$$F(T^*) = 1 + 0.0042 \left\{1 - \exp[0.33(1 - T^*)]\right\} \qquad (6.2)$$

The accuracy of this expression is estimated to be ±0.1%.

In Table 32 , we list the Eucken factors obtained with the aid of equation (6.1) for the five noble gases based on these data sources and our own thermal conductivity results at zero density.

Table 32 .

Experimental Eucken factors for the pure monatomic gases

Gas	η° μPa s	λ° mW/m/C	F(T*) -	Eucken factor -
He	20.31±0.02	158.4 ±0.3	1.0042	2.494±0.01
Ne	32.47±0.03	50.41 ±0.10	1.0035	2.503±0.01
Ar	23.24±0.02	18.18 ±0.03	1.0012	2.503±0.01
Kr	26.15±0.03	9.722±0.020	1.0006	2.497±0.01
Xe	23.84±0.02	5.656±0.010	1.0001	2.497±0.01
He^R	20.31±0.02	158.5 ±0.3	1.0042	2.496±0.01
Ar^R	23.24±0.02	18.17 ±0.03	1.0012	2.501±0.01
He^N	20.31±0.02	158.3 ±0.3	1.0042	2.493±0.01

At the bottom of the Table 32 , remeasured values for Helium(He^R) and Argon (Ar^R) are also presented. Measurements performed on Helium after all other results, using a new set of wires are also shown (He^N). It can be seen that within the combined uncertainty the experimental viscosity and thermal conductivity data are entirely consistent with the theoretical Eucken factor of 2.500. This provides supporting evidence for the claim that the accuracy of the present measurements is one of ±0.2%. Measurements performed on Helium with a new set of wires show that the reproducibility of the equipment is ±0.1%, and therefore consistent with our estimate of the precision of the apparatus.

6.1.2. THE DENSITY DEPENDENCE

The outstanding problem in the transport coefficients of moderately dense gases and gas mixtures remains the rigorous theoretical calculation of the first density coefficient of the thermal conductivity from first principles and known intermolecular potentials. Such calculations have only been carried out for rigid spherical molecules by Sengers et al. [152] . The reason that the calculations are restricted to such crude molecular models are related to the difficulty of accounting for the dimers (bound states) which may be formed in three body collisions. It will be sometime before a full theory is developed.

Two semi-theoretical approaches have been developed. The first is by Hoffman and Curtiss [154] and it basically neglects the presence of bound states but accounts for the effect of collisional transfer. The second, of Kim and Ross [153] incorporates the effect of bound states but it neglects collisional transfer. These two semi-theoretical approaches were put together by Olmstead and Curtiss [163] who proceeded to derive first density coefficients as a function of the reduced temperature.The basic assumption of their method is the neglect of an atom-diatom collision in the singlet distribution function. The consequence of this is that although the theory properly accounts for the effects of collisional transfer only approximate account of the effects of bound states is taken. Their results for the collisional transfer are the same as those by Snider and Curtiss [164] . The first density coefficient C_λ^* reduced in a dimensionless form is related to the previously discussed first density coefficient (§5.1.,p.104) c_1 by the expression :-

$$C_\lambda^* = \frac{c_1 \cdot M}{\lambda^\circ N \sigma^3} \qquad (6.3)$$

and it incorporates two contributions as :-

$$C_\lambda^* = (C_\lambda^*)_{SC} + (C_\lambda^*)_{BD} \qquad (6.4)$$

where $(C_\lambda^*)_{SC}$ is the collisional transfer contribution, first derived by Snider and Curtiss [164] and $(C_\lambda^*)_{BD}$ is the contribution of the bound states.Their results together with our experimental first density coefficients for the pure monatomic gases are plotted

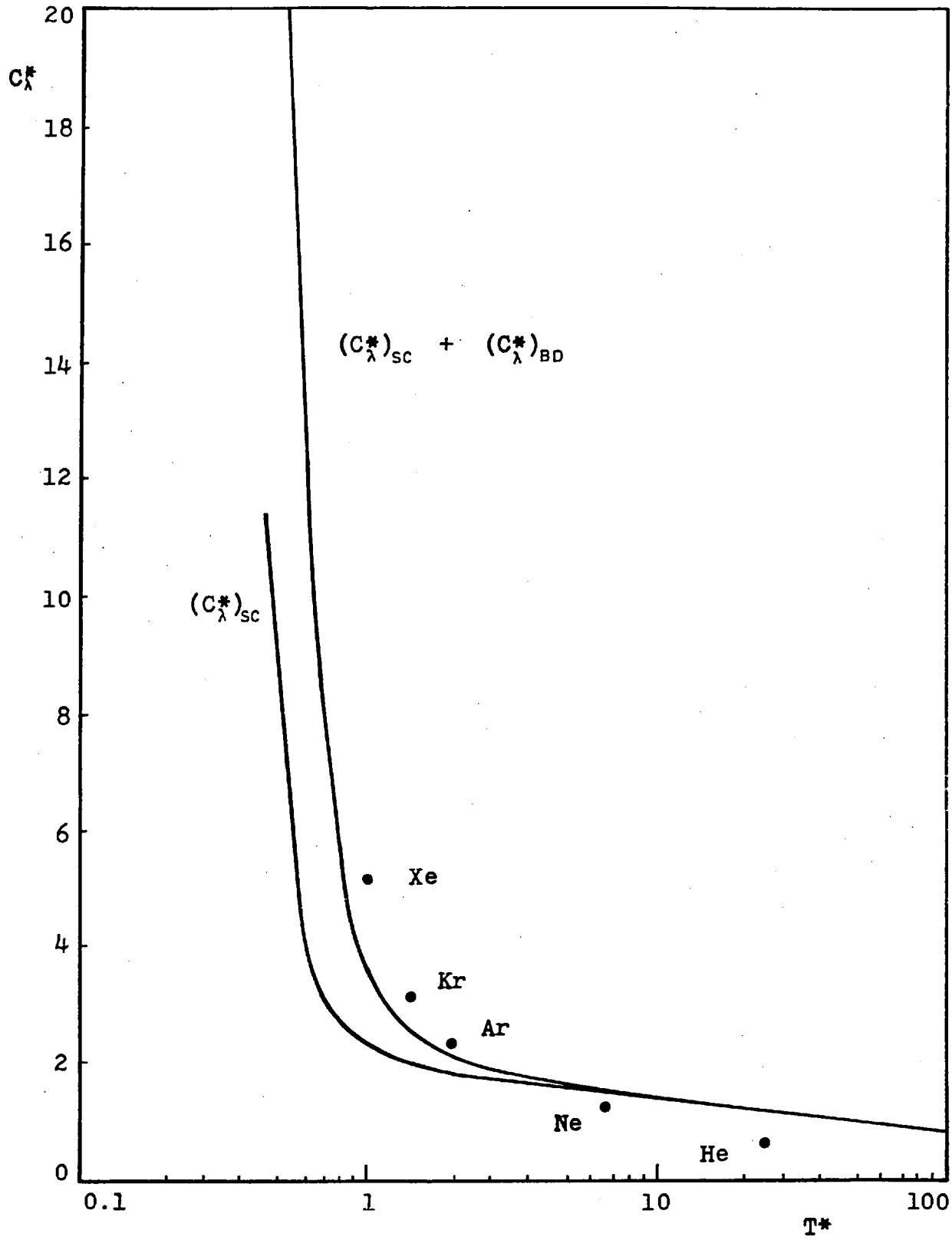

Figure 48 . Rigorous theoretical calculation of the first density coefficient C^*_λ for the monatomic gases
• Experimental coefficients

in Figure 48. Due to the complexity of the calculation involved the theoretical results are based on an unrealistic Lennard-Jones (12-6) potential.Their results , however, seem to produce only order of magnitude agreement . We believe that part of this may be atributed to using an unrealistic potential and part owing to an inadequate treatment of bound states. It is beyond the scope of this work to provide an improvement on their theory, although such improvement is necessary since the discrepancies shown in Figure 48 are larger than the experimental uncertainty.

The present measurements provide the means by which modification of their theory or further suggestions can be checked.

6.2. MONATOMIC MIXTURES

6.2.1. THE ZERO DENSITY LIMIT

In the case of monatomic mixtures the equivalent Eucken factor relation, equation (2.107),p. 42 , involves the interaction viscosity and thermal conductivity. For the two binary systems studied here, the interaction viscosity $[\eta_{ij}]_1$ has been derived from the measurements of Kestin and coworkers [140,141] using the analysis based on the second order kinetic theory expressions and described in detail elsewhere [142] . In the case of the thermal conductivity of the binary mixtures, the poorer convergence of the kinetic theory formulae requires a third order analysis in order to determine the interaction thermal conductivity $[\lambda_{ij}]_1$. This analysis has been based on the third order kinetic theory formulae (§2.3.2.,p. 33) as follows. For the analysis of both the viscosity and the thermal conductivity data it is necessary to assume an intermolecular pair potential for each of the three interactions in the binary mixture. Although the choice of the intermolecular potential has only a small effect on the computed values of $[\eta_{ij}]_1$ and $[\lambda_{ij}]_1$ it is desirable to use as reasonable a potential as possible. Accordingly, we have applied the inversion procedure of Gough et al. [122] to the universal collision integral $\Omega^{(2,2)}(T^*)$ of the extended law of corresponding states [58,60] so as to determine a 'universal' intermolecular pair potential for the interactions of the monatomic gases [143] . This pair potential has then been employed to compute all the collision integrals which occur in the third order expression for

the mixture thermal conductivity and thus the factor $f^{(3)}_{mix}$ which represents the ratio of the third order thermal conductivity to the first order, is computed via the explicit formulae of section §2.3.2. The experimental thermal conductivities are then assumed to be equal to the third order Chapman Cowling thermal conductivities. By means of the factor $f^{(3)}_{mix}$ these values are converted to first order thermal conductivities, using the following expression (§2.3.2.,p.33) :-

$$[\lambda_{mix}]_1 = \frac{[\lambda_{mix}]_3}{f^{(3)}_{mix}} = \frac{\lambda^{\circ}_{mix}}{f^{(3)}_{mix}} \qquad (6.5)$$

First order values for the pure components thermal conductivities are computed in a similar manner. The first order expression for the mixture thermal conductivity (§2.3.1.,p.32) is then solved to obtain iteratively the interaction thermal conductivity $[\lambda_{ij}]_1$ for every mixture. The resulting values are given in Table 33 , together with their estimated uncertainties.

Table 33 .

Experimental Eucken factors for the monatomic mixtures

Gas	Molefraction -	$[\eta_{ij}]_1$ μPa s	$[\lambda_{ij}]_1$ mW/m/C	Eucken factor -
He/Ne	$x_{He} = 0.2172$	22.21±0.2	102.5 ±1.0	2.472±0.05
	$x_{He} = 0.4662$	22.21±0.2	102.0 ±1.0	2.460±0.05
	$x_{He} = 0.6823$	22.21±0.2	102.5 ±1.0	2.472±0.05
	$x_{He} = 0.7156$	22.21±0.2	101.7 ±1.0	2.453±0.05
Ar/Kr	$x_{Ar} = 0.4088$	23.98±0.2	13.74±0.14	2.486±0.05
	$x_{Ar} = 0.7059$	23.98±0.2	13.80±0.14	2.496±0.05

The uncertainties in the computed values of $[\eta_{ij}]_1$ and $[\lambda_{ij}]_1$ are significantly larger than those in the mixture transport properties themselves, particularly when the mass ratio of the two species is much different from unity, as in the case of Helium/Neon mixture where the mass ratio is about five. We have confirmed by direct calculation that an error of only 0.0005 in the mole fraction of this particular mixture can contribute as much as ±0.4% to the uncertainty in the calculated value of $[\lambda_{ij}]_1$. In addition,

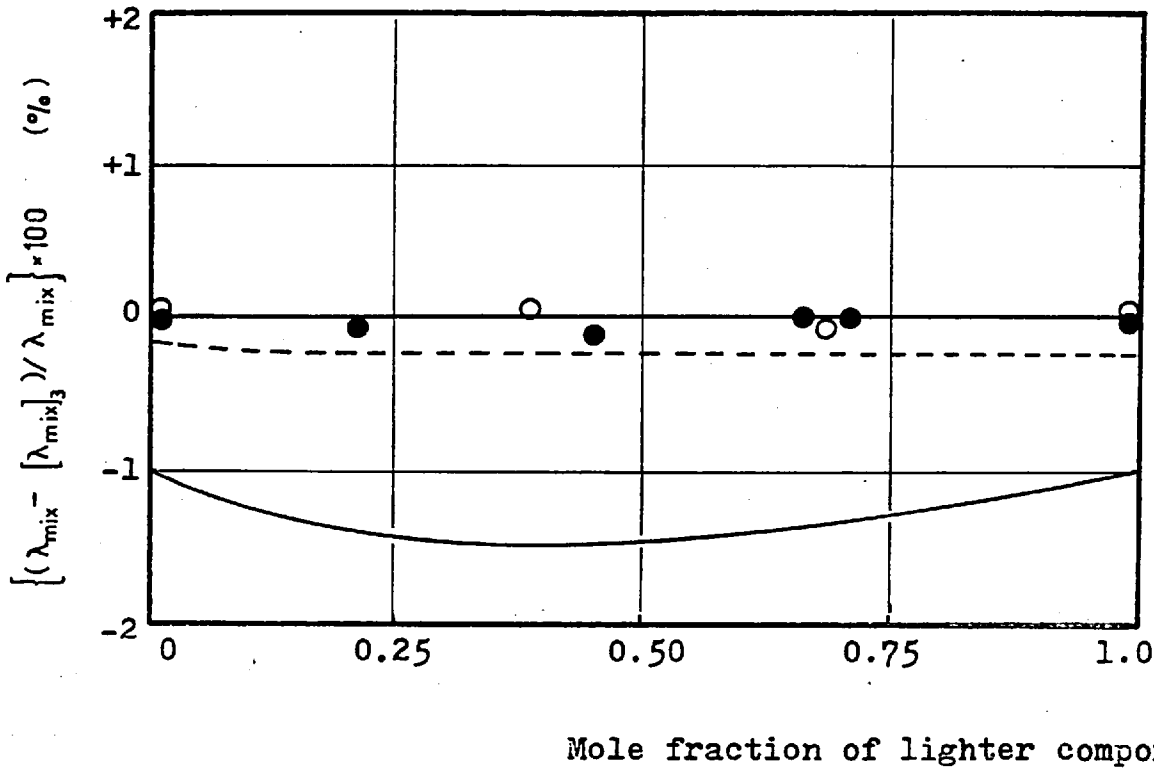

Figure 49 . Deviations of the experimental, zero density thermal conductivity of the binary mixtures from a calculation based on the third order kinetic theory formulae.

- ● Experimental data for Helium/Neon
- o Experimental data for Argon/Krypton
- ——First order calculation for Helium/Neon
- ----First order calculation for Argon/Krypton

errors of ±0.2% in the estimated collision integral ratios A* and B* each contribute to ±0.15% in the error in $[\lambda_{ij}]_1$,[75] . When account is taken of these uncertainties, together with the errors in the experimental thermal conductivity data of the mixtures and the pure gases, the overall uncertainty in the calculated value of $[\lambda_{ij}]_1$ is estimated to be one of ±1%.

From the Table 33 , it can be seen that fluctuations in the computed values of $[\lambda_{ij}]_1$, for the different composition mixtures lie within their estimated uncertainty and the corresponding experimental Eucken factors included in the same Table are consistent with the expected value of 2.500 .

In order to illustrate the importance of the higher-order

kinetic theory approximations to the thermal conductivity of binary mixtures, we have computed both the first order and third order approximations to the thermal conductivity of the mixtures studied here. For this purpose we have employed the mean value of $[\lambda_{ij}]_1$ determined above, the experimental values of the pure gas thermal conductivities and the collision integrals determined from the extended law of corresponding states [58,60] . Figure 49 ,p.161, contains a plot of the deviations of the experimental data from the third order calculation of the mixture thermal conductivity for the systems discussed here. The maximum deviation amounts to only $\pm 0.1\%$ so that the third order kinetic theory equations provide an adequate description of our experimental data. It can be seen in the same Figure that the first order formulae underestimate the thermal conductivity by up to 1.6% in the case of Helium/Neon mixtures although for Argon/Krypton the difference is only 0.2%. These calculations indicate the poor convergence of the kinetic theory formulae for the thermal conductivity of binary gas mixtures with a large mass ratio. In the case of polyatomic gas mixtures the only formulae which exist are those equivalent to the first order Chapman-Cowling approximation.

6.2.2. THE DENSITY DEPENDENCE

A rigorous treatment of the first density coefficient of the thermal conductivity of monatomic mixtures has not yet been given. A semi-empirical description of the density dependence of the thermal conductivity of dense monatomic gas mixtures, is provided by the Mason-Wakeham approximation (§2.5.1.,p.54) which was presented in Chapter two. Because the expressions involved are first order in the Chapman-Cowling sense, first order thermal conductivities for the pure components are required for consistency. These may be derived from our measurements by using the factor $f_\lambda^{(3)}$ in the manner described in the previous section and assuming that this factor is density independent, in the absence of other guidance.The same intermolecular potential as in the zero density case is used for the functionals A* and B* whereas virial coefficients have been derived from the corresponding states correlation of Kestin and Mason [58,60] . The pseudo-radial distribu-

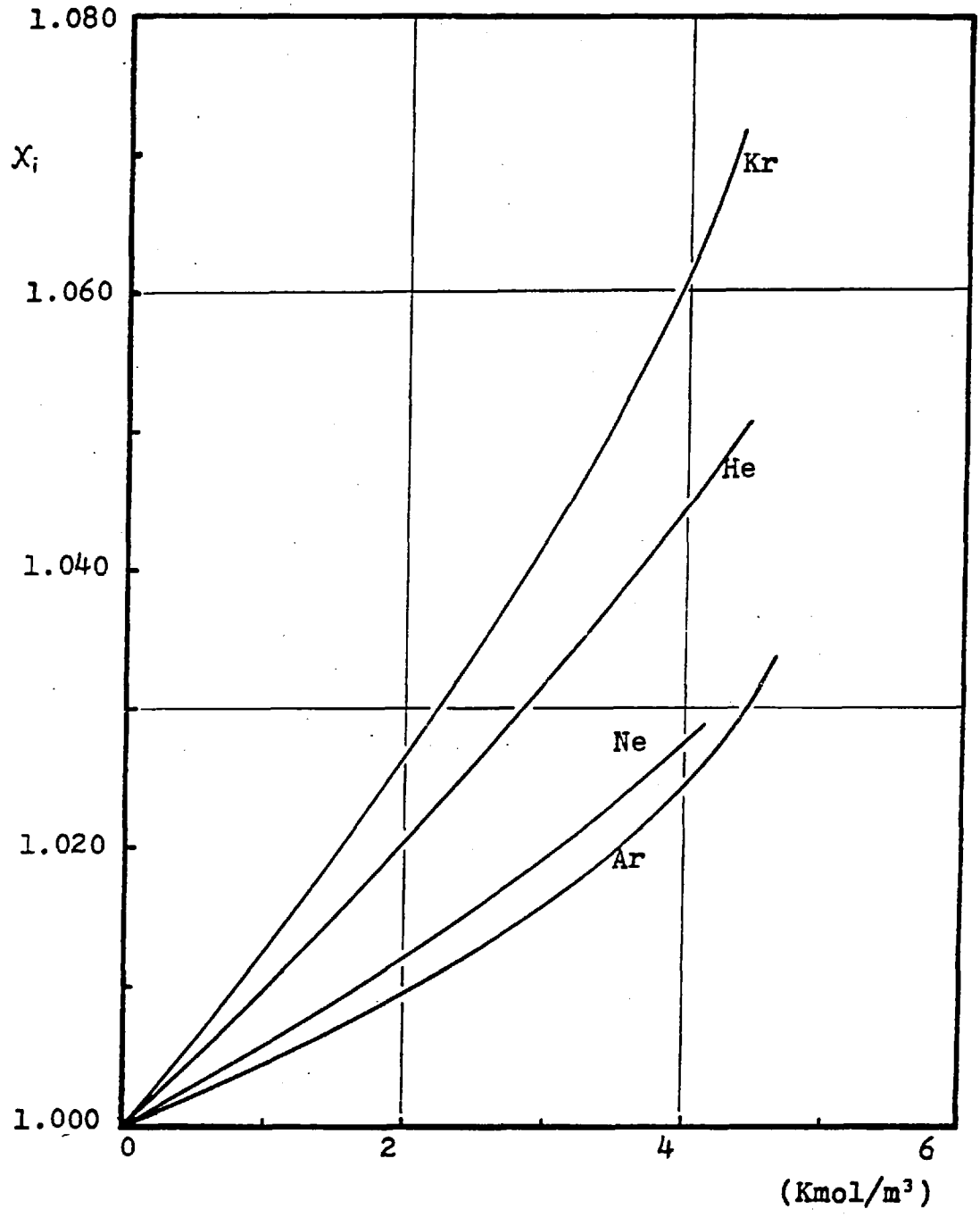

Figure 50 . The radial distribution function χ_i

tion functions (§2.5.1.,p.54) for the pure components are shown in Fig. 50,p.163. It can be seen that their behaviour is physically reasonable (real and greater than unity).

The thermal conductivity of the mixtures obtained by this scheme are plotted in Fig. 51,p.164 for the Helium/Neon mixtures and in Fig. 52,p.165 for the Argon/Krypton mixtures, where

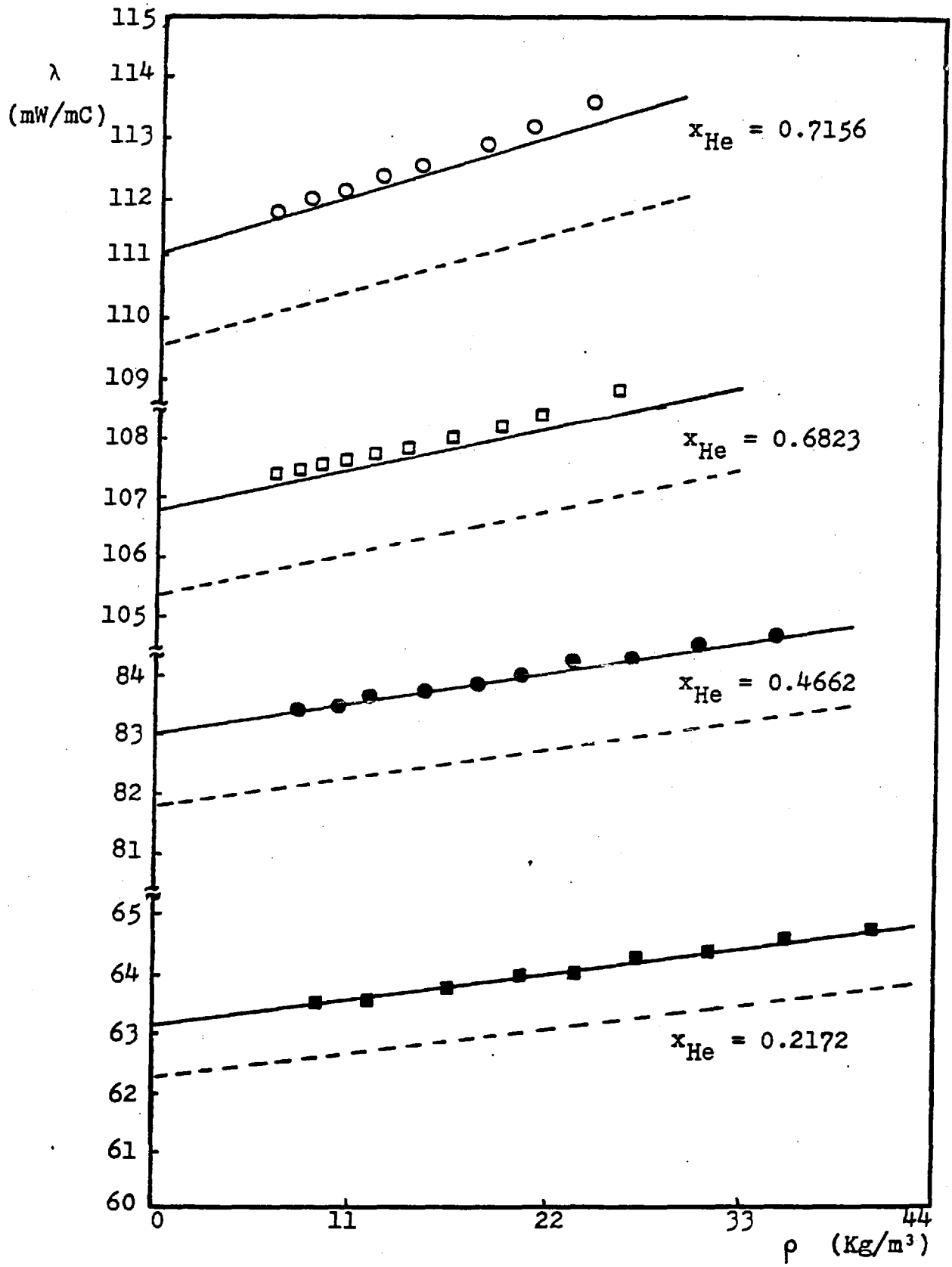

Figure 51 . Thermal Conductivity of Helium/Neon mixture as a function of density at 35.0 °C

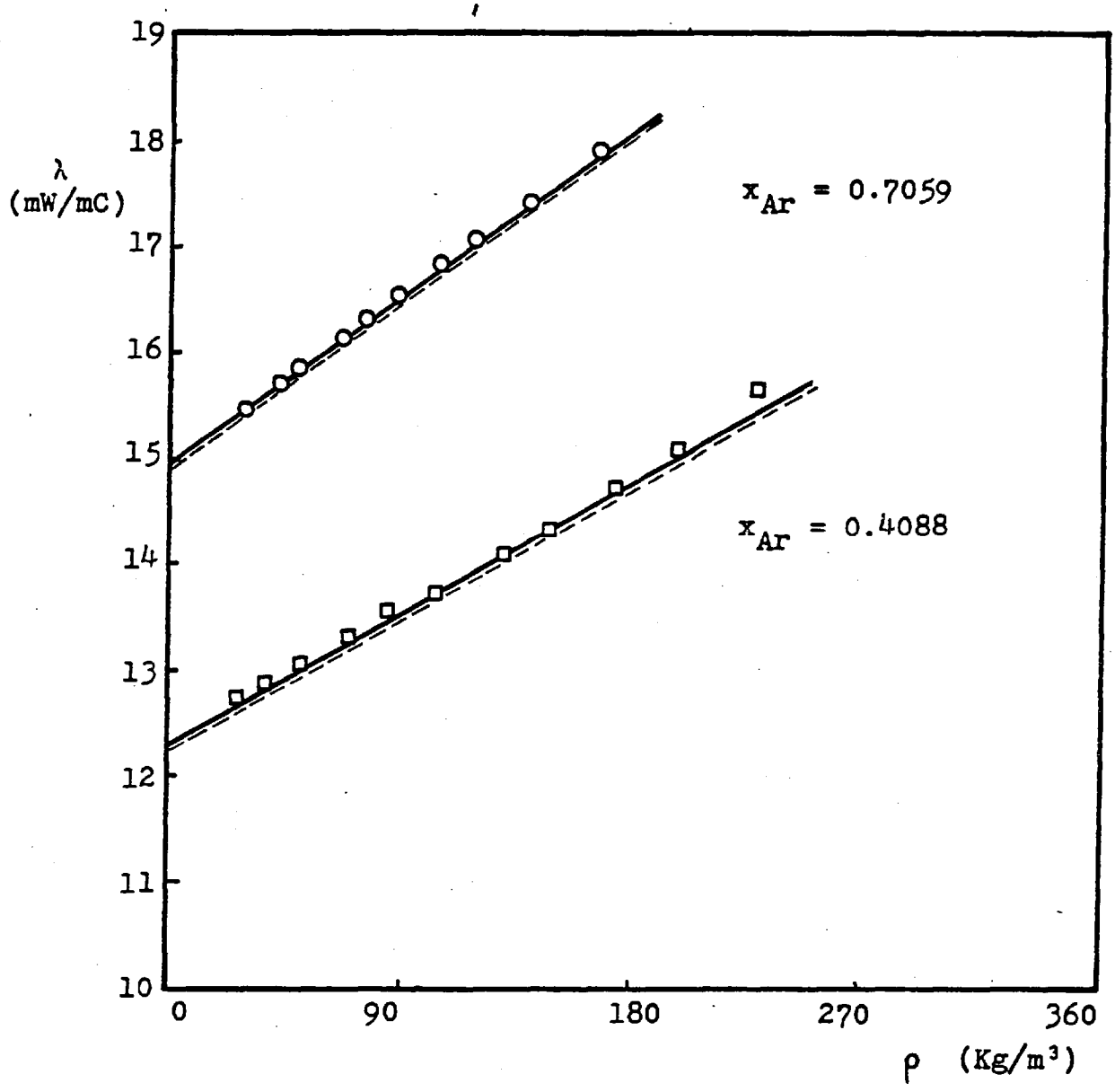

Figure 52 . Thermal Conductivity of Argon/Krypton mixture as a function of density at 35.0 °C

they are compared with experimental data.

The calculations for the Helium/Neon mixtures (dotted lines) lie systematically below the experimental results by up to 1.7%, a consequence of the first order nature of the calculations. For Argon/Krypton the calculations (dotted lines) differ by less than 0.3% from the experimental data. This improved agreement is a result of the smaller mass ratio of this mixture. Although no higher order approximations for the dense gas thermal conductivity

exist it is possible to make an empirical correction to the formulae to account for them. For this purpose we have computed a third order correction factor $f^{(3)}_{mix}$ according to the equation :-

$$f^{(3)}_{mix} = \frac{[\lambda_{mix}]_3}{[\lambda_{mix}]_1} \qquad (6.6)$$

using the explicit third order expressions for the zero density limit described previously. We have then applied this correction factor uniformly to the calculated thermal conductivity at all densities. The results of this procedure are included in Fig.51 and 52 (continuous lines); it can be seen that a greatly improved agreement with experimental values is obtained as the deviations now do not exceed 0.3%.

An alternative approach to the above procedure is to use the experimental thermal conductivities of the pure components directly in the equations. Although this method automatically ensures that the pure gas thermal conductivities are reproduced, it leads to worse agreement with the experimental values for the mixtures. This is probably due to the additional uncertainty introduced by using third order values in a first order expression.

6.2.3. MONATOMIC GASES & THEIR MIXTURES - CONCLUSION

From the foregoing discussion it can be seen that at low densities the available kinetic theory formulae are entirely adequate to describe the experimental results for monatomic gases and gas mixtures. Furthermore because intermolecular pair potentials for all such interactions are well known there is no need for further measurements at zero density for these gases and their mixtures.

At moderate densities the extensions of the modified Enskog theory to mixtures within the Mason-Wakeham approximation(§2.5.1) seem to be succesful in cases where the mass ratio of the constituent gases is about one. When the mass ratio is significantly different from unity (as in Helium/Neon mixtures, about five) semi-empirical schemes like the one described in this thesis seem to work well. However this is only possible in monatomic species where the thermal conductivity can now be calculated to a third order approximation with the aid of the equations derived in this thesis.

The problem of calculating the first density coefficient from first principles and known intermolecular potentials was shown here to be still in the early stages.

The measurements presented in this thesis, will, therefore provide in the future, a check on the theoretical predictions for more realistic potential models, and modifications of the present theories.

6.3. POLYATOMIC GASES

6.3.1. HYDROGEN

To a first order non-vanishing terms in the expansion of the velocity distribution function, the relationship between the thermal conductivity of a polyatomic gas and its viscosity in the limit of zero density can be written - as was shown by Mason (§2.4.1.,p.46,eq.(2.125))- in terms of the Eucken factor Eu as:-

$$Eu = \frac{\lambda^\circ M}{\eta^\circ C_v^\circ} = \frac{5}{2C_v^\circ}\left(\frac{3R}{2} - \Delta\right) + \frac{\rho D_{int}}{\eta^\circ C_v^\circ}\left(C_{v,int}^\circ + \Delta\right) \qquad (6.7)$$

where Δ is given by equation (2.126) and accounts for the effects of inelastic collisions in the gas. This expression is appropriate for the situation where only one mode of internal energy is excited. This, indeed, is the case for Hydrogen at 35 'C since the rotational modes are almost fully excited whereas the vibrational energy contributes less than 0.1% to the total energy of a molecule. In these circumstances we can identify the collision number ζ with the colision number for rotational energy relaxation ζ_{rot} ,and the diffusion coeffient D_{int} with the diffusion coefficient for rotational energy D_{rot}.

Furthermore, Hydrogen has relatively large collision numbers for rotational relaxation and thus inelastic collisions in the gas are rare although sufficient to maintain equilibrium between the different modes of motion of the molecule in the gas.For such cases, equation (6.7) was shown (§2.4.1.,p.47,eq.(2.127)) to simplify and yield the Modified Eucken relation reading:-

$$Eu = \frac{\lambda^\circ M}{\eta^\circ C_v^\circ} = \frac{15}{4}\frac{R}{C_v^\circ} + \frac{\rho D_{rot}}{\eta^\circ}\left(1 - \frac{3R}{2C_v^\circ}\right) \qquad (6.8)$$

The present thermal conductivity data at zero density, when combined with accurate measurements of the viscosity [60] give the opportunity to test equations (6.7) and (6.8) to a high degree of accuracy.

In order to perform these calculations we must first obtain values for ζ_{rot} and D_{rot} . The collision numbers for rotational relaxation of Hydrogen have been measured by Jonkman et al. [144] at low temperatures and their results have been extrapolated to 35 °C using the appropriate formula given by Parker [145] . As far as D_{rot} is concerned, to a first approximation it may be equated with the self diffusion coefficient D of the gas [80] which itself has been estimated with the aid of the first order kinetic theory relationship :-

$$\frac{\rho D}{\eta^\circ} = \frac{6}{5} A^* = \frac{8}{25} \frac{A^* m}{k} \lambda^\circ_{tr} \qquad (6.9)$$

where A^* is a ratio of collision integrals, which are functionals of the intermolecular pair potential. The ratio A^* has been obtained from calculations for an intermolecular potential deduced from molecular beam scattering data, second virial coefficients and dispersion energy calculations by Gegenbach et al. [146] . The collision integral calculations have been performed by a semi-classical evaluation of phase shifts to account for the small, but significant, quantum effects at room temperature [127] . The collision integral calculations are believed to be accurate to within $\pm 0.2\%$ at 35 °C .

Finally, we have used the zero density heat capacity given by McCarty [130] and computed the internal contribution to the molar heat capacity from the relationship :-

$$C^\circ_{v,int} = C^\circ_v - \frac{3}{2} R \qquad (6.10)$$

Table 34 presents the values of the parameters obtained from the foregoing discussion and the values of the consequent Eucken factors.

From the Table, it can be seen that the results of the Modified Eucken expression , eq.(6.8) and the more rigorous formula by Mason et al. eq.(6.7) , are identical essentially. We note also that although neither formula reproduces the experimental

Table 34 .

Eucken factors for pure Hydrogen

ζ_{rot} = 200	
A* = 1.1309	λ° = 192.21 mW/m/C
η° = 9.123 μPa s	λ_{tr} = 140.95 mW/m/C

Experimental	Modified Eucken eq. (6.8)	Mason et al. eq. (6.7)	Hirschfelder eq. (2.132)
2.068±0.008	2.0531	2.0529	2.0530

Eucken factor for Hydrogen within the experimental uncertainty, the maximum discrepancy amounts to no more than ±0.75%. However both theoretical formulae underestimate the Eucken factor.

There are several possible explanations for this discrepancy. It was thought that one of them might be related to the assumption that normal-Hydrogen is a single component gas. In order to assess the validity of this assumption we have treated Hydrogen as a two component gas - composed of ortho and para-Hydrogen - and used the Hirschfelder-Eucken formula (§2.4.2.,p.47, eq.(2.132)) to calculate the Eucken factor. The resulting Eucken factor, however, was found to be in complete agreement with the theoretical ones as can be seen from Table 34.

All the theoretical expressions employed so far, are essentially first order formulae in the Chapman-Cowling sense. From our discussion on the monatomic gases (§6.1.1.,p.155) we know that first order expressions can underestimate the thermal conductivity to viscosity ratio by about 0.3%. Assuming that the higher order corrections in polyatomic gases constitute a similar amount to the ratio, this could provide an explanation for some of this discrepancy.

A further point that must be considered is that the theoretical calculations of the Eucken factors are bounded by the uncertainty associated with the selection of the value for D_{rot} . An error of 2% in this value, is sufficient to contribute up to 1% to the uncertainty in the Eucken factor. We therefore estimate

that the overall uncertainty in the calculated Eucken factors may be as much as ±2%. Within this tolerance band the experimental and theoretical Eucken factors are consistent, although the theoretical predictions are less accurate than our measured values.

Viehland et al. [84] attempted to provide a better approximation to the Eucken factor for polyatomic gases by accounting for the spin polarisation contribution to the transport properties of a polyatomic gas (§2.4.4.,p.50). Their expression however restricted to cases for which the rotational energy level spacing is small compared to kT. Since this is not a valid assumption for Hydrogen their result can not be used in our analysis for the Eucken factors for Hydrogen.

The foregoing discussion indicates that before useful information can be deduced from the transport coefficients of polyatomic gases more accurate theoretical formulae must be obtained.

6.3.2. NITROGEN

In Nitrogen the rotational energy level spacing is small compared to kT. Therefore the most accurate available theoretical calculation of the Eucken factor is the one presented by Viehland [80] which incorporates spin polarization effects. This expression has the form (eq.(2.145),§2.4.4.,p.52):-

$$Eu = \frac{\lambda^\circ M}{\eta^\circ C_v^\circ} = \frac{5}{2C_v^\circ}\left(\frac{3R}{2} - \Delta\right) + \frac{\rho D_{int}}{\eta^\circ C_v^\circ}\left(C_{v,int}^\circ + \Delta\right)x \left\{1 - \frac{5}{3}\left(1 + \frac{\lambda_{tr}}{\lambda_{int}}\right)\left(\frac{\Delta\lambda_\mu}{\lambda}\right)_{sat}\right\} \qquad (6.11)$$

where Δ is defined by equation (2.126).

The only quantity in this expression for which experimental data are not available or for which accurate calculations can not be performed is D_{int} .Thus in this case we prefer to use our experimental data to calculate this quantity.

To carry out this calculation we have employed our experimental results for the zero density thermal conductivity and the zero density viscosity by Kestin et al. [157] . The collision number for rotational relaxation in Nitrogen has been taken from the experimental data of Prangsma et al. [158] . The heat capacity has been obtained from the values of Hilsenrath et al. [159]

and the value of $(\Delta\lambda_{ii}/\lambda)_{sat}$ from the measurements of Heemskerk et al. [160] . Finally in accordance with equation (6.9) we have written :-

$$\frac{\rho\, D_{int}}{\eta^\circ} = \frac{\rho\, D}{\eta^\circ}\left\{\frac{D_{int}}{D}\right\} = \frac{6}{5} A^* \left\{\frac{D_{int}}{D}\right\} \qquad (6.12)$$

where the functional A* can be obtained from the correlations of the extended law of corresponding states [58,60] .

Table 35

Eucken factor for pure Nitrogen

ζ_{rot}	A*	$(\Delta\lambda_i/\lambda)_{sat}$	η° μPa s	λ° mW/m/C	λ_{tr} mW/m/C	Experimental Eucken factor
5.7	1.0832	-8×10^{-3}	18.23	26.45	18.93	1.9550

The numerical values for all of the parameters discussed are presented in Table 35 . When these are employed in equation (6.12) we obtain :-

$$\frac{D_{int}}{D} = 0.93 \qquad (6.13)$$

To establish the significance of this result several observations must be made. If the spin polarization effect is neglected, as it only constitutes a 1.3% correction to the Eucken factor, the value of (D_{int}/D) is reduced by 3.5% and hence is further from unity. Furthermore, 10% fluctuations in the rotational relaxation number results in only a $\pm$0.5% change in the value of (D_{int}/D) .

The right hand side of equation (6.9) is, as shown before, a first order formula while in the left hand side we use experimental quantities. From our experience with monatomic gases, we know that using first order formulae can constitute errors of 0.3% in the theoretical ratio. Such an error would result in a 1% error on the ratio of (D_{int}/D). Finally, of course an error in A* contributes directly to the error in the calculated ratio of (D_{int}/D), but it is unlikely that even allowing for the effects of inelastic collisions on A* , its value could be in error by more then $\pm$1%.

Sandler[165] has performed the only theoretical calculation of the ratio (D_{int}/D) for a spherocylidrical molecular model. For this particular model the calculation of(D_{int}/D) is relatively straightforward and a correlation of his results reads :-

$$\frac{D_{int}}{D} = 1 + \frac{0.24}{\zeta_{rot}} - \frac{0.44}{\zeta_{rot}^2} - \frac{0.9}{\zeta_{rot}^3} \qquad (6.14)$$

For the value of $\zeta_{rot}= 5.7$ appropriate to Nitrogen this leads to the result :-

$$\frac{D_{int}}{D} = 1.023 \qquad (6.15)$$

so that the internal energy diffusion coefficient is greater than that for mass in contrast to our experimental results.

The physical significance of the result of equation (6.13) is that the internal, rotational energy in Nitrogen diffuses more slowly than do the molecules themselves. This in turn implies that there is a mechanism whereby rotational energy can be exchanged between Nitrogen molecules at a relatively long-range so that a fraction of the molecular collisions in the gas appear like head-on-collisions for rotational energy. It is possible that the long-range quadrapole-quadrapole interaction between Nitrogen molecules provides the means whereby this exchange is achieved.

6.3.3. CARBON MONOXIDE

The most accurate available theoretical calculation of the Eucken factor, as in the case of Nitrogen, is the one presented by Viehland [80] which incorporates spin polarisation effects eq.(6.11). As Carbon Monoxide displays very similar properties to Nitrogen, expression (6.11) was used to calculate the ratio of the internal energy diffusion coefficient to that for diffusio of mass.

We have employed our experimental data for the zero density thermal conductivity, The zero density viscosity was obtained from the measurements of Kestin *et al.* [161] whereas the collision number for rotational relaxation in Carbon Monoxide from the experimental data of Prangsma *et al.* [168] . The heat capacity has been obtained from the values of Hilsenrath *et al.*[159] and the value of $(\Delta\lambda_{\parallel}/\lambda)_{sat}$ from the measurements of Hermans *et al.*[162]. Finally the functional A* required for the calculation

of the dimensionless group $(\rho D_{int}/\eta^{\circ})$ from equation (6.12), was obtained from a (12-6) Lennard-Jones intermolecular potential for Carbon Monoxide suggested by Amdur et al. [170].

The numerical values for the parameters discussed are presented in Table 36 .

Table 36 .

Experimental Eucken factor for Carbon Monoxide

ζ_{rot}	A*	$(\Delta\lambda_{II}/\lambda)_{sat}$	η° μPa s	λ° mW/m/C	λ°_{tr} mW/m/C	Experimental Eucken factor
4.1	1.109	-8.1×10^{3}	18.23	25.73	18.61	1.898

Employing these parameters in equation (6.11) we obtain :-

$$\frac{D_{int}}{D} = 0.77 \qquad (6.16)$$

If the spin polarisation effect is neglected, as it only constitutes a 1.5% correction to the Eucken factor, the value of (D_{int}/D) is reduced by about 4% and hence further from unity. Furthermore, 10% fluctuations in the rotational relaxation number results in only a $\pm$0.5% change in the value of (D_{int}/D). An error in the functional A* ofcourse contributes directly to the error in the calculated ration of (D_{int}/D) but it is unlikely that even allowing for the effects of inelastic collisions in A*, its value could be in error by more than $\pm$1%. From the foregoing discussion we estimate the uncertainty involved in the ratio (D_{int}/D) to be at most $\pm$3%.

The result above for Carbon Monoxide is remarkable. First despite the similarity of Carbon Monoxide and Nitrogen the relationship between the mass and internal energy diffusion coefficients is considerably different. Secondly the experimental finding that the internal energy diffusion coefficient is some 20% smaller than that for mass is unusual. No experimental observations of such behaviour have been reported before although theoretical calculations based on approximate analyses have suggested the possibility for strongly polar molecules. The origin

of this gross discrepancy between D_{int} and D for polar gases is thought to be resonant exchange of internal energy brought about by the long range dipolar interaction for strongly polar molecules [171] . Carbon Monoxide is in fact weakly dipolar and so we have employed the analysis of resonant exchange given by Mason and Monchick[171] to investigate whether it can explain the above observation. According to their analysis :-

$$\frac{D_{int}}{D} = \frac{1}{1 + \delta} \tag{6.17}$$

where,

$$\delta = (1.7963 \cdot 10^3) \frac{\mu_d^2 M^{1/2} \theta_{rot}^{3/2}}{(C_{v,int}/R) \langle \Omega^{(1,1)*} \rangle \sigma^2 T^2} \tag{6.18}$$

Here, μ_d is the dipole moment in debyes, M the molecular weight in g/mole θ_{rot} the rotational temperature in 'K and σ the intermolecular pair potential parameter in A' .

We have evaluated δ using standard tabulations of the molecular properties [155] and find $\delta = 0.0005$. From this we infer that either the resonant exchange of internal energy is not responsible for our observations or that the appropriate analysis of Mason and Monchick[171] is not complete.

The only other means at present for estimating (D_{int}/D) are based on a model calculations. However neither the Sandler [165] spherocylinder model which yields $(D_{int}/D) = 1.019$, nor the rough sphere argument of Mason et al. [171] which yields the value $(D_{int}/D) = 1.11$, is capable of explaining our results. It appears therfore that an explanation of this observation will have to await calculations of internal energy diffusion coefficient based on the Wang Chang and Uhlenbeck equations for realistic potential models possibly with the aid of the recent Infinite Order Sudden (IOS) approximation [128] to the collision dynamics.

6.3.4. METHANE

The same analysis is applied to Methane. The zero density viscosity is obtained from the measurements of Kestin [161]. The functional A* is taken from the correlations of the extended law of corresponding states [58] whereas the value of $(\Delta\lambda_{\parallel}/\lambda)_{sat}$ from the measurements of Hermans et al.[162]. Finally the rotati-

onal relaxation number has been obtained from the experimental measurements of Prangsma et al. [158] .

The numerical values for the parameters discussed are presented in Table 37 .

Table 37 .

Experimental Eucken factor for Methane

ζ_{rot}	A*	$(\Delta\lambda_{\parallel}/\lambda)_{sat}$	η° μPa s	λ° mW/m/C	λ°_{tr} mW/m/C	Experimental Eucken factor
8,7	1.083	-1.8×10^{-3}	11.39	35.35	20.36	1.812

Employing these parameters in equation (6.11) we obtain :-

$$\frac{D_{int}}{D} = 1.006 \qquad (6.19)$$

For Methane the spin polarisation effect constitutes a 0.3% correction to the Eucken factor in contrast to Nitrogen or Carbon Monoxide. This is due to the smaller value of $(\Delta\lambda_{\parallel}/\lambda)_{sat}$. Fluctuations of 10% in the rotational relaxation number result in only a $\pm$0.4% change in the value of (D_{int}/D). We estimate, thus that the uncertainty involved in the ratio (D_{int}/D) is attributed mostly to the value of A* chosen and is about 1%.

Within this uncertainty, for Methane, the diffusion coefficient of inernal energy seems to be equal to the mass diffusion coefficient.

6.4. HYDROGEN/MONATOMIC MIXTURES

From the theoretical point of view, the mixtures of the monatomic gases with non-polar diatomic species are particularly interesting to study. The binary mixtures of the monatomic gases with Hydrogen are especially atractive because inelastic collisions in the gas mixtures are rare, Thus on the one hand, relatively simple kinetic theory formulae which neglect such collisions entirely should be quite adequate. On the other hand, the poorly known quantities related to inelastic collisions, which occur in the more rigorous kinetic theory formulae for the thermal conductivity have only a small effect on the calculated thermal conductivity.

6.4.1. THE ZERO DENSITY LIMIT

In the limit of zero density the most accurate available kinetic theory is the one presented by Mason and Monchick (§2.4.2., p.47).

The thermal conductivities of the pure gases at 35 °C have already been determined and reliable data for the viscosity of Hydrogen are available [60] . Therefore in order to carry out the theoretical calculation of the thermal conductivity of the mixtures from equations (2.131) to (2.144), it is necessary to obtain values for the various rotational collision numbers ζ_{ij} , the diffusion coefficients for internal energy $D_{i,int\,j}$, and the functionals of the unlike interactions in the mixture A^*_{ij} and B^*_{ij}.

The rotational collision numbers for the mixtures and pure Hydrogen have been obtained from the low temperature measurements of Jonkman [144] . The results have been extrapolated to 35 °C using the appropriate formula of Parker [145] and the values are listed in Table 38, p.177. For the diffusion coefficient of internal energy we have adopted the assumption employed by Monchick et al. [80], that it may be replaced by the ordinary mass diffusion coefficient calculated in turn from equation (6.9).

For the pure monatomic species we have computed the mass diffusion coefficient from the experimental thermal conductivities obtained in this work, and the functionals A^* of the extended law of corresponding states [58] via eq. (6.9). For pure Hydrogen we have employed the experimental viscosity [80] together with

A* computed from the intermolecular pair potential given by Gengenbach et al. [146] .

The necessary functionals of the unlike intermolecular pair potential have been computed for the potentials proposed by Bickes et al. [147] on the basis of molecular beam scattering data and Le Roy and van Kranendonk [148] on the basis of spectroscopic studies. In the case of Hydrogen/Argon interaction a further pair potential has been proposed by Le Roy et al. [149] from an examination of a greater range of experimental data.

Table 38 .

Parameters for the calculation of mixture thermal conductivities

Unlike Intermolecular Pair Potential		H_2/Ne	H_2/Ar	H_2/Kr
	λ_1° , mW/m/C	192.21	192.21	192.21
	$\lambda_{1,tr}^\circ$, mW/m/C	140.95	140.95	140.95
	λ_2° , mW/m/C	50.41	18.20	9.722
	ζ_{11}	250	250	250
	ζ_{22}	∞	∞	∞
	ζ_{12}	80	100	140
	ζ_{21}	∞	∞	∞
Bickes et al. [147]	A_{12}^*	1.105	1.096	1.904
	B_{12}^*	1.091	1.096	1.104
	$[\lambda_{12}]_1$, mW/m/C	108.06	78.58	67.57
Le Roy and Kranendonk [148]	A_{12}^*	1.109	1.098	1.097
	B_{12}^*	1.091	1.093	1.096
	$[\lambda_{12}]_1$, mW/m/C	105.37	76.97	67.81
Le Roy et al. [149]	A_{12}^*	-	1.108	-
	B_{12}^*	-	1.105	-
	$[\lambda_{12}]_1$, mW/m/C	-	77.81	-

The potentials suggested by Bickes et al. and Le Roy and van Kranendonk are both of Lennard-Jones (12-6) form and as they are therefore spherically symmetric the evaluation of their collision integrals is straightforward. However the potential proposed by Le Roy et al. [149] is orientation-dependent, and so in this case the collision integrals have been computed by the method of Parker and Pack [128].

Table 38 summarises all the data employed for the theoretical evaluation of the thermal conductivity of the mixtures. In these calculations we have employed experimental values for the thermal conductivity of the pure gases to ensure our calculation reproduces the thermal conductivity at each end of the composition range. The results of the calculations are listed in Table 39.

Table 39 :

Calculated thermal conductivities of the mixtures at zero density

Systems	λ°_{exp}	Bickes [147]		Le Roy [148]		Le Roy [149]	
		λ_{HE}	λ°_{mix}	λ_{HE}	λ°_{mix}	λ_{HE}	λ°_{mix}
	mW/m/C	mW/m/C	mW/m/C	mW/m/C	mW/m/C	mW/m/C	mW/m/C
H_2/Ne							
x_{H_2} = 0.2699	75.64	72.83	72.86	72.34	72.36	-	-
x_{H_2} = 0.5168	105.74	101.80	101.84	101.12	101.16	-	-
x_{H_2} = 0.7188	137.49	133.01	133.05	132.41	132.45	-	-
H_2/Ar							
x_{H_2} = 0.2614	42.89	41.79	41.81	41.25	41.27	42.17	42.21
x_{H_2} = 0.4847	71.49	69.43	69.47	68.48	68.52	70.09	70.13
x_{H_2} = 0.6402	97.35	94.96	95.02	93.86	93.91	96.76	95.81
x_{H_2} = 0.7504	120.24	117.66	117.71	116.60	116.65	118.45	118.50
H_2/Kr							
x_{H_2} = 0.4795	59.48	57.57	57.75	57.73	57.77	-	-
x_{H_2} = 0.7312	106.28	103.25	103.30	103.21	103.27	-	-

First, as expected, the contribution of inelastic collisions to the mixture thermal conductivity is very small (0.05%) so that the simpler Hirschfelder-Eucken result is entirely adequate. Secondly, the calculations consistently underestimate the thermal conductivity of the mixtures by up to 4%. The best agreement is achieved for H_2/Ar mixtures using the non-spherical HFD potential of Le Roy *et al.* [149] where the deviations are no more than 1.5%.

In view of the fact that the intermolecular pair potential employed have been derived without reference to transport properties, this agreement is encouraging. Nevertheless, the discrepancies between the experimental and calculated thermal conductivities lie well outside of the experimental uncertainty. It would be premature, however, to attribute all of this failure to the intermolecular pair potentials because the kinetic theory formulae employed for the calculation are only first-order approximations. It was shown (§2.3.2.,p.33) that for monatomic mixtures with species mass ratio much different from unity the first order formulae can underestimate the thermal conductivity by some 3%. Although no higher order expressions exist for the thermal conductivity of polyatomic gas mixtures it seems likely that the effect will be of a similar magnitude, particularly as for the mixtures studied here the mass ratio is greater than ten. It seems, therefore, that before polyatomic gas mixture properties at low density can be used as a test of intermolecular pair potentials more accurate kinetic theory expressions must be derived.

6.4.2. THE DENSITY DEPENDENCE

For moderate densities we have employed as for the monatomic mixtures the scheme proposed by Mason outlined in Chapter two, (§2.4.2.,p.47). In addition to the information needed for the calculation of the thermal conductivity in the low density limit the procedure requires the thermal conductivity of the pure gases as a function of density as well as estimates of the temperature dependent molecular size parameters γ_{ij} . These parameters have been obtained from the second virial coefficients as shown in equation (2.155),p.54. obtained from corresponding states [58] for the monatomic gases. For Hydrogen the second virial coeffi-

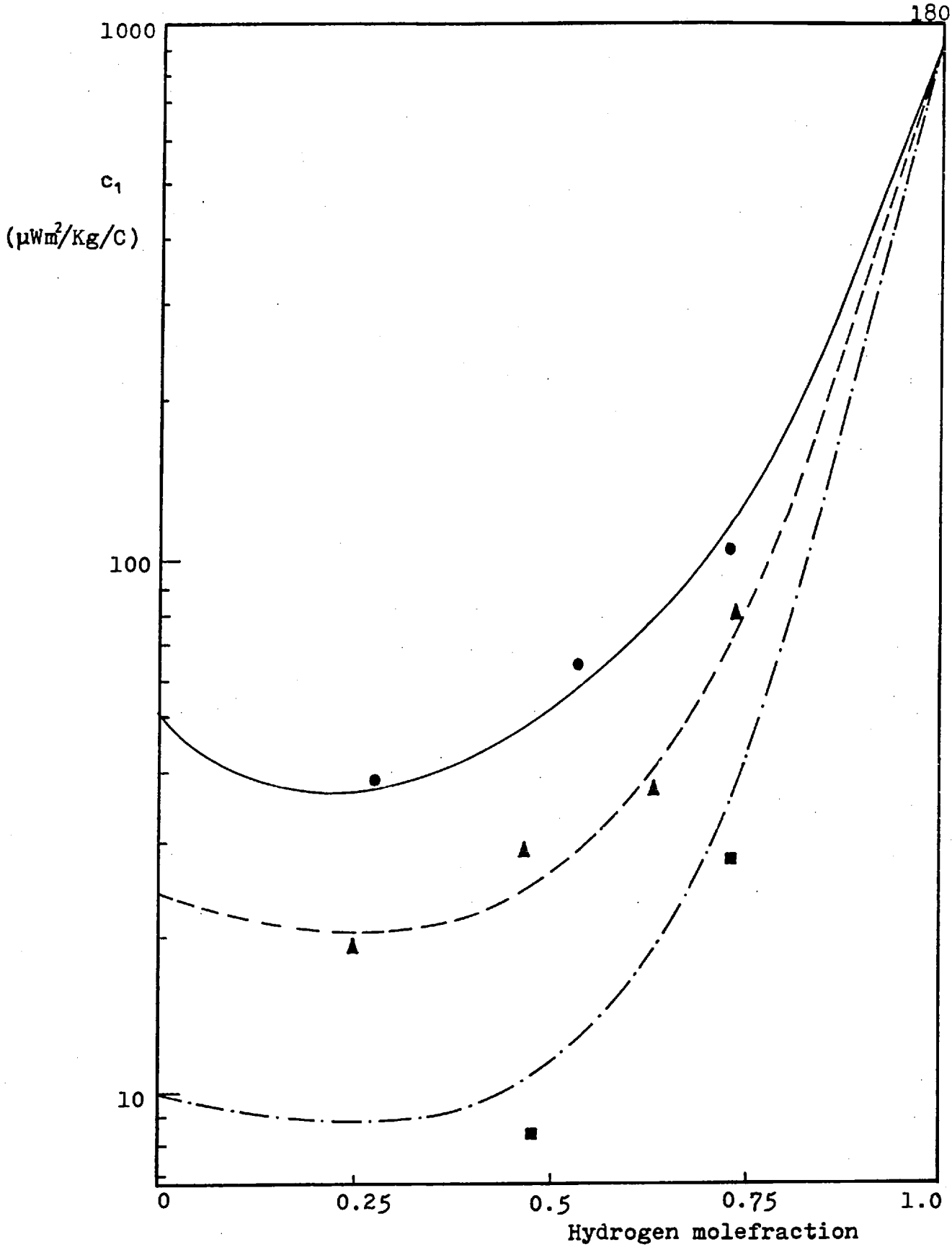

Figure 53. First density coefficient c_1 as a function of composition at 35 °C

Experimental :- ● H_2/Ne ▲ H_2/Ar ■ H_2/Kr

Theoretical :- —— H_2/Ne – – – H_2/Ar –·–·– H_2/Kr

cient was obtained from the work of Brewer et al. [150] as were the interaction virial coefficients B_{ij} .

At zero density this formulation of Mason et al. reduces to the Hirschfelder-Eucken result, which neglects explicit inelastic effects. Therefore, for the reasons given earlier, the absolute values of the dense gas mixture thermal conductivity lie systematically below the experimental values. Since there is no known method of correcting these calculations to a higher order of approximation we examine here only the predicted first density coefficient of the thermal conductivity defined in equation (5.2).

Figure 53,p.180, contains plots of the calculated and experimental values of the coefficient c_1 for the three binary mixtures as a function of the Hydrogen molefraction in the mixture. The agreement between the two sets of values is remarkably good, confirming the usefulness of the procedure of Mason and his collaborators.

6.5. HYDROGEN/NITROGEN MIXTURES

To complete the Hydrogen mixtures we chose to study a Hydrogen/polyatomic mixture because in this particular case, inelastic collisions play a more inportant role than before but only two rotational relaxation times are significant. The same analysis as the foregoing for the Hydrogen/monatomic mixtures is employed.

6.5.1. THE ZERO DENSITY LIMIT

As in the case of Hydrogen/monatomic mixtures (§6.4.1.,p.176) the only available kinetic theory is the semi-empirical approximation by Mason and Monchick (§2.4.2.,p.47).

The thermal conductivity of Hydrogen and Nitrogen have already been determined. The zero density viscosity of the mixtures has been obtained from the measurements of Kestin and Yata [164] and employed to compute the interaction viscosity.

The rotational collision numbers for the pure components and the mixtures have been obtained again from the low temperature measurements of Jonkman [144] and extrapolated to 35 °C using the approximate formula of Parker [145] . In order to calculate the diffusion coefficient for internal energy we have employed for the pure Nitrogen and the Hydrogen/Nitrogen interaction the experimental viscosities together with the functionals A* computed from a Lennard-Jones (12-6) intermolecular potential suggested by Kestin and Yata [169] , according to eq.(6.9). That is, the diffusion coefficientsfor internal energy have been assumed to be identical with the mass diffusion coefficients.

Table 40 .

Parameters for the calculation of mixture thermal conductivity at low density

$\lambda^{\circ}_{H_2}$ mW/m/C	$\lambda^{\circ}_{H_2,tr}$ mW/m/C	$\lambda^{\circ}_{N_2}$ mW/m/C	$\lambda^{\circ}_{N_2,tr}$ mW/m/C	ζ_{H_2}	ζ_{N_2}	$\zeta_{H_2N_2}$	$\zeta_{N_2H_2}$	A*	B*	$[\lambda_{H_2N_2}]_1$ mW/m/C
192.21	140.95	26.45	18.93	200	5.7	200	5.7	1.1023	1.0906	73.701

Table 40 summarises all the data employed for the theoretical evaluation of the thermal conductivity of the mixtures. In these calculations we have employed experimental values for the thermal conductivity of the pure gases to ensure our calculation reproduces the thermal conductivity at each end of the composition range. The results of the calculation are listed in Table 41.

Table 41 .

Calculated mixture thermal conductivities at zero density

	λ°_{exp} mW/m/C	λ_{HE} mW/m/C	λ°_{mix} mW/m/C
$x_{H_2} = 0.2136$	44.09	43.60	43.78
$x_{H_2} = 0.4865$	74.47	74.16	73.13
$x_{H_2} = 0.7338$	115.21	116.20	114.31

The contribution of the inelastic colisions is larger in this case than the one obtained for the Hydrogen/monatomic systems and it amounts up to 2%. Therefore, the Hirschfelder-Eucken result is not sufficiently accurate for this system. The calculations consistently underestimate the thermal conductivity of the mixtures by up to 1%. This seems to be better than the agreement obtained for the comparable Hydrogen/Neon cases (3%). However, this improved agreement is probably fortiutous.

One point that ought to be made is that since inelastic collisions constitute a 2% of the thermal conductivity an accurate value of the rotational relaxation number is important. Typically a 3% change in the rotational relaxation number for Nitrogen or Nitrogen/Hydrogen interaction constitutes a 27% change in the inelastic contribution term and therefore a 0.6% in the total thermal conductivity of the mixture. On the other hand, changes in the diffusion coefficient for internal energy of 3% produce only small changes ,0.01%, in the total thermal conductivity. Furthermore, changes in A* and B* of 3% produce only 0.6% change in the thermal conductivity. Hence if more accurate thermal con-

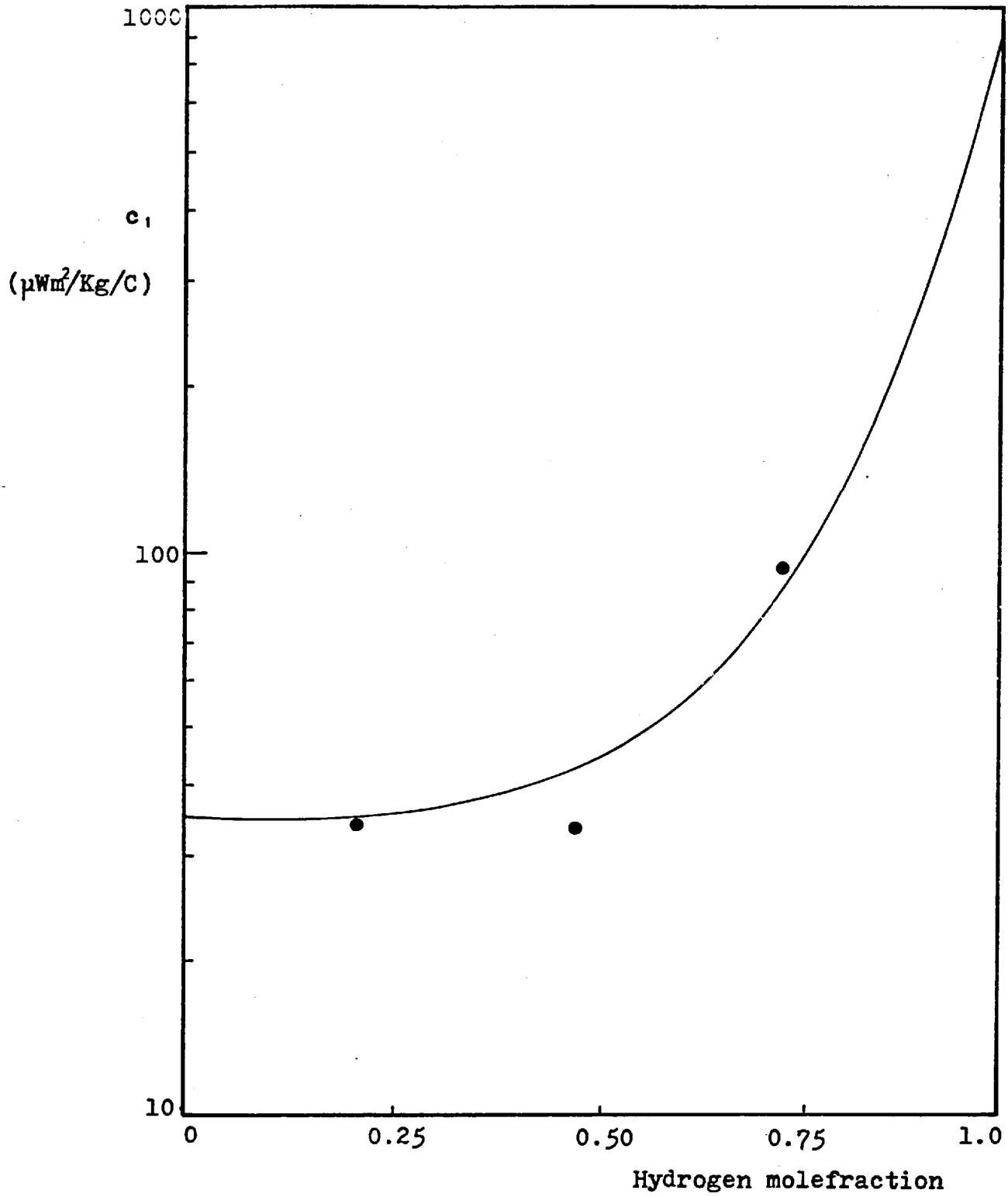

Figure 54 . First density coefficient c_1 as a function of composition at 35 °C

Experimental :- ● H_2/N_2

Theoretical :- —— H_2/N_2

ductivity expressions were available the measurements could be used to determine the rotational relaxation number for the Nitrogen/Hydrogen interaction.

6.5.2. THE DENSITY DEPENDENCE

For moderate densities the scheme proposed by Mason (§2.5.1., p.54) is again employed. Estimates for the temperature dependent molecular size parameter γ_{ij} have been obtained from the second virial coefficient, as shown by equation (2.167), from the measurements of Michels et al. [116] for Hydrogen, Michels and Wouters [117] for Nitrogen and Brewer [150] for the unlike interaction.

The functional B^* was obtained in the same way as A^* in the zero density limit previously examined. For the same reasons outlined in section(§6.4.2.,p.179) we examine here only the predicted first-density coefficient of the thermal conductivity of the mixtures as defined by the equation (5.2).

Figure 54,p.184, contains plots of the calculated and experimental values of the coefficient c_1 for the three binary mixtures as a function of the Hydrogen molefraction in the mixture. As in the Hydrogen/monatomic mixtures, the agreement between the two sets of values is remarkably good, confirming the usefulness of the procedure of Mason and his collaborators.

SEVEN

SUGGESTIONS FOR FUTURE WORK

In this thesis we have shown how very accurate measurements of the thermal conductivity of gases can be performed with the transient hot wire technique. We have also demonstrated the superiority of this technique over all other methods of measuring the thermal conductivity of gases.

Measurements on monatomic gases and their mixtures, at low density, were found to be adequately described by the available kinetic theory as extended to a third order approximation in this thesis. At elevated densities, semi-empirical schemes presented in this thesis were found to be adequate, whereas more rigorous theoretical predictions of the first density coefficient were not quantitatively accurate. For the polyatomic gases it was shown how molecular properties such as the internal energy diffusion coefficient can be derived from our results. Semi-empirical interpolation formulae for the polyatomic mixtures were found to be very useful in correlating the results in the absence of rigorous theoretical calculations which do not yet exist. It it thus concluded that we have reached a stage where the measurements can be performed with a higher accuracy than the existing theoretical calculations. Therefore, we believe that no further measurements at room temperature are needed, on the basis that they will not offer us more information until the kinetic theory is more advanced.

There are still however, insufficient experimental data on very low and high temperatures as well as very low pressures. As far as the very low pressures are concerned the present equipment has to be modified by using a thicker platinum wire. The reason for this, is that at very low pressures Knudsen effects become important , that is, the mean free path in the gas becomes compatible with the radius of the wire.

To perform measurements at very high or very low temperatures

the equipment must also be modified in two respects. Firstly, the cells were manufactured from stainless steel type 304 which has a much larger linear thermal expansion coefficient ($\approx 16 \cdot 10^{-6}$ m/m) than the platinum wire ($\approx 9 \cdot 10^{-6}$ m/m). Therefore at high temperatures the wire will be stretched and break while at low temperatures it will become slack. To overcome this difficulty it is proposed that the cells should be remade using another type of steel such as S80 which has a similar thermal expansion coefficient ($\approx 10 \cdot 10^{-6}$ m/m) to the wire. Secondly, in order to reach extreme temperatures, a vacuum must be introduced around the isothermal enclosure to avoid heat transfer to the environment. For low temperatures a system by which liquid Nitrogen is circulated around the vessel must be introduced. These two requirements can both be met by surrounding the pressure vessel itself with Helium contained in a sealed isothermal enclosure , fitted with heating cables and liquid Nitrogen circulation pipes, mounted in a vacuum chamber. The thermal inertia of the isothermal enclosure employed in the present measurements together with the vacuum jacket should be sufficient to ensure adequate temperature stability. In other respects the measurements can be performed as described in this thesis with due account being taken of the changes in the platinum wire length as a function of temperature.

SYMBOLS

GENERAL SYMBOLS

a - Wire radius
b - Van der Waals co-volume
B - Second virial coefficient
c_p - Molecular specific heat capacity at constant pressure
c_v - Molecular specific heat capacity at constant volume
$\tilde{c}_v$ - Specific heat capacity at constant volume per unit mass
$\underline{c}_i$ - Absolute velocity of species i
C - Third virial coefficient
$\underline{C}_i$ - Peculiar velocity of species i
C_v - Molar specific heat capacity at constant volume
$\underline{\xi}$ - Dimensionless velocity
D_{ij} - Multicomponent diffusion coefficient
D_{Ti} - Multicomponent thermal diffusion coefficient
D_{int} - Diffusion coefficient for internal energy
e - Extension
E - Energy
F - Force
g - Relative velocity of a molecule
g' - Gravitational constant
I - Electric current
k - Boltzmann's constant
k_d - Thermal diffusivity
K_{Ti} - Thermal diffusion ratio of species i
K_s - Spring constant of elasticity
ℓ - Length
m - Molecular mass
n - Number density
N - Avogadro number
N_t - Number of turns in a spring

P - Pressure
$\underline{P}$ - Pressure tensor
Pr - Prandtl number
q - Heat flux
Q - Heat flow
r - Radius
R - Resistance
S - Switch
t - Time
T - Temperature
u - Mean kinetic energy
$\underline{v}$ - Hydrodynamic velocity
$\underline{V}_i$ - Diffusion velocity vector
V - Voltage
x_i - Mole fraction of species i
Y - Young's modulus of elasticity

GREEK SYMBOLS

α - Temperature coefficient of resistance
β - Impact parameter for a collision
β' - Linear expansion coefficient
γ - Free path shortening parameter
δ_{pq} - Kronecker's delta
ε - Potential well depth parameter
ζ - Collision number for equilibrium of translational and internal energy
η - Viscosity
η - Order of approximation
λ - Thermal conductivity
λ' - Partial thermal conductivity
μ - Reduced mass
ν - Number of components in a mixture
$\bar{\nu}$ - Poisson's ratio
π - 3.141592.....
ρ - Mass density
σ - Potential parameter
$\bar{\sigma}$ - Resistance per unit length
σ_B - Stefan Boltzmann constant
τ - Tension

χ_i - Angle of deflection on a collision
χ'_i - Pseudo-radial distribution function
ψ - Angle defining the orientation of a collision plane
$\Omega^{(l,s)}$ - Collision integral

SUBSCRIPTS

cw - Compression work correction
e - Experimental conditions
tr - Translational contribution
id - Ideal conditions
int - Internal contribution
ℓ - Long wire
mix - Mixture
o - Initial equilibrium conditions
OB - Outer boundary correction
R - Radiation correction
s - Short wire
SH - Specific heat capacity correction
w - Wire

REFERENCES

[1] W.Nicholson,J.Nicholson,Proc.Roy.Soc.(LON) 5,197 (1802)
[2] J.Murray,J.Nicholson,Proc.Roy.Soc.(LON) 1,105 (1800)
[3] B.Rumford,J.Nicholson,Proc.Roy.Soc.(LON) 14,353 (1806)
[4] J.Biot,Biblioteque Brittanique 27,310 (1804)
[5] M.Depretz,Pogg.Ann. 46,340 (1839)
[6] R.Weber,Ann.Physik 15,1047 (1903)
[7] A.Berger,Compt.Rend. 105,224 (1885)
[8] K.O.Bates,Ing.Eng.Chem. 25,431 (1933)
[9] B.C.Sokiades,J.Coates,A.I.Chem.E.Journal 1,275 (1955)
[10] B.C.Sokiades,J.Coates,Eng.Expt.Stat.Louisiana Univ.B34(1952)
[11] A.Michels,A.Botzen,Physica 18,605 (1952)
[12] A.Michels,J.V.Sengers,P.S.Van der Gulick,Physica 28,586 (1962)
[13] W.Fritz,H.Poltz,Int.J.Ht.Mass Transfer 5,307 (1962)
[14] L.Riedel,Chemie Ing.Technik 29,321 (1958)
[15] G.N.Richter,B.H.Sage,Ind.Eng.Chem.,Chem.Eng.Data 2(1),61(1957)
[16] P.W.Bridgman,Proc.An.Acad.Arts & Sci. 59,141 (1923)
[17] L.Riedel,Chemie Ingenia Technik 13,321 (1951)
[18] R.J.Schmidt,W.Seleschop,Forsch.Gebiete Ingenier 3,277 (1932)
[19] R.J.Schmidt,S.W.Milverton,Proc.Roy.Soc.(LON) A152,586 (1935)
[20] D.Misic,G.Thodos,Physica 32,885 (1966)
[21] H.Schliermacher,Wied.Ann. 34,623 (1888)
[22] O.B.Cecil,R.H.Munch,Ind.Eng.Chem. 48,437 (1956)
[23] W.J.Taylor,H.L.Johnston,J.Chem.Phys. 14,219 (1946)
[24] H.L.Johnston,E.R.Grilly,J.Chem.Phys. 14,233 (1946)
[25] E.F.M.Van der Held,F.G.Van Drunen,Physica 15,866 (1949)
[26] F.G.Drunen,Diss.Utrecht, Netherlands (1949)
[27] E.F.M.Van Held,J.Hadebol,J.Kalshoven,Physica 19,208 (1953)
[28] D.A.Vries,Soil Science 73,83 (1952)
[29] K.Buettner,Trans.Am.Geophys.Union 36,831 (1955)
[30] D.G.Gillan,O.Lamm,Acta. Chemica Scand. 9,609 (1955)
[31] P.Grassman,W.Straumann,Int.J.Ht.Mass Transfer 1,50 (1960)
[32] E.M.McLaughlin,J.K.Horrocks,Proc.Roy.Soc.(LON) A273,259 (1969)
[33] J.Pittman,E.M.C.McLaughlin,Phil.Trans.R.Soc.(LON) A270 (1971)
[34] N.Mani,Thesis,University of Calgary,Canada (1971)

[35] B.H.Vos,Techniskh Wetenschapelijk Onderzoek 1,7 (1961)
[36] J.W.Haarman,Thesis,Technische Hogelschool Delft(1969) Neth.
[37] B.Stahlane,S.Pyk,Tecknish Tidskrift 61,38 (1931)
[38] C.A.N.Castro,W.A.Wakeham,Proc.1st Nat.Cong.on Pure & Applied Mathematics (LISBON) (1974)
[39] J.J.De Groot,J.Kestin,H.Sookiazian,Physica 75,454 (1974)
[40] M.J.Assael, M.Sc.Report,Imperial College,(LON) (1978)
[41] S.Weber,Ann.der Physik 54,437 (1917)
[42] J.Hammond,J.Kestin,R.Paul,A.Clifford,W.A.Wakeham, Physica,100A 349 (1980)
[43] B.Le Neindre,R.Tufeu,P.Bury,P.Johannin,B.Vodar,Ther.Cond. Proc.of 7th Conf.(NBS) 579 (1967)
[44] A.Michels,A.Botzen,A.Friedman,J.V.Sengers,Physica 22,121 (1956)
[45] R.Bailey,J.Kellner,Physica 39,444 (1968)
[46] Van Dael,H.Cauwenberch,Physica 40,173 (1968)
[47] F.G.Waelbroeck,P.Zuckerbroot,J.Chem.Phys. 28,524 (1958)
[48] F.G.Keyes,Trans.Am.Soc.Mining.Met.Engrs. 76,809 (1954)
[49] B.G.Dickins,W.B.Mann,Proc.Roy.Soc.(LON) A134,77 (1931)
[50] A.Eucken,Physik Zeitz 14,324 (1913)
[51] A.Clifford,J.Kestin,W.A.Wakeham,Physica 97A,287 (1979)
[52] A.Clifford,J.Kestin,W.A.Wakeham, (to be published)
[53] C.T.Archer,Proc.Roy.Soc.(LON) A165,474 (1938)
[54] W.Northdurft,Ann.D.Phys. 28,137 (1937)
[55] H.S.Gregory,Proc.Roy.Soc.(LON) A149,35 (1935)
[56] R.Tufeu,Thesis, University of Paris,France (1971)
[57] W.G.Kannuluik,L.H.Martin,Proc.Roy.Soc.(LON) A144,496 (1934)
[58] J.Kestin,E.A.Mason,Art.in 'Transp.Phen.'AIP Conf.11,193 (1973)
[59] P.E.Liley,Proc.4th Symp.Therm.Prop.Bladzijde 323(1968)
[60] J.Kestin,S.T.Ro,W.A.Wakeham,J.Chem.Phys.56,4036 (1972)
[61] J.C.Maxwell,Phil.Trans.Roy.Soc.(LON) 157,49 (1867)
[62] L.Boltzmann,Akad.der Wissenschaften 66(2),275 (1872)
[63] L.Boltzmann,Akad.der Wissenschaften 72(2),427 (1875)
[64] S.G.Brush,Kinetic Theory(Pergamon Press,Oxford) (1966)
[65] H.A.Lorentz,Akad.der Wissenschaften 95,684 (1887)
[66] D.Hilbert,Grundzuge Einer Allgemeinen Theorie der Lingaren Integralglekhungen Teubner,Leipzig (1912),Chelsea Pub.NY(1953)
[67] S.Chapman,Trans.Roy.Soc.(LON) 216,279 (1917)
[68] S.Chapman,Trans.Roy.Soc.(LON) 217,118 (1917)
[69] D.Enskog,Physik.Zeitschr. 12,533 (1911)

[70] D.Enskog,Thesis,Upsala (1917)
[71] J.H.Ferziger,H.G.Kaper,Mathematical Theory of Transport Processes in Gases,North Hol.Publ.Comp.(1972)
[72] G.C.Maitland,M.Rigby,E.B.Smith,W.A.Wakeham, Intermolecular forces - Their origin and determination, Oxf.Univ.Press(1980)
[73] S.Chapman,T.G.Cowling,Mathematical Theory of Non-Uniform Gases,3rd ed.,Cambridge Univ.Press,London (1972)
[74] C.Muckenfuss,C.F.Curtis,J.Chem.Phys. 29,1273 (1958)
[75] M.Assael,J.Kestin,W.A.Wakeham,Int.J.Thermophys., 1,5 (1980)
[76] J.O.Hirschfelder,C.F.Curtis,R.B.Bird,Molecular Theory of Gases and Liquids,Wiley, New York (1964)
[77] C.S.Wang-Chang,G.E.Uhlenbeck,Transport Phenomena in Polyatomic Gases,Univ.of Michigan,Eng.Res.Inst.Report CM-681
[78] C.S.Wang-Chang,G.E.Uhlenbeck,J.De Boer,Heat Conductivity & Viscosity of Polyatomic Gases,North Publ.Comp.Amsterdam(1964)
[79] L.Monchick,K.S.Yun,E.A.Mason,J.Chem.Phys. 39(3),654 (1963)
[80] L.Monchick,A.N.Pereira,E.A.Mason,J.Chem.Phys. 42(9),3241 (1965)
[81] J.O.Hirshfelder,J.Chem.Phys. 26,282 (1957)
[82] J.S.Dahler,N.F.Sather,J.Chem.Phys. 38,2363 (1963)
[83] J.S.Dahler,N.F.Sather,J.Chem.Phys. 44,1229 (1966)
[84] A.L.Viehland,E.A.Mason,S.I.Sandler,J.Chem.Phys. 68,5277 (1978)
[85] J.J.M.Beenakker,Acta Phys.Austeica Suppl. 10,267 (1973)
[86] F.R.McCourt,R.F.Snider,J.Chem.Phys. 41,3185 (1964)
[87] L.Waldmann,Quantum Theoretical Transport equations for Polyatomic Gases,ed.J.Meixner,North Hol.Publ.Comp.Amsterdam (1965)
[88] D.Enskog,Kungl.Svenska Vet.Ak.Hande 63,5 (1922)
[89] E.A.Mason,H.E.Khalifa,R.DiPippo,J.R.Dorfman,Physica 91A,377 (1978)
[90] J.Kestin,W.A.Wakeham,Ber.Bunsenges.Phys.Chem. (in press)
[91] L.Barajas,L.S.Garcia-Colin,E.Pina,J.Stat.Phys. 7,161 (1973)
[92] H.Van Beijeren,M.H.Ernst,Physica 68,437 (1973)
[93] H.Van Beijeren,M.H.Ernst,Physica 70,225 (1973)
[94] D.Enskog,Kinetic Theory,Vol.3,Pergamon Press,New York (1972)
[95] H.H.Thorne, ref. [94] p.292
[96] M.K.Tham,K.E.Gubbins,J.Chem.Phys. 55,268 (1971)
[97] T.M.Reed,K.E.Gubbins,Applied Statistical Mechanics,Chapter 9 McGraw-Hill,New York (1973)
[98] S.I.Sandler,J.L.Fiszdon,Physica 95A,602 (1979)
[99] J.H.Haarman,Physica 52,605 (1971)
[100] J.J.Healy ,J.J.De Groot,J.Kestin,Physica 82C,392 (1976)

[101] M.Smoluchowski,Ann.Phys.Chem. 35,983 (1911)
[102] M.Smoluchowski,Phil.Mag. 21,11 (1911)
[103] H.Sookiazian, Ph.D. Thesis, Brown University USA (1972)
[104] J.Menashe, Imperial College,London (Private communication)
[105] J.Kestin,W.A.Wakeham,Physica 92A,102 (1978)
[106] J.Fischer,Ann.Phys. 34,669 (1939)
[107] W.A.Wakeham, N.E.L.Report No 144 (1976)
[108] J.Anderson,K.Leaver,G.S.Rawlings,Materials Science-Nelson 2nd edt.(1974)
[109] R.H.Perry,C.Chilton,S.D.Kirkpatrick,Chemical Engineers' Handbook,4th edt.McGraw-Hill,(1963)
[110] A.Michels,H.J.Wijker,H.Wijker,Physica 7 ,627(1949)
[111] A.Michels,H.Wouters,Physica 8,923 (1941)
[112] A.Michels,T.Wassenaar ,P.Louwerse,Physica 26,539 (1960)
[113] A.Michels,T.Wassenaar ,P.Louwerse,Physica 20,99 (1954)
[114] N.J.Trappeniers,T.Wassenaar ,G.Wolkers,Physica 32,452 (1966)
[115] A.Michels,G.Nederbragt,Physica 2,1000 (1935)
[116] A.Michels,M.Goudeket,Physica 8,347 (1941)
[117] A.Michels,H.Wouters,J.de Boer,Physica 1,587 (1934)
[118] A.Michels,T.Wassenaar,W.Van Seventer,Appl.Sci.Res.A 5,121 (1961)
[119] A.Clifford,P.Gray,A.Johns,A.Scott,J.Watson N.E.L.(in press)
[120] A.Clifford, Leeds University (Private correspondance)
[121] A.Clifford,J.Kestin,W.A.Wakeham, Physica (in press)
[122] D.W.Gough,G.C.Maitland,E.B.Smith,Mol.Phys. 24,151 (1972)
[123] D.W.Gough,E.B.Smith,G.C.Maitland,Mol.Phys.23,1433 (1973)
[124] G.C.Maitland,W.A.Wakeham,Mol.Phys. 35,1443 (1978)
[125] R.Fleeter,J.Kestin,R.Paul,W.A.Wakeham, Physica (in press)
[126] A.Michels,J.V.Sengers,L.J.M.van der Klunder,Physica 29,149 (1963)
[127] V.Vesovic,Imperial College,London (private communication)
[128] G.A.Parker,R.T.Pack,J.Chem.Phys. 68,1585 (1978)
[129] L.Monchick,E.A.Mason,J.Chem.Phys. 35,1676 (1961)
[130] R.D.McCarty,Hydrogen Technological survey - Thermophysical Properties NASA 5P-3089 (NASA,Washington,1975)
[131] H.J.M.Hanley,R.D.McCarty,E.G.D.Cohen,Physica 60,322 (1972)
[132] N.Taxman,Phys.Rev. 110,1235 (1958)
[133] H.Senftleben,Physik.Zeitschr. 31,961 (1930)
[134] J.J.M.Beenakker,F.R.McCourt,Ann.Rev.Phys.Chem 21,47 (1970)

[135] H.Holsen,F.G.van Kuik,K.W.Walstra,J.J.M.Beenakker, H.F.P.Knaap, Physica 57,501 (1972)
[136] J.R.Dorfmann,H.van Beijeren,Stat.Mech.Part B- Time dependent processes,ed.B.J.Berne (Plenum,New York,1977)
[137] J.V.Sengers, AIP Conf.Proc.,Transport Phenomena,11,229 (1973)
[138] International Practical Temperature Scale of 1968 (NPL) (HMSO London,1968)
[139] International Practical Temperature Scale of 1976 (NPL) Revised ed. (HMSO London,1976)
[140] J.Kestin,S.T.Ro,W.A.Wakeham,J.Chem.Phys. 56,5837 (1972)
[141] J.Kestin,W.A.Wakeham,K.Watanabe,J.Chem.Phys.53,3773 (1970)
[142] J.Kestin,H.E.Khalifa,W.A.Wakeham,Physica 90A,215 (1978)
[143] A.Boushehri,L.A.Viehland,E.A.Mason,Physica 91A,424 (1978)
[144] R.M.Jonkman,G.J.Prangsma,I.Erias,H.F.P.Knaap,J.J.M. Beenakker, Physica 38,441 (1968)
[145] J.G.Parker,Phys.Fluids 2,449 (1959)
[146] R.Gengenbach,C.Hahn,W.Schrader,J.P.Toennies,Theor.Chim.Acta 34,199 (1974)
[147] R.W.Bickes,G.Scoles,K.M.Smith,Can.J.Phys. 53,435 (1975)
[148] R.J.Le Roy,J.van Kranendonk,J.Chem.Phys.61,4750 (1974)
[149] R.J.Le Roy,J.S.Carley,J.Crabenstetter,Far.Disc.of Chem.Soc. 62,169 (1977)
[150] J.Brewer,W.Vaughn,J.Chem.Phys. 40,2960 (1969)
[151] H.J.M.Hanley,M.Klein,J.Chem.Phys. 53,4722 (1970)
[152] J.V.Sengers,Ph.D.Thesis,Van der Waals Lab.Univ.Van Amsterdam, Amsterdam (1962)
[153] S.K.Kim,J.Ross,J.Chem,Phys. 42,263 (1965)
[154] D.K.Hoffman,C.F.Curtiss,Phys.Fluids 8,890 (1965)
[155] Handbook of Chemistry and Physics,56th ed.CRC Press (1975)
[156] A.Clifford,J.Kestin,W.A.Wakeham,Ber.Bunsenges.Phys.Chem. 84,9 (1980)
[157] J.Kestin,E.Paykoc,J.V.Sengers,Physica 54,1 (1971)
[158] G.J.Prangsma,L.J.M.Borsboom,H.F.P.Knaap,C.J.N.van der Meijdenberg,J.J.M.Beenakker,Physica 61,527 (1972)
[159] J.Hilsenrath,C.W.Beckett,W.S.Benedict,L.Fano,H.J.Hodge, J.F.Masi,R.L.Nutall,Y.S.Touloukian,H.W.Woolley - Nat.Bur. Stand.Circ. No 564 (1955)
[160] J.P.J.Heemserk,F.G.van Kuik,H.F.P.Knaap,J.J.M.Beenakker. Physica 71,484 (1974)

[161] J.Kestin,S.T.Ro,W.A.Wakeham,Tr.of Far.Soc.584,67 (1971)
[162] L.J.F.Hermans,J.M.Koks,A.F.Hengenveld,H.F.P.Knaap, Physica 50,410 (1970)
[163] R.D.Olmsted,C.F.Curtiss,J.Chem.Phys. 63,1966 (1975)
[164] R.F.Snider,C.F.Curtiss,Phys.Fluids 1,122 (1958)
[165] S.I.Sandler,Phys.Fluids 11,2549 (1968)
[166] J.van Oosten, Ph.D.Thesis,Amsterdam (1974)
[167] J.A.A.Snel,N.J.Trappeniers,A.Botzen,Proc.Kon.Ned.Akad. Van Wet. 82B,316 (1979)
[168] G.J.Prangsma,A.H.Alberga,J.J.M.Beenakker,Physica 64, 278 (1973)
[169] J.Kestin,J.Yata,J.Chem.Phys. 49,4780 (1968)
[170] I.Amdur,L.M.Shuler,J.Chem.Phys. 38,188 (1963)
[171] E.A.Mason,L.Monchick,J.Chem.Phys. 36,1622 (1962)
[172] J.P.J.Michels,N.J.Trappeniers,Physica 90A,179 (1978)
[173] H.E.Khalifa,J.Kestin,W.A.Wakeham,Physica 97A,273 (1979)

LIST OF PUBLICATIONS

1. THE ECONOMIC ADVANTAGES OF ACCURATE TRANSPORT PROPERTY DATA
   M.Assael,C.A.N.Castro,W.A.Wakeham,Proc.of Chempor 78 ,
   Braga, Portugal (1978)

2. THE ECONOMIC ADVANTAGES OF ACCURATE TRANSPORT PROPERTY DATA FOR HEAT TRANSFER EQUIPMENT DESIGN
   A.J.F.Mendonca,C.A.N.Castro,M.Assael,W.A.Wakeham,
   Chem.Eng.Comm. (1980)

3. HIGHER ORDER APPROXIMATIONS TO THE THERMAL CONDUCTIVITY OF MONATOMIC GAS MIXTURES
   M.Assael,W.A.Wakeham,J.Kestin,Int.J.Thermophys.Prop.1,5 (1980)

4. AN ABSOLUTE DETERMINATION OF THE THERMAL CONDUCTIVITY OF THE NOBLE GASES AND TWO OF THEIR MIXTURES AS A FUNCTION OF THE DENSITY
   M.Assael,M.Dix,A.Lucas,W.A.Wakeham,Faraday Soc. (1980)

5. THE THERMAL CONDUCTIVITY OF HYDROGEN WITH THE MONATOMIC GASES
   M.Assael,W.A.Wakeham, Ber.Bunsenges.Phys. Chem. (1980)

6. THE THERMAL CONDUCTIVITY OF FOUR POLYATOMIC GASES
   M.Assael,W.A.Wakeham (1980)